Thesis submitted for the degree of Doctor of Philosophy
King's College London

The role of the Jun N-terminal kinase (JNK) pathway in neuronal morphogenesis

Andrew Sam Rallis

September, 2009

MRC Centre for Developmental Neurobiology
King's College London

This PhD thesis is especially dedicated to my deceased mother Elaine, my father George and my sister Julia who have helped me throughout my career. I would also like to thank my supervisor Dr Julian Ng, for his continuous help, advice and guidance throughout the four years of my PhD, Michael Fletcher and Coralie Moore, for their technical assistance in the lab and numerous members of the Tear, Williams and Chia Lab for providing constructive ideas, which have helped me improve my PhD.

ABSTRACT

Understanding how signalling molecules regulate various processes in neurodevelopment is a fundamental question in the field of neurobiology. One confounding factor towards a complete understanding of the topic is the constant reiteration of the same proteins being implicated in diverse morphogenetic events, how can the same molecule regulate so many aspects of cell morphology? The Jun N-terminal kinase (JNK) pathway, typifies such a pleiotrophic factor and in neurons has been demonstrated to be involved in neurodegeneration, axon extension, dendrite formation and synaptic growth.

Here I show that two parameters are critical in defining JNK-dependent axonal stability: signal strength and signal duration. Using mushroom body (MB) neurons in the *Drosophila* brain as a model, the data acquired shows that complete absence of the *Drosophila* JNK (Basket), results in a failure of MB axons to stabilise and subsequent neurodegeneration in the later stages of development. Surprisingly loss of one of the upstream JNK kinases (JNKKs) Hemipterous or Mkk4, resulted in a contrasting axon overextension phenotype, whereas concomitant loss of both JNKKs phenocopied the neurodegeneration observed in *Bsk* null MB neurons. I resolved this conundrum by demonstrating that it is the partial inactivation of *Bsk* signals that results in axon overextension. This suggests that *Bsk* signals safeguard against neurodegeneration at lower thresholds and prevent axon overextension at higher levels.

I also present evidence demonstrating that sustained Bsk signals are essential throughout development of MB neurons to maintain proper axonal morphogenesis but are dispensable at adulthood. This suggests a change in requirements for JNK signalling between the developing and adult brain. Finally I hypothesise that the AP-1 transcription factor complex regulates axon stability downstream of *Bsk*. Weak AP-1 signals are able to protect against neurodegeneration, while stronger AP-1 signals prevent axon overextension. I therefore propose that graded Bsk inputs are translated into AP-1 transcriptional outputs consisting of Fos and Jun proteins.

CHAPTER 5: Bsk threshold activity levels and sustained Bsk signalling throughout development regulate axon stability

CHAPTER 6: A graded AP-1 response regulates axon stability

CHAPTER 7: Discussion

LIST OF FIGURES AND TABLES

CHAPTER 1: Introduction

1.1 Introduction

The establishment of functional neural circuits in the developing brain is dependent upon the ability of individual neurons to accurately navigate their axonal and dendrite projections to the appropriate target. To accomplish this developing neurons rely on growth cones located at the navigating tips of axons for proper cell motility. The trajectories of individual axons are defined by the response of the growth cone to attractive or repulsive extracellular cues. Each extending neuronal growth cone is required to make a series of guidance decisions, in order to reach the correct destination, which may be some considerable distance away. Growth cone motility and guidance, which is responsible for numerous changes in the directionality of axons such as turning, retraction, branching and advancement is mediated by the rearrangement of the dynamic actin and microtubule cytoskeleton. The axonal growth cone is localised towards the leading edge of a developing neuron and consists of both filopodia and lamellipodia (Dent and Gertler, 2003, Kalil and Dent, 2005), dynamic structures of filamentous actin (Bray and Chapman, 1985; Goldberg and Burmeister, 1986) which are strategically located to sample the extracellular environment for instructive guidance cues that direct the trajectory of axons. Filopodia are localised in the distal region of the growth cone and are composed of narrow cylindrical spikes capable of extending microns from the periphery of the growth cone, whereas lamellipodia are flattened, veil-like extensions at the periphery of the growth cone.

Microtubule dynamics have also been implicated as integral in the directional guidance of nerve growth cones (Gordon-Weeks, 2004). Although acetylated, stable

microtubules are confined to the central region of the growth cone, a population of dynamic microtubules is able to extend into the periphery of the growth cone to interact with actin filament bundles in the filopodia and actin filaments in lamellipodia, this flexible property of microtubules, to continuously expand and retract is termed 'dynamic instability'. Studies carried out in Aplysia neurons; divide the growth cone in to three structural domains, the peripheral domain consisting of actin filaments, the microtubule rich central domain and the transitional zone where there is an association of actin filaments and dynamic microtubules (Bridgman and Dailey, 1989; Forscher and Smith, 1988; Smith, 1988). The fast growing (plus) ends of microtubules are directed towards the peripheral region of the growth cone and the minus ends towards the central domain of the growth cone. Microtubule dynamics are regulated by microtubule associated proteins (MAPs) and plus end tracking proteins (+TIPS), which are highly conserved (Howard and Hyman 2003; Gundersen et al, 2004; Akhmanova and Hoogenraad, 2005). The plus ends of microtubules can be stabilised by specific associations with TIPS. These interactions are able to regulate the frequency at which microtubules shorten (catastrophe) or re-expand (rescue). The location of actin filaments and microtubules in the neuronal growth cone is displayed in Figure 1.1. A model demonstrating how the actin and microtubule cytoskeleton of the nerve growth cone reorganises itself in response to attractive and repellent cues is shown in Figure 1.2.

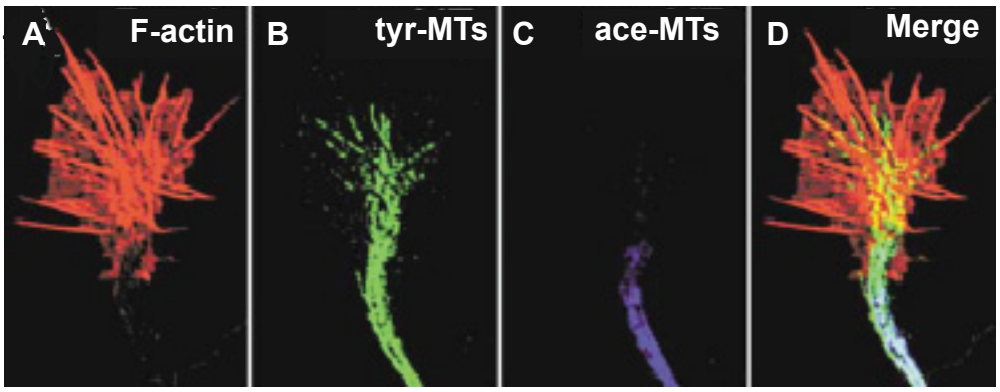

Figure 1.1 The Neuronal Growth Cone

Image of a rapidly extending hippocampal nerve growth cone that has been fixed and labelled for **(A)** F-actin (with phaillodin – red), **(B)** tyrosinated microtubules (tyr-MTs – Green), and **(C)** acetylated microtubules (ace-MTs – blue), with specific antibodies. **(D)** The prominent F-actin bundles are present in the (P) region and the tyr-MTs extend into this actin rich P-domain along the F-actin bundles. In contrast ace-MTs are confined to the central region and are unable to co-localise with F-actin. Adapted from: (Dent and Gertler, 2003).

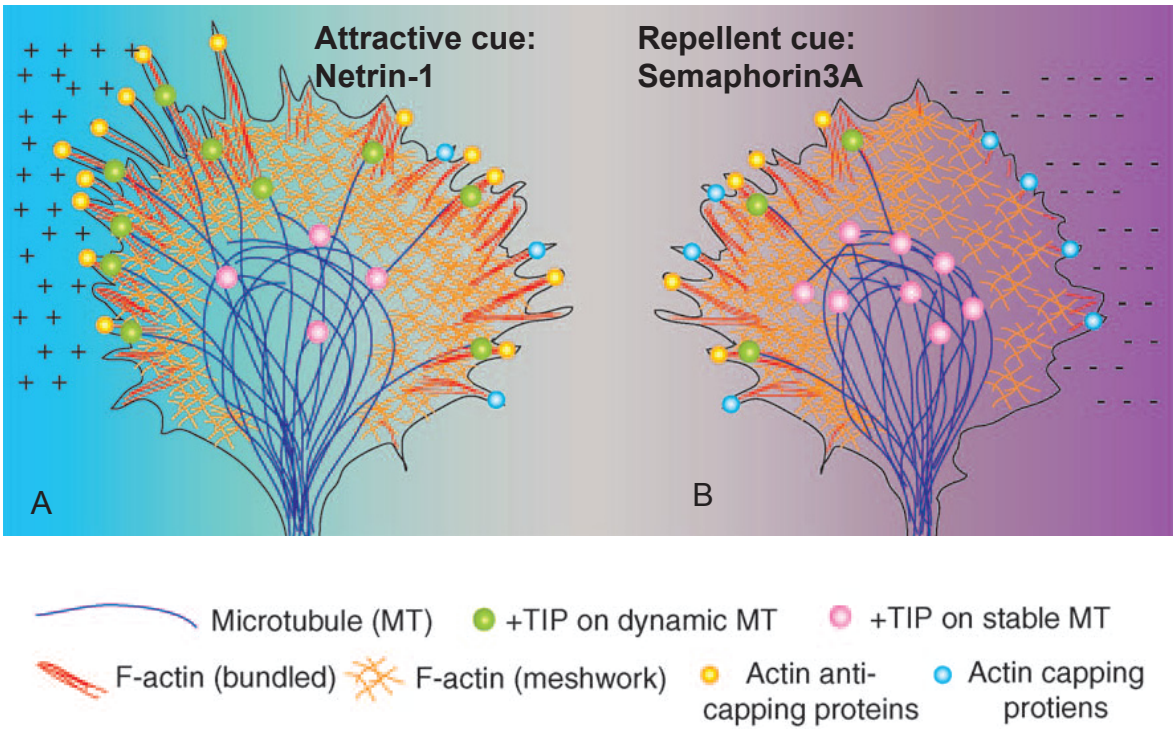

Figure 1.2 Model demonstrating the reorganisation of the neuronal growth cone cytoskeleton in response to attractive and repellent cues.

The region of the growth cone facing towards the guidance cues is the stimulated region. The growth cone consists of a dense area of stable microtubules in the centre, a network of actin filaments in the lamellipodium, actin filament bundles that enter into the filopodia and a population of dynamic microtubules that extends into the periphery of the growth cone, interacting with actin filaments. **(A)** In response to an attractive cue such as netrin-1, the number of filopodia increase and actin filament elongation occurs, due to the action of anticapping proteins such as Ena/VASP, which have been shown to antagonise capping proteins that normally terminate elongation of actin filaments (Lebrand et al, 2004). In the growth cone periphery a population of dynamic microtubules, along with associated +TIP proteins such as APC (adenomatous polyposis coli) are able to interact with actin filaments in the filopodia and lamellipodia, facilitating movement of the growth cone towards the attractive cue (Zho et al, 2004). **(B)** Conversely repellent cues such as semaphorin3A causes a disruption of the actin filament meshwork, and the subsequent loss of dynamic microtubules, which culminates in growth cone collapse and repulsive turning. It has been demonstrated that +TIP proteins such as CLASP, unlike APC, (which stabilises microtubules) induce microtubule looping culminating in growth cone pausing and/or repulsion (Lee et al, 2004). Diagram adapted from: (Kalil and Dent, 2005).

1.2 Signalling at the Neuronal Growth Cone

Directed movement of the growth cone is mediated by response of the growth cone to the concerted action of attractive or repulsive cues, which operate in either a contact-dependent fashion or at a distance via secreted molecules (Figure 1.3). The growth cone receives a vast array of these cues during development and detects a particular selection of these cues through receptors at its surface, to elicit the appropriate morphogenetic response and guide axons to their specific targets. These instructive extracellular signals can be relayed to diverse downstream signaling pathways which can either directly interact with the cytoskeleton or initiate translation and synthesis of the relevant cytoskeletal proteins (Figure 1.4). The subsequent remodeling of the cytoskeleton then alters the trajectory of the growth cone's leading edge. In recent years, rapid progress has been made in identifying molecules that function as either attractive or repulsive cues (for reviews see Huber et al, 2003; Wen and Zheng, 2006). The well documented guidance molecules belong to families of signaling molecules such as netrin, slit, sempahorin and ephrin. These guidance molecules have been shown to be evolutionarily conserved both structurally and functionally. Many are also bifunctional, capable of attracting some axons, whilst repelling others, depending on the neuronal subtype and the nature of the extracellular milieu.

1.3 How is cytoskeletal remodeling of the growth cone regulated by axon guidance cues?

The directed motility of the nerve growth cone is a highly specific process. This specificity is determined by the differential expression of specific membrane receptors

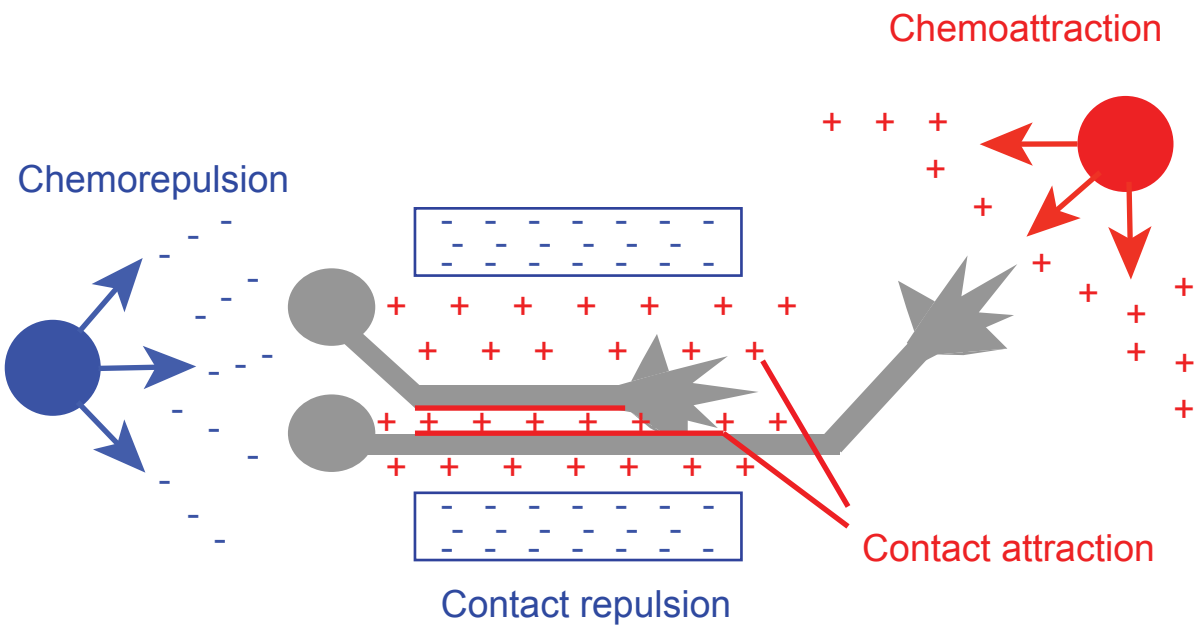

Figure 1.3 Schematic diagram illustrating the effects of guidance cues.
The correct navigation of the nerve growth cone towards its correct target is directed by four classes of guidance forces: long range chemoattraction and chemorepulsion and contact mediated attraction and repulsion. In the above example growth cones are avoiding inhibitory guidance cues from a chemorepulsive source, are directed into a channel through contact mediated attraction and repulsion and forced towards a chemoattractive source. Selective fasciculation is also occurring, where the 'follower' neuron is using contact mediated attraction to follow the projection of the pre-existing 'pioneer' axon. (Adapted from Tessier-Lavigne and Goodman, 1996).

for guidance molecules. In an archetypal scenario signals received by the neuron in the form of guidance cues are transduced by cytoplasmic signaling pathways and converege onto regulatory mechanisms that can elicit changes in cytoskeletal dynamics, enabling the axon to reach its required destination. Adaptors are able to specifically interact with the cytoplasmic domain of the receptors and form a link between diverse membrane receptors and common downstream signaling pathways. For instance neurotrophin stimulated axon outgrowth requires the activation of transcription factors and continuous gene expression and protein synthesis, to supply the necessary components for axon growth (Markus et al, 2002). This is achieved by nerve growth factor (NGF), a neurotrophin, binding to its specific receptor tyrosine kinases (TRKs) and activating both the MAPK and PI3K pathways in neurons (Segal, 2003), which in turn upregulate the expression of the desired genes, required for *de novo* axon growth.

In addition to gene expression, PI3 kinase has also been implicated as a central signal transducer in neurotrophin-mediated axon morphogenesis including elongation and guidance. *In vitro* studies have confirmed the mechanism by which local NGF signaling mediates assembly of the axonal cytoskeleton. In the growth cone of mammalian DRG neurons PI3K is activated at the leading edge in response to NGF stimulation. Spatial activation of PI3K at the axon tip induces the phosphorylation and local inactivation of GSK-3β through Integrin-linked kinase (ILK). ILK acts as receptor kinase regulating integrin-mediated signal transduction, through its interaction with the cytoplasmic domain of β1 integrin. Inactivation of GSK-3β, disassociates the GSK-3β/APC complex and allows the dephosphorylated APC protein to bind to the microtubule plus ends and therefore promote microtubule assembly. It is thought that

APC may play an integral role in mediating microtubule-actin interactions in neurons, which has been suggested as a means of regulating microtubule stability in growth cones (Zhou et al, 2004; Zhou and Cohan, 2004). Furthermore the withdrawal of NGF or inhibition of PI3K culminated in decreased levels of β-catenin protein in DRG axons. β-catenin binds directly to the cadherins and links the cadherins to the actin cytoskeleton. GSK-3β when activated, in resting cells, is able to phosphorylate β-catenin, (when bound to axin). This subsequently induces a signal for the rapid ubiquitin-dependent degradation of beta-catenin by proteosomes. Inhibition of GSK-3β by NGF can promote APC microtubule interactions and simultaneously stabilize β-catenin. Therefore coordinated microtubule assembly regulated by APC and cell adhesion mediated by β-catenin is essential in regulating axon morphology.

Different extracellular cues can often result in distinct axonal processes such as branching or elongation, depending on the location of the extracellular cue and its downstream signaling molecules. For instance NGF activates the GSK-3β/APC pathway at the distal axon, thereby promoting elongation, whereas Wnt signaling activates this pathway more proximally along the axon and induces branching. This is consistent with a recent study in which Wnt signaling has been demonstrated to act as an attractive guidance cue when it is presented as a distal-proximal gradient (Lyuksyutova et al, 2003). In addition to regulating axon growth it has also been demonstrated that GSK-3β is implicated in axon growth inhibition or growth cone collapse (Eickholt et al, 2002). Unlike NGF stimulation, which inactivates GSK-3β, Semaphorin 3A (Sem3A) signaling at the axon growth cone of DRG explant cultures induced GSK-3 activity at the leading edge of the growth cone. Sem3A an inhibitory guidance cue, by inducing GSK-

3β activity, may potentially phosphorylate APC which would in turn inhibit microtubule stabilization thereby suppressing axon elongation (Zumbrunn et al, 2001). Overall these studies suggests that the highly localized concentration of GSK-3β at the growth cone serves as a central switch for the behavior of the growth cone in response to semaphorin, neurotrophin and Wnt guidance cues. A schematic diagram illustrating the signaling pathways by which guidance cues mediate axon growth via the regulation of GSK3 activity is shown in Figure 1.4.

1.4 The Rho family of GTPases provides critical links between guidance signals and the growth cone cytoskeleton.

One important class of molecules that regulate the cytoskeleton are the Rho GTPases. Rho GTPases are small G proteins, which are active when bound to guanine triphosphate (GTP) and in this state are able to interact with effector molecules that regulate the cytoskeleton. GTPases are inactivated when bound GTP is hydrolysed to GDP, this disrupts binding of GTPases to downstream effector molecules. The activity of Rho GTPases is regulated by the opposing actions of guanine nucleotide exchange factors (GEFs) and GTPase activating proteins (GAPs). Rho GTPase signalling is switched 'on' by GEFs and swiched 'off' by GAPs facilitating the hydrolysis of GTP to GDP. Axon guidance receptors can be directly or indirectly coupled to GEFs and GAPs, conferring these receptors direct control over Rho GTPases. It is thought that the large number of GEFs and GAPs contributes to a huge diversity of downstream signals which can be activated by various guidance cues, since Rho GAPs and GEFs can couple to different

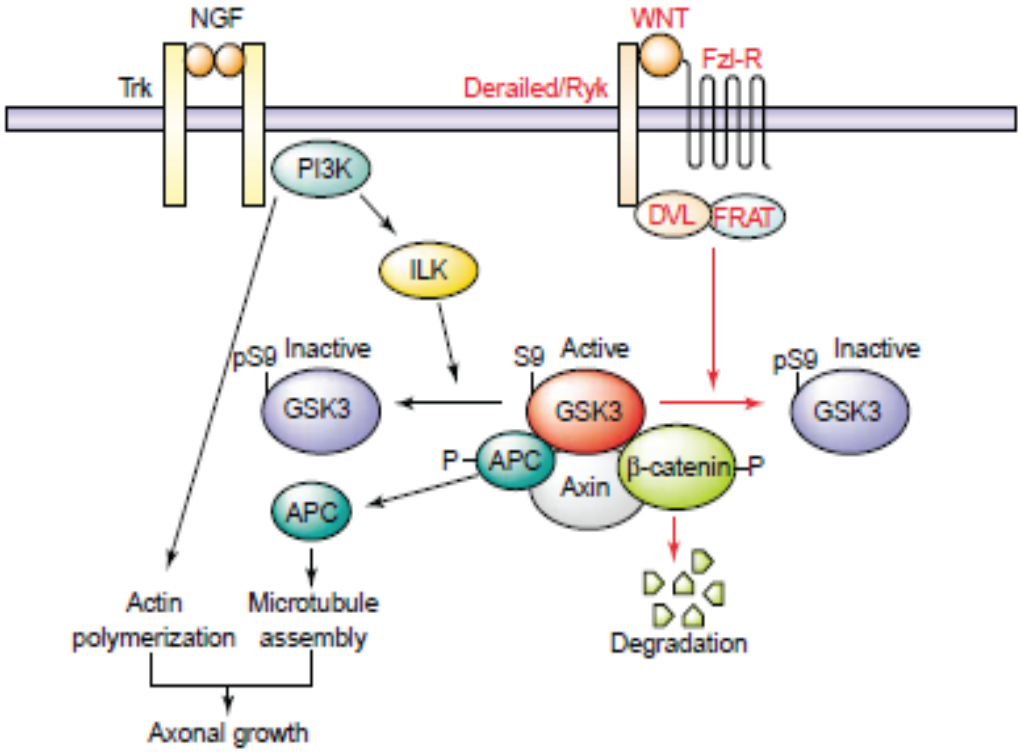

Figure 1.4. GSK-3β is a central modulator for the behaviour of growth cones in response to semaphorins and neurotrophins.

PI3K is activated at the distal tip of the axon in response to the binding of NGF a neurotrophin to Trk receptors, this induces the activation of ILK, which phosphorylates GSK-3β at serine 9 and inactivates it in the growth cone. Consequentially APC and β–catenin are no longer phosphorylated and are freely available to modify cytoskeletal dynamics and promote axonal growth. GSK-3β is also inactivated through the activation of the Fzl-R and Derailed/Ryk receptors by the Wnt family of ligands. (Adapted from Arévalo and Chao, 2005).

axon growth pathways (Luo, 2000). The schematic in Figure 1.5 illustrates the cycle by which the Rho GTPase activity is regulated.

The Rho GTPases have been identified as key molecules in transducing extracellular signals to the actin cytoskeleton (Tapon and Hall, 1997; Van Aelst and D'Souza-Schorey, 1997; Hall, 1998). Extensive functional analysis identified Rho GTPases as regulators of the actin cytoskeleton in mammalian fibroblast cells (Ridley and Hall, 1992). Microinjection of a constitutively activated form of Rac1, Cdc42 and RhoA in fibroblast cells induced the formation of lamellipodia, filopodia and stress fibers respectively. The location of lamellipodia, filopodia and stress fibers in both fibroblasts and growth cones is illustrated in Figure 1.6. In neuronal growth cones Rac1 and Cdc42 have also been found to regulate both movement of filopodia and lamellipodia, which are needed in axon guidance and extension (Kuhn et al, 1998; Brown et al, 2000). In addition studies in Drosopholia post-mitotic neurons show that activation or inactivation of Rac1 and Cdc42 results in axon growth defects (Luo et al, 1994). Conversely in various types of neurons, Rho-A activation increases myosin-II activity and promotes growth cone collapse and axon retraction (Katoh et al, 1998; Wahl et al, 2000; Jurney et al, 2002).

The widely accepted view is that the attractive extracellular cues activate Rac or Cdc42 to promote growth cone advance whereas repulsive cues activate RhoA to induce growth cone retraction (Dickson, 2001; Matsuura et al, 2004). However conflicting data exists partly due to the fact that the functional consequences of these small Rho GTPases can very depending on the type of neurons and the type of substrate on which neurons are cultured (Gallo and Letourneau, 1998; Kuhn et al, 2000). By generating asymmetries in the activities of the Rho GTPases, guidance cues could potentially instruct the growth

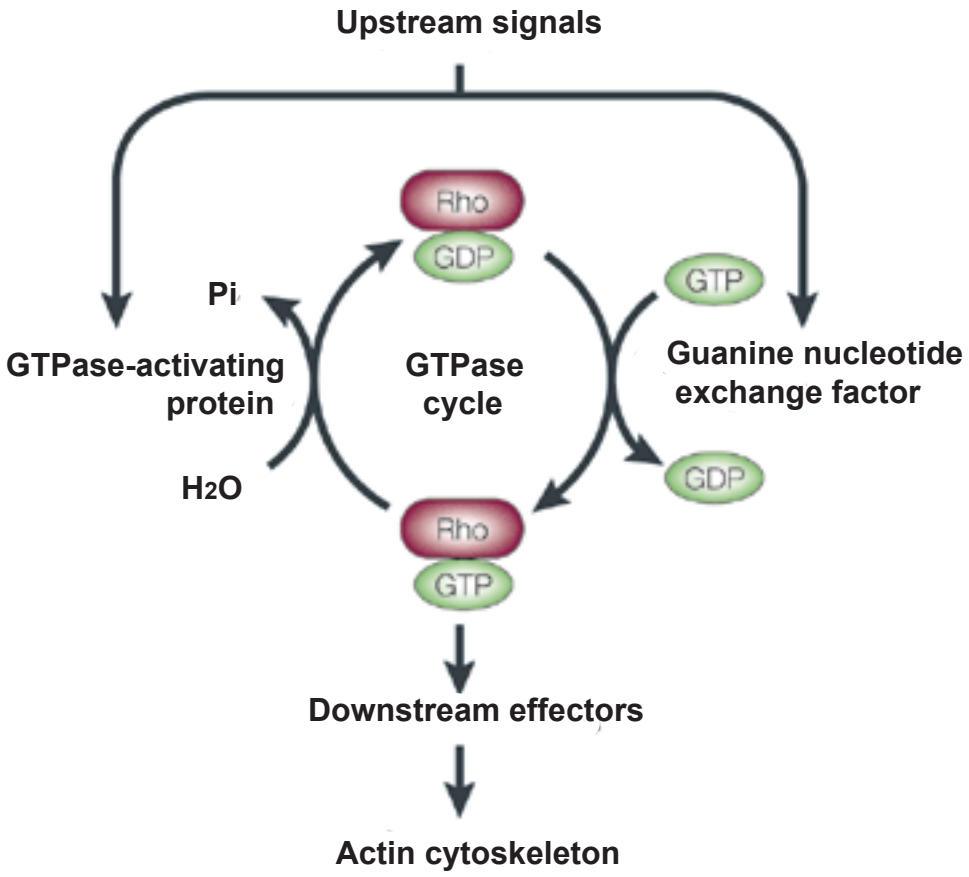

Figure 1.5. Schematic diagram of the cycle illustrating how Rho GTPase activity is regulated.

Upstream signalling molecules regulate the activities of guanine nucleotide exchange factors or GTPase activating proteins, thereby transducing signals to the Rho GTPases and thus enabling the Rho GTPases to be switched on or off. Rho GTPases are able to activate their effectors and transduce the relevant downstream signals, when in their active GTP-bound conformation (Adapted from: Luo, 2000).

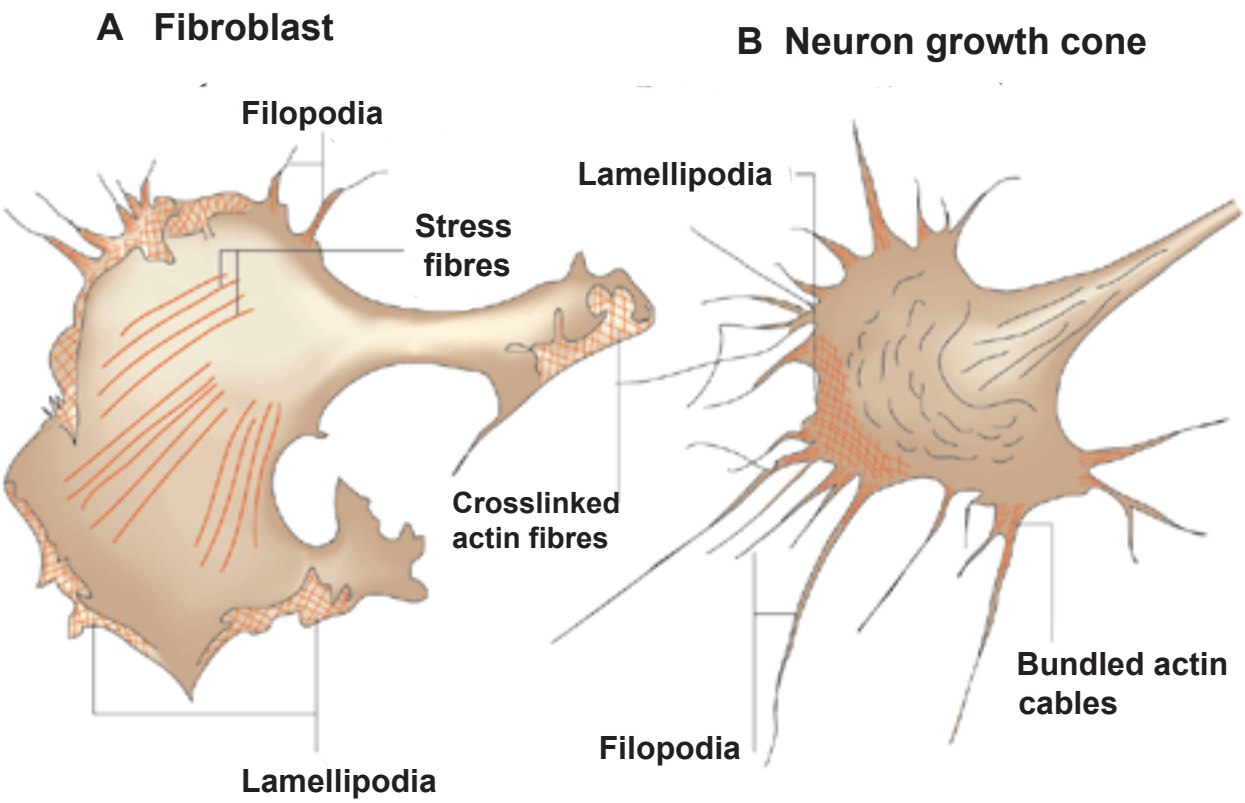

Figure 1.6. The location of filopodia, lamellipodia and stress fibres in migrating fibroblasts and the growth cone.

Rho GTPase signalling co-ordinates cytoskeletal remodelling of prominent F-actin based structures including filopodia, lamellipodia and stress fibres in both **(A)** migrating fibroblasts and **(B)** the neuronal growth cone in order to induce the required morphological changes in these structures (Adapted from Luo, 2000).

cone to turn (Figure 1.7A). Alternatively the Rho GTPases might act as permissive factors for guidance cues providing the dynamic actin structures, such as lamellipodia and filopodia required to detect and respond to extracellular guidance cues. In this scenario growth cone motility would be mediated by signals that regulate the cytoskeleton independently of the Rho GTPases (Figure 1.7B). However the strongest evidence to date testifies that extracellular guidance cues can directly modulate the activities of the Rho GTPases as predicted by the instructive model (Shekerabi and Kennedy; Li et al, 2002; Gitai et al, 2003; Wong et al, 2001).

1.5 Rho GTPase Signalling in Neuronal Morphogenesis *in vivo*.

How are cytoskeletal dynamics within the growth cone regulated by axon guidance cues? It has been demonstrated that particular Rho GTPases (RhoA, Rac and Cdc42) play a critical role in receiving signalling inputs from the receptors of guidance cues belonging to the netrin, slit, semaphorin and ephrin families (Luo, 2000; Huber et al, 2003; Govek et al, 2005), and in turn activating the relevant downstream pathways to regulate cytoskeletal remodelling in the nerve growth cone. For instance netrin-1 can activate Rac1 and Cdc42, facilitating neurite outgrowth (Shekerabi and Kennedy, 2002; Li et al, 2002, Gitai et al, 2003). In contrast the Slit ligand, once bound to the Robo receptor can recruit slit-robo (sr) GAPs to inactivate Cdc42, which induces chemorepulsion of various neuronal migratory cells in mice. This slit-mediated repulsion can be blocked with a dominant negative srGAP1 (Wong et al, 2001).

In Drosophila it has been demonstrated that axon branching, turning and outgrowth are distinct processes which can be modified by differential activation of Rac

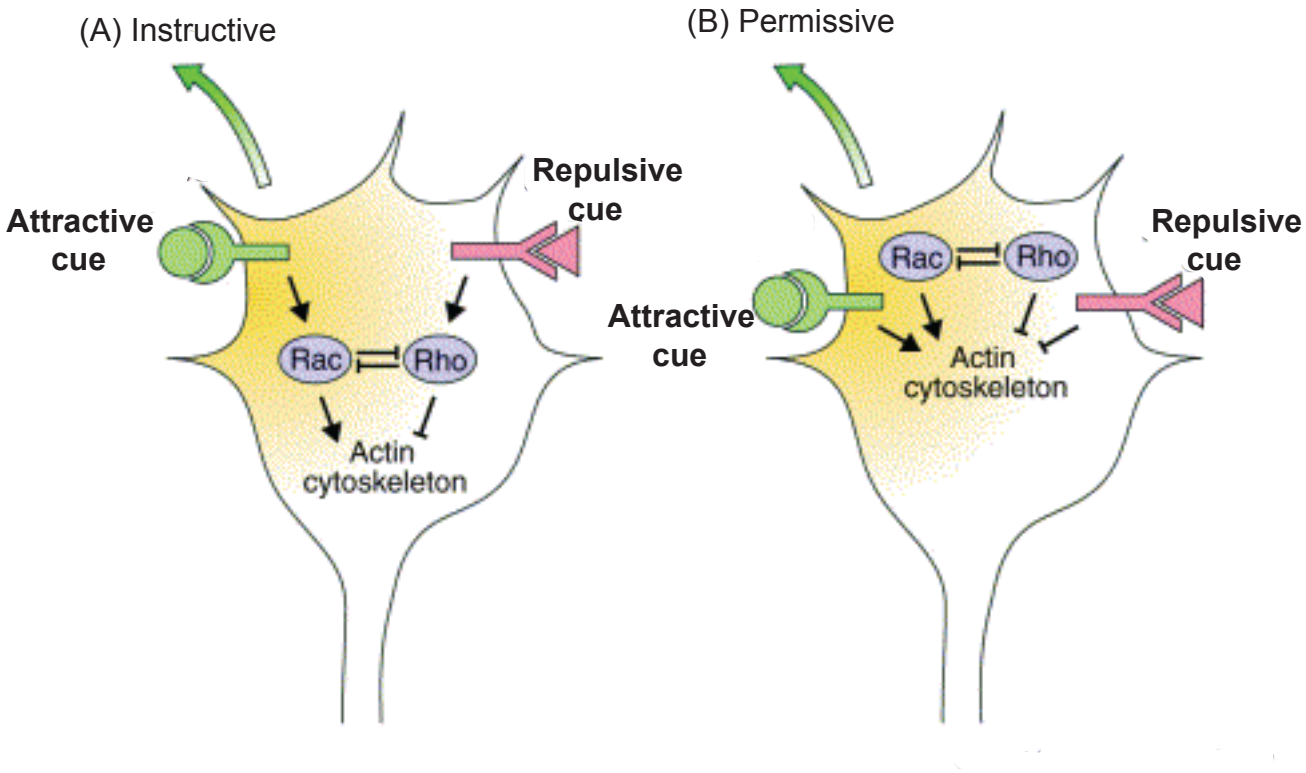

Figure 1.7 Models for the functions of Rho GTPases in Growth cone motility **(A)** In the instructive model extracellular guidance cues regulate the activity of the Rho GTPases. It is widely thought that attractive cues activate Rac or Cdc42, whereas repulsive cues activate Rho. A bias towards Rac signalling causes the growth cone to be directed towards attractive cues. **(B)** In the permissive model the Rho GTPases regulate the growth cone cytoskeleton, but do not act as signal transducers for directional cues. Adapted from: (Dickson, 2001).

signalling pathways. Analysis of loss-of-function phenotypes of three Rac GTPases in Drosophila mushroom body neurons, showed that the progressive loss of Rac-1, Rac2 and Mtl, leads to defects in axon branching, then guidance and finally growth (Ng et al, 2002, Hakeda-Suzuki et al, 2002). Studies in C. elegans show that inactivation of two or more Rac-like genes also perturbs axon outgrowth and guidance (Lundquist et al, 2001). Rho GTPases activate diverse downstream pathways to regulate distinct events of the cytoskeleton such as actin polymerisation, depolymerisation, cross-linking, anchoring and myosin-motor activities (Pollard et al, 2000; Etienne-Manneville and Hall, 2002). However how Rho GTPases are linked to the actin cytoskeletal machinery during axon growth remains unclear?

It has been demonstrated that Rho GTPases act by regulating an actin depolymerisation factor, Cofilin through LIM kinase (LIMK) (Arber et al, 1998; Yang et al, 1998; Maekawa et al, 1999). In vivo it has been shown that Rho GTPases Rac and Cdc42 or RhoA act via the effector kinases Pak and ROCK respectively to activate LIMK, which inhibits axon growth through phosphorylating Cofilin (Ng and Luo, 2004). The function of cofilin is highly conserved in eukaryotes and is required to promote the rapid turnover of actin filaments and depolymerise actin filaments from their pointed ends (Bamburg, 1999). However genetic analysis has indicated that Rac GTPases do not act solely through the LIMK/cofilin pathway to regulate neuronal morphogenesis and there exists an alternative Pak-independent pathway(s) that promotes axon growth and acts antagonistically to LIMK. This was deduced from the fact that although overexpression of wild type Rac1 strongly enhanced the LIMK axon inhibited (gain-of-function) phenotype, transgenic overexpression of Rac1Y40C (a mutated form of Rac1,

unable to bind to and activate Pak-1) strongly suppressed the LIMK (gain of function) axon inhibited phenotype. (Ng and Luo, 2004).

1.6 Examination of the candidate pathways downstream of the Rho GTPases, which promote axon growth.

Genetic studies suggest that Rac mediated axon growth is promoted via a pathway antagonistic to Pak and LIMK1. The mechanism by which this pathway "X" , promotes axon growth is not known. Since Rac is known to activate various downstream effector pathways (Chen et al, 2005), it is likely that these pathways may promote axon growth. A number of pathways have been tested and thus far, none of these pathways have exhibited any effect in antagonising LIMK as well as promoting axon growth (Ng et al, 2004).

One candidate is the SCAR-Arp2/3 complex, which mediates actin dynamics and has been shown to promote de novo actin polymerisation via interaction with Rac (Eden et al, 2002). WASp/SCAR double mutants were also tested since WASp is an integral component of the Arp2/3 complex and is required for filament extension. Loss-of function of SCAR and WASp, or Arp1 did not result in axon growth defects in either MB single cell or neuroblast clones nor did they antagonise the LIMK phenotype.

The other candidate genes tested include the actin polymerisation stimulators profilin (encoded by *chic*) and Ena, which are known to be essential for axon growth and guidance in Drosophila (Wills et al, 1999) and C elegans (Yu et al, 2002). Although both Ena and profilin are required for axon growth, genetic interaction experiments found no evidence that either gene acts antagonistically to LIMK.

Finally the Formin-class protein Diaphanous (*dia*), which has also been implicated in regulating actin polymerisation downstream of Rho GTPases (Evangelista et al, 1997; Palazzo et al, 2001) was analysed. Dia loss-of-function MB neurons did not exhibit axon growth and guidance defects in both single cell or neuroblast clones and reducing *dia* activity (loss of one copy of dia) suppressed the LIMK gain-of-function axon inhibited phenotype, suggesting that dia acts in a pathway that enhances, but does not antagonise LIMK activity (Ng and Luo, 2004). The Rho GTPase signalling pathways that have been mentioned hitherto, that are known to regulate cytoskeletal dynamics and neuronal morphogenesis are summarized in a schematic diagram (Figure 1.8).

1.7 Rho GTPase signalling through the JNK pathway regulates neuronal morphogenesis.

Substantial evidence demonstrates that the Rho family GTPases act upstream of the JNK signal transduction cascade, therefore JNK may be considered as a potential candidate for regulating axon growth. (Weston and Davis, 2002; Stronach, 2005). Constitutively activated forms of Rac and Cdc42 have been shown to activate the JNK cascade (Coso et al, 1995, Minden et al, 1995). Furthermore the Drosophila JNKKK, slipper is composed of a CDC42/Rac interactive binding domain (CRIB) motif (Burbelo et al, 1995), which is necessary for binding active Rac/Cdc42 and is required in dorsal closure and eye development, Both *slipper* and *misshapen* (a JNKKKK protein) have been shown to genetically interact with and lie downstream of Rac (Su et al, 1998, Stronach and Perrimon, 2002; Gallo and Johnson, 2002). In neurons, Rac signals through JNK to regulate dendritic morphogenesis in hippocampal neurons (Rosso et al, 2005), neurite

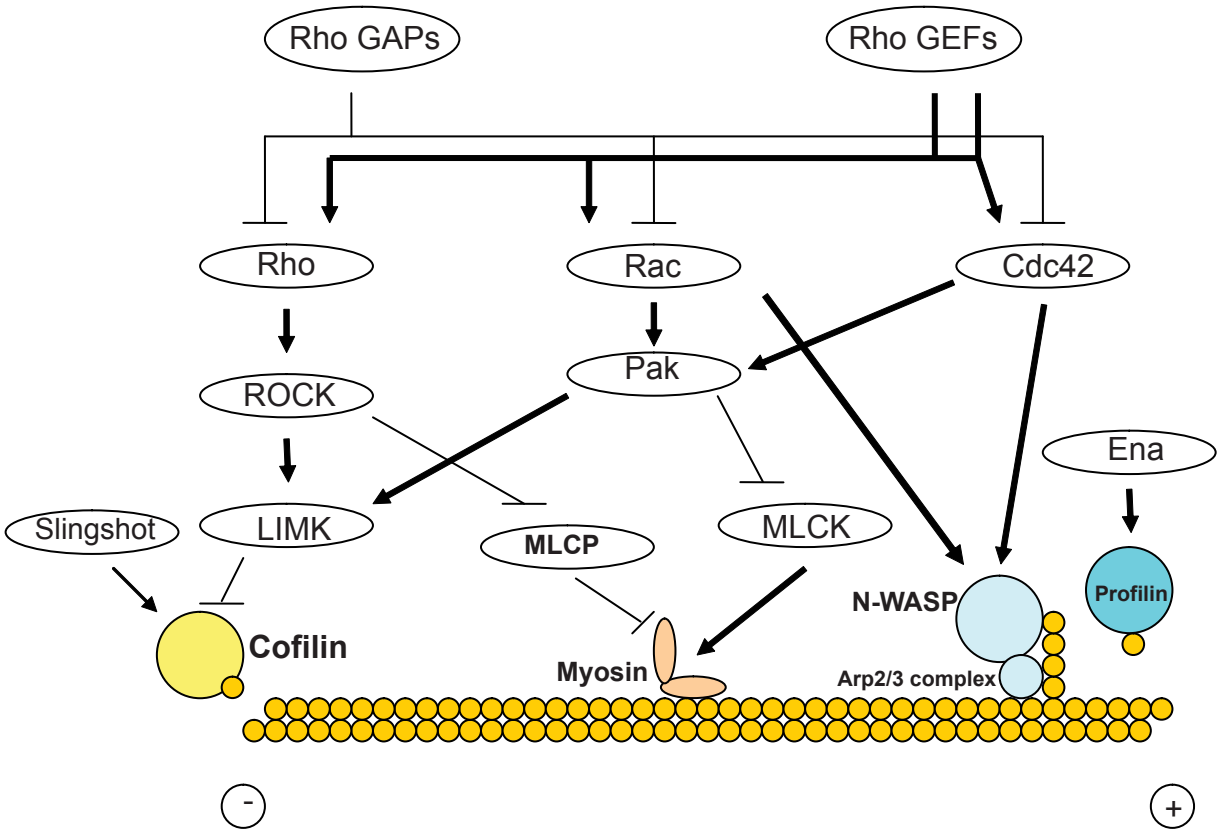

Figure 1.8 Regulation of actin dynamics by the Rho GTPases

Schematic diagram illustrating the various signalling pathways that link Rho GTPases to the actin cytoskeleton. Rac signalling activates proteins of the Wiskott-Aldrich syndrome protein (WASP) family. N-WASP binds directly to the Arp2/3 complex, and co-localises with the Arp2/3 complex at the tip of growth cone filopodia and stimulates its ability to promote the nucleation of new actin filaments and promote elongation of the growth cone. Profilin also promotes actin polymerisation by catalysing the elongation of newly formed actin filaments. Conversely Rho activation increases Myosin II activity via the phosphorylation of myosin II regulatory light chain (MRLC), which subsequently induces growth cone collapse and axon retraction. Myosin light chain kinase (MLCK) phosphorylates MRLC whereas MLC phosphatase (MLCP), dephosphorylates MRLC and inhibits its activity. Finally the Rho GTPases Rac and Cdc42 or RhoA act via the effector kinases Pak and ROCK respectively to activate LIMK, which inhibits axon growth through phosphorylating Cofilin. Cofilin is required to promote the rapid turnover of actin filaments. Adapted from: (Huber et al, 2003).

extension in mouse N1E-115 neuroblastoma cells (Yamauchi et al, 2006) and neurite outgrowth in Neuro2A cells (He et al, 2006). In Drosophila *misshapen* mutants have been implicated in axon guidance in photoreceptor axons (Su et al, 2000). Furthermore the loss of function of *misshapen* (msn^{102}) results in MB axon growth phenotypes similar to those acquired for loss-of-function of Rac (unpublished data).

Thus based on a multitude of previous data from different systems and preliminary data, it may be postulated that Rac signals through the JNK cascade to promote axon growth antagonistically to LIMK. In fact genetic analysis has revealed that the *Drosophila* JNK *Bsk* is able to promote axon growth and suppress the LIMK gain-of function stalled phenotypes, observed in MB neurons (unpublished data).

1.8 Structure and homology of the JNKs

Since *Drosophila* JNK *(D-JNK)* has been found to be a candidate gene for axon growth regulation a detailed analysis of its structure is necessary. The mammalian JNKs are encoded for by three distinct genes (*JNK-1, JNK-2* and *JNK-3*). Additonally alternative splicing generates up to ten different isoforms varying in size from 46kDa to 55kDa (Gupta et al, 1996; Barr and Bogoyevitch, 2001). JNK1 and JNK2 are both expressed in a variety of tissues whereas JNK-3 expression is confined primarily to the brain, heart and testes (Matin et al, 1996; Mohit et al, 1995). *D-JNK* expression is highly dynamic during embryonic development and high levels of *D-JNK* mRNA are detected in groups of cells that undergo morphogenetic movements. During larval stages high levels of JNK are maintained in the CNS and the peripheral nervous system, similarly *JNK-3* also exhibits a specific non-homogenous expression pattern, when it is expressed in subsets of pyramidal

cells in the CNS (Mohit et al, 1995). *D-JNK* (*bsk*), the sole JNK homologue in *Drosophila* (49kDa in size) shares a large degree of homology with its mammalian counterparts. The degree of amino acid homology between the *Drosophila* JNK sequence and its mammalian counterparts is approximately 70% (Riesgo-Escovar et al, 1996). *D-JNK* is composed of all the conserved residues of protein kinases in the kinase domains, which have been classified as kinase subdomains I-XI, originally defined by Hanks and colleagues (Hanks et al, 1988). The JNK Threonine-Proline-Tyrsoine (TPY) motif between kinase subdomains VII and VIII which can be activated by dual phosphorylation via the MAPK kinases MKK4 and MKK7 (Hep in Drosophila), is also 100% conserved between mammalian *JNKs 1-3* and *D-JNK* (Figure 1.9). It has also been found *in vitro* that MKK4 has a preference for phosphorylating the Tyrosine residue and MKK7 the Threonine residue (Lawler et al, 1998), providing the potential for integrating diverse upstream signals. These MAPK kinases are able to catalyse the transfer of a terminal phosphoryl group of ATP to JNK. JNK1 itself is known to phosphorylate the archetypal transcription factor Jun, and the amino acid sequence, which determines the efficiency for D-JNK binding to *c-Jun*, shares 64% homology with *JNK-2*. Phosphorylation is crucial in regulating numerous aspects of cellular function including metabolism, movement, survival and death (Bogoyevitch and Kobe, 2006).

Numerous studies have also underlined the importance of docking interactions for enzymatic specificity and efficient signalling of MAPK pathways (Sharrocks et al, 2000, Tanoue and Nishida, 2003, Enslen and Davis, 2001). Docking motifs are distinct from phosphoacceptor sites and have been demonstrated to be present in the JNK signalling cascade, downstream substrates of JNK, phosphatases and JNK scaffolding proteins, such

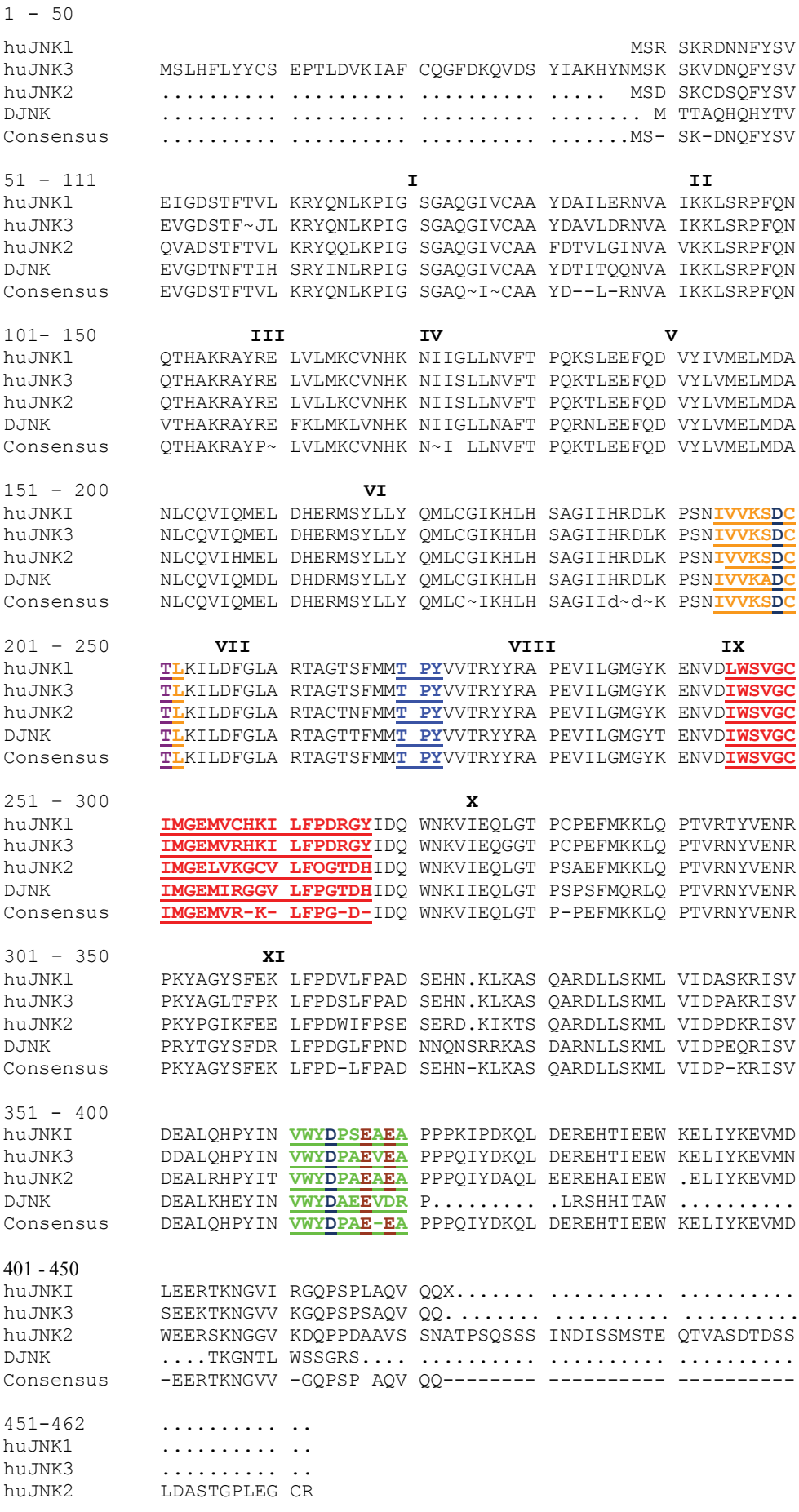
1 - 50
huJNKl MSR SKRDNNFYSV
huJNK3 MSLHFLYYCS EPTLDVKIAF CQGFDKQVDS YIAKHYNMSK SKVDNQFYSV
huJNK2 .... MSD SKCDSQFYSV
DJNK .... M TTAQHQHYTV
Consensus ....MS- SK-DNQFYSV
51 - 111 I II
huJNKl EIGDSTFTVL KRYQNLKPIG SGAQGIVCAA YDAILERNVA IKKLSRPFQN
huJNK3 EVGDSTF~JL KRYQNLKPIG SGAQGIVCAA YDAVLDRNVA IKKLSRPFQN
huJNK2 QVADSTFTVL KRYQQLKPIG SGAQGIVCAA FDTVLGINVA VKKLSRPFQN
DJNK EVGDTNFTIH SRYINLRPIG SGAQGIVCAA YDTITQQNVA IKKLSRPFQN
Consensus EVGDSTFTVL KRYQNLKPIG SGAQ~I~CAA YD--L-RNVA IKKLSRPFQN
101- 150 III IV V
huJNKl QTHAKRAYRE LVLMKCVNHK NIIGLLNVFT PQKSLEEFQD VYIVMELMDA
huJNK3 QTHAKRAYRE LVLMKCVNHK NIISLLNVFT PQKTLEEFQD VYLVMELMDA
huJNK2 QTHAKRAYRE LVLLKCVNHK NIISLLNVFT PQKTLEEFQD VYLVMELMDA
DJNK VTHAKRAYRE FKLMKLVNHK NIIGLLNAFT PQRNLEEFQD VYLVMELMDA
Consensus QTHAKRAYP~ LVLMKCVNHK N~I LLNVFT PQKTLEEFQD VYLVMELMDA
151 - 200 VI
huJNKI NLCQVIQMEL DHERMSYLLY QMLCGIKHLH SAGIIHRDLK PSNIVVKSDC
huJNK3 NLCQVIQMEL DHERMSYLLY QMLCGIKHLH SAGIIHRDLK PSNIVVKSDC
huJNK2 NLCQVIHMEL DHERMSYLLY QMLCGIKHLH SAGIIHRDLK PSNIVVKSDC
DJNK NLCQVIQMDL DHDRMSYLLY QMLCGIKHLH SAGIIHRDLK PSNIVVKADC
Consensus NLCQVIQMEL DHERMSYLLY QMLC~IKHLH SAGIId~d~K PSNIVVKSDC
201 - 250 VII VIII IX
huJNKl TLKILDFGLA RTAGTSFMMT PYVVTRYYRA PEVILGMGYK ENVDLWSVGC
huJNK3 TLKILDFGLA RTAGTSFMMT PYVVTRYYRA PEVILGMGYK ENVDIWSVGC
huJNK2 TLKILDFGLA RTACTNFMMT PYVVTRYYRA PEVILGMGYK ENVDIWSVGC
DJNK TLKILDFGLA RTAGTTFMMT PYVVTRYYRA PEVILGMGYT ENVDIWSVGC
Consensus TLKILDFGLA RTAGTSFMMT PYVVTRYYRA PEVILGMGYK ENVDIWSVGC
251 - 300 X
huJNKl IMGEMVCHKI LFPDRGYIDQ WNKVIEQLGT PCPEFMKKLQ PTVRTYVENR
huJNK3 IMGEMVRHKI LFPDRGYIDQ WNKVIEQGGT PCPEFMKKLQ PTVRNYVENR
huJNK2 IMGELVKGCV LFOGTDHIDQ WNKVIEQLGT PSAEFMKKLQ PTVRNYVENR
DJNK IMGEMIRGGV LFPGTDHIDQ WNKIIEQLGT PSPSFMQRLQ PTVRNYVENR
Consensus IMGEMVR-K- LFPG-D-IDQ WNKVIEQLGT P-PEFMKKLQ PTVRNYVENR
301 - 350 XI
huJNKl PKYAGYSFEK LFPDVLFPAD SEHN.KLKAS QARDLLSKML VIDASKRISV
huJNK3 PKYAGLTFPK LFPDSLFPAD SEHN.KLKAS QARDLLSKML VIDPAKRISV
huJNK2 PKYPGIKFEE LFPDWIFPSE SERD.KIKTS QARDLLSKML VIDPDKRISV
DJNK PRYTGYSFDR LFPDGLFPND NNQNSRRKAS DARNLLSKML VIDPEQRISV
Consensus PKYAGYSFEK LFPD-LFPAD SEHN-KLKAS QARDLLSKML VIDP-KRISV
351 - 400
huJNKI DEALQHPYIN VWYDPSEAEA PPPKIPDKQL DEREHTIEEW KELIYKEVMD
huJNK3 DDALQHPYIN VWYDPAEVEA PPPQIYDKQL DEREHTIEEW KELIYKEVMN
huJNK2 DEALRHPYIT VWYDPAEAEA PPPQIYDAQL EEREHAIEEW .ELIYKEVMD
DJNK DEALKHEYIN VWYDAEEVDR P..... .LRSHHITAW .....
Consensus DEALQHPYIN VWYDPAE-EA PPPQIYDKQL DEREHTIEEW KELIYKEVMD
401 - 450
huJNKI LEERTKNGVI RGQPSPLAQV QQX..... ....
huJNK3 SEEKTKNGVV KGQPSPSAQV QQ..... ....
huJNK2 WEERSKNGGV KDQPPDAAVS SNATPSQSSS INDISSMSTE QTVASDTDSS
DJNK ....TKGNTL WSSGRS.... ....
Consensus -EERTKNGVV -GQPSP AQV QQ-------- ---------- ----------
451-462 ....
huJNK1 ....
huJNK3 ....
huJNK2 LDASTGPLEG CR

Figure 1.9

Figure 1.9. Sequence alignment of *D-JNK* with its mammalian homologues
The conserved TPY phosphorylation motif is in bold blue type and underlined. The specificity determining region, which binds to the transcription factor *c-Jun* is underlined in bold red type for the four sequences. The dark yellow bold underlined type represents the conserved sequences encompassing the ED domain of the JNKs. The residues within the ED domain that are necessary for docking of MKK4 to JNK are shown in Dark Blue bold type (Asp ^{162} for *JNK-2* and Asp^{160} for *D-JNK*) and in Purple bold type (Thr^{164} for *JNK-2*, Thr^{162} for *D-JNK*). The light green bold underlined type represents the conserved sequences encompassing the CD domain of the JNKs. The residues within the CD domain that are needed for the docking of JIP-1 or MKK4 to JNK-2 are shown in Brown bold type (Glu^{329} and Glu ^{331} for JNK-2; Glu^{328} and Asp^{162} for *D-JNK*). Additionally residues within the CD domain that contribute to the docking of MKK4 to JNK are highlighted in Dark Blue bold type (Glu ^{326} for *JNK-2* and Glu^{325} for *D-JNK*).

as JIP-1 (Mooney and Whitmarsh, 2004). In JNK-2 itself it has been revealed that there are distinct determinants which are responsible for binding to upstream MAPKKs and JIP-1 (Figure 1.10). Furthermore amino acid alignment of the ED and CD (common docking) domains of human JNK isoforms and those from lower eukaryotes including Drosophila (*D-JNK*) reveal that these specific residues required for the docking of JNK to *JIP-1*, *MKK4* and c-Jun are highly conserved (Figure 1.9), suggesting that they serve to carry out the same function. This is likely to involve temporal and spatial regulation of JNK, through sequential association and disassociation of JNK to and from MAPK scaffolding complexes, in order to elicit varying biological responses.

1.9 Organisation of the JNK signalling pathway

The JNK signalling pathway, is highly conserved in eukaryotes and consists of a terminal JNK that is activated through a sequential MAPK phosphorylation cascade (Figure 1.11), composed of several diverse upstream kinases that include JNKKs, JNKKKs and JNKKKK (Gallo and Johnson, 2002; Stronach, 2005).

The JNK signalling pathway is spatially organised to elicit specific cellular processes. For instance upon bacterial infection, the Immune Deficiency (IMD) signalling pathway activates Hep (Davis et al, 2008). Activated JNKK, Hemipterous (HEP) binds to the scaffolding protein, Connector of kinase to AP-1 (CKA), bringing it into close proximity to the JNK protein, Basket (BSK) which it then phosphorylates. CKA is also phosphorylated which results in the dissociation of BSK which then translocates to the nucleus. Here it binds with a nuclear-residing CKA molecule which additionally recruits the AP-1 transcription factor consisting of the c-Jun orthologue, JRA, and the c-Fos

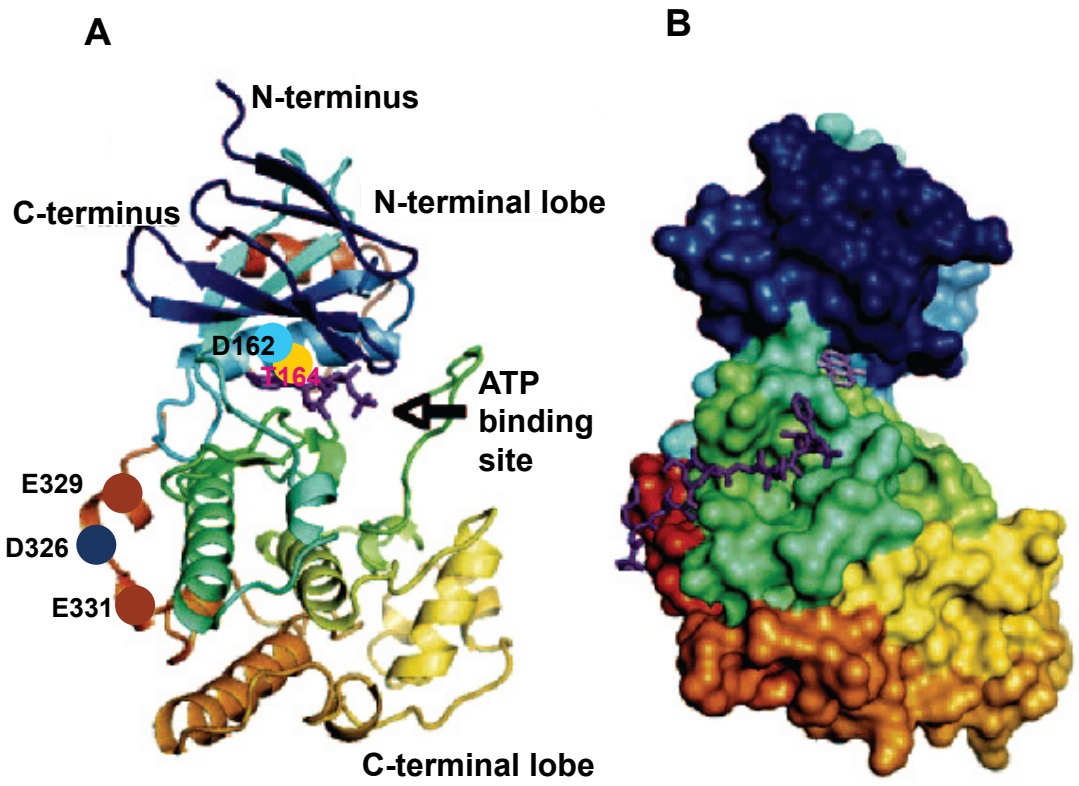

Figure 1.10. Structure of the JNKs.

(A) Crystal structure of *JNK-3*. The structure of JNK-3 is similar to that of other eukaryotic MAPKs. *JNK-3* exhibits typical eukaryotic kinase folds, with an N-terminal region rich in β-structure: (residues 45-159 and 370-400 in *JNK-3*) and a C-terminal domain rich in α-helices (residues 150-374 in *JNK-3*). The ATP binding site is located in close proximity to the domain interfaces in the C-terminal region. This region is typical of MAPKs and it is though that peptide substrates of JNK bind between the two lobes of JNK. This diagrammatic ribbon representation of *JNK-3*, portrays the inactive, non-phosphorylated form of JNK, in this case the catalytic residues are misaligned and obstructed by the 'activation loop', which is located between the two domains. It is assumed that docking of upstream MAPK kinases will induce subtle but important conformational changes, which will facilitate access of ATP into the active site. The positions of equivalent residues to those in *JNK-2* required for the docking interactions of MKK4 (D162, T164) are indicated as are those required for docking of both JIP-1 and MKK4 (E329, E331), each amino acid residue is indicated as a coloured circle. **(B).** Surface representation of the crystal structure of JNK-1 in complex with the peptide corresponding to residues 153-163 of the substrate and scaffolding protein JIP-1 (magenta in stick representation) and the ATP competitive inhibitor SP600125 (dark pink in stick representation). Adapted from: (Bogoyevitch and Kobe, 2006; Mooney and Whitmarsh, 2004).

Components of the *Drosophila* JNK signalling cascade		
Activity	**Drosophila gene**	**Mammalian homolog**
JNKKKK	***msn***	**MINK, NIK, HGK, TNIK**
JNKKK	***Pk92B***	**ASK1**
	Tak1	**TAK**
	Tak12	**TAK**
	Slpr	**MLK**
	CG8789	**DLK, ZPK**
	Mekk1	**MEKK 1-4**
JNKK	***Hep***	**MKK7**
	Mkk4	**MKK4**
JNK	***Bsk***	**JNK 1-3**
Transcription factor	***Jra***	**c-JUN**
	Kay	**c-Fos**

Figure 1.11 Components of the JNK signal transduction pathway

The *Drosophila* gene is indicated in *italics* and its equivalent Mammalian homologue is in CAPITALS (Adapted from Stronach, 2005)

orthologue, Kayak (KAY). BSK may phosphorylate both JRA and KAY which dissociate from CKA and activate transcription of genes involved in the early immune response thought to be involved in wound repair and stress mechanisms. Additionally, the gene responsible for encoding the phosphatase Puckered (PUC) is activated which is responsible for dephosphorylating BSK, an example of a negative regulatory loop (Chen et al, 2002). Figure 1.12 gives an overview as to how CKA regulates the JNK signalling pathway in *Drosophila*.

Scaffold proteins provide a means by which the JNK pathway can achieve signal specificity by bringing together specific and consecutive members of the JNK signaling cascade (Figure 1.13). For instance in mammals, the JNK interacting protein 1 (JIP-1), provides a scaffold for the MLK3/MKK7/JNK module (Yasuda et al, 1999), whereas JSAP1, an alternatively spliced isoform of JIP3, is able to bind MEKK1, MKK4 and JNK3 (Akechi et al, 2001). Additionally it is thought that scaffold proteins provide a mechanism that dictates Rho GTPase-signalling specificity. The physical interaction with scaffold proteins may represent a means by which GEFs can govern the selection of signal outputs upon Rho GTPase activation. In fact it has been found that the Rac GEF Tiam-1 and p115-Rho GEF are able to bind JIP-1 and connector enhancer of *ksr* (CNK1) respectively (Buchsbaum et al, 2002; Marinissen and Gutkind, 2005). This in turn assembles the JNK pathway (Morrison et al, 2003) resulting in enhanced JNK activity in various cellular contexts. Additionally, many JNK scaffold proteins have been found to be strongly expressed in the brain, spinal cord and peripheral neurons, underlining their importance for the regulation of JNK activity in the nervous system (Raivich and Behrens, 2006). Finally the scaffolding proteins, JIP-1, JIP-2 and JSAP1 also regulate

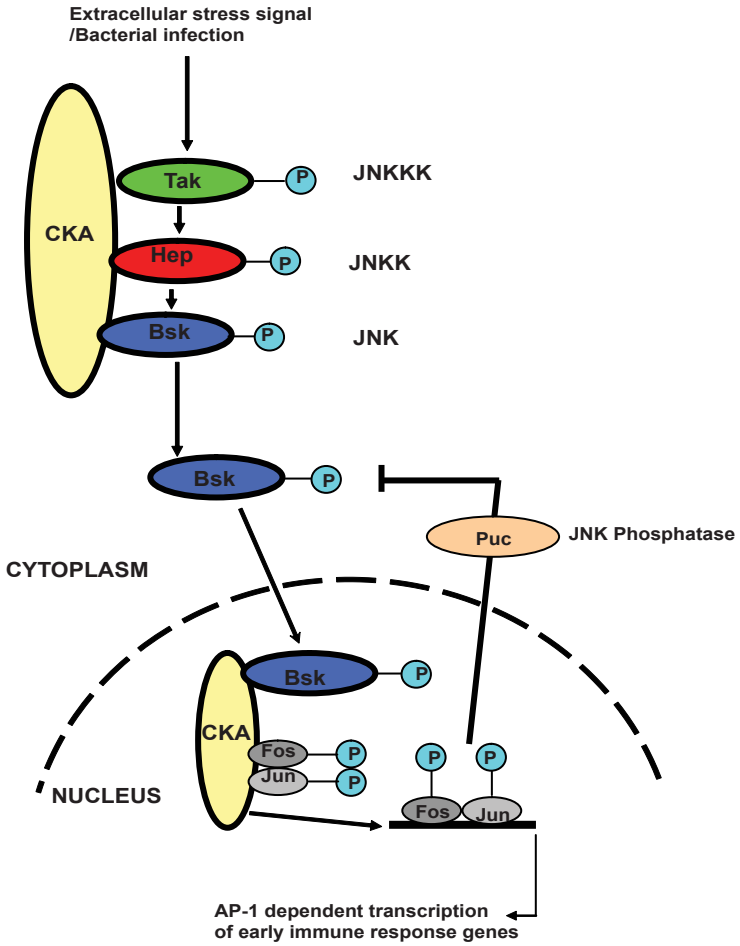

Figure 1.12. Schematic diagram illustrating how CKA regulates the JNK signal transduction pathway in *Drosophila*

Upon Bacterial infection the immune deficiency (IMD) signalling pathway is activated in *Drosophila*. Upstream IMD signals activate the JNKKK Tak1. Tak-1 then phosphorylates its JNKK substrate Hep, enabling it to bind to CKA. Once Hep is coupled to CKA, it is situated in close proximity to its JNK substrate Bsk, which it can then phosphorylate. Activated Bsk then dissociates from the CKA complex and enters the nucleus, where its associates with the nuclear residing CKA molecules. The activated CKA complex then recruits the AP-1 transcription factor consisting of Fos and Jun heterodimers. Bsk is then able to phosphorylate the AP-1 transcription factor complex. AP-1 then dissociates from the CKA complex and activates genes involved in the early immune response. Bsk activity is negatively regulated by the AP-1 dependent transcription of the JNK phosphatase Puckered, which dephosphorylates Bsk. CKA also regulates the JNK signalling pathway in Drosophila, through the mechanism outlined above to co-ordinate epithelial cell sheet movement during the process of dorsal closure (Chen et al, 2002).

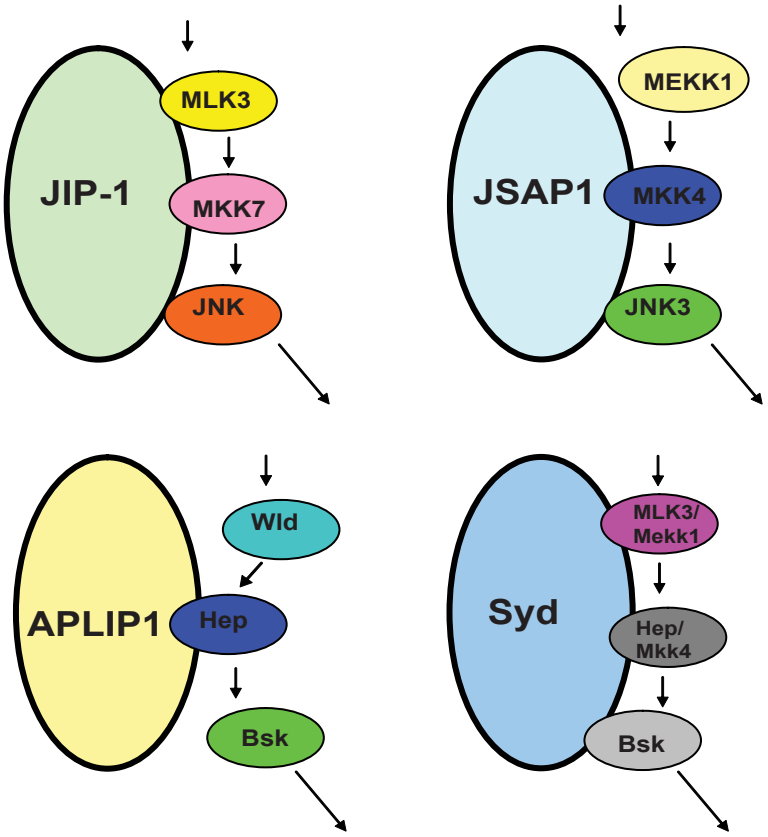

Figure 1.13. JNK scaffolding proteins provide a means by which the JNK signalling cascade can achieve a high level of specificity.

The JNK scaffolding proteins bring together consecutive members of the JNK signalling cascade: JIP-1 serves as a binding partner for MLK3, MKK7 and all three JNK isoforms, JSAP-1 for MEKK1, MKK4 and JNK3. The *Drosophila* homologue of JIP-1, APLIP1 only binds directly to the JNKK *Drosophila* MKK7 (Hep) and the *Drosophila* homologue of JIP-3, Sunday Driver has been demonstrated to bind to the JNKKKs MLK3 and MEKK1, the JNKKs: MKK4 and MKK7 and the sole *Drosophila* JNK: Bsk. It has been proposed that JNK scaffolding proteins transport JNK kinases to specific subcellular locations, this is mediated by microtubule-based transport of JNK-JIP complexes (Bowman et al, 2000; Verhey et al, 2001). Diagram adapted from: (Raivich and Behrens, 2006).

microtubule associated axonal transport between neuronal cell bodies and the axon terminal, by acting as linking molecules for the cargo of the kinesin motors (Verhey et al, 2001) and numerous JNK signaling components (Lindwall and Kanje, 2005).

1.10 Role of the JNK scaffolding proteins in axonal transport

JNKs through their interaction with the JNK scaffold proteins are thought to be associated with axon transport; this may be to ensure that JNK signalling components are transported to the appropriate region of a neuron, to elicit the necessary biological response. Long distance axonal transport of signal transduction components is principally carried out by dyneins and kinesins, two families of microtubule dependent motors. The direction in which any given signal transduction component will travel is regulated by the directionality of microtubule dependent motors and the polarity of microtubules (Blasius et al, 2007; Horiuchi et al, 2007). In the majority of axons the fast growing microtubule plus ends are orientated towards the periphery of the growth cone, where a synapse will eventually occur, (once the axon has stabilised) and minus end microtubules are orientated towards the neuronal cell body. Thus anterograde transport, from the cell body to the growth cone is principally regulated by the kinesins, whereas retrograde transport from the synapse to the cell body, is mainly controlled by the dyneins (Hirokawa and Takemura, 2004).

Kinesins form a large superfamily of genes that are categorised by a discrete domain which binds microtubules and hydrolyses ATP. The kinesin-1 motor is the most extensively studied of the kinesin superfamily and is composed of two heavy chains (KHC) and two light chains (KLC). KHC binds to and moves along microtubules,

whereas KLC binds to specific cargoes, such as signalling modules and scaffolding proteins and assists in keeping the motor inactive. JIPs (JNK interacting are scaffolding molecules) are able to bind to different components of the JNK canonical phosphorylation cascade, such as JNK, MAPKK and MAPKKK (Figure 1.13). It has also been demonstrated that physical interactions between JIP scaffolding molecules and JNK cascade kinases can enhance JNK signalling (Mooney and Whitmarsh, 2004; Whitmarsh, 2006). There are four mammalian JIPs: JIP-1, JIP-2, JIP-3 and JIP-4, which all contain a JNK binding domain, but differ slightly in their structural domains. JIPs 1-3 have been shown to directly interact with Kinesin and provide a link between kinesin and plasma membrane cargo proteins (Verhey et al, 2001). In fact APLIP1 the *Drosophila* homologue of JIP-1, named based on its interaction with Drosophila APP-like protein (APPL), a homologue of the β-amyloid precursor protein is functionally conserved with the mammalian JIP's and shares homologous binding domains with its mammalian counterparts. They also share properties such as interaction with APPs, JNKKs and kinesin (Figure 1.14).

JIP-1 and APLIP1, its Drosophila homologue both function as adaptors linking motor to cargo during axonal transport. KLC is able to bind directly to both JIP-1 and APLIP1 and JIP-1 transport is dependent on kinesin-1 motor activity (Verhey et al, 2001; Horiuchi et al, 2005). Mammalian JIP-1 is able to bind various neuronal cargoes including JNK cascade kinases (DLK, MKK7 and JNK), (Whitmarsh, 2006; Nihalani et al, 2001; Whitmarsh et al, 1998), RhoGEF190 (Meyer et al, 1999) the β amyloid precursor protein (APP) (Matsuda et al, 2001) and apolipoprotein E receptor-2 (ApoER2) (Stockinger et al, 2000). It is probable that some JNK cascade signalling components are

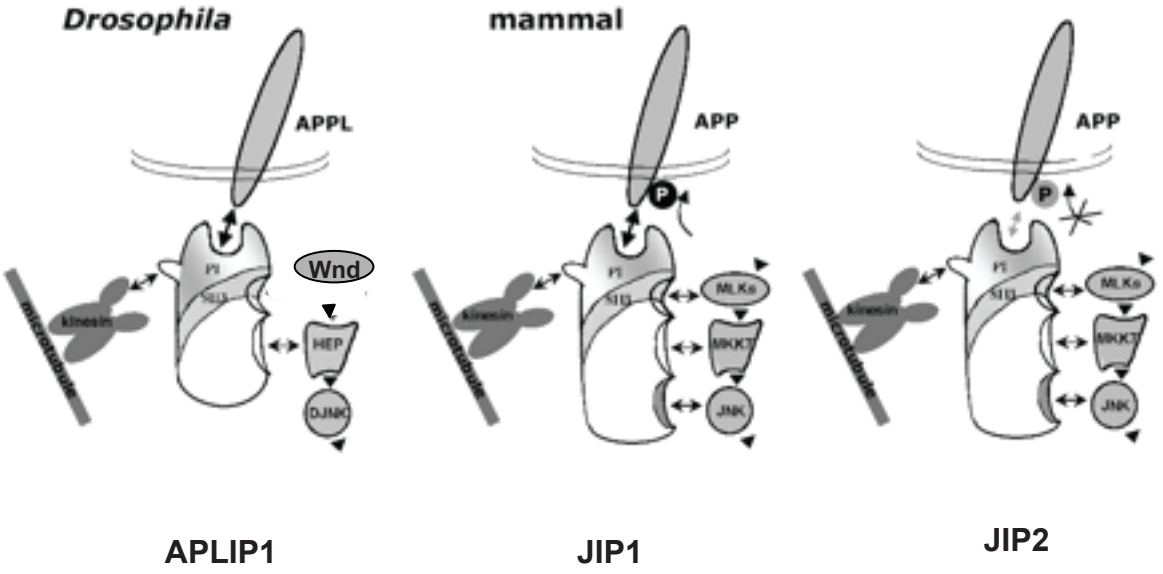

Figure 1.14. Schematic diagram illustrating the protein interactions of JNK scaffold proteins with kinesin, JNK signalling components and APPs.

JIP proteins form a scaffold on which on which cytoplasmic JNK signalling components as well as plasma membrane proteins are assembled. The entire complex is transported down an axonal process by conventional kinesin. The binding of proteins, to their specific protein site on the JIPs are indicated with double headed arrows. The sequential phosphorylation and activation cascade of JNK signalling components are designated with arrow heads. Phosphorylation of APP by JNK is indicated as P. The phosphorylation of APP is suppressed by JIP2. Kinesin binds to APLIP1, JIP1 and JIP2 and associates with the microtubules (Adapted from Taru et al, 2002).

transported bound to JIP-1 and kinesin-1, since DLK has been shown to be in the same complex as kinesin-1 and JIP-1. If an activated JIP-1-JNK signalling module is transported by kinesin-1 and JNK activation is known to inhibit JIP-1-KLC binding, how is it possible that a JIP-1 complex with activated JNK signalling modules can be transported with kinesin-1? There are numerous ways this paradox, could be overcome. Firstly the JNK signalling module could be carried in an inactive state, until it reaches its appropriate targets such as the neuronal cytoskeleton or the cell body, in order for this to occur JIP-1 levels would have to be stringently regulated. At the moment it is not completely clear the mechanism by which JIP-1 via its association with kinesin-1 acts to transport and release activated JNK to its appropriate target (Koushika et al, 2008). In *Drosophila* it has be shown that activation of a JNK signalling pathway, can influence axonal transport by functioning as a kinesin-cargo dissociation factor (Horiuchi et al, 2007). Interactions between APLIP1 the *Drosophila* orthologue of JIP-1 and kinesin-1 are disrupted, when Wallenda (DLK) and Hemipterous (MKK7) are activated, thus in this manner JNK can be activated in a spatiotemporal manner (Figure 1.15). APLIP-1 unlike its mammalian homologue is only known to bind directly to Hep (MKK7), in the JNK signalling cascade (MAPKKK: Wnd; MAPKK:Hep; MAPK:JNK).

A recent publication has demonstrated that JIP-1 can also make a contribution in activating the kinesin-1 motor. In order to prevent kinesin-1 from moving along microtubules in the absence of cargo a mechanism known as KHC autoinhibition is utilised. In this instance KLC participates in maintaining KHC in its folded inactive conformation, in this orientation the tail of the KHC motor can autoinhibit its motor activity. This inactivation is reversed by the simultaneous binding of both JIP-1 to KLC

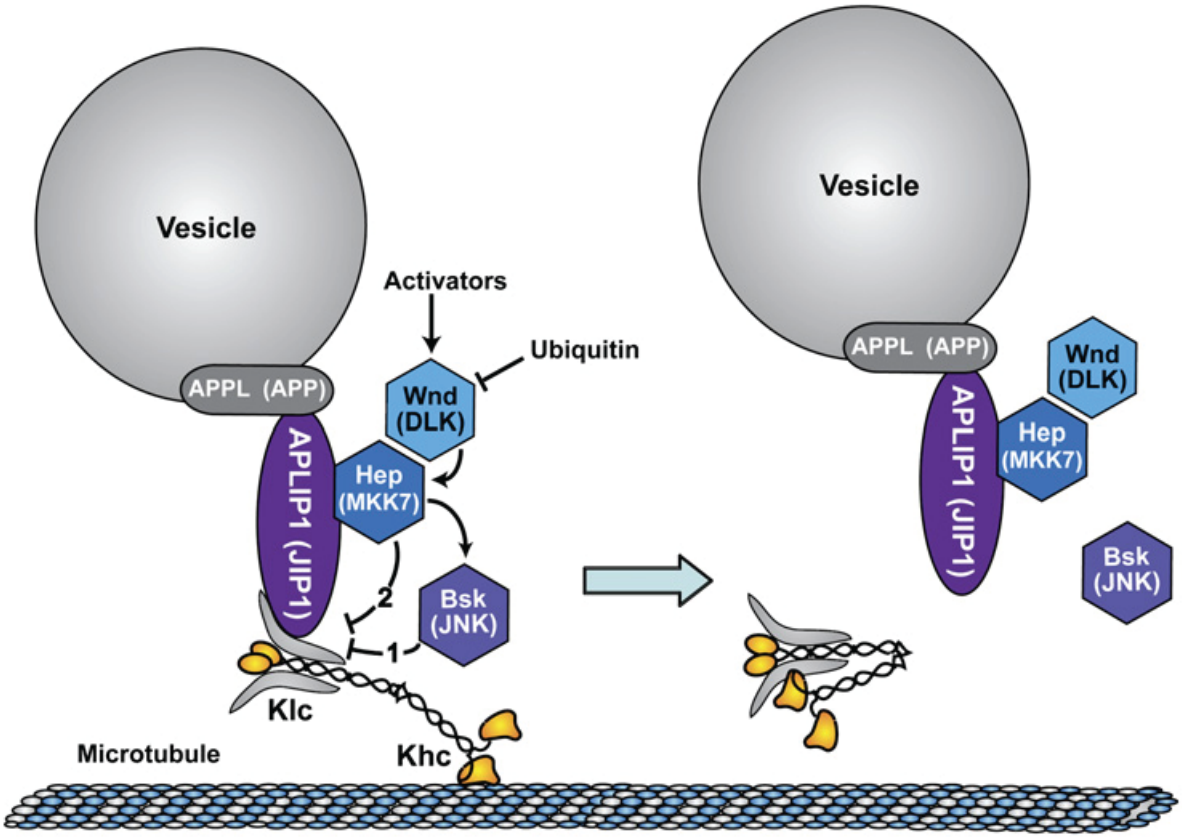

Figure 1.15. A schematic diagram demonstrating how the JNK signalling pathway operates to mediate APLIP-1/JIP-1 linked Kinesin-1 cargo transport.

Wallenda (MAPKKK), whose levels can be mediated by ubiquitination, is activated by an unidentified upstream signal. Wallenda activates Hep (MAPKK) by phosphorylation, and activated Hep, subsequently causes dissociation of APLIP1 (JIP-1) from KLC, possibly through phosphoactivation of Bsk (JNK) which can then modify the linkage complex (pathway 1). Alternatively activated Hep could modify the linkage between KLC and APLIP1, by inducing a conformational change that inhibits the KLC-APLIP1 interaction, independently of Bsk (pathway 2). Disruption of this APLIP-1-KLC binding may enable kinesin to adopt a folded inactive conformation which cannot bind microtubules. [Components are labelled with their Drosophila names and their equivalent vertebrate homologues, in brackets. Lines with arrowheads depict activation and those with crossbars indicate inhibition]. Adapted from: (Horiuchi et al, 2007).

and FEZ-1 to KHC, this in turn facilitates the binding of KHC to microtubules, ensuring that only the kinesin-1 motor possessing cargoes begins movement on microtubules (Blasius et al, 2007; Koushika et al, 2008), see Figure 1.16. Furthermore evidence suggests that JIP-1 has a more wide-ranging effect on axonal transport beyond those related to kinesin-1. It is possible that there is a direct physical interaction of JIP-1 with a component of the dynein-dynactin complex, since in APLIP1 mutants retrograde flow of both mitochondria and synaptobrevin (a synaptic vesicle protein) is substantially decreased (Horiuchi et al, 2005). This is not inconceivable and is consistent with the function of JIP-3 in retrograde transport. JIP-3 has been shown to immunoprecipitate with p150 glued, a component of the dynactin complex and is known to retrogradely transport activated JNK-3 from the site of nerve injury (Cavalli et al, 2005). JIP-1 and JIP-3 could also influence axonal transport by affecting microtubule dynamics. Since JIP-1 amplifies JNK phosphorylation this can assist in regulating microtubule stability via increased phosphorylation induced binding to MAP2 and MAP1B (Chang et al, 2003) and enhanced negative regulation of SCG10, a microtubule depolymeriser (Tararuk et al, 2006). Additionally JIP-3 docking to JNK3 enhances the activation of Tau, a well known stabilising microtubule associated protein (Goedert et al, 1997; Reynolds et al, 1997).

1.11 The role of the JNK signalling pathway cellular morphogenesis.

The JNK signalling pathway is crucial to various cellular processes, which require changes in cellular morphology co-ordinated by the actin cytoskeleton including dorsal closure, innate immunity, wound healing, apoptosis and eye development (Riesgo-Escovar et al, 1996; Sato et al, 2005; Ramet et al, 2002; Bosch et al, 2005; Tobiume et al,

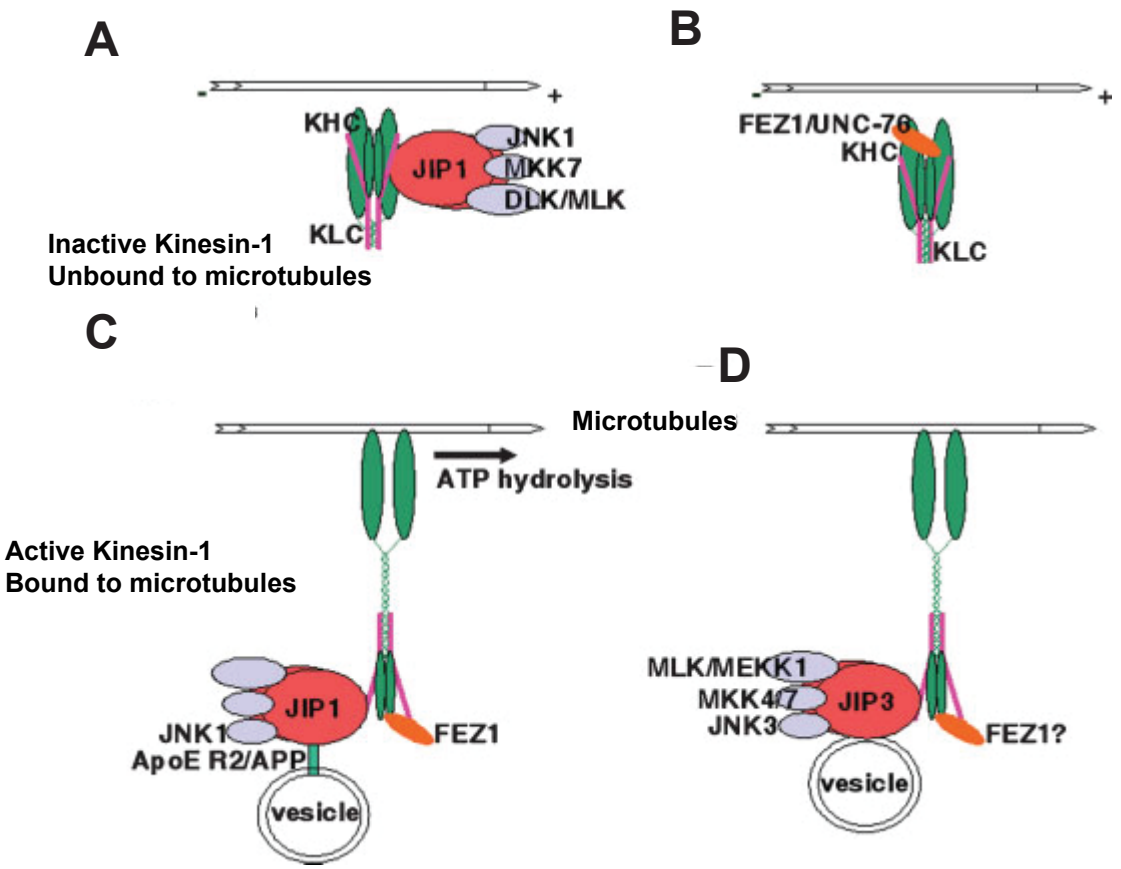

Figure 1.16. **Diagrammatic representation of the activation of kinesin-1 by docking of both JIP-1 and FEZ-1**.

(A) Docking of JIP-1 to KLC alone is not sufficient to activate Kinesin-1 mediated transport. **(B)** Docking of FEZ-1 is also not sufficient to facilitate KHC-microtubule interactions. **(C)** JIP-1 attaches to vesicular cargoes, such as APP or APoER2, and once FEZ-1 and JIP-1 are bound to kinesin-1, it is activated and can transport multiple cargoes along microtubules (such as JNK signalling kinases and APP containing vesicles). **(D)** JIP-3 may also act in conjunction with FEZ-1, allowing interaction of KHC with microtubules, thereby activating kinesin-1. JIP-3 is also able to interact with membranous cargoes and can also homodimerise like JIP-1. Adapted from: (Koushika et al, 2008).

2001; Stronach and Perrimon, 2002). Dorsal closure in the fly occurs in mid-embryogenesis and involves the movement of the dorsal ectoderm on each side of the embryo towards the midline to close the embryo in a surrounding, protective epidermis, However mutations removing the function of JNK pathway components result in a failure of dorsal closure giving a characteristic non-viable 'dorsal open' phenotype (Glise et al, 1995; Riesgo-Escovar et al, 1996; Hou et al, 1997; Su et al, 1998; Stronach and Perrimon, 2002). Consequently the Drosophila homologue of JNK has acquired the name '*Basket*' (*Bsk*) due to the morphology of *Bsk* null mutant embryos.

1.12. The role of the JNK signalling cascade in neurodevelopment

As well as being central to numerous morphogenetic processes in *Drosophila* development. JNK has also been implicated as being integral in diverse neural functions. For instance the development of cerebellar granule neurons (Coffey et al, 2000; Bjŏrkblom et al, 2005) is dependent on JNK signalling, additionally mice null for the *JNK-1* gene exhibit abnormalities in axonal tracts (Chang et al, 2003). Furthermore mice exhibit severe neurological defects and die during embryogenesis, when dually null for *JNK-1* and *JNK-2* (Sabapathy et al, 1999). It has also been demonstrated that JNK signalling is necessary for axon regeneration in dorsal root ganglion neurons (Kennedy and Kocsis, 1998) as well as regulating transcriptional events that promote neurite outgrowth in PC12 cells (Yao and Osada, 1997; Kita et al, 1998). In hippocampal neuronal cultures it has been demonstrated that JNK is needed for the formation of axons (as oppose to dendrites) and in both *in vitro* hippocampal cultures and Drosophila dorsal

cluster neurons it has been established that JNK is needed for axonal outgrowth and stabilisation (Srahna et al, 2006; Oliva et al, 2006).

The localisation of JNK reflects the ability of this MAPK to regulate diverse neural functions. For instance it has been demonstrated that phosopho-JNK is necessary for the axonogenesis of hippocampal neurons in culture. Activated JNK is solely present in the axons of fully mature hippocampal neurons, but completely absent in the dendrites (Figure 1.17A). Additionally *in vitro* studies on developing hippocampal neurons reveals that a proximal-distal gradient of phospho-JNK exists in the axon, with activated levels of JNK being highest at the growth cone and in the neuronal cell body (Figure 1.17B), (Oliva et al, 2006). Thus the extent to which JNK is preferentially activated in the axon and the high concentration of phospho-JNK in both the growth cone and the cell body of a developing axon, demonstrates that JNK is a central effector molecule in relaying upstream signals to the cytoskeleton or promoting transcription of the necessary proteins needed in order to direct the correct navigation of the axon growth cone. In fact it is well known that JNK phosphorylates a large array of nuclear and cytoplasmic targets including transcription factors (Sanyal et al, 2002; Weston and Davis, 2002; Stronach, 2005) as well as proteins that interact with the microtubule and actin cytoskeleton (Reynolds et al, 2000; Chang et al, 2003; Yoshida et al, 2004; Björkblom et al, 2005; Gdalyahu et al, 2004; Huang et al, 2003).

1.12 JNK signals to the cytoskeleton to regulate axon growth

Regulation of the neuronal cytoskeleton plays an integral role in channeling growth to the emerging axon. Extensive research has demonstrated that JNK also regulates components

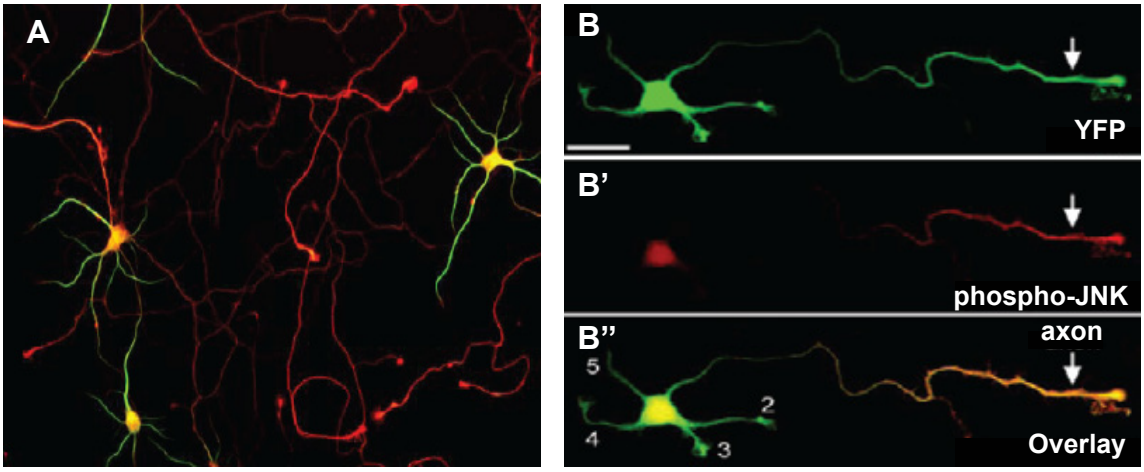

Figure 1.17. Activated JNK is enriched in mouse hippocampal axons.

(A) After 7 days in culture (stage 4), phospho-JNK is completely absent in dendrites (labelled with antibodies against phospho-JNK (red). **(B-B'')** A representative neuron (stage 3), 24 hours in culture. **(B)** A hippocampal neuron transfected with an YFP construct, to reveal its morphology. **(B')** Immunostaining with a phospho-JNK antibody reveals a proximal-distal gradient of phospho-JNK in the axon. **(B'')** Overlay between phospo-JNK and transfected YFP. It is important to note that phospho JNK is completely absent from the dendritic processes labelled 2, 3, 4 and 5. Adapted from (Oliva et al, 2006).

of the nerve growth cone cytoskeleton. Although JNK has principally been studied for its role in transcriptional regulation and apoptosis, there is an increasing amount of evidence showing that JNK can directly modulate the cytoskeleton. JNK phosphorylates microtubule (MT) associated proteins such as MAP2 and MAP1B resulting in changes in microtubule dynamics (Chang et al, 2003). For instance Wnts function as molecules that guide axons to their appropriate targets (Schmitt et al, 2006, Liu et al, 2005, Lyuksyutova et al, 2003) and as instructive cues are able to elicit profound changes in the organisation and stability of microtubules during axon remodelling. Wnts increase the population of stable (acetylated) microtubules and induce unbundling of MTs and the formation of looped MTs at the distal region of the axon (Krylova et al, 2000; Hall et al, 2000; Lucas et al, 1998). In mouse Neuroblastoma (NB2a) cells Wnt signals through Dishevelled (Dsh) to activate JNK. Dishevelled is able to both increase the level of active JNK associated with microtubules and inhibit GSK-3β, culminating in an increased quantity of stable microtubules at the axon shaft and inducing the formation of looped microtubules at enlarged growth cones (Ciani and Salinas 2007).

Furthermore, it has also been demonstrated *in vivo* that JNK physically interacts with the stathmin family of microtubule destabilising proteins SCG10, SCLIP, RB3 and RB3'. Moreover in the developing forebrain and in cerebrocortical cultures JNK phosphorylates SCG10 on sites that regulate its microtubule depolymerising activity (Tararuk et al, 2006). Stathmin proteins negatively regulate microtubule dynamics *in vitro* by binding to tubulin heterodimers (Horwitz et al, 1997; Charbaut et al, 2001; Ravelli et al, 2004). However in order to extend long axons and dendrites, neurons must exert tight control over microtubule dynamics and neurite outgrowth would be impeded,

if the stathmins were not stringently regulated. JNK acts to phosphorylate SCG10 in the neurite and suppresses inappropriate destabilising events. In *Drosophila* cells, disruption of the stathmin homologue using RNAi knockdown produces anomalies in nervous system development, characterised by migration and commisure defects (Ozon et al, 2002). JNK is also able to phosphorylate doublecortin (DCX) a microtubule associated protein, which stabilises microtubules, however it is postulated that DCX is involved in a variety of functions, regarding regulation of the neuronal cytoskeleton, these have yet to be elucidated (Reiner et al, 2004; Gdalyahu et al, 2004). Mutations in DCX show a lamination defect in the hippocampus resulting in lissencephaly. Loss of function mutations for the JNK phosphorylation sites on DCX decreases the length and quantity of neurites in PC12 cells and primary cerebellar neurons, whereas DCX containing artificial gain of function mutations replicating JNK phosphorylation increases them (Gdalyahu et al, 2004), signifying the involvement of JNK in the DCX regulation of neuronal morphogenesis.

Paxilin has also been proposed to be a JNK substrate. Paxilin is a focal adhesion adaptor protein that is able to couple cell adhesion proteins such as integrin to the actin cytoskeleton (Brown and Turner, 2004), facilitating cell locomotion. Paxilin co-localises with JNK in focal adhesions, it is able to function as an adaptor protein involved in organisation of adhesion and cell migration and *in vitro* kinase assays have demonstrated that JNK phosphorylates paxilin at Ser178 (Huang et al, 2003). Additionally a paxilin mutant, unable to be phosphorylated by JNK (containing a Ser178 → Ala mutation) slowed cell migration in NBT-II cells and delayed wound healing in monolayers of these cells (Huang et al, 2003). This suggests that JNK-mediated phosphorylation of the focal

adhesion protein paxilin enhances cell movement. Additionally similar evidence was obtained in wound healing assays for varying cell types, including Chinese hamster ovary K1 cells and MDA-MB-231 human breast cancer cells (Huang et al, 2003). Furthermore it has been demonstrated that JNK localises to the actin-dense membrane ruffles localised at the cell leading edge following growth cone factor exposure, implying a crucial role for JNK in migration (Amagasaki et al, 2006). The process of neuronal migration is dependent upon the formation of lamellipodia and filopodia, which are regulated by the activities of Rac1 and Cdc42 in a large diversity of cell types, including fish keratocytes, rat bladder tumour epithelial NBT-II cells, fibroblasts and neurons (Luo, 2000; Hall et al, 2000). In mouse N1E-115 neuroblastoma cells it has been revealed that JNK phosphorylation of paxilin acting downstream of Rac1 and Cdc42 signalling, mediates neurite extension and a paxilin construct consisting of a mutation in the JNK phosphorylation domain (Ser178 → Ala) inhibits neurite outgrowth (Yamauchi et al, 2006. Additionally both activated JNK and paxilin were found to co-localise in the tips of extending neurites (Yamauchi et al, 2006). Although Rho and Rac regulate Drosophila *paxilin* to transduce signals to the actin cytoskeleton in various morphogenetic events including eye development and imaginal disc morphogenesis (Chen et al, 2005), no homologous JNK Ser178 phosphorylation site, equivalent to that present in humans and mice, has been found in Drosophila *paxilin*, suggesting that paxilin may be regulated in an alternative way (Llense and Blanco, 2008).

1.13 JNK signals to transcription factors to regulate axon growth

In numerous cell signalling and morphogenetic events including synaptic plasticity in Drosophila neurons, JNKs function through activating the AP-1 transcription factor complex (Sanyal et al, 2002, Weston and Davis, 2002; Stronach, 2005). Proteins that act as transcription factors regulate gene expression in eukaryotic cells. Typically a transcription factor is composed of a structure that includes a transactivation domain along with a DNA binding domain that is able to recognise specific DNA elements within the promoters of target genes. The range of transcription factors that are known to be JNK substrates are illustrated in Figure 1.18. Active AP-1 complexes are composed of a variety of dimers, which consist of members of the Fos and Jun families of proteins. In mammals, the Fos proteins (c-Fos, FosB, Fra1 and Fra2) can only heterodimerise with members of the Jun family (c-Jun, Jun-B and Jun-D) to form transcriptionally active complexes. Jun proteins in addition to Fos are able to efficiently heterodimerise with other transcription factors such as ATF2 (Hai et al, 1999). In mammals, AP-1 activation is principally mediated by phosphorylation of c-Jun by JNK (Davis, 2000). It has been demonstrated that c-jun is highly expressed in the nervous system in response to inujury (Herdegen and Leah, 1998) and it is an important regulator of axonal regeneration in the injured central nervous system (Herdegen et al, 1997; Raivich et al, 2004).

It is thought that c-jun dependent axonal outgrowth occurs by the upregulation of galanin, $\alpha 7\beta 1$integrin and CD44, since the promoters of these genes contain identified AP-1 sites (Anouar et al, 1999, Lee et al, 1993, Raivich et al, 2004). Additionally *in vitro* studies have also conferred a role for c-Jun in neuronal sprouting and survival in PC12 cells (Dragunow et al, 2000) and c-Jun has also found to be expressed during

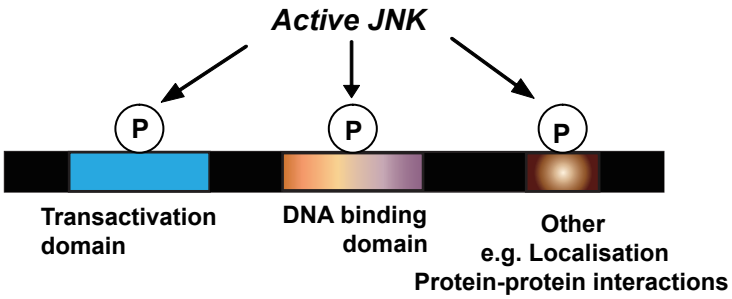

Transcription factor substrates

Example Substrates:

c-Jun, Jun-D
ATF-2,JDP, Elk1, Net
HSF1, c-Myc, p53,
NFATc3, NFATc1α
NFATc2
FOXO4, **STAT3**
STAT1, PAX2, TCFβI
Fos, ATF3
[(AP-1) Fos and Jun Heterodimers]
BIM

Figure 1.18. Major classes of transcription factor substrates, known to be activated by the JNKs.

JNK mediated phosphorylation may occur on the transactivation domains, DNA binding domains or other protein domains. Transcription factors which regulate diverse functions in neurons such as outgrowth, survival, regeneration and synaptic plasticity are highlighted in red.

neurogenesis and in the adult brain (Raivich et al, 2004). Moreover the c-Jun related bZIP transcription factor ATF3 can enhance c-Jun mediated neurite sprouting and when upregulated in conjunction with c-Jun can induce axonal regeneration in response to axotomy (Pearson et al, 2003). During development of neuronal polarity in cultured hippocampal neurons phospho-JNK can activate another transcription factor ATF-2. ATF-2 is a member of the ATF/CREB (cAMP responsive element binding protein) family that binds to CRE (cAMP responsive element) consensus sites to regulate numerous neuronal genes (Gupta et al, 1995, 1996; van Dam et al, 1995; Herdegen and Leah, 1998). ATF-2 is highly expressed in retinal ganglion cells after axotomy and partial optic nerve crush and is necessary for neuronal survival and regeneration (Robinson, 1996, Kreutz et al, 1999).

As mentioned the AP-1 complex of Fos and Jun is a common downstream effector of JNK-mediated changes in gene expression, for instance AP-1 can regulate synaptic growth at the Drosophila neuromuscular junction (NMJ) (Sanyal et al, 2003). However it has been shown that highwire, (a ubiquitin ligase which regulates MAPK signalling) signals through JNK towards a distinct pathway to regulate synaptic overgrowth, which requires Fos and is Jun independent (Collins et al, 2006). This is consistent with the AP-1 independent functions of D-Fos, which have been described previously in *Drosophila* (Riese et al, 1997; Riesgo-Escovar and Hafen, 1997a). Unlike its mammalian homologue Fos is able to homodimerise or operate in conjunction with a third bZIP transcription factor ATF2 (Perkins et al, 1990; Riesgo-Escovar and Hafen, 1997). Thus this MAPK signalling pathway which regulates synaptic growth could

possibly involve a homodimer of D-Fos or another transcription factor that interacts with Fos.

In *Drosophila*, there is a precedent for Fos rather than Jun being the principle AP-1 component, mediating varied morphological events in diverse cell types. For instance during Drosophila endoderm induction it is Fos and not Jun, which is responsible for activating labial, a selector gene with a role in cellular differentiation in the larval midgut. Furthermore Fos inactivation interferes with cell differentiation in the larval midgut whereas as Jun inactivation does not (Riese et al, 1997). Additionally in imaginal discs *Jun* mutant clones display only mild mutant phenotypes and do not affect proliferation/survival, whereas as strong loss of function Kayak/Fos alleles exhibit severe defects. Consistent with this, recent studies on the role of Fos, show it is required for cell cycle regulation and proliferation in wing and eye discs. In fact cyclin B was identified as a direct downstream transcriptional target of Fos *in vivo* (Hyun et al, 2006). Fos also controls the expression of ecdysone inducible genes to regulate glial cell number and differentiation in the developing ventral nerve cord of Drosphila (Giesen et al, 2003).

It has been well documented that multiple Fos isoforms exist in Drosophila, whereas this is not the case for Jun, this could account for the fact that Fos rather than Jun is able to elicit a wide diversity of morphogenetic processes in Drosophila. (Giesen et al, 2003, Weber et al, 2008).

1.14 The role of the JNKs in neurodegeneration and apoptosis

While JNK signalling is essential for many aspects of neurodevelopment, there is also substantial evidence that JNK signalling plays a crucial role in neurodegeneration.

Defective JNK signalling has been heavily implicated in neurodegenerative disorders such as Alzheimer's, (Okazawa et al, 2002; Legalwar et al, 2007), Parkinson's (Pen and Andersen, 2003) and Huntington's Disease (Perrin et al, 2009). The importance of JNK signalling in neurodegeneration has been corroborated in a wide range and extensive series of research findings. For instance JNK has been shown to induce neurodegeneration and axonal loss in response to a wide range of genetic, environmental and stress stimuli, including ischaemia and trophic factor deprivation (Miller et al, 2009, Morfini et al, 2006; Waetzig et al, 2006). The JNKs have principally been considered as degenerative signal transducers and cental activators of neuronal apoptosis, this is partly based on the neuroprotective affects exerted upon inactivation of JNKs. For example genetic deletion of JNK3 protects against axotomy or induced death of dopaminergic neurons (Brecht et al, 2005), furthermore neuroprotective effects are also observed in JNK3 knockout mice following excitotoxicity (Yang et al, 1997). Conversely a neuroprotective role of the JNKs has also been uncovered. In ischemia-induced neurodegeneration, caused by permanent occlusion of the middle cerebral artery in mice, JNK1 knock out exacerbates ischemic damage indicating a protective function for JNK-1 in this scenario (Brecht et al, 2005). Additionally JNK1 null mice exhibit degeneration of the anterior commisure during development (Chang et al, 2003), thus conferring a protective role of JNK1.

What is the mechanism by which JNKs exert their neurodegenerative and apoptotic effects? JNK is a central mediator of apoptosis and is able to activate the pro-apoptotic Bcl-2/BH3 only proteins and promote the release of cytochrome C from mitochondria, which can subsequently activate the caspase dependent death pathway

(Chipuk et al, 2008). JNKs are able to activate transcription factors in the nucleus to elicit caspase dependent apoptosis. For instance trophic factor deprivation in rat sympathetic (SCG) or cerebellar granule (CG) neurons *in vivo* and *in vitro* activates nuclear JNKs (primarily JNK2 and JNK3) and subsequently induces the activation of the AP-1 transcription response. In this context, the AP-1 transcription factor response induces the transactivation of the pro-apoptotic Bcl-2 family members BIM$_{EL}$ and HRK (Harris and Johnson, 2001; Putcha et al, 2001; Whitfield et al, 2001). These pro-apoptotic Bcl-2 molecules are able to inhibit the anti-apoptotic Bcl-2 family members BCL-2 and BCL-$_{XL}$, culminating in the BAX-, BAK, and/or BOX-dependent release of mitochondrial apoptogens. In *Drosophila* there are two homologs of the Bcl-2 family proteins Debcl and Buffy. Debcl has been shown to have a pro-apoptotic function in Drosophila (Brachmann et al, 2000; Colussi et al, 2000; Igaki et al, 2000), whereas Buffy has been demonstrated to be a pro-survival Bcl-2 relative (Quinn et al, 2003). These pro-apoptotic Bcl-2 proteins therefore promote mitochondrial permeability and cytochrome c release, facilitating the formation of the Apaf-1 apoptosome and subsequent caspase dependent cell death, whereas pro-survival Bcl-2 members prevent the release of cytochrome c from mitochodria required for the formation of the Apaf-1 apoptosome and therefore caspase activation (Zou et al, 1997). Apaf-1 is known to be required for the activation of the initiator caspase-9, which induces cleavage of the effector caspases 3 and 7, in Drosophila the equivalent process is carried out by Dark, which interacts with the Drosophila caspase Dronc and is required for its activation (Richardson and Kumar, 2002).

The inhibitor of apoptosis (IAPs), pro-survival proteins bind to inhibit caspases (Deveraux and Reed, 1999), two IAP homologs have been reported in *Drosophila* Diap1 and Diap2 (Hay, 2000), which are antagonized by IAP inhibitors Reaper (Rpr), Hid (Head involution defective) and Grim (McCall and Steller 1997). In fact it has been widely reported that activation of JNK signalling induces cell death via the transcriptional activation of the pro-apoptotic genes *reaper*, *grim* and *hid*. (Griswold et al, 2008; Hong et al, 2009). The mammalian apoptosis inducer Smac/Diablo appears to act as a functional homolog of Rpr, Hid or Grim, since it also acts to neutralize caspase inhibitory function of the IAP protein family (Du et al, 2000, Verhagen et al, 2000).

The JNK signalling pathway is also able to operate via a transcription independent mode to induce neuronal apoptosis. Activation of extranuclear JNKs culminates in direct substrate phosphorylation of the pro-apoptotic Bcl-2 molecule BIM. The JNK substrate BIM is able to inhibit the anti-apoptotic Bcl-2 molecules (Putcha et al, 2003, Tournier et al, 2000) and facilitate subsequent activation of the 'intrinsic' caspase dependent apoptotic signalling cascade. Regulation of the apoptotic signalling cascade by the JNK signalling pathway is summarised in Figure 1.19.

Recently, a study has also demonstrated that individual isoforms of JNK have specialised functions in mitochondria, depending on the *in vivo* environment. For instance under normal physiological conditions brain mitochondria contain all three JNK isoforms, with basal activity being mediated by JNK1. However following middle cerebral artery occlusion (MCAo) and subsequent ischemia, the phosphorylation profile on the JNK isoforms drastically changes. There is a pronounced rise of phosphorylated JNK2 and to a greater degree JNK3, accompanied with a sharp decline in phosphorylated

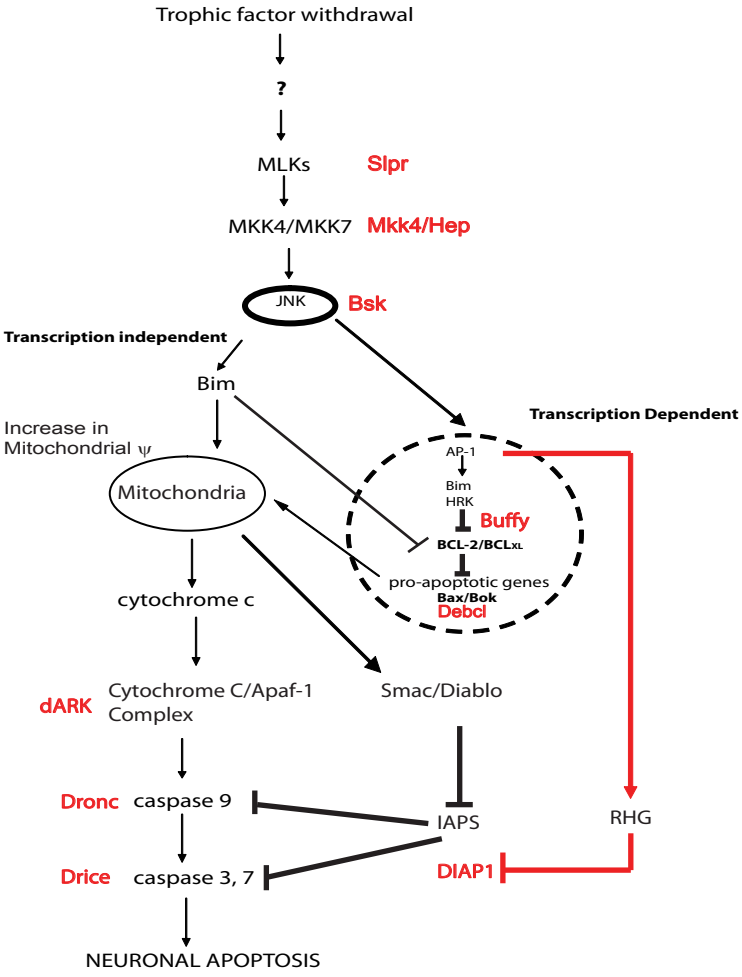

Figure 1.19. Model of the signalling pathway for transcription-dependent and independent JNK-Induced apoptosis

Trophic factor deprivation in SCG and CG neurons culminates in the activation of the nuclear JNKs which mediates the transcription dependent pro-apoptotic effects of the JNKs, characterised by the induction of the pro-apoptotic Bcl-2 family members BIMEL and HRK. These molecules inhibit the activity of the pro-survival Bcl-2, Bcl-XL proteins which act as inhibitors of caspase activation and function upstream of Apaf-1. This facilitates the activation of the pro-apoptotic Bcl-2 family members Bax and Box, which promote an increase in mitochondrial permeability. This change in permeability (ψ) culminates in the release of mitochondrial apoptogens, which induce cell death via a caspase dependent pathway and Smac/Diablo which sequesters the Inhibitor of Apoptosis Proteins (IAPs). In *Drosophila reaper* [R], *hid* [H] or *grim* [G] act to neutralise caspase inhibitory function of the IAP family and are therefore considered functional homologues of Smac/Diablo. JNK signalling induces the activation of the pro-apoptotic gene *reaper*, *hid* and *grim* via transcriptional regulation of AP-1. Concomitantly transcription independent pro-apoptotic effects of JNKs are mediated by the MLK/JNKK-dependent activation of extranuclear JNKs. This in turn culminates in the activation of cellular substrates such as BIM, which is facilitates the activation of the caspase dependent apoptotic signaling cascade. The *Drosophila* homologues of mammalian JNK signalling and apoptotic pathway components are in red. Adapted from: (Putcha et al, 2003).

JNK1, between 2-6 hours after the onset of ischemia (Zhao and Herdegen, 2009). This finding suggests that JNK-1 does not have a degenerative-apoptotic function, but could be needed in a neuroprotective capacity, to prevent degeneration. A number of studies have shown that inactivation of the JNK-1 isoform leads to degeneration and defective neuronal morphogenesis during development (Chang et al, 2003; Kuan et al, 1999; Sabapathy et al, 1999), furthermore JNK1 protects against ischemic death since genetic deletion of JNK-1 aggravates ischemic injury in CG neurons of mice (Brecht et al, 2005). Conversely JNK3 knockout protects neurons against excitotoxicity, (Yang et al, 1997), ischemia induced neurodegeneration and axotomy (Brecht et al, 2005). Overall the evidence implicates JNK-3 as the isoform required to exert degenerative effects in varied neuronal subtypes, whereas JNK-1 has been shown to have a neuroprotective function.

1.15 How do the vertebrate JNKs generate signal specificity to regulate neuronal morphogenesis?

In vertebrates the JNK family consist of at least ten different expressed isoforms from three genes (jnk1, jnk2 and jnk3) and isoform specific JNK functions have been identified in various neuronal subtypes *in vitro* and *in vivo* (Yang et al, 1997; Kuan et al, 1999; Chang et al, 2003, Brecht el al, 2005, Zhao and Herdegen, 2009). The JNKs have been associated with a pleathora of diverse function in neuronal morphogenesis; this is principally based on the fact that the different JNK isoforms are able to generate distinct substrate specificity. Firstly different JNK isoforms vary in their binding affinity to certain transcription factors such as ATF-2, Elk1 and Jun (Gupta et al, 1996). Furthermore differential subcellular localisation of the JNKs determines their functions.

For instance withdrawal of trophic support in cerebellar neurons culminates in the intanuclear translocation of JNK2/3 but not JNK1, this in turn activates Jun and a stress response is induced in these neurons. However although JNK-1 is constitutively activated it is predominantly associated with cytoplasmic structures and is unable to phosphorylate c-Jun in the nucleus (Coffey et al, 2002).

Furthermore it has been demonstrated that distinct pools of JNKs serve different function in developmental and stress responses in cerebellar granule neurons. A major cytosolic pool of MKK4 colocalises with JNK in the neurites and during differentiation cytoplasmic JNK (colocalised with MKK4) is activated threefold, this is accompanied with the concomitant activation of nuclear JNK (colocalised with MKK7) which is activated 10-fold and is possibly able to promote the transcription of maturation specific gene products such as glut2. Furthermore a minor stress-sensitive pool of JNK exists, which translocates in the nucleus in response to anisomycin treatment. Increased active JNK in the nucleus is able to phosphorylate c-Jun, culminating in the activation of stress induced genes (Coffey et al, 2000). The evidence therefore suggests that MKK4 and MKK7 may have distinct functions as JNK activators in *vivo* and this may be attributed to their subcellular localisation, with MKK7 being exclusively localised to the nucleus, whereas as MKK4 exhibits predominantly cytoplasmic localisation (Coffey et al, 2000).

1.16 How does the *Drosophila* JNK *Bsk* generate signal specificity to regulate neuronal morphogenesis?

The sequence alignment data (Figure 1.9) demonstrates that there is a large degree of conservation between Drosophila JNK (*Bsk*) and its mammalian JNK homologues. In fact

the TPY phosphorylation motif, which can be activated by dual phosphorylation via the MAPK kinases MKK4 and MKK7 (Hep in *Drosophila*) is 100% conserved between *Bsk* and its human JNK homologues. This suggest that activation of *Bsk*, in crucial in regulating diverse processes in neuronal morphogensis in a similar manner to which JNK phosphorylation is crucial in regulating morphogenetic changes in vertebrate neurons. In genetic studies, *Bsk* has been implicated in axon extension in *Drospohila* dorsal cluster (DC) neurons (Srahna et al, 2006), and at the *Drosophila* neuromuscular junction (NMJ) *Bsk* has also been found to regulate synaptic plasticity and growth (Collins et al, 2006, Sanyal et al, 2002). However the literature up to data has not addressed how a single gene *Bsk* is able to regulate multiple aspects of JNK-dependent neuronal morphogenesis. In mammals diverse neuronal processes are regulated by three JNK genes. Additionally although isoform specific function of the JNKs have been identified extensive functional overlap between the different JNK isoforms adds a further level of complexity in determining the role of the JNKs in various aspects of neuronal morphogenesis such as neuron extension, axon stabilisation, axon growth and neurodegeneration. Therefore evaluation of JNK signalling in a genetically amenable organism, such as *Drosophila*, could assist in clarifying how JNK operates in *vivo* to generate signal specificity and elicit particular morphogenetic changes during neuronal development.

1.17 Principle objectives of research

Given that JNK signalling is integral to diverse aspects of both neurodegeneration and neurodevelopment, I decided to examine the role of the JNK signalling pathway *in vivo* by analyzing the function of the sole *Drosophila* JNK homologue Bsk in MB neurons of

the *Drosophila* brain. The objectives of my PhD thesis can therefore be described as follows.

1. **Understand the mechanistic basis of how *Bsk* is able to regulate multiple functions in MB neurons:** In order to address how *Bsk* activation mediates various aspects of neuronal morphogenesis, I will genetically manipulate the relative level of Bsk activity in *vivo*, to determine the importance of JNK signal strength. To accomplish this I will use a variety of techniques, including the generation of *Bsk* null MB neuroblast clones (loss of function scenario), Bsk RNAi knockdown and the use of Bsk hypomorphic mutations to ensure partial reduction of *Bsk* activity and overexpression of JNKK-Bsk fusion transgenes to enable *Bsk* to be constitutively activated (gain of function scenario).
2. **Determine the role of the two JNKKs Hep and Mkk4 in neuronal morphogenesis:** Unlike Hep the in vivo role of MKK4 in *Drosophila* neuronal morphogenesis has yet to be determined. Here I evaluate the roles of the JNKKs in MB neuronal morphogenesis, by loss of function analysis, and gain of function studies. I also generate Hep-Bsk and Mkk4-Bsk fusion transgenes to determine if Hep and Mkk4 differential regulate Bsk activity. In order to investigate the function of Hep, Mkk4 and Bsk, I used the relevant antibodies on whole mount *Drospohila* Brains. These experiments provided crucial information regarding the localisation of activated Bsk during development and adulthood in MB neurons, and also gave insight into the functional role of Hep and MKK4 in MB neurodevelopment.

3. **Establish if temporal expression of *Bsk* activity plays a significant role in regulating MB axonal morphogenesis during development:** It has already been established that transient or prolonged JNK inactivation using JNK mutant mice can affect distinct JNK-dependent immune responses (Ventura et al, 2006). Here I use different experimental paradigms to control the timing of *Bsk* activity in MB neurons. This is achieved by expressing *Bsk* RNAi at different developmental phases (to induce Bsk inactivation) and expressing *Bsk* WT transgenes in a null *Bsk* background (to examine the extent of rescue at different developmental stages). These experiments enabled me to determine whether Bsk activity is required to be sustained throughout MB neuron development or is required at critical points during development.
4. **Determine how Bsk regulates MB neurodevelopment and diverse aspects of MB neuronal morphogenesis through regulation of AP-1 transcription:** Here I investigate the role of AP-1 in MB neuronal morphogenesis by inactivating Fos and/or Jun activity. Furthermore in order to determine if JNK signalling operates through AP-1 to regulate morphogenetic changes in MB neurons, I also determine if JNK can genetically interact with AP-1 components.
5. **Investigate the mechanism by which Bsk and AP-1 are able to regulate diverse axonal behaviors in *vivo*:** In order to examine whether Bsk and AP-1 are able to interact with the cytoskeleton, I established co-expression assays to determine if Bsk and/or AP-1 can rescue the axon stalled phenotype induced by LIMK overexpression. Finally I set up another co-expression assay to determine if inactivation of AP-1 could rescue the neuronal death phenotype induced in a Bsk

gain-of-function background. This enabled me to determine whether Bsk signals through AP-1 transcription to regulate MB neuronal death.

CHAPTER 2: Materials and Methods

2.1 *Drosophila* methods

2.1.1 *Drosophila* lines

bsk^{147e} and *hep* mutant strains (*hep*^{R39} and *hep*^{R75}) are null mutations, as previously described (Glise et al., 1995; Sluss et al., 1996). *Bsk*^{147e} is a caused by an imprecise excision of a mobilised p-element, resulting in the deletion of the entire *Bsk* kinase domain. *Hep*^{R39} and *Hep*^{R75} are deletions of the entire coding region of Hep caused by imprecise excision of a p-element insertion, located 179 base pairs upstream of the ATG start codon (Glise et al, 1995). The *bsk*^{H15} allele (Berger et al., 2008) encodes a missense mutation (I212F–PB isoform) within the kinase domain, which is likely to result in a hypomorphic allele (see quantifications in Figure 3.5.1G). The *Mkk4*^{e01458} allele is derived from a *PiggyBac* insertion. This *PiggyBac* insertion is located in close proximity to 3' end of Mkk4 and therefore potentially interferes with Mkk4 transcription (Thibault et al., 2004). *Mkk4*^{e01458} complemented the chromosomal deficiencies *Df(3R)Dhod15, Df(3R)BSC195* and *Df(3R)BSC197* but failed to complement *Df(3R)p13* and *Df(3R)Exel6149* (www.flybase.org). Ubiquitous expression of Mkk4 (*tub-GAL4>MKK4::YFP*) fully rescued the lethality associated with *Mkk4*^{e01458}*/Df(3R)p13* transheterozygotes, confirming that the insertion disrupts the *Mkk4* locus.

The following additional strains were also used in our study: *UAS-p35* (Hay et al, 1994), *UAS-zipper::GFP DN* gives a mutant gene product, where only amino acid residues 775-1972 of the zip fragment are expressed (Franke et al, 2005)*; UAS:DLIMK1-F4::HA* (Niwa et al, 2002); *p38a*^{1} is a null mutation. Deletion of the entire *p38* gene is

caused by the excision of two flanking p-elements (Craig et al, 2004); *UAS-p38b.DN gives a* nonactivable mutant gene product, the phospho-site Threonine 183 is replaced by Alanine (Adachi-Yamada et al, 1999); *UAS-rl^{SEM},* a constitutively active form of the rl kinase; Aspartic acid is replaced by Asparagine at amino acid 334 at the C-terminal domain of kinase domain XI (Ciapponi et al, 2001); *UAS-Bsk::myc, UAS-Bsk::myc$^{T181A, Y183F}$*, a phospho-inactive *Bsk* transgene (this study); *UAS-Mkk4::Venus* (this study); *UAS-Bsk RNAi* (VDRC lines 34138 and 34139) - the Bsk RNAi constructs are inserted on chromosome II and designed against the 5'UTR of *Bsk,* cDNA bases 738-1196; *UAS-Dcr2* (Dietzl et al., 2007); *UAS-Bsk*, *UAS-Bsk DN, gives a* nonactivable mutant gene product, the phospho-site Threonine 181 is replaced by Alanine, *UAS-Hep.B^{2}*, *GAL80^{ts7}* (McGuire et al, 2003); UAS-Hep*::RFP* (this study); *UAS-Hep^{CA},* a constitutively active form of Hep (Adachi-Yamada et al, 1999), three amino acids are replaced: S346D, T350D and S352D; *UAS:Hep-Bsk::HA*, a Hep-Bsk fusion transgene (this study); *UAS:Hep^{K226M}-Bsk::HA*, a kinase dead Hep-Bsk fusion transgene (this study); *UAS: Mkk4-Bsk::myc*, a Mkk4-Bsk fusion transgene (this study); *UAS: Mkk4^{K151M}-Bsk::myc,* a kinase dead Mkk4-Bsk fusion transgene (this study); *Jun^{1}* is an EMS induced mutant allele, the Jun^{1} open reading frame is prematurely terminated and can only be translated into a truncated gene product of 176 amino acids, which lacks the basic region and leucine zipper; *Jun^{2}*, is also an induced EMS mutant allele, a stop codon at amino acid 72, results in a truncated protein lacking the DNA binding and dimerization domain and the amino terminal phosphorylation sites (Kockel et al., 1997); *UAS-Jun^{Asp}*, a constitutively active form of *Jun,* Asp replaces Ser or Thr at positions 58, 62, 73, 91 and 93 (Treier et al, 1995) *UAS-Fos*, *UAS-Jun, UAS-Jbz* (Bohmann et al, 1994) and *UAS-Fbz,* (Eresh et al., 1997) are both dominant negative mutants in which the transcriptional

activation domains are deleted, these transgenes consist of the bZIP, fragment and act dominant negatively since they are able to dimerize and bind DNA, without being able to stimulate transcription; *UAS-Fos*$^{PAN-ALA}$, *UAS-Fos*$^{N-ALA}$, *UAS-Fos*$^{C-ALA}$ *are* phospho inactive forms of the Fos transgene, at the specified termini, (Ciapponi et al, 2001); *kay*^{1} is a deletion caused by breaks between the first and second exons of kay and the first exon is removed extending to an upstream region of kay. This particular deletion is in the 5' region of kay and removes exon 1 including the translation start site (Riesgo-Escovar and Hafen, 1997a; Zeitlinger et al., 1997); *kay*^{ED6315} is a deletion that begins upstream of exon 1 and removes exons 1-3 (Weber et al., 2008); the *kay* RNAi construct (NIG-FLY, Mishima, Japan) is inserted on chromosome III and is designed against the 5' UTR of *kay* cDNA bases 657-1252. *Drosophila* strains for MARCM analysis have previously been described (Lee and Luo, 1999) and mutant strains were generated by standard recombination techniques.

2.1.2 Genetics

Generation of MARCM clones

Homozygous mutant clones that are positively labeled were generated using the MARCM method (Lee and Luo, 1999). MB neuroblast and single-cell clones were generated as previously described (Wu and Luo, 2006b). A single neuroblast clone can give rise to ~600 Kenyon cells (Ito et al., 1997). Neurons were visualized using the OK107-Gal4 driver expressing UAS-mCD8::GFP. Later born α/β MB neuroblast clones were generated by heat shocking the relevant fly progeny at 0HR APF to induce Flp-mediated recombination at this developmental stage.

GAL4 mediated expression of UAS-transgenes

The UAS/GAL4 system (Brand and Perrimon, 1993) was used to ectopically express particular genes in specific cell types or genetic backgrounds. For instance, in this study the GAL4-OK107 driver was used to misexpress UAS: transgenes, along with one copy of CD8::GFP in MB neurons. Flies were reared at 25°C, unless otherwise stated such as in RNAi and TARGET experiments.

RNAi knockdown analysis

For 'high' level of RNAi knockdown, flies were cultured at 29°C in the presence of ectopic Dicer (Dcr2), to increase the level of UAS expression and RNAi efficiency (Dietzl et al., 2007). For 'medium' RNAi activity, flies were raised at 29°C without ectopic Dcr2. We found that even at low levels of RNAi expression (18°C), Dcr2 expression can significantly enhance RNAi phenotypes. Ectopic expression of Dcr2 alone does not disrupt MB axon projections (data not shown). Flies were dissected within 3-7 days post-eclosion. The UAS/GAL4 system is temperature sensitive, therefore higher temperatures will induce greater degrees of RNAi knockdown. For Bsk RNAi knockdown the particular region targeted within the Bsk kinase domain is 2L 10,248,239..10,248,697 and it is known that the Bsk RNAi transgene exhibits no non-specific off-target effects (VDRC; www.flybase.org).

TARGET expression analysis

The TARGET system (McGuire et al, 2003) was utilised to control the temporal expression of *Bsk* activity in MB neurons. For the TARGET protocol, flies were grown at 18°C and UAS-GAL4 expression was induced by transferring to 29°C at the indicated

stages. In the 'reverse' protocol, flies were grown at 29°C and shifted to 18°C. These flies were maintained in the shifted temperatures and analyzed at 3 days post-eclosion, unless indicated otherwise.

2.1.3 Immunohistochemistry

Fly brains were dissected at various stages and stained as previously described (Wu and Luo, 2006a). For MARCM neuroblast and single-cell clones, axon projections were visualized using anti-FasII (1:5) and anti-mCD8, 1:200. The following additional antibodies were used: anti-JNK1 (Santa-Cruz Biotechnology, sc-571, 1:250), anti-Phospho JNK (Cell Signalling, no.9255, 1:250), anti-Myc (Santa Cruz Biotechnology, clone 9E10; 1:100 or Cell Signalling, no.2272; 1:200), anti-GFP (Molecular Probes, A11122, 1:100 or Roche, 11814460001, 1:200), anti-cleaved Caspase-3 (Cell Signalling 1:25), anti-MKK4 (1:50) and anti-Hep (1:100). Anti-Hep and Anti-Mkk4 antibodies were generated commercially using rabbit and guinea pig hosts, respectively, using a DXP protocol (Eurogentec, Seraing, Belgium). The following peptide sequences were used as immunogens (QSLEAKLQAQNESHDC and CLRANGDPTLQRLPNS for the JNKK Hep; MAERPKNLFATGSSRC and CKDGITQFTANQQAES for JNKK Mkk4).

2.1.4 Microscopy and image analysis

Stained brains were imaged by confocal microscopy (using Zeiss 510, and processed using Zeiss LSM and Image J software).

2.2 Molecular Biology Methods

Standard molecular biology techniques were carried out according to Sambrook et al, 1989. Additional methods or modifications are mentioned below.

2.2.1 Cloning strategy

PCR Primer design

The polymerase chain reaction was used to amplify the relevant cDNA inserts for cloning into a pENTR vector (Invitrogen) using TOPO® cloning. The primers designed used the following cDNAs as template DNAs:

- Full length Mkk4 cDNA (BDGP clone RE70055)
- Full length Bsk cDNA (a gift from D. Bohmann)
- The full length Hep RC transcript cDNA

Generation of the *UAS-Bsk::myc* and *UAS-Mkk4::YFP* expression vectors

The following primers were used.

(Red: Indicates the four base pair sequence on the 5'end of the forward primer, necessary for directional TOPO® cloning of the cDNA PCR product into the pENTR vector; Blue: ATG start site).

DJNK_Forward1:

5'-CACC ATG ACG ACA GCT CAG CAC CAA CA-3'

DJNK_Reverse2:

5'- CCG CGT TCT ATT ATT TGT TGT ATT GTG TGC-3'

DMKK4_Forward1:

5'-CACC ATG GCC GAA CGA CCG AAA AAT TTG-3'

DMKK4_Reverse2:

5'-ACT CTC CGC CTG CTG ATT GGC-3'

The resulting pENTR-*Bsk* and pENTR-Mkk4 clones were ligated to their respective destination vectors (pTWM or pTWV; Terence Murphy, Carnegie *Drosophila* Gateway® vectors) using the Gateway® system (Invitrogen). Germline transformations were performed commercially (Aktogen, Cambridge, UK)

Generation of the *UAS-Hep::RFP* expression vector

I next used PCR amplification to generate a Hep cDNA insert, consisting of a 3'-XbaI/XhoI overhang. To this end I designed the following primers (XbaI and XhoI restriction sites are in dark green and light green respectively).

HepRC_Forward1:

5'-CACC ATG TCC ACC ATT GAG TTC GAA ACG-3'

HepRC_Reverse2:

5'-TCT AGA CTC GAG GGA ATT AGG TAA CCT CTG-3

The resulting PCR product was cloned into a pENTR vector and the *pENTR-Hep* clone then underwent Xba-1/XhoI restriction. [All restriction endonuclease enzymes and buffers (for this and all subsequent restriction digests) were supplied by New England Biolabs (NEB) and restriction reactions were set up according to NEB protocols.]

Following agarose gel electrophoresis which confirmed the presence of the restricted pENTR-Hep fragment, the band of interest was excised for purification using QIAquick gel extraction kit, (Crawley, UK) using the manufacturers protocol. Once

compatible Xba1/Xho1 overhangs had been generated on both the pENTR-Hep fragment and the RFP insert, the vector and insert were ligated together. The resulting pENTR-*Hep::RFP* clone was then ligated into the pTW destination vector (Terence Murphy, Carnegie *Drosophila* Gateway® vectors) using the Gateway® system (Invitrogen). Germline transformations were performed commercially (Best Gene, California, USA).

Generation of *UAS:Hep-Bsk::HA and UAS:Mkk4-Bsk::Myc* fusion constructs

In order to generate a Bsk cDNA fragment consisting of an Xba1/Xho1 restriction site, followed by a peptide linker at the 5'end, PCR amplification was used with the following primers (the peptide linker is shown in light blue):

DJNK-fusion_Forward1:

5'-CACC CTC GAG TCT AGA GGT GGC GGT GGC TCT GGA GGT GGT GGG TCC TCC GGA ATG ACG ACA GCT CAG CAC CAA CA-3'

DJNK_Reverse2:

5'- CCG CGT TCT ATT ATT TGT TGT ATT GTG TGC-3'

The resulting PCR product was then cloned into a pENTR VECTOR. The pENTR-Bsk clone produced subsequently contains the following important features: 5'-Not1 restriction site – CACC-Xba/Xho-I restriction site-peptide linker – Bsk cDNA-3'. I then used PCR amplification to generate Hep/Mkk4 cDNA fragments, which consist of an Xba1/XhO1 restriction site at the 3'end. The following primers were used to achieve this aim:

HepRC_Forward1:

5'-CACC ATG TCC ACC ATT GAG TTC GAA ACG-3'

HepRC_Reverse2:

5'-TCT AGA CTC GAG GGA ATT AGG TAA CCT CTG-3

DMKK4_Forward1:

5'-CACC ATG GCC GAA CGA CCG AAA AAT TTG-3'

DMKK4-fusion_Reverse2:

5'- TCT AGA CTC GAG ACT CTC CGC CTG CTG ATT GGC-3

The resulting PCR products were then cloned into a pENTR vector. The pENTR Hep/Mkk4 clones subsequently contained the following important features: 5'-Not1 restriction site-CACC-Mkk4/Hep cDNA-Xba1/Xho1 restriction site-3'. The modified pENTR Hep/Mkk4 and pENTR Bsk clones then underwent Not1/Xba1 restriction. Following agarose gel electrophoresis which confirmed the presence of the restricted Hep/Mkk4 fragment(s) and pENTR Bsk fragment, the relevant bands were then excised for purification using the QIAquick gel extraction kit, (Crawley, UK) using the manufacturers protocol. Once compatible Not1/Xba1 overhangs had been generated on both the Hep/Mkk4 insert(s) and pENTR Bsk vector, the insert and vector were ligated to one another. The resulting *pENTR Hep-Bsk::HA* and *pENTR Mkk4-Bsk::Myc* entry clones were then ligated into their respective destination vectors pTWH and PTWM (Terence Murphy, Carnegie *Drosophila* Gateway® vectors) using the Gateway® system

(Invitrogen). Germline transformations were performed commercially (Best Gene, California, USA).

PCR

The reaction mix contained 300nM of each primer, 0.1-0.5µg of template DNA, 250µM of each dNTP, 10X coral load PCR buffer and 5U *Taq* DNA polymerase (Invitrogen) with a final volume of 100µl. The following PCR program was used:

Thermal Cycler conditions:

Initial denaturation	94°C	3 mins	1 cycle
3 Step Cycling			
Denaturation	94°C	45 seconds	30 cycles
Annealing	58°C	30 seconds	30 cycles
Extension	72°C	120 seconds (2min/kb of PCR target)	30 cycles
Final extension	72°C	10 minutes	1 cycle

2.2.2 Site Directed Mutagenesis

Generation of *UAS-Bsk::Myc^{T181A,Y183F}*

The following primers were used to generate the phospho mutant pENTR Bsk clone. The amino acids which have been mutated are highlighted in Green: Threonine 181 (T) → Alanine (A) and Tyrsoine 183 (Y) → Phenylalanine (F). The actual codons which are substituted to induce the mutation are highlighted in Purple.

DJNK-T181AF183Y_Forward1

5'-GGA ACT ACC TTT ATG ATG GCT CCC TTT GTG GTC ACC CGA T-3'
A181 P182 F183

DJNK-T181AF183Y_Reverse2

5'-A TCG GGT GAC CAC AA A GGG AGC CAT CAT AAA GGT AGT TCC-3'

Generation of *UAS:Hep^{K226M}-Bsk::HA and UAS:Mkk4^{K151M}-Bsk::Myc* fusion vectors

The following primers were used to generate the kinase dead pENTR *UAS:Hep^{K226M}-Bsk::HA* and *UAS:Mkk4^{K151M}-Bsk::Myc*. The amino acids which have been mutated are highlighted in green. Hep: Lysine 226 (K) → Methionine (M); Mkk4: Lysine 151 (K) → Methionine (M). The actual codons which are substituted to induce the mutation are highlighted in Purple.

HEP-K226M_Forward1

5'-G ATC ATC GCC GTG ATG CAG ATG CGA CGC ACT GG-3'
M226

HEP-K226M_Reverse2

5'-GCC AGT GCG TCG CAT CTG CAT CAC GGC GAT GAT-3'

MKK4_K151M_Forward1

5'-AC AAG GTG ATG GCC GTC ATG CGC ATT CGA TC-3'
M151

MKK4_K151M_Reverse2

5'-GA TCG AAT GCG CAT GAC GGC CAT CAC CTT GT-3'

PCR

The reaction mix contained 150nM of each primer, 10-50µg of template DNA (pENTR-Bsk vector or Hep-Bsk/Mkk4-Bsk), 250µM of each dNTP, 10X *pfu* ULTRA™ HOTSTART Reaction Buffer and 2.5U *pfu* ULTRA™ HOTSTART DNA Polymerase (Quickchange®, Statagene) with a final volume of 100µl. The following PCR program was used for site directed mutagenesis:

Thermal Cycler conditions:

Initial denaturation	95°C	30 seconds	1 cycle
3 Step Cycling			
Denaturation	95°C	30 seconds	25 cycles
Annealing	58°C	30 seconds	25 cycles
Extension	72°C	4 mins (2min/kb of PCR target)	25 cycles

The amplification products were then restricted with Dpn-1 (New England Biolabs) at 37°C for 1 hour to ensure digestion of the parental methylated and hemimethylated DNA. The mutated DNA was then transformed into one shot of TOPO® competent cells (Invitrogen) using the manufactures protocol (QuikChange® II Site-Directed Mutagenesis Kit, Statagene). The subsequent cloning strategy outlined in the pENTR™ Directional TOPO® cloning kit (Invitrogen) was then used to clone the mutated pENTR vectors, *Bsk*^{T181A,Y183}, *Mkk4*^{K151M}*-Bsk, Hep*^{K226M}*-Bsk* into the relevant pTWM and pTWH destination vectors (Terence Murphy, Carnegie *Drosophila* Gateway® vectors) using the Gateway® system (Invitrogen). Germline transformations were performed commercially (Best Gene, California, USA).

2.2.3 Sequencing

Double stranded plasmid DNA was sequenced commercially (Geneservice, Cambridge, UK) using M13 Forward and M13 reverse primers as well as internal Hep, Mkk4 and Bsk primers. Data analysis was carried out using Sequencher® 4.9.

DNA samples were sequenced at the following stages:

- Sequencing took place to ensure that PCR had correctly amplified the DNA template, free of mutations.
- The pENTR clones containing the relevant gene, i.e. Hep, Mkk4 or Bsk, were then sequenced to ensure that the required gene had been successfully incorporated and correct directional cloning had taken place.
- Sequencing of the final destination vector, containing the gene of interest was carried out, to ensure that the construct was free of errors and ready to send off for microinjection.

2.2.4 Ligations

Ligation and transformant conditions had to be optimized to ensure a sufficient number of transformant colonies containing the successfully ligated construct were obtained. Prior to ligation the vector was dephosphorylated by adding 10 Units of Calf Intestinal Alkaline Phosphotase (CIP) for 1 hour at 37°C (New England Biolabs), to prevent self-ligation. Optimised ligation conditions included using a low final reaction volume (10µl) approximately 50ng of previously digested and dephosphorylated vector (pENTR clone, containing the gene of interest), 20ng of insert (DNA fragment), 400U of T4 DNA ligase and 10 X ligase buffer (New England Biolabs). The ligation mix was incubated overnight

at 18°C and 1µl of the total reaction mixture was used to transform one shot of DH5α™ cells (Invitrogen).

2.2.5 Transformations and DNA plasmid preparation

Transformation of DH5α™ cells (Invitrogen) or one shot of TOPO® competent cells (Invitrogen) with plasmid DNA occurred at the following stages:

● 2 µl of DNA plasmid containing the pENTR vector (with the relevant gene of interest) was used to transform one shot of TOPO® competent cells (Invitrogen) using the manufactures protocol (pENTR™ Directional TOPO® cloning Kits, Invitrogen). A quantity of 250µl of the transformation reaction was then plated onto LB plates containing 50 µg/ml of kanamycin and incubated for 16 hours at 37°C. Five colonies of transformed TOPO® competent cells were selected at random and cultured in 5ml of LB growth media (Q biogene) containing 50 µg/ml of kanamycin, for 16 hours at 37°C with shaking at 225 rpm. The following day 1.5 ml of each cell suspension was centrifuged for 10 minutes at 13,000 rpm and supernatant discarded. Purified plasmid was extracted from the resulting pellet by use of the QIAGEN miniprep kit (Qiagen, Crawley, UK). The fidelity of the purified DNA was confirmed by sequencing (Geneservice, Cambridge, UK).

● 1 µl of DNA plasmid containing the final destination vector (with the relevant gene of interest) was used to transform one shot of TOPO® competent cells (Invitrogen). The following protocol was used as above with the exception of ampicilin LB plates (100µg/ml) being used to plate the transformation reaction. This is since unlike the pENTR vector which contains a kanamycin resistance gene, the destination vectors

consist of an ampicilin resistance gene. The QIAGEN miniprep kit was then used to obtain purified plasmid and the fidelity of the purified was confirmed by sequencing (Geneservice, Cambridge, UK). To obtain a sufficient quantity of plasmid DNA for microinjection (50-100 μg), 100 μl of the relevant glycerol stock (containing E-coli cells incorporating the relevant plasmid DNA) were grown for 16 hours in 200ml of LB growth media with 100 μg/ml of ampicilin. The following day the cells were centrifuged at 4,000 rpm for 10 minutes at 4°C. Purified plasmid was then obtained from the resulting pellet via the use of the QIAGEN maxiprep kit (Qiagen, Crawley, UK). The DNA was then eluted in 100 μl of TE buffer.

2.2.6 Glycerol stocks

*Glycerol stocks are composed of 500 μl of the transformant reaction mixture, (which consists of E-coli cells in mid-log phase, with the relevant incorporated plasmid DNA) and 500 μl of 80% glycerol. Glycerol stocks of all the relevant pENTR clones and destination constructs were preserved at -80°C.

2.2.7 Quantification of plasmid DNA

Purified plasmid DNA was quantified using a spectrophotometer. The DNA was diluted 1:200 in dH_2O and the absorbance was read at 260nm, using dH_2O as the blank. The following formula was used to calculate the DNA concentration of the plasmid:

$$\frac{OD_{260} \times 50 \times \text{dilution factor} \times \text{initial sample volume}}{1000} = \text{concentration } \mu g/\mu l$$

2.2.8 Agarose Gel Electrophoresis

To determine the size of linearised DNA fragments or to detect the presence of plasmid double stranded DNA, 1–5µl of the DNA sample, along with 2 µl of 6x blue loading buffer (Promega), made up to a final volume of 12 µl (with dH_2O) was run on an agarose gel (containing 0.5µg/µl of ethidium bromide) at 100V for 30 minutes. DNA bands of interest were then visualized under UV light.

2.3 *Drosophila* S2 cells in culture

Drosophila S2 cells were maintained at 25°C in Schneider's media, supplemented with 10% fetal bovine serum.

2.3.1 S2 cell transfections using the pMT-GAL4 system

S2 transfections were performed using the pMT-GAL4 binary system (Klueg et al., 2002). Briefly, 2 x 10^6 cells (50% confluent) were plated in 2 mls of medium 24 hrs prior to the transfection. 2µg of pUAST and 2µg of pMT-GAL4 plasmids were then added per well (90% cell confluent stage), along with 30µl of Cellfectin (Invitrogen) in 2 ml of Schneiders antibiotic-free Media. The media was removed 3 hrs post- transfection and replaced with Schneider's media, supplemented with 10% fetal bovine serum, 1% streptomycin (Gibco BRL). 12 hours later, media was replaced with media containing 1% $CuSO_4$ to induce protein expression.

2.3.2 Protein harvesting from S2 cells

S2 cells were subsequently harvested 24 hrs later. Cells were harvested by centrifugation at 1000*g* for 5 minutes and lysed on ice for 30 minutes in RIPA buffer [10mM Tris (pH 7.4), 10mM NaH_2PO_4, 150mM NaCl, 1% Triton X-100], supplemented with protease and phosphatase inhibitors (Halt® protease inhibitor from Pierce, 10mM NaF and 1mM Na_3VO_4). Lysates were spun for 10 minutes at 21,000*g*. The supernatant was added to reducing sample loading buffer (2X) in equal quantity.

2.3.3 Western Blotting and Protein detection

Reduced protein samples were run on 10% polyacrylamide Tris-HCl gels and transferred to Invitrolon® membranes (Invitrogen), using standard methods (Bio-Rad). Immunoblots were probed with phospho-JNK (Cell Signalling, no.9255, 1:1000) and JNK1 (Santa Cruz Biotechnology, sc-571, 1:4000), Hep (ab1956; 1:2000 and ab1957; 1: 250) and Mkk4 antibodies (ab1954 and 1955; both at 1:5000). Additional antibodies used were GFP (Molecular Probes, A11122, 1:4000) and myc (Santa Cruz Biotechnology, clone 9E10, 1:4000) using standard protocols. Blots were developed with Pico-ECL chemiluminescence reagents (Pierce) and exposed to ECL hyperfilm (Amersham Biosciences).

CHAPTER 3: Bsk is required for mediating axon stabilisation in MB neurons by preventing axon degeneration.

3.1 Introduction

In this chapter I show that the activity level of the Drosophila JNK *Bsk* is crucial in mediating axon stability *in vivo*. Complete loss of the Drosophila JNK Basket (*Bsk*), using a null mutation, results in axon degeneration of Mushroom Body (MB) neurons in the fly brain, whereas a *Bsk* hypomorphic mutation culminates in a higher frequency of MB axon overextensions. Furthermore axon degeneration is a late onset phenotype in *Bsk* null MB neurons and becomes manifest in later stages of pupal development. Loss of function of *Bsk* also affects OL and AL axon projections, and culminates in axon targeting defects in both neuron subtypes.

MB neurons were used as a primary model to analyse Bsk signalling *in vivo*, however to determine whether Bsk regulates the patterning of different types of neurons, antennal lobe (AL) and optic lobe (OL) contralateral projection neurons were analysed (Figure 3.1.1 A). The Drosophila MB neuron is a paired neuropile structure (Figure 3.1.2 A) involved in higher order processes such as memory, learning and courtship. The three sets of MB neurons which form the adult MB are known as γ, α'/β' and α/β and are sequentially derived from common neuroblast precursors (Lee et al., 1999). Each MB neuron extends a primary neurite that gives rise to dendritic branches in the calyx (located in close proximity to the cell body) and an axon that extends anteriorly and ventrally through the peduncle. Each adult γ-neuron consists of only a medial branch, whereas the α'/β' and the α/β neurons bifuricate to form a dorsal and medial branch (Figure 3.1.1 B). The dorsal lobes of wild type axons terminate close to the anterior

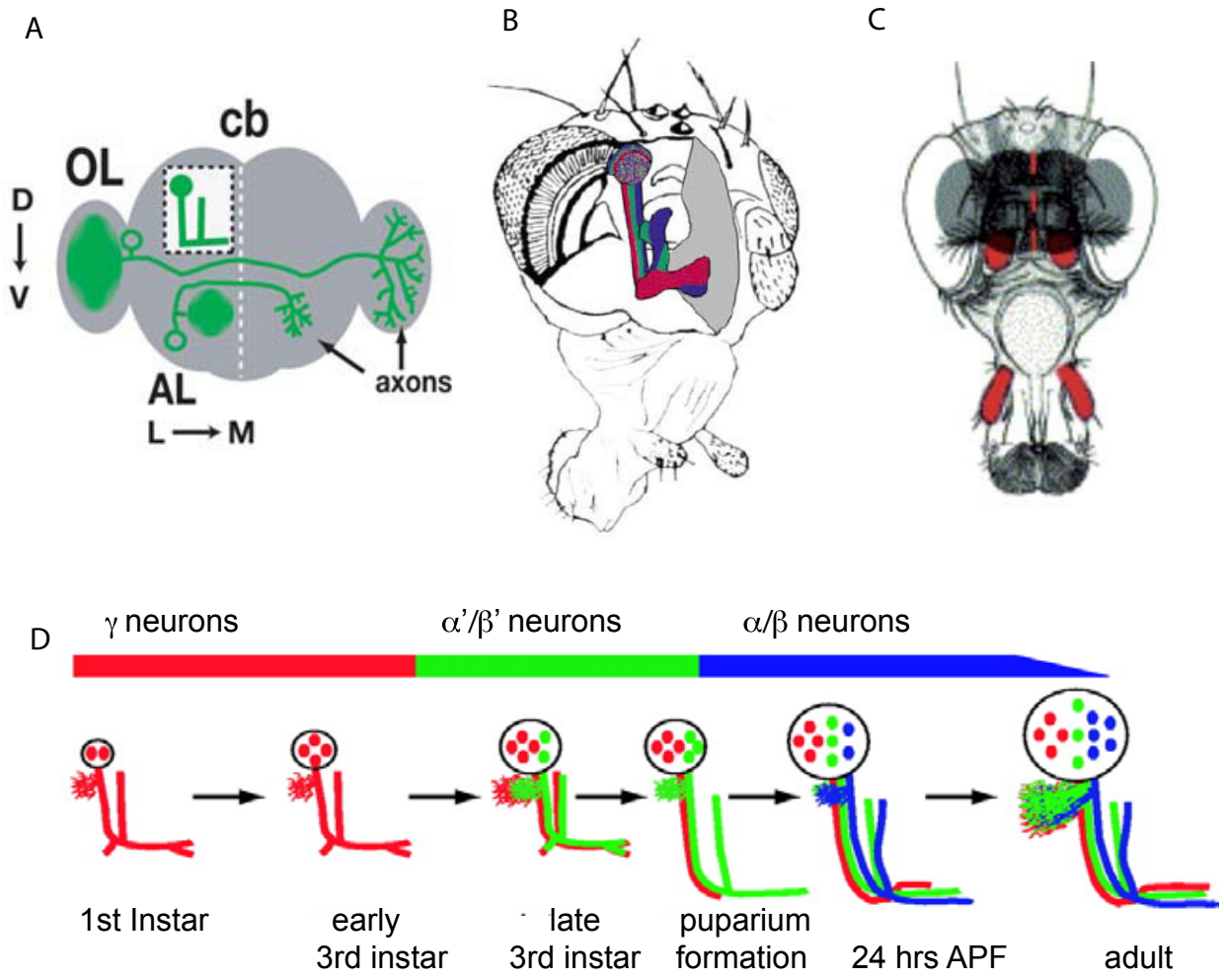

Figure 3.1.1 MB neurons in the Drosophila Brain

(A) Schematic diagram of the Drosophila adult brain displaying the location of the OL, AL and MB neurons. Dashed white line represents the midline (Adapted from Ng and Luo, 2004). **(B)** Lateral view of the fly head, cut away to reveal the location of the γ, α'/β' and α/β neurons in the adult MB, each subset of neurons is depicted as red, green and blue respectively. (Adapted from Martini and Davis, 2005) **(C)** Anterior view of the fly head, with the location of the brain superimposed. Red dashed lines represent the midline (Adapted from Wu and Luo, 2006a). **(D)** Schematic diagram of mushroom body development. Each separate class of MB neurons is colour coded and the developmental time period in which they are born is also indicated (Adapted from Lee et al, 1999)

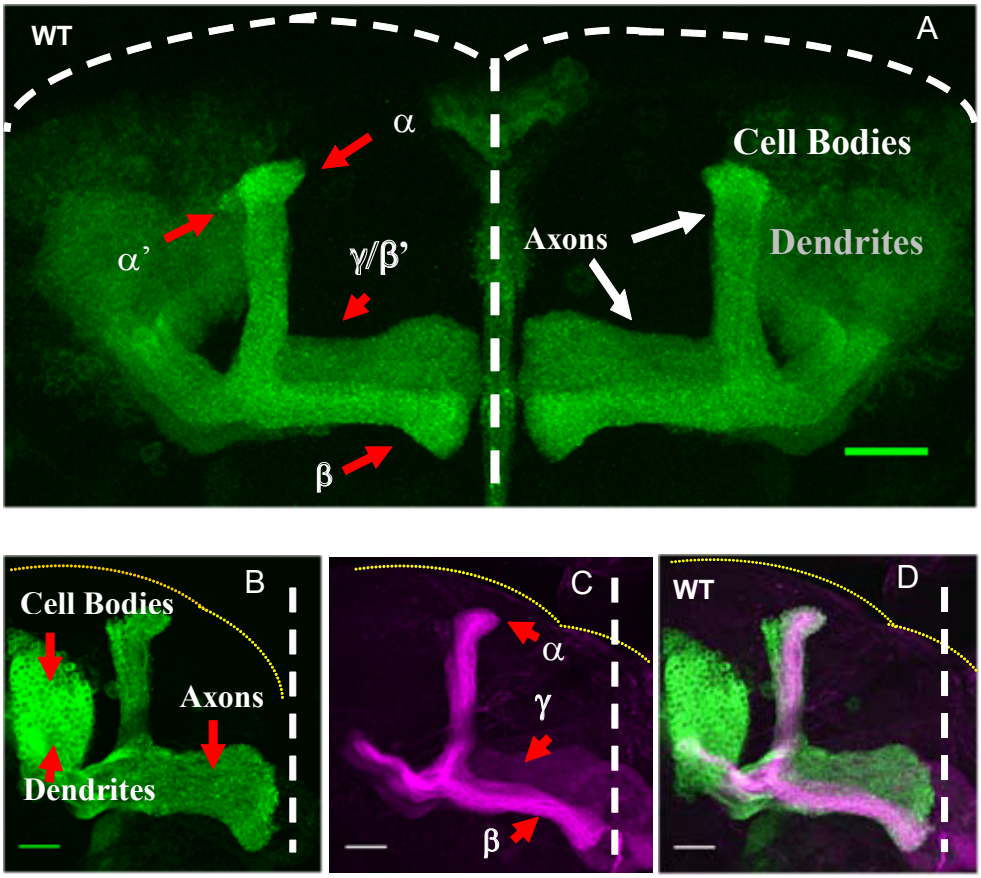

Figure 3.1.2 Wild Type MB neuron projections

(A) Image of Wild Type MB neurons, labelled with the epifluorescent CD8-GFP marker using an inducible GAL4-OK107 enhancer trap line. The Drosphila MB neuron is a paired neuropile structure exhibiting bilateral symmetry. Each neuropile consists of 2500 neurones. **(B)** Image of a wild type MB neuroblast clone, consisting of approximately 400 MB neurons. The OK107-GAL4 driver was used together with one copy of the epifluorescent CD8::GFP market to visualise MB neurons. Red arrows indicate the location of cell bodies, dendrites and axons. **(C)** The early-born class of γ neurons and the later-born subsets of α/β neurons can be discerned, since they were immunostained with FasII, an axonal marker. FasII staining is absent in the α′/β′ neurons, weak in the γ lobes and strong in the α/β neurons. **(D)** Overlap between CD8-GFP positive axons and FasII labelled MB axons. The white dashed line denotes the midline and the yellow dotted line demarcates the boundary of the Drosophila brain. Scale Bars: 20 μm. Genotypes are as follows: (A) *UAS-mCD8-GFP/+;GAL4-OK107/+* (B) *hs-Flp, UAS-mCD8-GFP/+;FRT40A, GAL80/FRT40A; GAL4-OK107/+*

cortex and the medial lobes of wild type axons terminate at the proximity of the midline.

In Drosophila, the three major subsets of MB neurons: γ, α'/β' are α/β recognised by morphological characteristics and by the developmental time period in which they born. The γ class of MB neurons are born in embryos and early larvae; the α'/β' class in late larvae; and the α/β class after puparium formation (Lee et al, 1999). During metamorphosis, pruning occurs, the larval specific axon branches re-elaborate and only the medial projections that give rise to the adult γ lobe remain (Figure 3.1.1 D). The expression pattern of Fascilin II (FasII) an axonally localised cell adhesion molecule is revealed by FasII staining in MB neurons (Figure 3.1.2 C), which strongly stains the α and β lobes, whereas the faint staining of the γ lobe corresponds to the relative low expression of FasII in this region (Crittenden et al, 1998).

3.2 *Drosophila* JNK is highly active in MB neurons

In order to determine *Bsk* activity in MB neurons, antibodies were used in whole-mount immunohistochemistry. Using a human JNK-1 antibody that cross-reacts with the Drosphila protein, I detected *Bsk* in MB axons, although the staining was at an overall high level in the whole Drosophila Brain (Figure 3.2.1 A''). I next used a phospho-specific antibody that is able to detect active forms of JNK. Bsk was highly phosphorylated in adult MB axons and AL neurons (Figure 3.2.1 A'). As antibody controls, JNK and phospho-JNK immunoreactivity were not present when *Bsk* was lost or its activity inhibited. Since it was very difficult to visualise phospho-JNK staining in *Bsk* mutant neuroblast clones, due to the small proportion of mutant clonal tissue in the adult brain, I consequently decided to express either *Bsk* RNAi or *Bsk* Dominant Negative

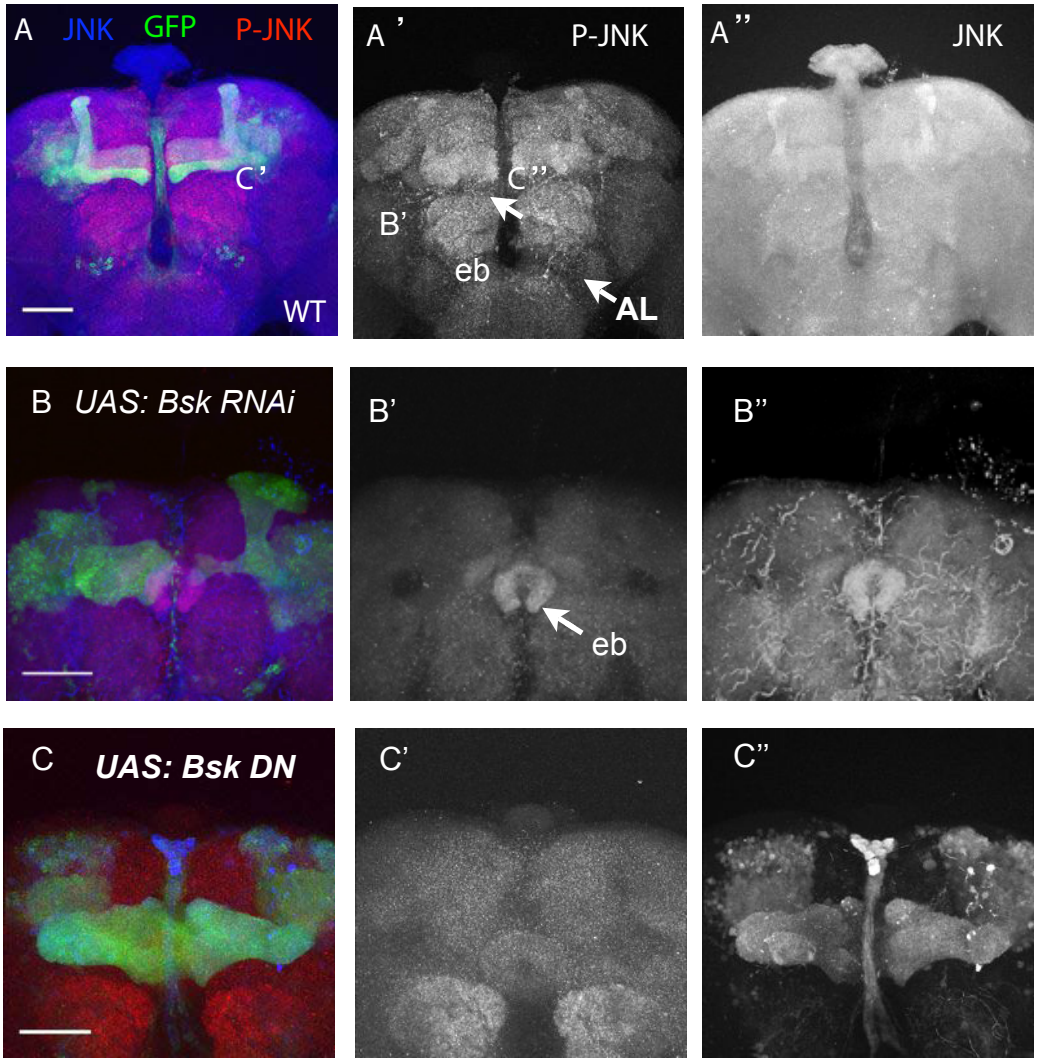

Figure 3.2.1 JNK is highly expressed in Adult MB axons and dendrites (A-A''). In whole-mount brains, wild type MB neurons, labelled with the CD8-GFP **(A)** and immunostained with anti-phospho JNK **(A')** and anti-JNK1 **(A'')** showed high levels of P-JNK/JNK signals. **(B-C'').** In identical immunostaining protocols MB neurons expressing Bsk RNAi **(B)** or DN Bsk **(C)** showed a strong reduction in P-JNK levels **(B', C')**. Loss of JNK signals were also observed by Bsk RNAi treatment **(B'')**, together with the expected increase in JNK signals due to ectopic DN Bsk expression **(C'')**. High P-JNK activity was also observed in other brain regions such as the antennal lobe (AL) and ellipsoid body (eb) as indicated. Scale Bar: 50 μm. Genotypes are as follows: *(A) UAS-mCD8-GFP/+; GAL4-OK107/+* (B) *UAS-mCD8-GFP/+; UAS-Bsk RNAi VDRC 31439/+; UAS: Dcr2; GAL4-OK107/+* (C) *UAS-mCD8-GFP/UAS-Bsk DN(X); UAS-Bsk DN(III)/+;GAL4-OK107/+*

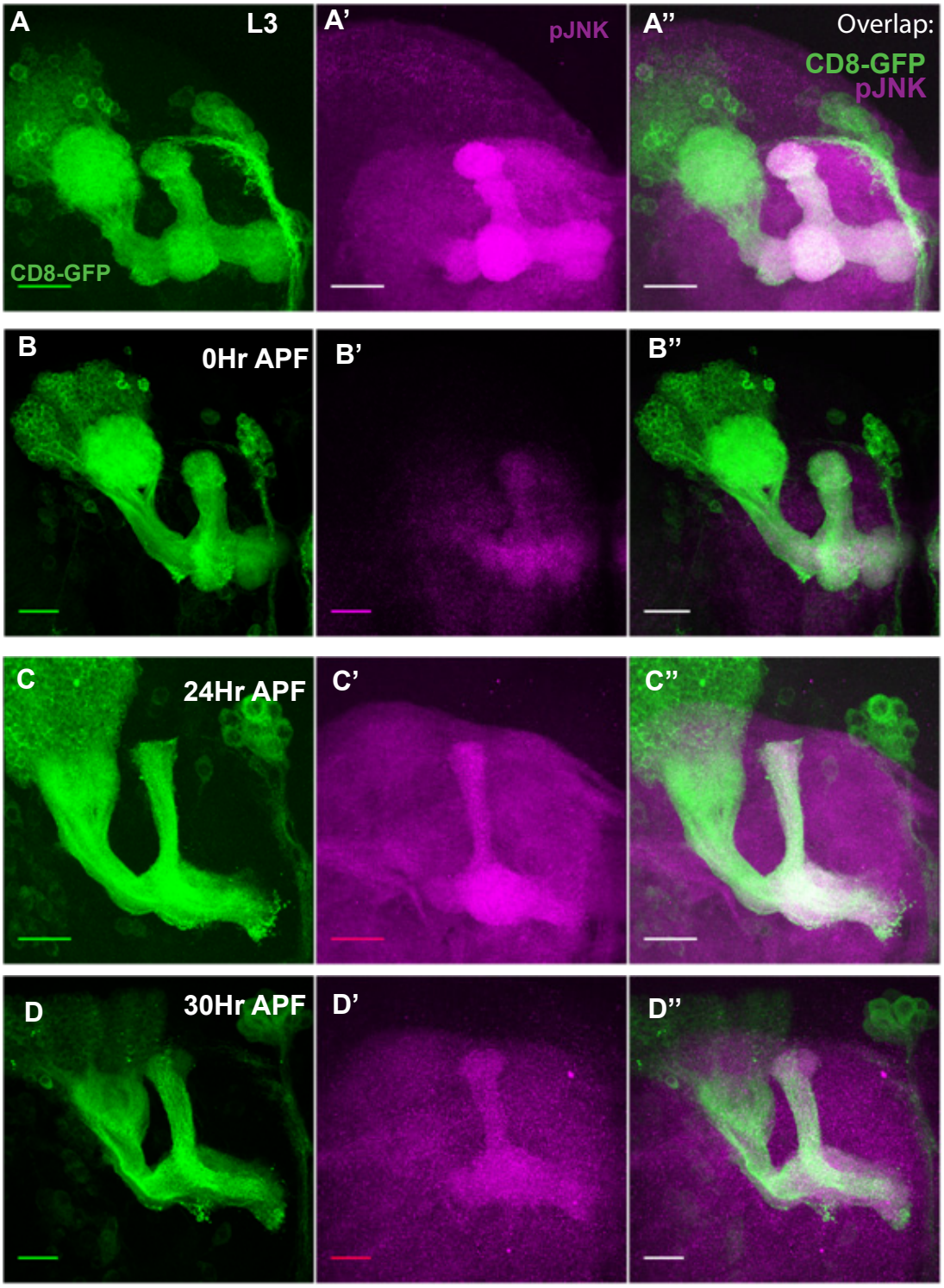
A
L3
CD8-GFP
A'
pJNK
A''
Overlap:
CD8-GFP
pJNK
B
0Hr APF
B'
B''
C
24Hr APF
C'
C''
D
30Hr APF
D'
D''

Figure 3.2.2

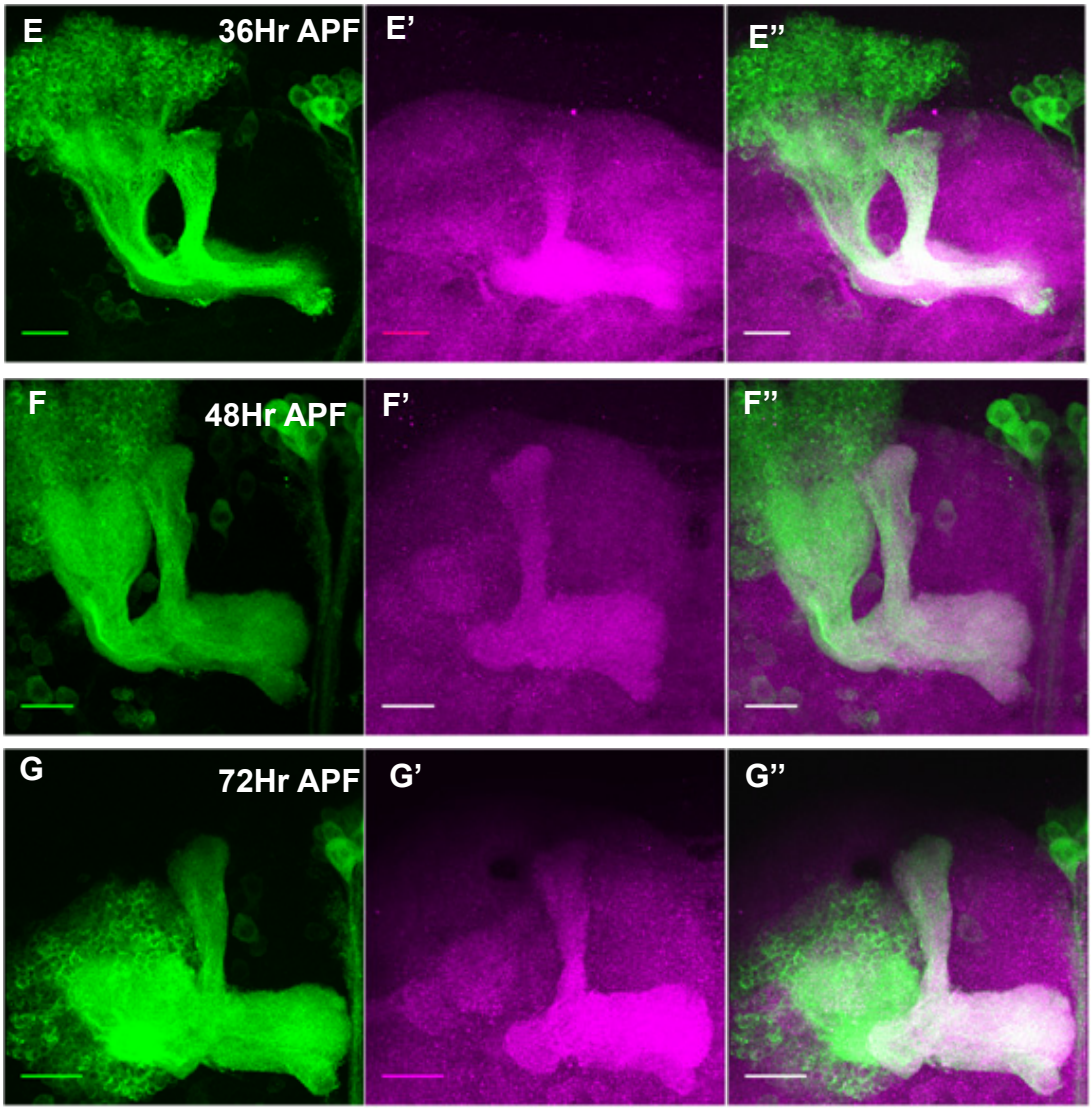

Figure 3.2.2 JNK is highly expressed in MB axons and dendrites during development. The left panels show GFP labelled axons at various developmental stages from wandering larvae L3, **(A)** and different time points After Puparium Formation as indicated in hours in descending order: 0Hr APF **(B),** 24Hrs APF **(C)**, 30Hrs APF **(D)**, 36Hrs APF **(E)**, 48Hrs APF **(F)**, 72Hrs APF **(G).** The corresponding Phospho JNK stainings of the same brain at various developmental stages, are indicated in hours in descending order **(A'-G')**. Forty samples were analysed for each time point, and the representative image at each developmental period is shown. The right panels display the corresponding overlap between phospho JNK and the GFP labelled MB axons at these particular stages **(A''-G'').** Green, CD8-GFP, Magenta, pJNK. Scale Bars 20 μm. Genotypes are as follows: (A-G): *UAS-mCD8-GFP/+;GAL4-OK107/+*

transgenes in MB neurons utilising the UAS-GAL4 system (See Chapter 2 – Methods). This enabled me to clearly visualise the absence of phospho JNK immunoreactivity in a larger population of MB neurons (Figure 3.2.1 B-C). I also analysed Bsk activity at different time points during development, the results clearly show that Bsk activity is maintained at a high level throughout MB neuron development, from the wandering L3 larvae stage to adulthood (Figure 3.2.2). It is also interesting to note that there maybe possible fluctuations in the levels of phospho JNK during MB neuron development, however I have not yet analysed this in depth. Nevertheless the immunohistochemical data in Figure 3.2.2 clearly shows that an elevated level of phospho JNK staining is solely confined to MB neurons during development.

3.3 *Bsk* loss results in axon destabilisation culminating in degeneration in MB neurons

Since, JNK signalling was highly active in MB neurons throughout development and in adulthood this shows it may be playing a crucial function in axonal morphogenesis; I then examined the effect of *Bsk* inactivation. To analyse the loss of function of Bsk, homozygous null *Bsk* clones were generated in newly hatched larvae. In contrast to wild type adult MB neuroblast clones (Figure 3.3.1 A) which consist of approximately 216 ± 24 neurons per MB neuroblast clone (Ito and Hotta, 1992), Bsk^{147e} adult neuroblast clones contained a reduced quantity of γ, α'/β' and α/β neurons (Figure 3.3.1 B-D). Additionally when analysed at the adult stage, the majority of Bsk^{147e} neuroblast clones axons' failed to reach their wild type termination points, this was the case for 92% of the samples analysed (Figure 3.3.1 B-D). However, a minority of *bsk* mutant axons displayed

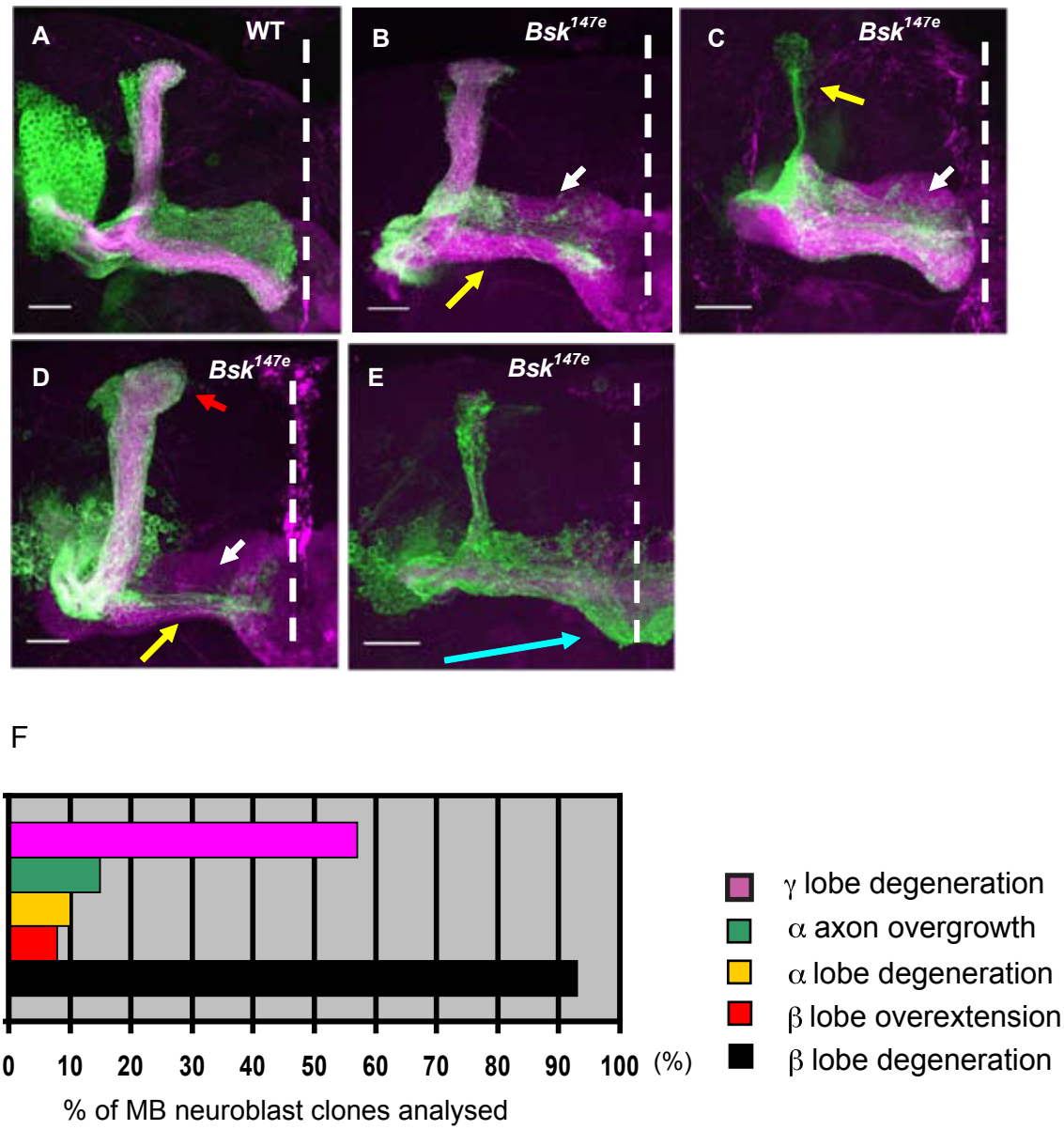

Figure 3.3.1 *Bsk* loss results in axon destabilisation.

(A) Image of a wild Type MB neuroblast clone. **(B-C)** Adult MB *bsk*^{147e} neuroblast clones exhibiting frequently observed neurodegeneration phenotypes, with axon loss/thinning of the γ neurons (white arrows) and α/β neurons (yellow arrows). Representative images show phenotypes exhibiting β-lobe degeneration **(B)**, and α-lobe degeneration **(C)**. **(D)** Adult MB *Bsk*^{147e} neuroblast clones exhibiting β/γ lobe neurodegeneration and the infrequently observed α axon overgrowth phenotype (red arrow). **(E)** Image of an adult MB *Bsk*^{147} neuroblast clone exhibiting an infrequently observed axon overextension phenotype (Blue arrow). Scale Bars 20 μm. **(F)** Quantification of phenotypes observed in adult *Bsk*^{147e} MB neuroblast clones (n=181). Genotypes are as follows (A) *hsFLP, UAS-mCD8-GFP/+; FRT40A, GAL80/FRT40A; GAL4-OK107/+* (B-E) *hsFLP, UAS-mCD8-GFP/+; Bsk*^{147e}*, FRT40/FRT40A, GAL80; GAL4-OK107/+*

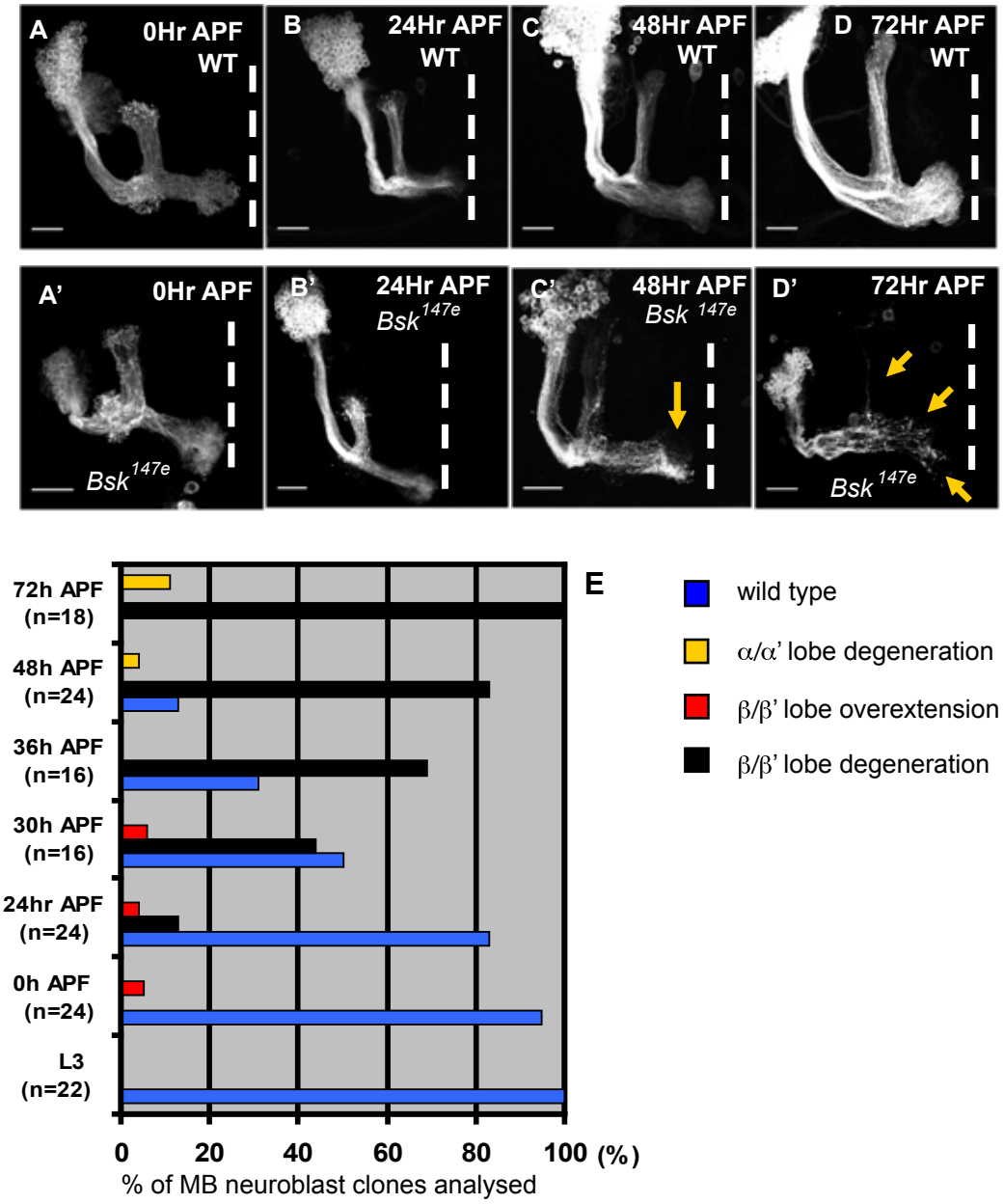

Figure 3.3.2. Progressive neurodegeneration in *Bsk* null MB neuroblast clones occurs in late pupal phases of development

Images of wild type MB neuroblast clones at specific development time points: 0Hr APF **(A)**, 24Hr APF **(B)**, 48Hr APF **(C)** and 72Hr APF **(D)**. Corresponding images of *Bsk*^{147e} MB neuroblast clones: 0Hr APF **(A')**, 24Hr APF **(B')**, 48Hr APF **(C')** and 72Hr APF **(D')** Areas of neurodegeneration are indicated by yellow arrows. Scale Bars 20μm. **(E)** Quantification of phenotypes observed for *Bsk*^{147e} MB neuroblast clones at the outlined time points. It is important to note that any mutant phenotypes observed prior to 24hrs APF are those of the γ neurons, since they are the only neuronal subset which are fully developed at this stage. Genotypes are as follows (A-D) *hsFLP, UAS-mCD8-GFP/+; FRT 40A, GAL80/FRT40A; GAL4-OK107/+;* (A'-D') *hsFLP, UAS-mCD8-GFP/+; Bsk*^{147e}*, FRT40/, FRT40A, GAL80; GAL4-OK107/+*

overextensions beyond their normal termination points, this phenotype was observed in 8% of the samples analysed (Figure 3.3.1 E, quantifications: Figure 3.3.1 F)

I next tested whether this majority phenotype observed for Bsk^{147e} neuroblast clones was caused from a failure of initial axon extension during initial MB neuronal development or was due to axons reaching their correct termination point and then degenerating? By analysing *bsk* null MB neuroblast clones at different stages of development. During early development of MB neurons, *Bsk* null neurons are wild type (Figure 3.3.2 A'-B'), however axonal phenotypes characteristic of the adult stage were apparent from 30 hours after puparium formation (APF) onwards. These axon defects were often subtle at early-mid pupal stages (Figure 3.3.2 C'), but become more acute at late pupal (Figure 3.3.2 D') and adult stages (Figure 3.3.1 B-D) with increasing frequency as development progresses (quantified in Figure 3.3.2 E). Together these results strongly suggest that *Bsk* loss does not result in an initial defect of axon extension but in the subsequent failure in axon stabilisation, leading to neurodegeneration and axon loss.

The vast majority of *Bsk* neuroblast clones analysed exhibited thinning of axon tracts along the main shaft of the β axon, suggesting possible axon degeneration and subsequent axon loss (yellow arrow in Figure 3.3.1 B). In order to analyse whether this axon loss can be attributed to degeneration I studied Bsk^{147e} single cell clones, which have the advantage of giving a fine resolution of the axon morphology. Multiple breaks and thinning were found along the axonal shafts of single cell Bsk^{147e} clones (Figure 3.3.3 E-F; H-I). I also uncovered similar axon breaks and thinning in the main processes close to the cell body (Figure 3.3.3 B-C), suggesting that an overall degeneration is occurring.

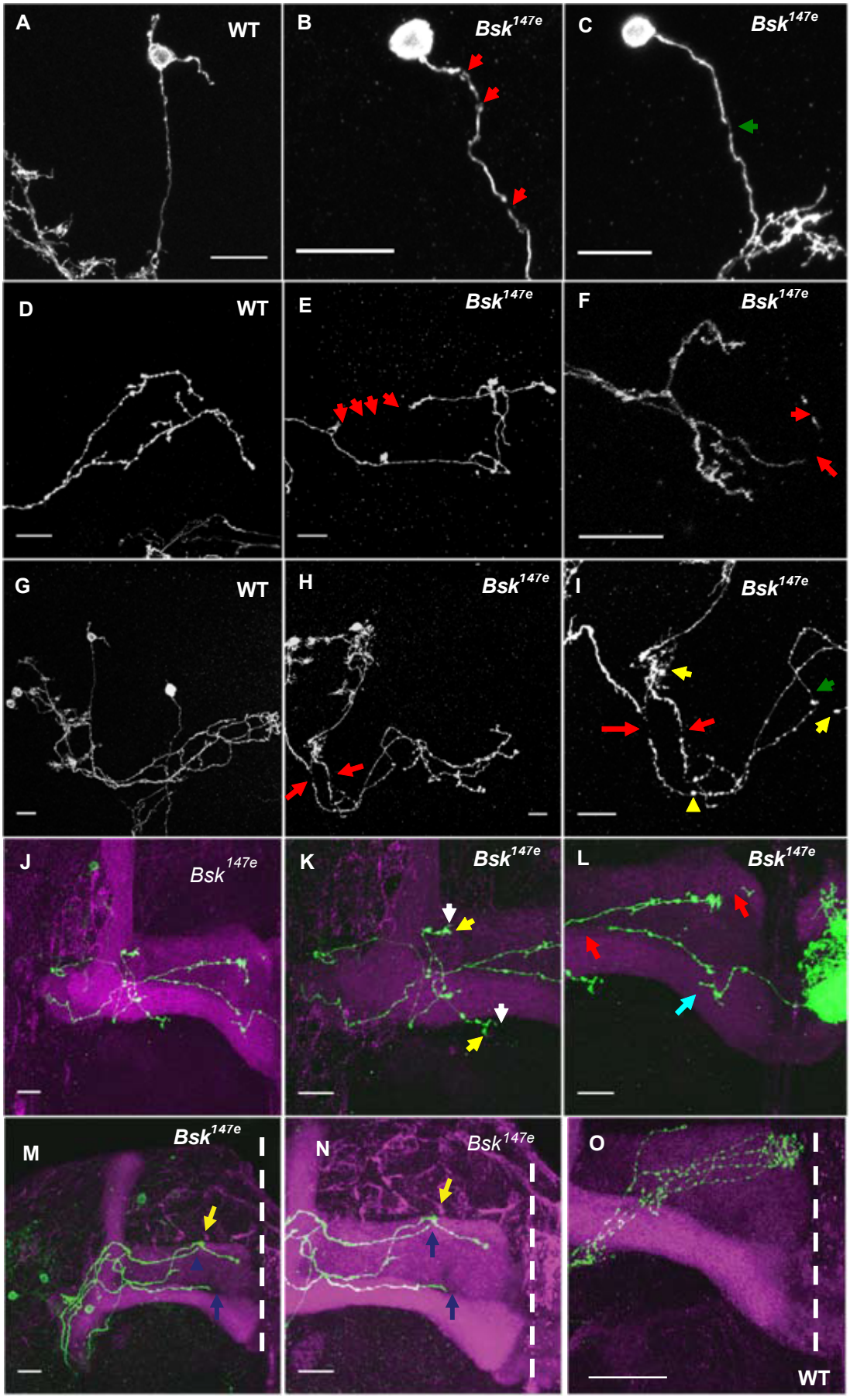
A
WT
B
Bsk147e
C
Bsk147e
D
WT
E
Bsk147e
F
Bsk147e
G
WT
H
Bsk147e
I
Bsk147e
J
Bsk147e
K
Bsk147e
L
Bsk147e
M
Bsk147e
N
Bsk147e
O
WT

Figure 3.3.3

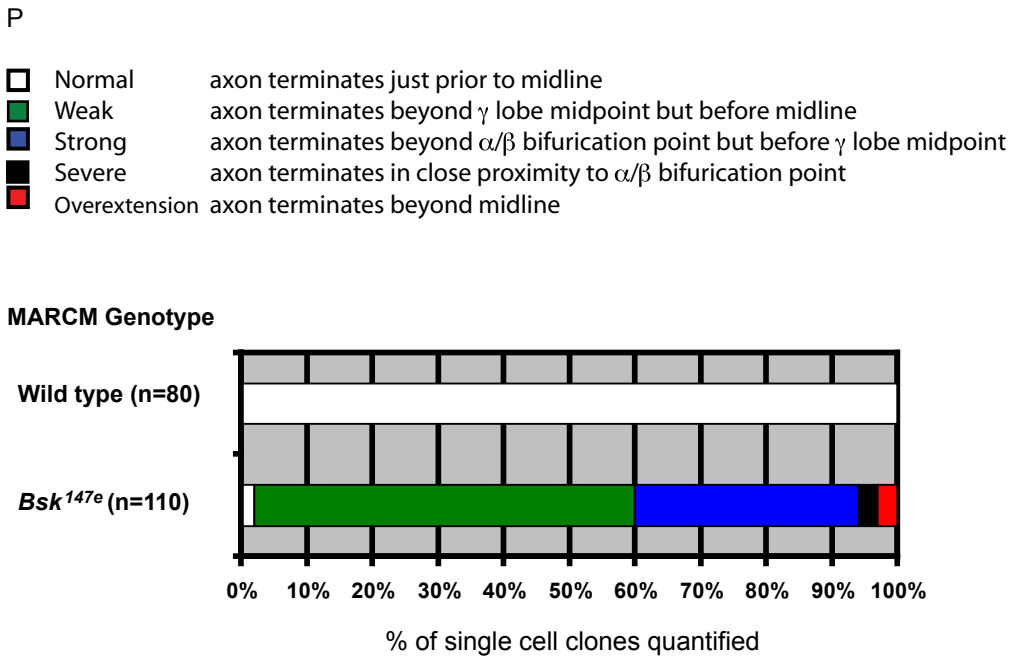

Figure 3.3.3 Neurodegeneration in *Bsk*^{147e} single cell clones of γ neurons

(A) Magnified image of a wild type single cell clone, showing the processes emanating from the cell body. **(B-C)**: Representative images of a *Bsk*^{147e} single cell clones exhibiting characteristic neurodegenerative phenotypes in the axon processes close to the cell body such as axon breaks **(B)** and axon thinning **(C)**. Axons breaks are indicated by the red arrows and axon thinning is indicated by the green arrows. **(D)** Magnified image of a wild type single cell clone, showing the mid to distal region of the axon. Representative phenotypes of *Bsk*^{147e} single cell clones exhibiting a large break in the mid-distal axon region **(E)** and smaller breaks in the axon termini **(F)**. **(G)** Overall image of entire wild type single cell clones. **(H)** *Bsk*^{147e} single cell clones exhibiting axon breakages in the proximal-mid axon region. A magnified image of this degeneration is shown in the right panel **(I)**. **(J)** Overall image of an entire *Bsk*^{147e} single cell clones exhibiting changes in axonal architecture, characterised by the presence of swellings, thin filopodia and protrusions (yellow arrows). Magnified images of mid-axon **(K)** and distal axon regions **(L)** of *Bsk*^{147e} single cell clones **(J)**. An overextending *Bsk* mutant single neuron is indicated by the turquoise arrow and a single mutant Bsk neuron terminating at the α/β bifurication point is categorised as 'strong' and indicated by the white arrow. **(M):** Overall image of entire *Bsk*^{147e} single cell clones terminating short of the midline, *Bsk*^{147e} single cell clones **(N)**, either terminate beyond the γ lobe midpoint but before the midline and can be classified as 'weak' (dark blue arrows) or terminate beyond the αβ bifurication point but before γ lobe midpoint, these neurons are categorised as 'strong' (white arrow). In contrast axons of wild type single cell clones terminate just prior to the midline, as shown in a magnified image of the axon termini **(O).** All scale bars 10μm. White dashed lines indicate the midline. **(P)** Quantification of position of axon termini in *Bsk* mutant single cell clones of γ neurons. Genotypes are as follows (A,D,G and O) *hsFLP, UAS-mCD8-GFP/+; FRT40A, GAL80/FRT40; GAL4-OK107/+* (B, C, E, F, H, I, J-N) *hsFLP, UAS-mCD8-GDP/+; Bsk*^{147e}*, FRT40A/FRT40A, GAL80; GAL4-OK107/+*

(A)

Sample no.	*Location of neurodegeneration in axon*											
	Cell Processes				Mid axon				Distal axon			
	Axon breaks		Axon thinning		Axon Breaks		Axon thinning		Axon breaks		Axon thinning	
1	0	1	0	2	0	1	0	3	0	1	0	3
2	0	0	0	1	0	1	0	4	0	1	0	4
3	1	4	0	1	0	4	1	3	0	0	0	3
4	0	3	0	3	0	0	0	4	0	0	0	3
5	0	1	0	1	0	2	0	3	0	1	0	3
6	0	0	0	2	0	1	1	4	0	0	0	1
7	0	3	0	1	0	3	0	3	0	2	0	3
8	0	0	0	2	0	2	0	3	0	1	0	3
9	0	3	0	2	0	1	0	4	0	5	0	4
10	0	1	0	1	0	1	0	3	0	0	0	1
Mean ($\bar{x}$)	0.1	1.6	0	1.6	0	1.6	0.2	3.4	0	1.1	0	2.8

(B)

	Location of neurodegeneration in axon											
	Cell Processes				Mid axon				Distal axon			
	Axon breaks		Axon thinning		Axon Breaks		Axon thinning		Axon breaks		Axon thinning	
Mean ($\bar{x}$)	0.1	1.6	0	1.6	0	1.6	0.2	3.4	0	1.1	0	2.8
SD	0.32	1.51	0	0.70	0	1.17	0.42	0.70	0	1.52	0	1.03
SEM	0.10	0.48	0	0.22	0	0.37	0.13	0.22	0	0.48	0	0.33
$(\bar{x})^2$ - $(\bar{x})^1$	1.5		1.6		1.6		3.2		1.1		2.8	
CI (95%)	0.32-2.68		1.10 – 2.10		0.76-2.44		2.54-3.86		0.01-2.19		2.06-3.54	
P value	0.0183		< 0.0001		0.0020		< 0.0001		0.0484		< 0.0001	

Figure 3.3.4

(C)

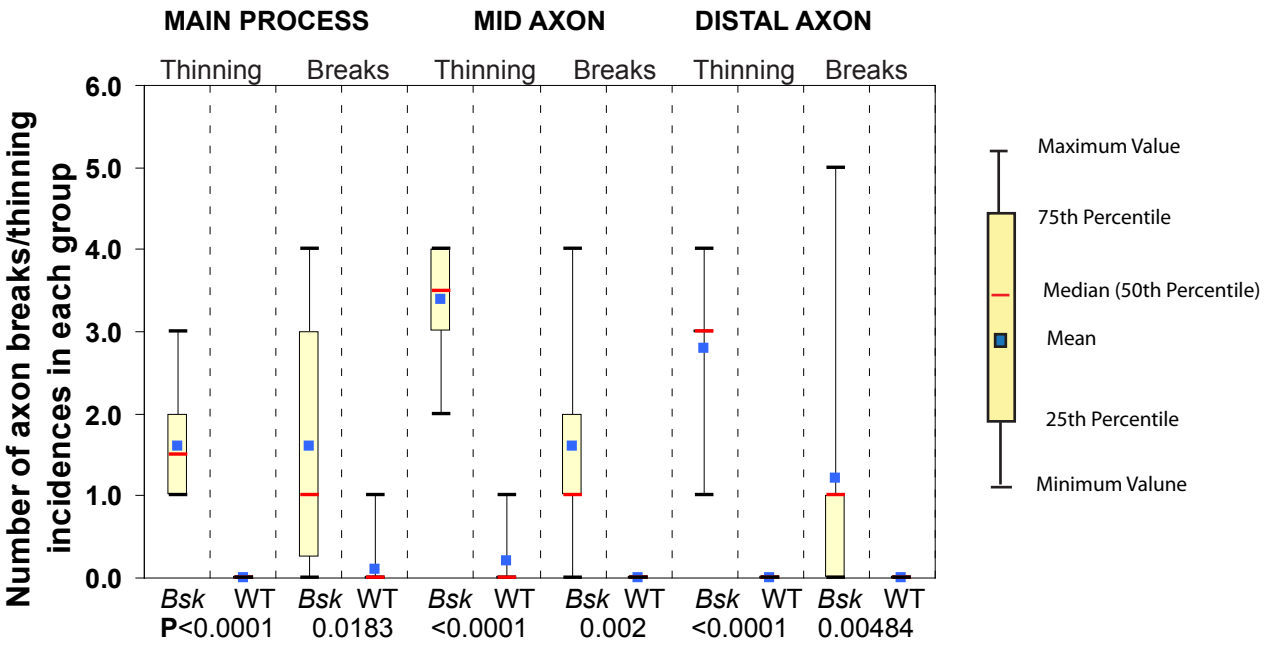

Figure 3.3.4 Neurodegeneration is statistically significant in *Bsk* null single cell clones compared to wild type single cell clones.

(A) Quantifications of axon thinning and axon breaks in Bsk^{147e} and WT single cell clones. Ten Bsk^{147e} and ten WT single cell clones were quantified. Grey cells contain wild type data; white cells contain Bsk^{147e} data. **(B)** Table showing that neurodegeneration (quantified as axon breaks and axon thinning) is statistically significant in mutant *Bsk* single cell clones of γ neurons compared with wild type single cells of γ neurons. All probability values (p values) are less than the threshold value of 0.05 therefore the null hypothesis that there is no difference in neurodegenerative phenotypes between wild type and *Bsk* single cell clones of γ neurons can be rejected. **($\bar{x}$) =** mean; SD = standard deviation, SEM = Standard Error Mean; $(\bar{x})^1 - (\bar{x})^2$ = Group 1 (mutant Bsk^{147e} mean quantity) – Group 2 (control wild type mean quantity); CI (95%) = 95% confidence interval between (specified values). **(C)** Corresponding Box plot, demonstrating that neurodegeneration is statistically significant in mutant *Bsk* single cell clones of γ neurons compared with wild type single cell clones of γ neurons.

Furthermore these neurodegenerative phenotypes in Bsk^{147e} single cell clones were also accompanied by axonal loss at the distal ends of the axons (Figure 3.3.3 M-N and quantifications Figure 3.3.3 P). The loss of *Bsk* also results in numerous alterations in the axonal architecture, I identified the presence of swellings, thin filopodia and protrusions, which do not occur in wild type axons (Figure 3.3.3 J-L). Overall these results suggest that loss of Bsk leads to axon degeneration. This neurodegeneration in *Bsk* mutant single cell clone γ-neurons occurs in all regions of the axon and is not specific to a particular region (Figure 3.3.3). Moreover when observing the frequency of axon breaks and thinning in *Bsk* mutant single cell clones compared with wild type single cell clones, statistical analysis using a paired student t-test revealed that neurodegeneration in Bsk mutant single cell clones was statistically significant in all axon regions over the control wild type group (Figure 3.3.4).

3.4 Mechanism of neurodegeneration in *Bsk* null MB neurons

In order to test whether the axon degeneration observed (Figure 3.3.1 B) was a result of a myosin II-based axon retraction process; I overexpressed dominant negative *Zipper* (the gene which encodes *Drosophila* Myosin II) in *Bsk* null Neuroblast clones. Myosin II activity has been implicated in inducing axon retraction in both in vitro (Gallo et al, 2004, Gallo, 2006, Wylie and Chantler, 2003) and in vivo settings (Billuart et al, 2001) by interacting with F-actin bundles and generating contractile forces. Therefore it would be expected that if a myosin II based mechanism was operating in *Bsk* null Neuroblast clones, to induce axon retraction, overexpression of dominant negative *Zipper* should restore wild type projection in Bsk null MB neuroblast clones. However this was not the

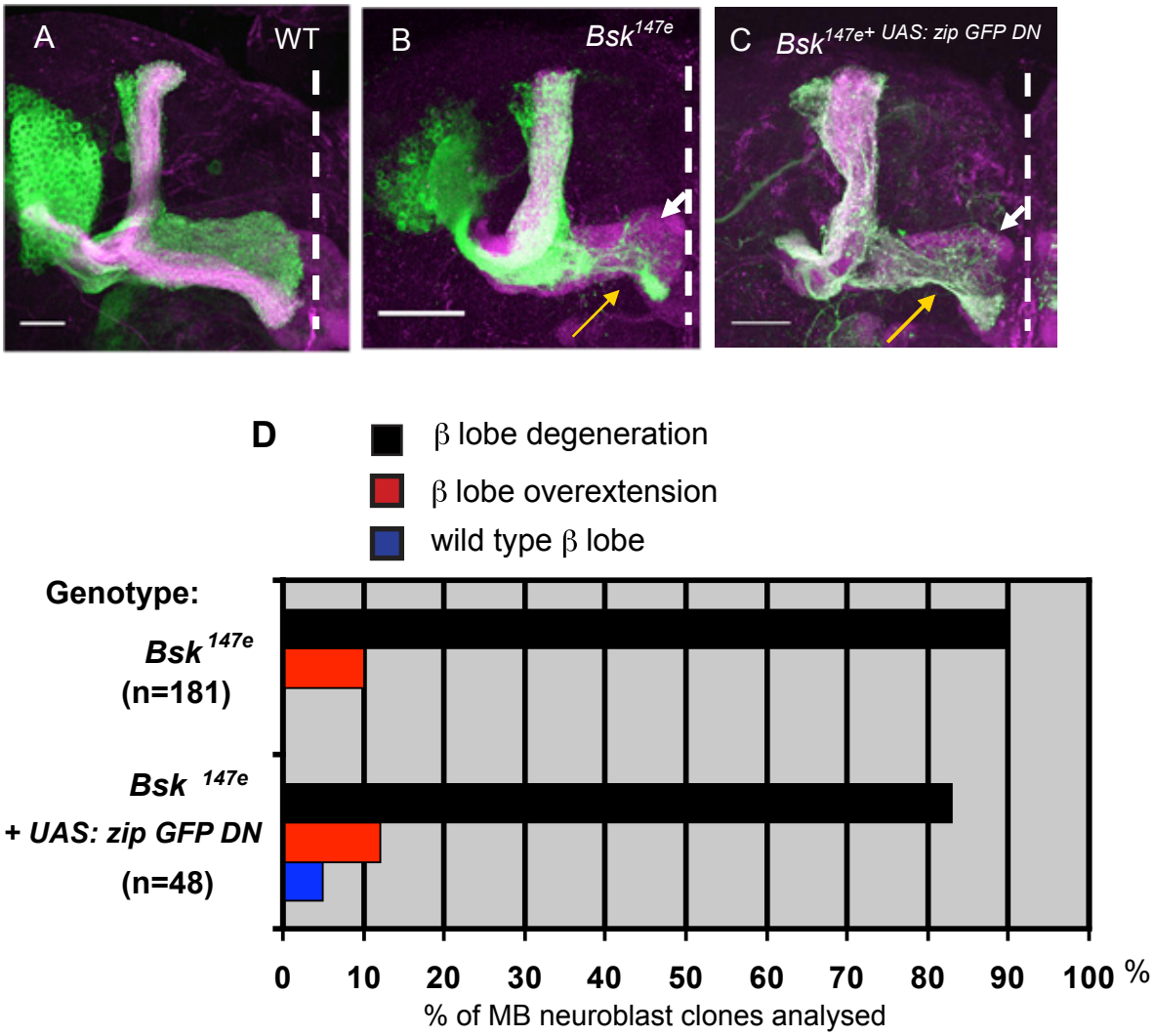

Figure 3.4.1 Axon retraction observed in *Bsk*^{147e} MB neuroblast clones in not dependent on Myosin II driven contractility.

(A) Representative image of a wild type MB neuroblast clone**. (B)** Representative image of a *Bsk*^{147e} MB neuroblast clone, exhibiting β neurodegeneration (indicated by the yellow arrow). **(C)** Overexpression of a dominant negative zipper transgene is unable to rescue the *Bsk*^{147e} null phenotype. The γ neurons which fail to terminate at their wild type termination points are indicated by the white arrows. **(D)** Quantification of the aforementioned β neuron phenotypes. Scale Bars, 20 μm. Genotypes are as follows (A) *hsFLP, UAS-mCD8-GFP/+; FRT40A, GAL80/FRT40A; GAL4-OK107/+* (B) *hsFLP, UAS-mCD8-GFP/+; Bsk* ^{147e}*, FRT40A /FRT40A, GAL80; GAL4-OK107/+* (C) *hsFLP, UAS-mCD8-GFP/+; Bsk* ^{147e}*, FRT40A /FRT40, GAL80; UAS-zip DN GFP /+; GAL4-OK107/+*

case, misexpression of dominat negative *Zipper* did not modify the morphology of axon projection in either MB or OL *Bsk* null neuroblast clones (Figure 3.4.1 C, Figure 3.7.2 H). This suggests that neurodegeneration phenotypes observed in *Bsk* null MB neuroblast clones, as well as the axon termination defects observed in *Bsk* null OL neuroblast clones, do not occur as a result of myosin mediated axon retraction.

I next decided to examine whether the neurodegeneration observed in *Bsk* null MB neurons could be rescued by ectopically expressing the baculovirus pan-caspase inhitor gene p35 in Bsk^{147e} MB neuroblast clones. Purified recombinant p35 has been shown to inhibit human caspase-1, caspase-3, caspase-6, caspase-7, caspase-8 and caspase-10 (Zho et al, 1998), additionally in *Drosphila,* expression of p35 eliminates the majority of cell death in the developing embryo and eye as well as X-irradiation induce death (Hay et al, 1994). This suggests that p35 targets an evolutionary conserved cell death pathway. In fact overexpression of *p35* in *Bsk* null MB neuroblast clones, fully rescued the vast majority of neurodegeneration phenotypes observed, restoring wild type axonal projections (Figure 3.4.2 B, quantifications, Figure 3.4.2D). This suggests that the neurodegeneration observed in *Bsk* null MB neurons is a caspase dependent process.

3.5 The Bsk^{H15} hypomorphic mutation results in a higher proportion of MB axon overextension phenotypes than in a *Bsk* null scenario

The *Bsk* deficiency *Df(2L)flp147e* (Riesgo-Escovar et al., 1996) is a small, 3-kb deletion produced by p-element imprecise excision. *Df(2L)flp147e* deletes the majority of the Bsk coding sequence, along with the kinase domain and is therefore a null allele for Bsk. I also analysed a number of *bsk* hypomorphic alleles, by generating MB neuroblast clones.

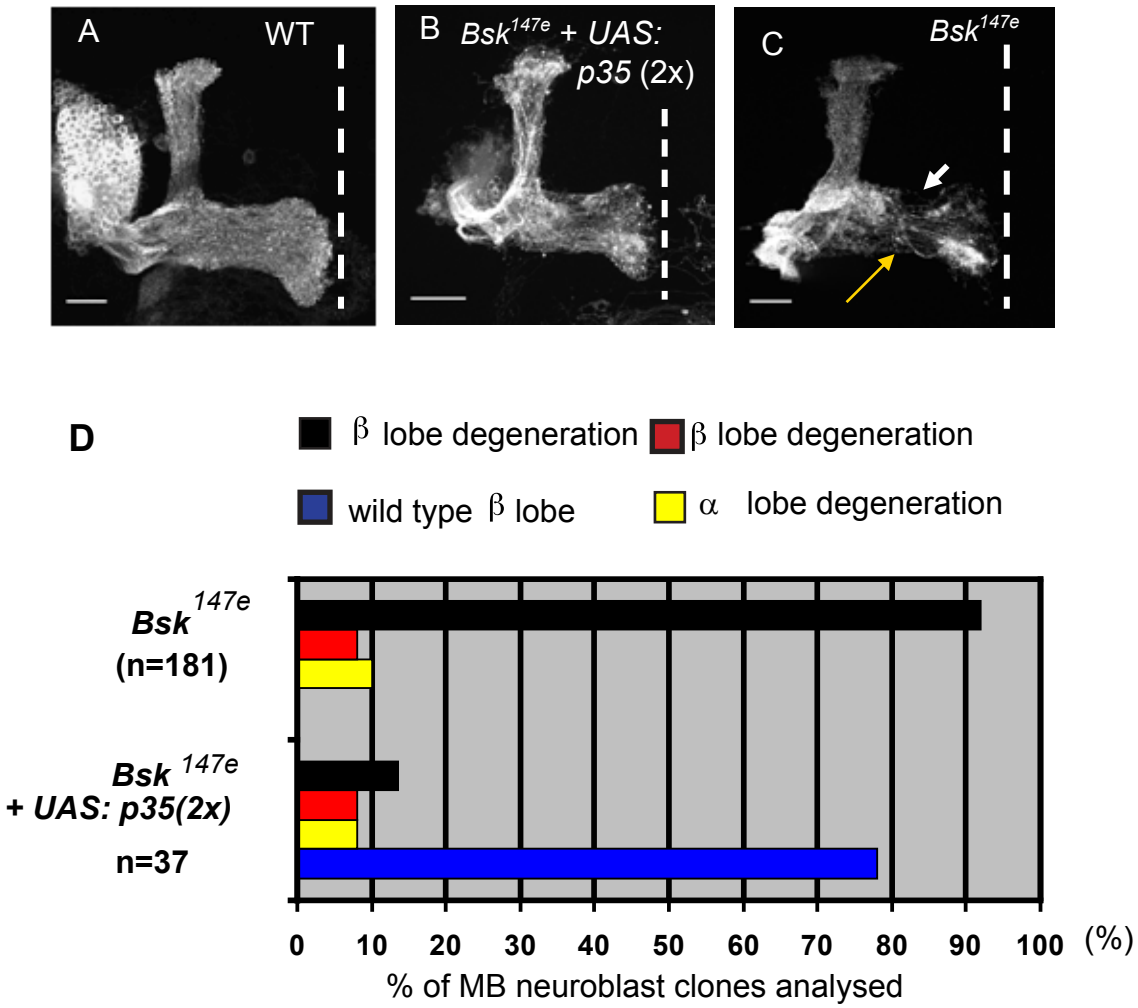

Figure 3.4.2 Overexpression of *p35* (a pan-caspase inhibitor gene), rescues the neurodegeneration phenotype observed in *Bsk* null MB neuroblast clones

(A) Representative image of a wild type MB neuroblast clone. **(B)** Ectopic expression of *UAS-p35* is able to fully rescue the degenerating axonal phenotype observed in *Bsk* null MB neuroblast clones **(C)** and restore wild type axon projections. **(D)** Quantification of the above phenotype. Scale Bars, 20 μm; CD8-GFP, white; 2 copies of *UAS-p35* are indicated in parenthesis as 2x. Yellow arrows indicate degenerating β neurons, while white arrows signify γ-lobe degeneration. Genotypes are as follows (A) *hsFLP, UAS-mCD8-GFP/+; FRT40, GAL80/FRT40A; GAL4-OK107/+* (B) *hsFLP, UAS-mCD8 /UAS-p35; FRT40A, GAL80/Bsk^{147e}, FRT40A; UAS-p35/+; GAL4-OK107/+* (C) *hsFLP, UAS-mCD8/+; FRT40A, GAL80/Bsk^{147e}, FRT40A; GAL4-OK107/+*

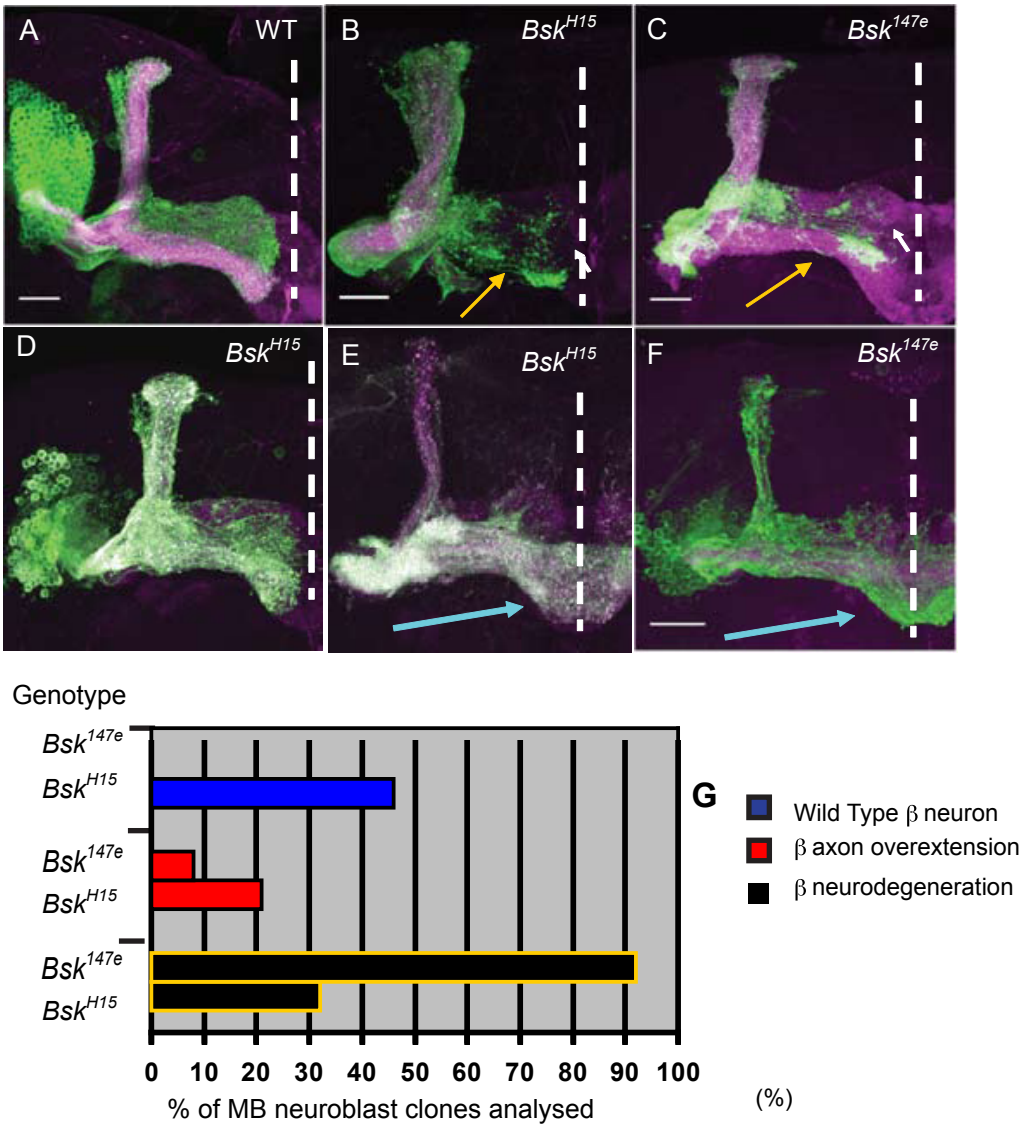

Figure 3.5.1. *Bsk*^{H15} Adult MB neuroblast clones exhibit hypomorphic phenotypes

(A) Image of a wild type adult MB neuroblast clone. **(B-C)** Representative images of *Bsk*^{H15} **(B)** and *Bsk*^{147e} adult MB neuroblast clones **(C)** exhibiting neurodegeneration in the mid axonal region of the β lobe (indicated by the yellow arrow). Since the degree of neurodegeneration seems to have occurred at a faster rate in this area, a dense accumulation of axons remain at the distal end of the β lobe (indicated by the white arrow). **(D)** Represenentative image of a *Bsk*^{H15} adult MB neuroblast clone exhibiting wild type β axon projections. **(E-F)** Representative images of *Bsk*^{H15} **(E)** and *Bsk*^{147e} MB adult neuroblast clones **(F)** displaying overextension of the β lobe (indicated by the light blue arrow). **(G)** Quantification of phenotypes observed in β axons of adult *Bsk*^{H15} MB neuroblast clones (n = 28). For comparative purposes the equivalent quantifications for adult *Bsk*^{147e} MB neuroblast clones (n = 181) are also included. n, number of neuroblast clones analysed, scale bars = 20 μm. *Genotypes are as follows* (A) *hsFLP, UAS-mCD8-GFP/+; FRT40, GAL80/FRT40A; GAL4-OK107/+* (B, D, E) *hsFLP, UAS-mCD8-GFP/+; FRT40A, GAL80/Bsk*^{H15} *, FRT40A; GAL4-OK107/+* (C, F) *hsFLP, UAS-mCD8-GFP/+; FRT40A GAL80/Bsk*^{147e}*, FRT40A; GAL4-OK107/+*

Bsk^{1} and *Bsk*^{2} MB neuroblast clones exhibited wild type projections. However *Bsk*^{H15} MB neuroblast clones displayed axonal defects. The *Bsk*^{H15} genetic lesion is a missense mutation (I212F) consisting of single amino acid substitution in the *Bsk* kinase domain (Berger et al, 2008). Loss of function analysis showed that a large proportion of the *Bsk*^{H15} β axons were wild type, 46% in total (Figure 3.5.1 D), 32 % gave degeneration defects, resembling those observed in *Bsk* null MB neuroblast clones (Figure 3.5.1 B-C), while 21% exhibited axon overextension phenotypes (Figure 3.5.1 E-F). Overall this data demonstrates that while the *Bsk* null allele results in predominantly axon degeneration, weaker loss of function alleles result in a shift towards axon overextension and a lower frequency of neurodegeneration (quantifications, Figure 3.5.1 G).

3.6 JNK phosphorylation is critical for axonal morphogenesis

Two JNKKs Hep (also known as Drosophila MKK7) and MKK4 are predicted to phosphorylate Bsk at two residues on threonine 181 and tyrosine 183 (Glise et al., 1995); (Han et al., 1998). I decided to investigate the relevance of these sites by generating a Bsk mutant construct that removes the phospho-acceptor sites: UAS: Bsk::Myc$^{T181A, Y183F}$. The UAS: Bsk::Myc$^{T181A, Y183F}$ construct was co-transfected with a pMT-GAL4 vector into S2 cells and the protein harvested, the same procedure was also carried out for the UAS: Bsk::Myc construct (see Chapter 2). A Myc 9E10 antibody (Santa Cruz) detected, ectopic Bsk-Myc and Bsk-Myc$^{T181A, Y183F}$ expression in S2 cell protein lysates (Figure 3.6.1 A). Further, western blotting of these S2 cell lysates revealed that the phospho-JNK antibody could only detect activated JNK with ectopic expression of Bsk-Myc and not the phospho inactive Bsk-Myc$^{T181, Y183F}$ mutant. As expected the human

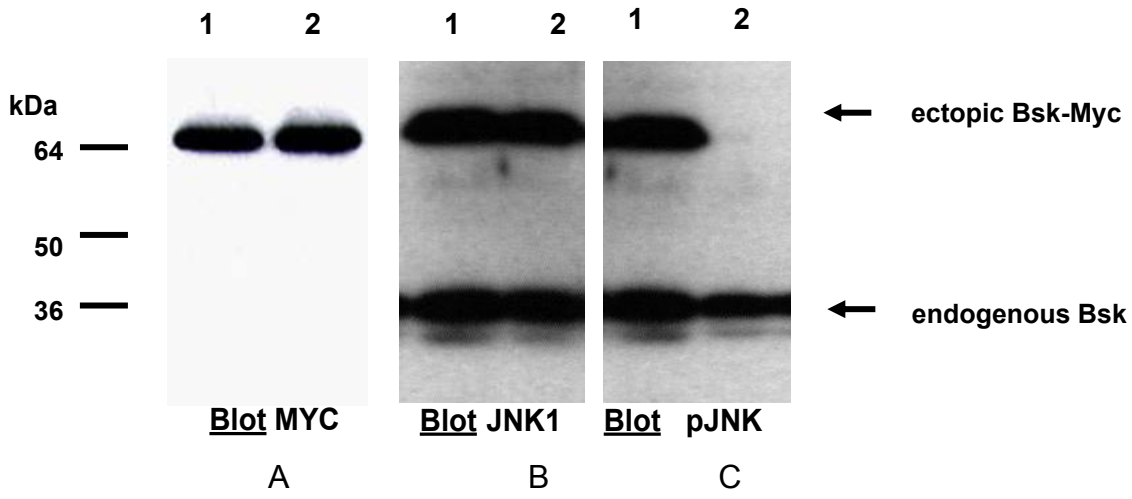

Figure 3.6.1. Threonine 181 and Tyrosine 183 are the sole residues on *Bsk* responsible for its phosphorylation.

(A) MYC Blot: Detection of ectopic Bsk-Myc (lane 1) and *Bsk-Myc*$^{T181,\ Y183F}$ (lane 2) expression in S2 cell protein lysates by a Myc 9E10 antibody (Santa Cruz). Measurement of protein mass is in kilodaltons (kDA). **(B) JNK1 Blot:** Detection of ectopic Bsk-Myc (lane1) and Bsk-Myc$^{T181A,\ Y183F}$ (lane 2) expression in S2 cell protein lysates by a JNK1 antibody (Santa Cruz). **(C) Phospho-JNK blot:** The phospho JNK antibody (cell signalling) is only able to detect expression of ectopic Bsk-Myc (lane 1) but not Bsk-Myc^{T181,Y183F} (lane 2) from S2 cell protein extracts, indicating that Threonine 181 and Tyrosine 183 are the sole residues responsible for Bsk phosphorylation

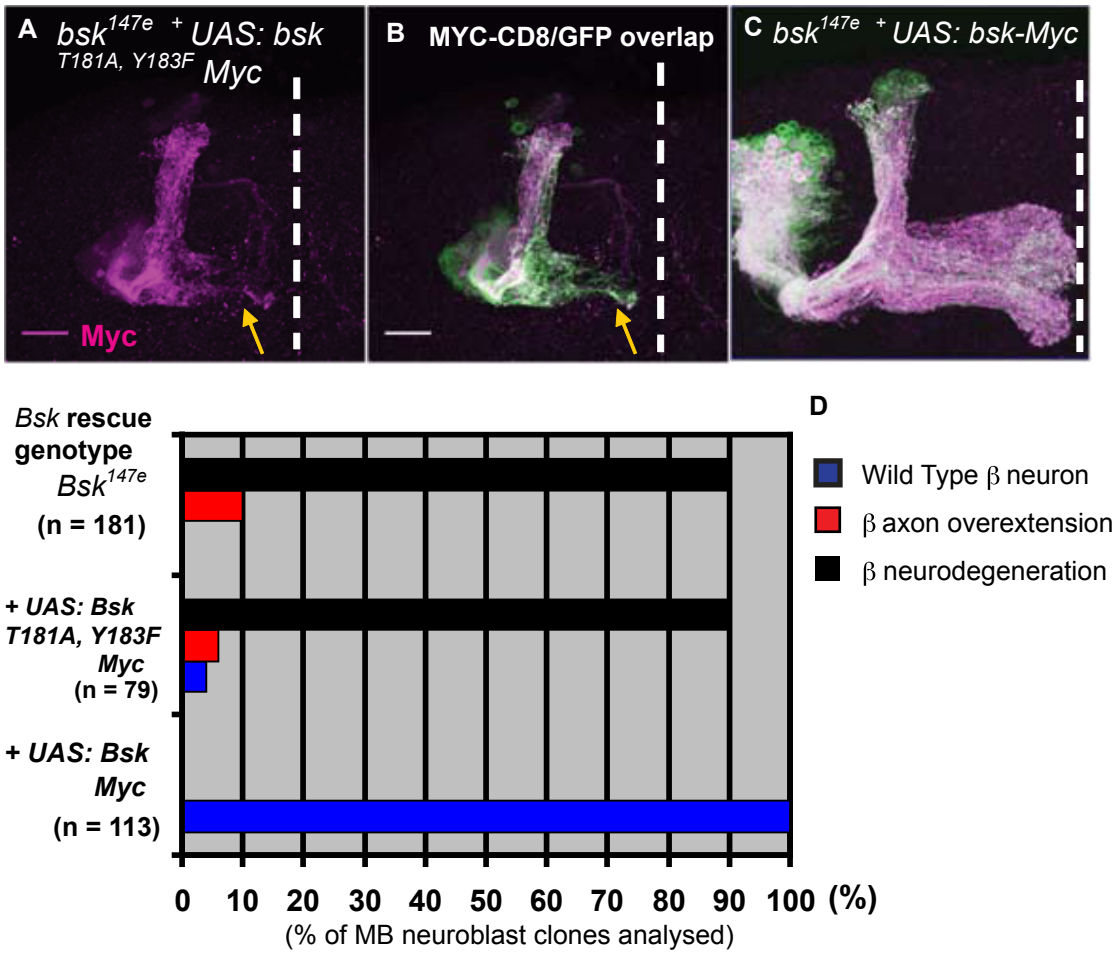

Figure 3.6.2. *Bsk* dependent axonal morphogenesis requires Threonine 181 and Tyrosine 183 Phosphorylation sites

(A-B) Representative images of *bsk*^{147e} adult MB neuroblast clones in the presence of ectopic *Bsk-Myc*$^{T181A,\ Y183F}$ or wild type *Bsk*-Myc **(C)**. The presence of the rescue transgenes: *Bsk-Myc*$^{T181A,\ Y183F}$ **(A)** and *Bsk-Myc* **(C)** was detected using a Myc antibody (Cell signalling). Regions of β neurodegeneration are observed in the *Bsk* mutant neuroblast clones which contain the phospho mutant transgene *Bsk-Myc*$^{T181A,\ Y183F}$ **(B)**. In contrast introduction of the wild type transgene into *Bsk* mutant clones, fully rescues the neurodegeneration phenotype giving wild type projections **(C)**. Scale Bars 20μm. Myc staining is shown in magenta; the MB mutant clonal tissue is shown in Green (CD8-GFP) with the Myc/CD8-GFP overlap being displayed in white. Yellow arrows indicate areas of neurodegeneration. **(D)** Quantifications of MB adult *Bsk*^{147e} axonal phenotypes (solely of the β lobe) in the presence of wild type *Bsk* and phospho inactive *Bsk* transgenes. Genotypes are as follows (A-B) *hsFLP, UAS-mCD8/+; FRT40A, GAL80/Bsk*^{147e}*, FRT40A; UAS-Bsk* $^{T181A,\ Y183F}$ *-Myc/+; OK107/+* (C) *hsFLP, UAS-mCD8/+; Bsk* ^{147e}*; FRT40A/ FRT40A, GAL80; UAS-Bsk-Myc /+; OK107/+*

JNK-1 antibody, which had previously detected Bsk in MB neurons, also detected ectopic Bsk expression in Bsk-Myc$^{T181, Y183F}$ and Bsk::Myc protein extracts (Figure 3.6.1 B-C).

I next set out to determine if *Bsk-Myc$^{T181, Y183F}$* expression could rescue the *Bsk* null degeneration phenotype. As oppose to wild type *Bsk* expression, which rescued the *Bsk* null phenotypes, expression of Bsk-Myc$^{T181, Y183F}$ did not (Figure 3.6.2). This suggests that the residues threonine 181 and tyrosine 183 are solely responsible for Bsk being phosphorylated and I can therefore safely assume that phospho-JNK antibody serves as a valid marker of JNK activity in MB neurons. The results also suggest that Bsk phosphorylation is required for correct axonal morphogenesis and that the phospho-JNK antibody gives an accurate readout of JNK activity in vivo.

3.7 Bsk loss results in axonal defects in Antennal Lobe and Optical Lobe neurons

Loss of *Bsk* function was also analysed in Antennal lobe (AL) and Optical Lobe (OL) projections. Wild type contralateral AL neurons, elaborate their dendrites ipsilaterally to one antennal lobe but project axons contralaterally to the opposite antennal lobe (Figure 3.7.1 A). However, *Bsk^{147e}* mutant AL lobe neuroblast clones exhibit axon targeting defects in the majority of cases (Figure 3.7.1 C, quantifications, 3.7.1 E). In this scenario the axons failed to innervate the correct region of the Antennal lobe. In the minority of samples, axon loss was exhibited, where only a relatively few axons fasciculate together and project contralaterally to the opposite side of the antennal lobe (Figure 3.7.1 B). These mutant *Bsk* AL phenotypes can be rescued when ectopic wild type *Bsk* is introduced into *Bsk ^{147e}* mutant AL lobe neuroblast clones (Figure 3.7.1 D).

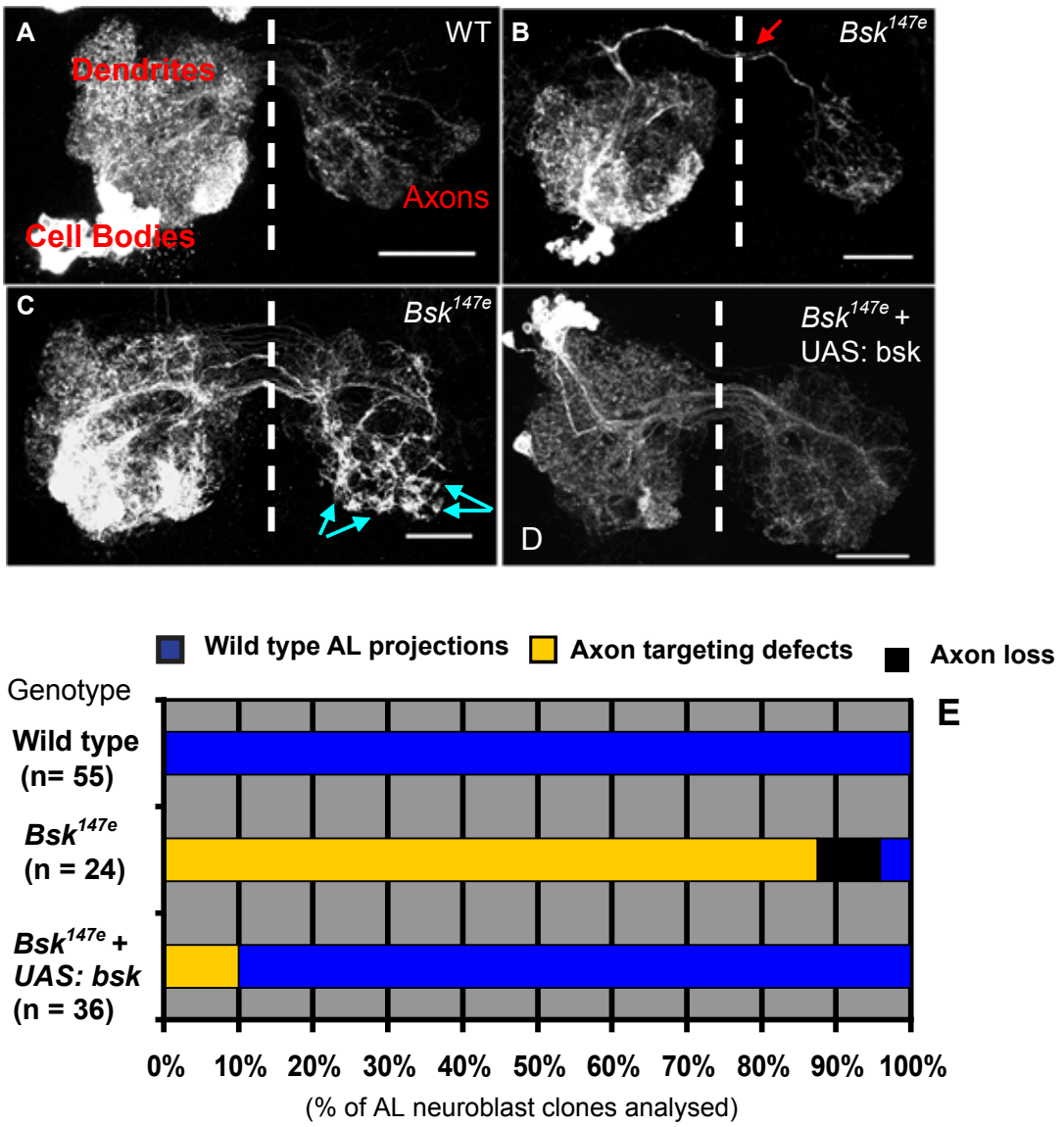

Figure 3.7.1 *Bsk* null AL neuroblast clones exhibit axon targeting defects

(A) Representative image of a wild type antennal lobe neuroblast clone. **(B)** *Bsk* mutant antennal lobe neuroblast clone, exhibiting axon loss and fasciculation defects. This phenotype is infrequently observed. In this particular sample only a few neurons bypass the midline to innervate the contralateral antennal lobe region (indicated by the red arrow). **(C)** Frequently observed *Bsk* mutant antennal lobe neuroblast clone, exhibiting axon targeting defects at the axon termini (indicated by the turquoise arrows). **(D)** Introduction of a *Bsk* WT transgene is able to fully restore WT axonal projections and rescue the axon targeting defects, which are characteristic of *Bsk* mutant antennal lobe neurons. Scale Bars, 50μm. **(E)** Quantification of the above phenotypes observed in **A-D**. Genotypes are as follows (A) *hsFLP, UAS-mCD8-GFP/+; FRT40A , GAL80/FRT40A; GAL4-OK107/+* (B-C) *hsFLP, UAS-mCD8-GFP/+; Bsk ^{147e}, FRT40A/FRT40A, GAL80 ;GAL4-OK107/+* (D) *hsFLP, UAS-mCD8-GFP/+; Bsk ^{147e}, FRT40A/FRT40A, GAL80* ; *UAS-Bsk /+; GAL4-OK107/+*

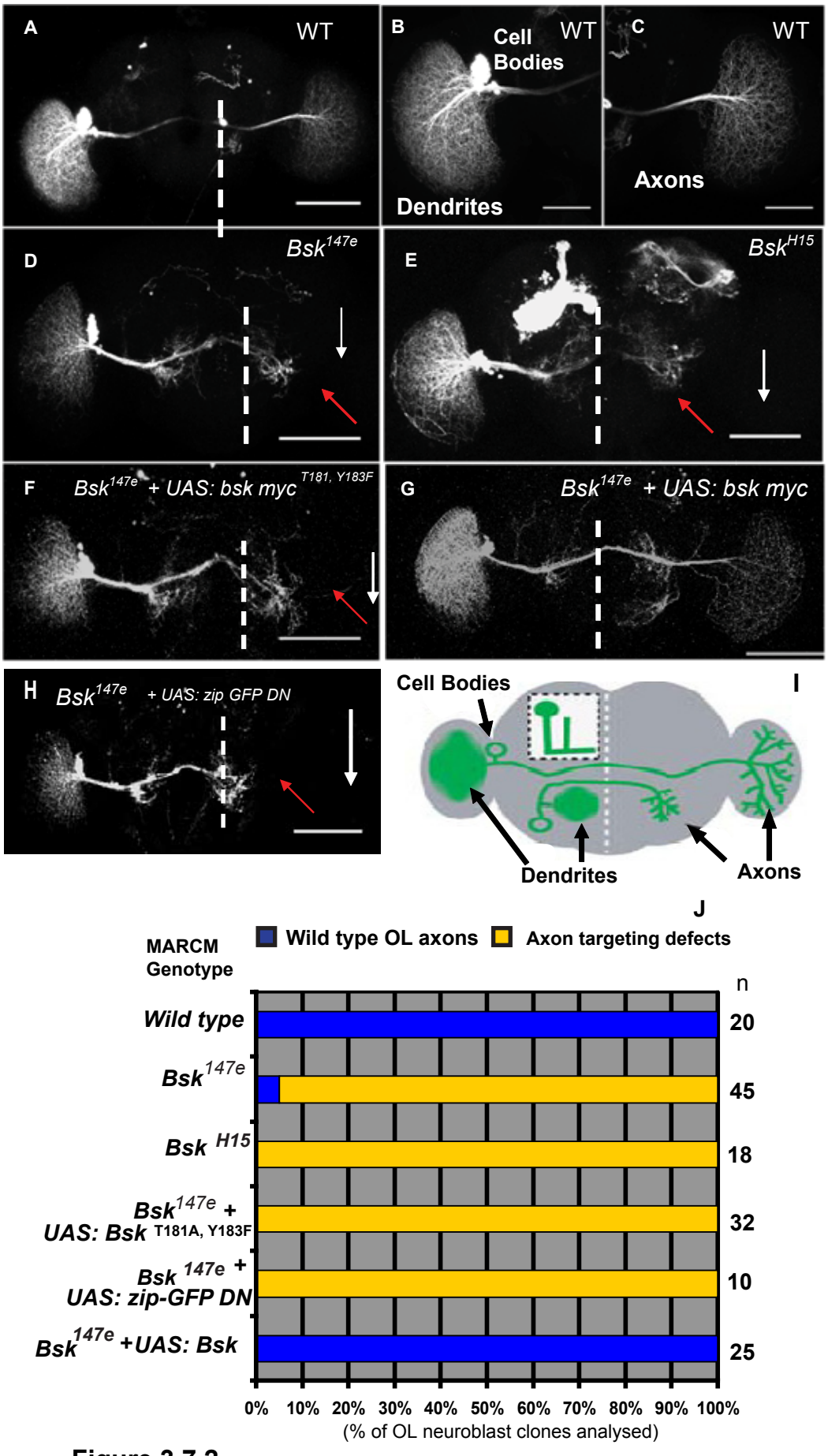
A
WT
B
Cell Bodies
WT
Dendrites
C
WT
Axons
D
Bsk147e
E
BskH15
F
Bsk147e + UAS: bsk myc T181, Y183F
G
Bsk147e + UAS: bsk myc
H
Bsk147e + UAS: zip GFP DN
Cell Bodies
I
Dendrites
Axons
J
MARCM Genotype
Wild type OL axons
Axon targeting defects
n
Wild type
20
Bsk147e
45
Bsk H15
18
Bsk147e + UAS: Bsk T181A, Y183F
32
Bsk 147e + UAS: zip-GFP DN
10
Bsk147e +UAS: Bsk
25
0% 10% 20% 30% 40% 50% 60% 70% 80% 90% 100%
(% of OL neuroblast clones analysed)

Figure 3.7.2

Figure 3.7.2. *Bsk* mutant OL neuroblast clones exhibit axon growth defects.

Representative images of CD8-GFP labelled wild type **(A-C)**, bsk^{147e} **(D)**, bsk^{H15} **(E)** OL neuroblast clones and bsk^{147e} OL neuroblast clones, in the presence of $Bsk^{T181A,\ Y183F}$ **(F)** or wild type *Bsk* **(G)** or dominant negative zipper **(H)**. Magnified images of the cell bodies and the dendrites of a WT OL neuroblast clone in the left hemisphere **(B)** and the axon termini in the right optic lobe **(C)**, the intricate axon and dendrite projections are clearly visible. White arrows indicate the supposed OL axon termination points, when axons have prematurely terminated and red arrows point to OL axon terminal branching phenotypes. Scale Bars, 100μm. **(I)** Schematic of the Drosophila brain, displaying the location of the MB, OL and AL neurons. **(J)** Quantifications of the OL neuroblast clone phenotypes, n = number of Drosophila brains analysed. Genotypes are as follows (A-C) *hsFLP, UAS-mCD8/+; FRT40, GAL80/FRT40A; GAL4-OK107/+* (D) *hsFLP, UAS-mCD8/+; Bsk ^{147e}, FRT40A/ FRT40A , GAL80; GAL4-OK107/+* (E) *hsFLP, UAS-mCD8/+; Bsk ^{H15}, FRT40A / FRT40A, GAL80; GAL4-OK107/+* (F) *hsFLP, UAS-mCD8/+; Bsk^{147e}, FRT40A/ FRT40A, GAL80; UAS-Bsk-Myc$^{T181A,\ Y183F}$/+; GAL4-OK107/+* (G) *hsFLP, UAS-mCD8-GFP /+; Bsk^{147e}, FRT40A/FRT40A, GAL80; UAS-Bsk-Myc/+; GAL4-OK107/+* (H) *UAS-mCD8-GFP/+; Bsk ^{147e}, FRT40A/ FRT40A, GAL80; UAS-Zip-GFP DN/+; GAL4-OK107/+*

In a wild type scenario, contralateral projection optical lobe (OL) neurons, elaborate dendrites ipsilaterally to one optic lobe but project axons contralaterally to the opposite optical lobe, to form an intricate network of axons innervating the optic lobe (Figure 3.7.2 A). However in 96% of the Bsk^{147e} neuroblast clones analysed, OL neurons exhibited axon targeting defects and failed to correctly innervate the optic lobe. This phenotype was characterised by axons stalling beyond the midline and forming collateral branches (Figure 3.7.2 D). Using the MARCM system, I then performed transgenic rescue experiments, expressing wild type *Bsk* and $Bsk^{T181A,\ Y183F}$ in Bsk^{147e} OL clones. I also examined the ability of these transgenes to rescue the collateral branching phenotypes observed in Bsk^{147e} OL neuroblast clones. Overexpression of wild type Bsk fully restored the axon targeting defects in Bsk^{147e} OL neuroblast clones (Figure 3.7.2 G). Like in MB neurons, overexpression of the phospho inactive $Bsk^{T181A,\ Y183F}$ mutant transgene in Bsk^{147e} OL neuroblast clones also failed to rescue the bsk null OL axon defects (Figure 3.7.2 F, quantification 3.7.2 J).

3.7 Discussion

In this chapter, I have shown that *Bsk* regulates distinct aspect of axonal morphogenesis in MB neurons, namely to prevent axon overextension and axonal degeneration. The basis of these phenotypes is most likely dependent on the level of JNK activity. This is underlined in the genetic results, where complete loss of *Bsk*, using a null allele (Bsk^{147e}) results in neurodegeneration of MB neurons, whereas partial loss of *Bsk*, using a hypomorphic mutation (Bsk^{H15}) favours a shift towards a higher frequency of overextension phenotypes. As expected the results confirmed that Bsk mediated axon

morphogenesis is kinase dependent and the particular amino acid residue of this domain, as Isoleucine 212 is integral to kinase function (this residue is conserved in all members of the MAPK family). Following on from this finding, I have also shown that Bsk regulates MB axonal morphogenesis *in vivo* through phosphorylation of residues Threonine 181 and Tyrosine 183. Since these resides are required for Bsk activity, the next objective would therefore be to investigate the function of the upstream JNK kinases: Mkk4 and Hep (also known as Drosophila Mkk7) and determine their relevance in regulating *Bsk* dependent axon morphogenesis.

As well as regulating MB neuron morphogenesis, *Bsk* and its phosphorylation sites were also shown to be essential in the correct axon targeting of OL and AL contralateral projecting axons, demonstrating that *Bsk* is able to regulate axon morphogenesis in a wide range of neuronal subtypes that have different axonal morphologies. This suggests that *Bsk* is a central regulator of axonal development in many varied neuronal populations and is able to react to different stimuli, which govern these diverse types of neurons during development.

I have also uncovered a neuroprotective role for *Bsk* during MB neuron development, reminiscent of that observed in *JNK1* null mice (Chang et al, 2003). Adult *Bsk* null MB muticellular and single cell neuroblast clones exhibit axon degeneration phenotypes characterised by axon thinning and axon breaks, respectively. Additionally the degeneration progressively worsens and accelerates in the latter stages of development and appears to be a late onset phenomenon. From the data acquired it can be clearly observed that axons of *bsk* null MB neuroblast clones in all samples analysed at 30hrs after puparium formation (APF), reach their termination points, i.e. the midline and

the anterior cortex respectively, confirming that axon extension is not defective during development. However after the 30hr APF time period, subtle axon degeneration phenotypes begin to appear.

Interestingly ectopic expression of the pan-caspase inhitor gene *p35*, rescues the neurodegeneration phenotype observed in *Bsk* null MB neuroblast clones. The neuroprotective role of p35, I have uncovered in MB neurons, is also consistent with the findings outlined in various studies on p35. For instance one study that found that neuronal expression of p35 attenuated neurodegeneration associated with excitotoxic glutamate analogue kainic acid *in vitro* and *in vivo* (Viswanath et al, 2000). Moreover expression of p35 was also demonstrated to prevent blindness in *Drosophila* mutants that undergo retinal degeneration (Davidson et al, 1998). Overall the results I acquired in MB neurons suggests that a caspase signalling pathway may be implicated in the neurodegeneration and axon loss observed in Bsk null MB neurons, this can be deduced from the fact that inhibiting caspase activity by overexpressing p35, restores wild type projections in *Bsk* null MB neurons. However the issue remains unresolved as to whether caspase signalling is a precursor to neurodegeneration or is invoked by it.

Finally using MB neurons in the Drosophila brain as a model I have shown that JNK signalling is highly active throughout different stages of MB neuron development and in adulthood. I have demonstrated this *in vivo* by utilising a phospho JNK1 antibody that recognises the two conserved epitopes on *Bsk.* Therefore it would be of interest to investigate how *Bsk* signals affects MB neuronal morphogenesis during different periods of development. Furthermore the fact that JNK signalling is highly active throughout

development and into adulthood suggests that the upstream JNKKs Hep and Mkk4, may possibly act as regulators of Bsk activity and JNK-dependent neuronal morphogenesis.

CHAPTER 4: Role of the JNK kinases Hep and MKK4 in neuronal morphogenesis

4.1 Introduction

In this previous chapter I presented evidence demonstrating that Bsk is required to maintain axon stability in MB neurons. In the *Drosophila* MAPK signalling cascade, Bsk is phosphorylated by two JNK kinases (JNKKs), Hemipterous (Hep) and MAP kinase kinase 4 (Mkk4) (Riesgo-Escovar et al, 1997; Han et al, 1998; Glise et al, 1995). Here I investigate the role of the JNK kinases Hep and Mkk4, the potential regulators of Bsk activity *in vivo*. In order to gain an insight into the role of the JNKKs in neuronal morphogenesis, I have employed various strategies including loss and gain-of function analysis. The generation of Hep/Mkk4-Bsk fusion transgenes, has also enabled me to uncover, whether the individual JNKKs Hep and Mkk4 differentially regulate Bsk activity *in vivo* as well as allowing me to analyse the potential differences that Hep-Bsk or Mkk4-Bsk signalling have on MB neuronal morphogenesis. Finally, I have obtained Hep and Mkk4 antibodies to determine the localisation of these JNKKs in MB neurons.

4.2 Hep is localised to all subsets of MB axons

Anti-Hep antibodies were generated commercially using rabbit hosts (Eurogentec, Seraing Belgium), to determine the expression pattern of the JNKK Hep. The following peptide sequences used as immunogens were: QSLEAKLQAQNESHDC and CLRANGDPTLQRLPNS; these peptide sequences are located on the N and C-terminus of the protein coding transcript 'Hep PC' respectively (Figure 4.1.1). Pre-screening confirmed that these antibodies Hep 1956 (N-terminal immunogen) and Hep 1957 (C-

terminal immunogen) did not cross react with non-specific antigens in the fly brain. Furthermore western blotting revealed the specificity of both Hep1956 and Hep1957 antibodies, since in S2 cell protein homogenates (which had been transfected with UASt: Hep-RFP constructs) both the endogenous Hep protein with a predicted molecular weight of 53.1 kDa and the protein band corresponding to the ectopic expression of Hep-RFP with a predicted molecular weight 80.6 kDa were detected (Figure 4.1.2).

Antibody staining of whole mount fly brains was carried out using the 1957 Hep antibody since it gave a clearer profile of Hep localisation in MB neurons. Endogenous Hep was highly detected in all MB axons subsets but was less prominent in the cell bodies. (Figure 4.1.3 A-C'). Furthermore Hep signals were also observed throughout the brain, particularly in the antennal lobe of the fly brain. I also visualised the expression profile of ectopic Hep in MB neurons through *Hep* overexpression. I constructed a UAS: Hep-RFP construct, which was microinjected into fly embryos to give UAS: Hep-RFP transgenic lines (see Chapter 2 - Material and Methods). This tagged *Hep* transgene enabled me to observe the localisations patterns of Hep protein *in vivo*. By overexpressing Hep-RFP in MB neurons, ectopic Hep staining also showed preferential localisation to axons (Figure 4.1.3 D-D'').

4.3 *Hep* loss results in axon overextension

Given the substantial quantity of data available consistently describing Hep as a central regulator of Bsk (Stronach, 2005), *hep*-null clones might be expected to phenocopy the *bsk* null neurodegeneration phenotype to the same degree. In order to test this hypothesis, I generated mutant *Hep* MB neuroblast clones. However in the majority of samples

```
1-50            MSTIEFETIGSRLQSLEAKLQAQNESHDQIVLSGARGPVVSGSVPSARVP
51-100          PLATSASAATSATHAPSLGAGSVSGSGISIAQRPAPPVPHATPFGSASAS
101-150         SSSSSASAFASAAPATGTFGGTYTPPTTRVSRATPTLPMLSSGPGGGLNR
151-200         TRPVILPLPTPPHPPVSETDMKLKIIMEQTGKLNINGRQYPTDINDLKHL
201-250         GDLGNGTSGNVVKMMHLSSNTIIAVKQMRRTGNAEENKRILMDLDVVLKS
251-300         HDCKYIVKCLGCFVRDPDVWICMELMSMCFDKLLKLSKKPVPEQILGKVT
301-350         VATVNALSYLKDKHGVIHRDVKPSNILIDERGNIKLCDFGISGRLVDSKA
351-400         NTRSAGCAAYMAPERIDPKKPKYDIRADVWSLGITLVELATARSPYEGCN
401-450         TDFEVLTKVLDSEPPCLPYGEGYNFSQQFRDFVIKCLTKNHQDRPKYPEL
451-492         LAQPFIRIYESAKVDVPNWFQSIKDNRLRANGDPTLQRLPNS
```

Figure 4.1.1 Peptide sequence of the Hep 'PC' protein isoform.

The red and blue highlighted sequences show the regions used as immunogens at the N and C-terminus of Hep, which are recognized by the Hep 1956 and Hep 1957 antibodies respectively. The conserved amino acid lysine (K226), shown in green (bold type), is located in the catalytic region of the kinase domain of Hep and corresponds to the ATP binding site. It is responsible for the kinase dependent activity of Hep.

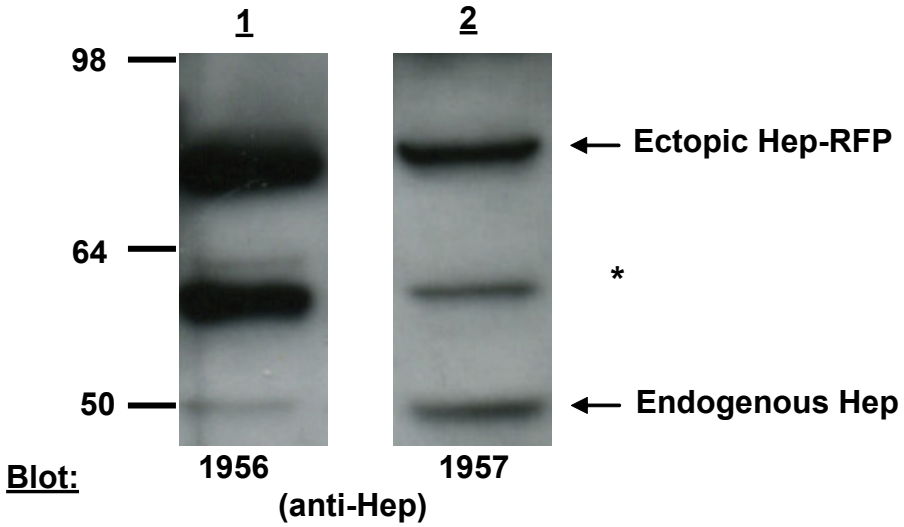

Figure 4.1.2 Detection of Hep Protein

S2 cells were transfected with pUASt Hep-RFP. Transfected S2 cell lysates were then subjected to SDS-PAGE and immunoblot analysis using both ant-Hep antibodies 1956 (column 1) and 1957 (column 2) revealed the presence of both ectopic and endogenous Hep. Molecular markers are in kDA. The asterisk indicates a degradation product derived from Hep-RFP.

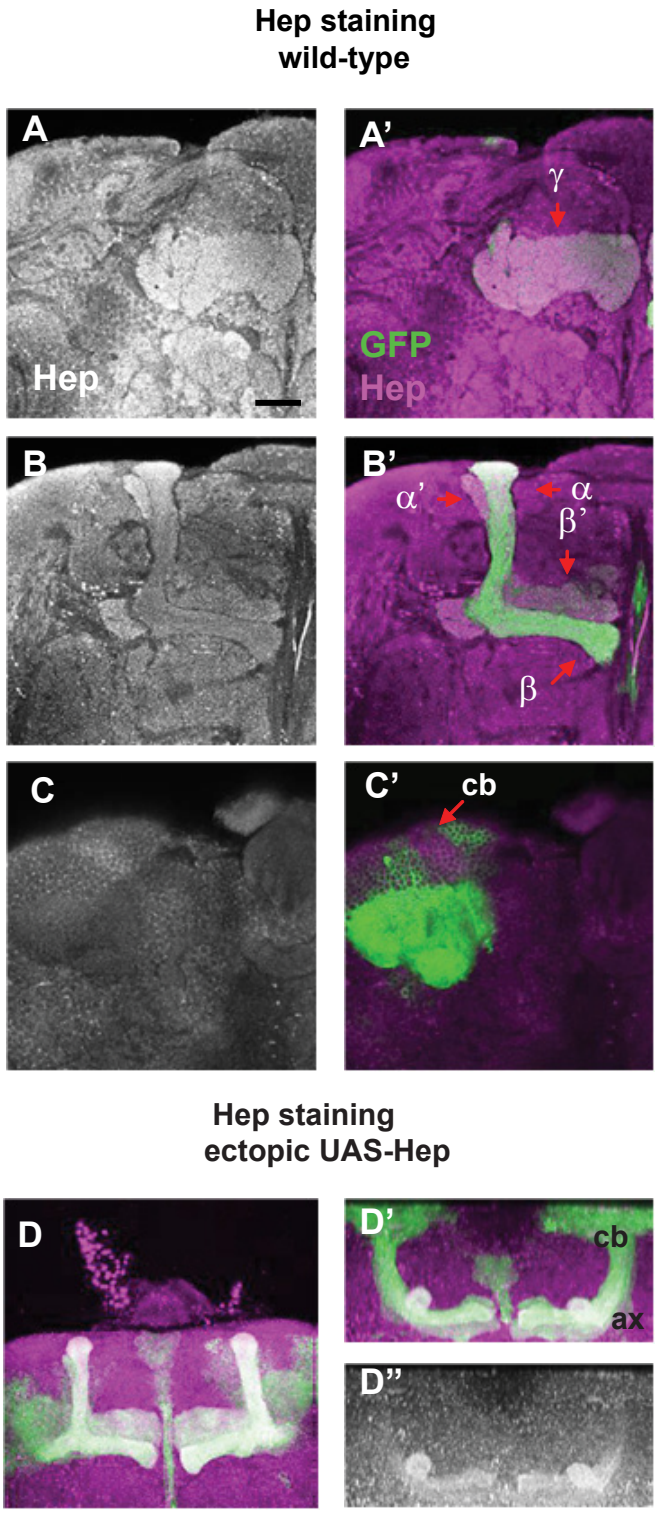

Figure 4.1.3 Expression study of the JNK kinase Hep

(A-C') Single confocal sections of MB neurons labeled with CD8-GFP and immunostained with Hep antibodies **(A-C)**. The corresponding panels **(A'-C')** shows overlap between Hep and CD8-GFP labeling. Single sections show γ **(A)**, α/β and α'/β' axons (ax) **(B)** and MB cell bodies (cb) **(C)** as indicated in **A'-C'**. **(D-D'')** MB neurons expressing CD8-GFP (green) and ectopic Hep (shown in magenta in **D** and **D'** and white in **D''**). Dorsal (y-projection) view (**D'** and **D''**) show Hep is mainly localized to axons (ax). Scale Bar 20μm (x-only). Genotypes are as follows (A-D'') *UAS-mCD8-GFP/+; GAL4-OK107/+*

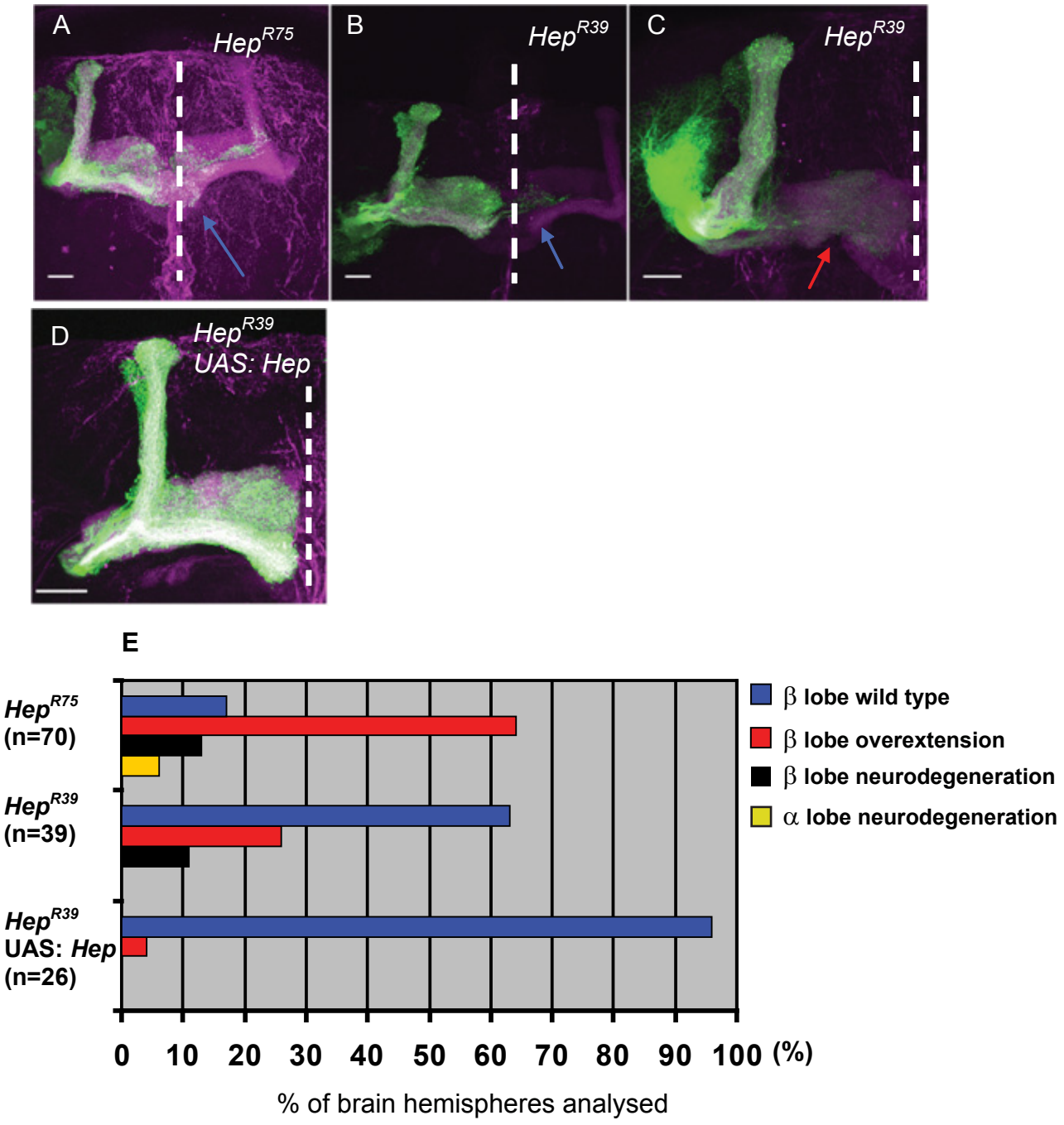

Figure 4.2.1 Loss of function of *Hep* culminates in MB axon overextension. Representative images of *hep*^{R75} **(A)** and *hep*^{R39} neuroblast clones **(B)** exhibiting axon overextension and degeneration **(C)** and *hep*^{R39} neuroblast clones in the presence of ectopic Hep, displaying wild type projections **(D)**. Scale bars: 20μm. Green, CD8-GFP. Magenta, FasII. Blue arrows indicate axon overextension, red arrows indicate axon degeneration. Quantification of these axon phenotypes **(E)**. Genotypes are as follows (A) *hsFLP122, FRT19A, GAL80/FRT19A, Hep*^{R75} *; UAS-mCD8-GFP (2x)/+; GAL4-OK107/+* (B-C) *hsFLP122, FRT19A, GAL80/FRT19A, Hep*^{R39} *; UAS-mCD8-GFP (2x)/+; GAL4-OK107/+* (D) *hsFLP122, FRT19A, GAL80/FRT19A, Hep*^{R39} *; UAS-mCD8-GFP(2x)/UAS-Hep; GAL4-OK107/+*

analysed axon overextension was observed. *Hep*^{R75} *and Hep*^{R39} MB neuroblast clones exhibited overextension of the β-axons past their wild type termination points in 64% and 26% of the samples analysed (Figure 4.2.1A, and Figure 4.2.1 B respectively). Only a minor proportion of the phenotypes analysed exhibited neurodegeneration. *Hep*^{R75} and *Hep*^{R39} mutant MB neuroblast clones exhibited neurodegeneration in 19% and 11% of the samples analysed respectively (Figure 4.2.1 E). Additionally ectopic wild type *Hep* expression was able to rescue all neurodegeneration and axon overextension phenotypes observed in the *Hep*^{R39} MB neuroblast clones, proving that the *Hep*^{R39} mutation is cell autonomous (Figure 4.2.1 D, quantifications Figure 4.2.1 E). Since *Hep* null clones did not phenocopy the neurodegeneration phenotype observed with *Bsk* null MB neuroblast clones, I then decided to study the role of the other JNK kinase *Mkk4,* in neuronal morphogenesis.

4.4 Mkk4 is localised to the later born α/β and α'/β' neuron subsets

Given that *Hep* mutant MB neuroblast clones did not phenocopy the *Bsk* null neurodegeneration phenotype, one possibility is that Mkk4 could regulate Bsk dependent axonal morphogenesis. In order to determine the expression pattern of Mkk4, antibodies to Mkk4 were produced. Anti-Mkk4 antibodies were generated commercially using guinea pig hosts. The following peptides used as immunogens were: MAERPKNLFATGSSRC and CKDGITQFTANQQAES (Figure 4.3.1); these peptide sequences are on located on the N-terminus and C-terminus of the Mkk4 protein coding transcripts PA and PB respectively. Pre-screening confirmed that these antibodies Mkk4

```
1-50          MAERPKNLFATGSSRSRNPPDQLSLNNLSIRHPPSSTSSTSSGSTSSGSS
51-100        SSSQHNHVTRCFGAQQPQQTPPVASSQVPPVPAASSSSAADRHRERIRQQ
100-150       ACGKLQFGEGGANTHTFTSDDLEDEGEIGRGAFGAVNKMTFKKLDKVMAV
151-200       KRIRSTVDEKEQKQLLMDLEVVMKSNECIYIVQFYGALFKEGDCWICMEL
201-250       MDTSLDKFYKYIYEKQQRHIPESILAKITVATVNALNYLKEELKIIHRDV
251-300       KPSNILLHRRGDIKLCDFGISGQLVDSIAKTKDAGCRPYMAPERIDPERA
301-350       KGYDVRSDVWSLGITLMEVATGNFPYRKWDSVFEQLCQVVQGEPPRLLTS
351-400       YNGMEFSKEFVDFVNTCLIKKESDRPKYSRLLEMPFIRRGETSHTDVAVY
401-424       VADILESMEKDGITQFTANQQAES
```

Figure 4.3.1 Peptide sequence of the Mkk4 'PA' protein isoform.

The red and blue highlighted sequences show the regions used as immunogens at the N and C-terminus of Mkk4, which are recognized by the Mkk4 1954 and Mkk4 1955 antibodies respectively. The amino acid lysine (K151), shown in green (bold type), is a conserved amino acid located in the catalytic region of the kinase domain of Mkk4, responsible for the kinase dependent activity of Mkk4 and corresponds to the ATP binding site.

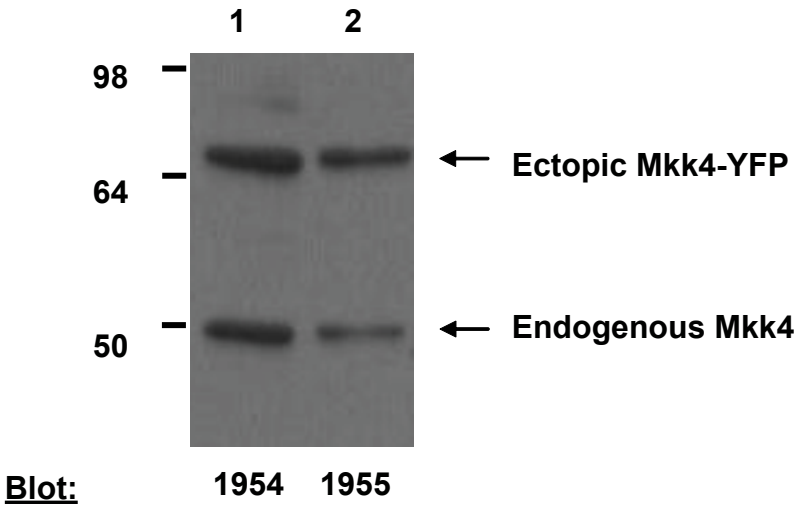

Figure 4.3.2. Detection of Mkk4 Protein.

S2 cells were transfected with pUAST MKK4-YFP. Transfected S2 cell lysates were then subjected to SDS-PAGE and immunoblot analysis using both anti-Mkk4 antibodies 1954 (column 1) and 1955 (column 2) revealed the presence of both ectopic and endogenous Mkk4. Molecular markers are in kDA.

1954 (N-terminal immunogen) and Mkk4 1955 (C-terminal immunogen) did not cross react with non-specific antigens in the fly brain. Additionally the specificity of each of these antibodies to MKK4 was revealed by western blotting. In S2 cell protein extracts which has been transfected with UASt: MKK4-YFP constructs, both the endogenous Mkk4 protein with a predicted molecular weight of 47.5 kDA and the protein band corresponding to the ectopic expression of MKK4-YFP with a predicted molecular weight of 72.5 kDA (Mkk4 protein, PA isoform = 47.5 kDA, + YFP tag = 25 kDA) were detected by both Mkk4 1954 and Mkk4 1955 antibodies (Figure 4.3.2).

To determine the expression pattern of Mkk4 in the Drosophila brain, antibody staining of whole mount wild type fly brains was carried out with the Mkk4 1954 antibody. Endogenous Mkk4 was detected in MB axons, particularly in α/β and α'/β' axons (Figure 4.3.3 A-C'). Furthermore ectopic Mkk4-YFP expression in MB neurons revealed that unlike Hep, Mkk4 was preferentially localised in the axons and cell bodies (Figure 4.3.3 D-D''). Thus the differential localisation of the JNK kinases Hep and Mkk4, suggests it is possible that they act non-redundantly and function in a differential manner to regulate Bsk.

4.5 *Mkk4* loss results in axon overextension

I next decided to examine whether loss of the JNK kinase *Mkk4* was able phenocopy the neurodegeneration observed in *Bsk* null MB neuroblast clones. Using a recently described *Mkk4* mutant allele (Thibault et al, 2004), I generated $MKK4^{e01458}$ neuroblast clones. In this case only a relatively small population of the earliest born subset of γ-neurons were present (Figure 4.4.1 A), whereas the later born α/β and α'/β' neuron subsets were absent, possibly due to a failure to proliferate. This would be consistent with recent

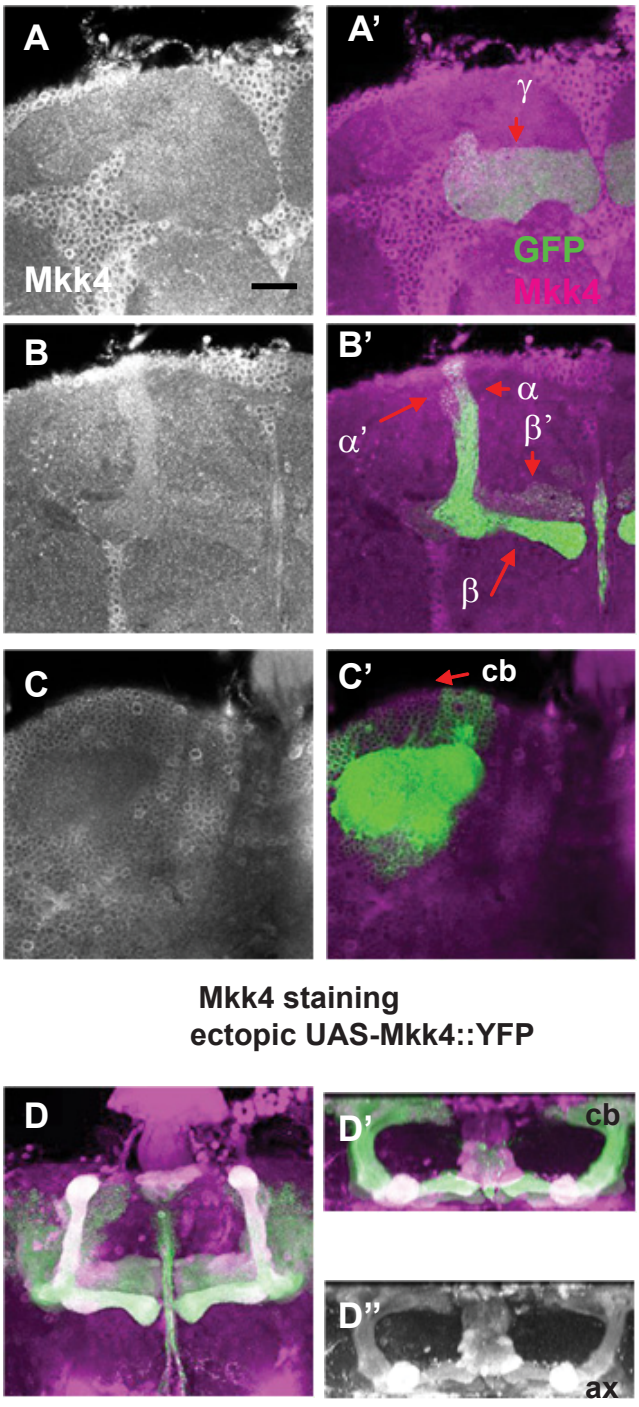

Figure 4.3.3 Expression study of the JNK kinase Mkk4

(A-C') Single confocal sections of MB neurons labeled with CD8-GFP and immunostained with Mkk4 antibodies **(A-C)**. The corresponding panels **(A'-C')** shows overlap between Mkk4 signals and CD8-GFP labeling. Single sections show γ **(A)**, α/β and α'/β' axons (ax) **(B)** and MB cell bodies (cb) **(C)** as indicated in A'-C'. **(D-D'')** Representative image of MB neurons expressing Mkk4-YFP (green) and stained with anti-MKK4 (magenta in **D** and **D'** and white in **D''**). Dorsal views (**D'** and **D''**) show Mkk4 is localised to axons and cell bodies (cb), Scale bar: 20 μm (x-only). Genotypes are as follow (A-D'') *UAS-mCD8/+; GAL4-OK107/+*

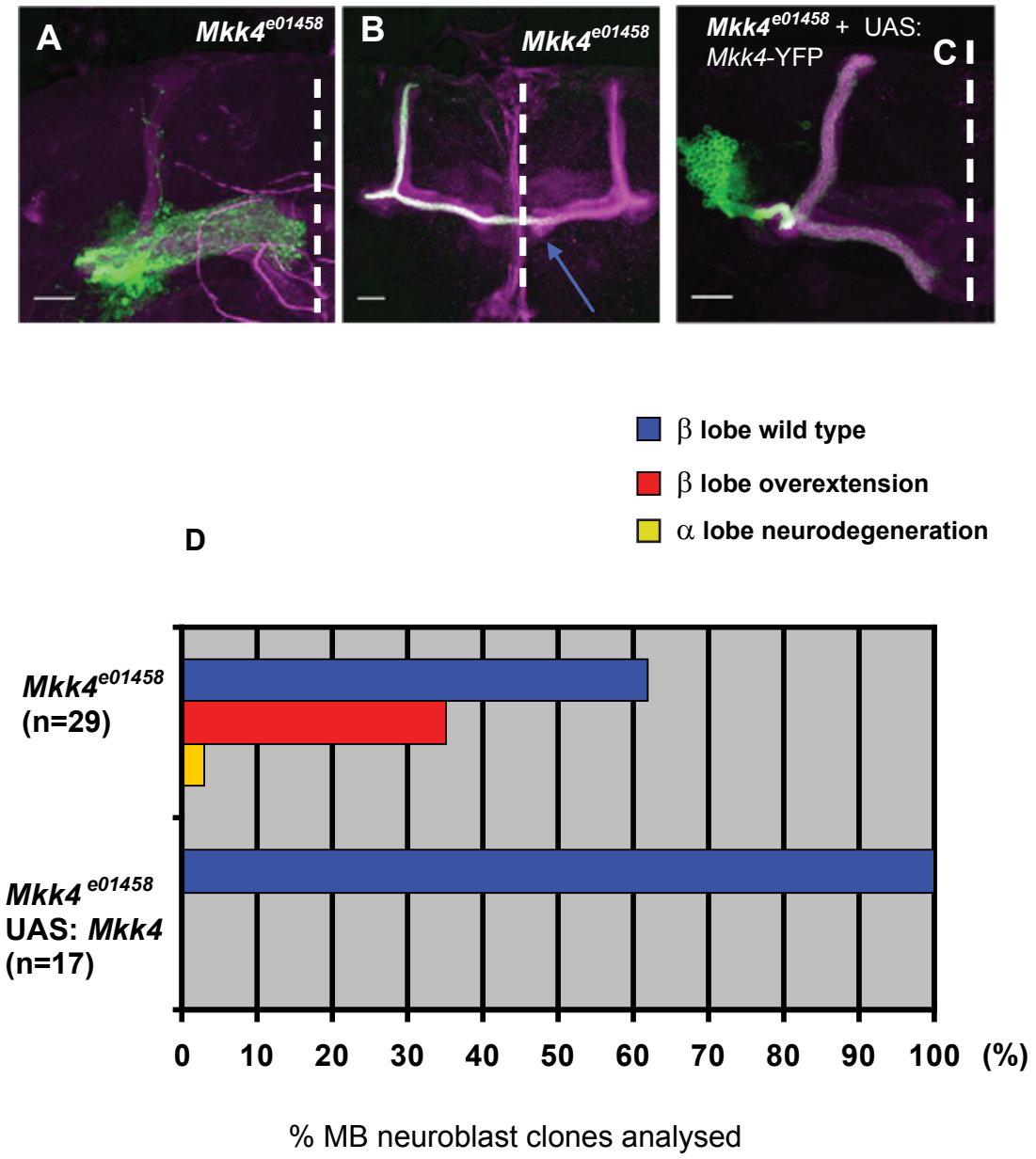

Figure 4.4.1 Loss of function of *Mkk4* in MB neurons.

Representative images of *Mkk4*^{e01458} MB neuroblast clones exhibiting **(A)** absence of the later born α/β and α'/β' neuron subsets and **(B)** axon overextension. **(C)** Representative image of *Mkk4*^{e01458} MB neuroblast clones in the presence of ectopic *Mkk4*::YFP. **(D)** Quantification of these β axon phenotypes. n, number of neuroblast clones analysed. Scale bars, 20 μm. Genotypes are as follows (A-B) *hsflp122/+; UAS-mCD8-GFP/+; FRT82B, GAL80/ FRT82B, Mkk4* ^{e01458} *; GAL4-OK107/+* (C) *hsflp122/+; UAS-mCD8-GFP/UAS-Mkk4-YFP; FRT-82B, GAL80/FRT82B, Mkk4* ^{e01458} *; GAL4-OK107/+*

reports which show *Mkk4* loss results in cytokinesis defects in cultured S2 cells (Bjorklund et al, 2006; Bettencourt-Dias et al, 2004).

In order to establish the role of Mkk4 in axon morphogenesis, I decide to generate later born $Mkk4^{e01458}$ neuroblast clones, which are comprised solely of α/β and α'/β' neuron subsets (see chapter 2). These later-born $Mkk4^{e01458}$ MB neuroblast clones also exhibited axon overextension phenotypes; although this phenotype was less frequently observed than in Hep^{R75} clones. (Figure 4.4.1 B, quantifications Figure 4.4.1 D). Additionally overexpression of wild type *Mkk4* was able to rescue the axon overextension phenotypes observed in $Mkk4^{e01458}$ clones (Figure 4.4.1 C), confirming that the $Mkk4^{e01458}$ mutation is cell autonomous.

4.6 Ectopic expression of either JNK kinase *Hep* or *Mkk4* does not modify the *Bsk* null phenotype

Both JNK kinases Hep and Mkk4 have been established as activators of Bsk (Riesgo-Escovar et al, 1996; Han et al, 1998; Glise et al, 1995). However it is important to ascertain if either of these JNK kinases can operate via an alternative signalling pathway to regulate neuronal morphogenesis or solely through *Bsk*. It is known that mammalian *MKK4* can phosphorylate MAPK p38 in vitro while *MKK7* cannot (Davis et al, 2000; Ho et al, 2003). Thus it is possible *Drosophila Mkk4* signals to p38 in vivo to regulate MB axon morphogenesis, although this has been ruled out by Han, et al. 1998. In order to resolve this issue of whether either JNK kinase Hep or Mkk4 signals independently of *Bsk* to regulate axon morphogenesis, I decided to ectopically express *Mkk4* and *Hep* in *Bsk* null MB neuroblast clones and observe any modification to the *Bsk* null

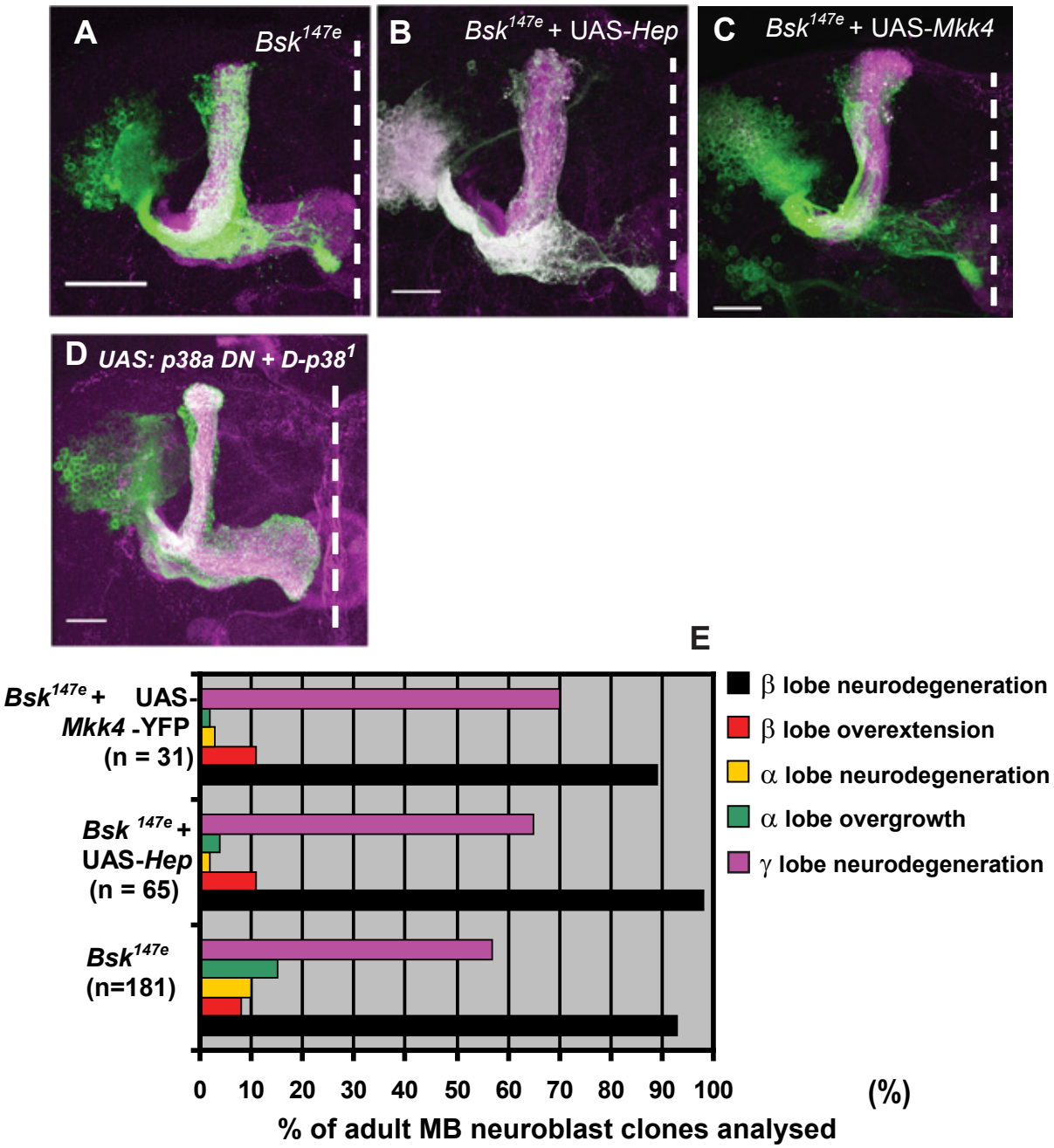

Figure 4.5.1 Ectopic expression of *Hep* or *Mkk4* cannot modify the *Bsk* null neurodegeneration phenotype

Representative image of a *Bsk*^{147e} MB neuroblast clone **(A)** in the presence of ectopic *Hep* **(B)** or *Mkk4*-YFP **(C)**. Ectopic expression of either of these JNKKs does not modify the *Bsk* mutant phenotype. **(D)** Representative image of *D-p38a*^{1} mutant MB neuroblast clones in the presence of a transgene overexpressing dominant negative *p38b*, the MB neuroblast clones display wild type axon projections (n = 18, 100% wild type). **(E)** Quantification of phenotypes observed in **(A)**, **(B)** and **(C)**, Scale Bars, 20μm. Genotypes are as follows: (A) *hsFLP, UAS mCD8-GFP/+; Bsk*^{147E}*, FRT40A/FRT40A, GAL80; GAL4-OK107/+* (B) *hsFLP, UAS-mCD8/+; Bsk* ^{147E}*, FRT40A/FRT40A, GAL80; UAS-Hep/+; GAL4-OK107 /+;* (C) *hsFLP, UAS-mCD8/+; Bsk*^{147E}*, FRT40A/FRT40A, GAL80; UAS-Mkk4-YFP /+; GAL4-OK107/+* (D) *hsFLP, UAS-mCD8/UAS-p38a DN; D-p38*^{1}*, FRT82B /FRT82B, GAL80; GAL4-OK107/+*

neurodegeneration phenotype (Figure 4.5.1 A). When either kinase is overexpressed in *Bsk* null MB neuroblast clones, there is no modification to the *Bsk* mutant phenotypes observed in MB neuroblast clones (Figure 4.5.1 B-C).

I also tested the role of *p38*, to determine if this MAPK plays a role in axonal morphogenesis. Two Drosophila homologs of p38, p38a and p38b have been identified on the basis of their homology to mammalian p38 and to one another (Han et al, 1998). *Drosophila* p38a provides protection against several environmental stresses including heat shock, oxidative stress and starvation (Craig et al, 2004) while p38b is involved in wing vein patterning and differentiation in Drosophila (Adachi-Yamada et al, 1999b). Furthermore p38 signalling has been implicated in human neurodegenerative diseases such as Alzheimer's, Parkinson's, amyotrophic lateral sclerosis and cerebral ischemia (Bendotti et al, 2006). I generated Drosophila $p38a^{1}$ null MB neuroblast clones (Craig et al, 2004), that expressed a dominant negative *p38b* transgene (Adachi-Yamada et al, 1999b). This mutant p38 *Drosphila* strain gave wild type MB neuronal projections (Figure 4.5.1 D, quantifications Figure 4.5.1 E), suggesting that p38 signalling does not play a role in MB neuronal morphogenesis.

4.7 Genetic redundancy of the JNK kinases *Hep* and MKK4

Given the similar axon overextension phenotypes observed in *Mkk4* and *Hep* loss of function MB neuroblast clones, a feasible assumption to make would be that Mkk4 and Hep could potentially compensate for each other's function in MB neuronal morphogenesis. In order to examine JNKK genetic redundancy I tested whether Hep and Mkk4 are interchangeable, ectopic *Mkk4* was expressed in *Hep* mutant MB neuroblast

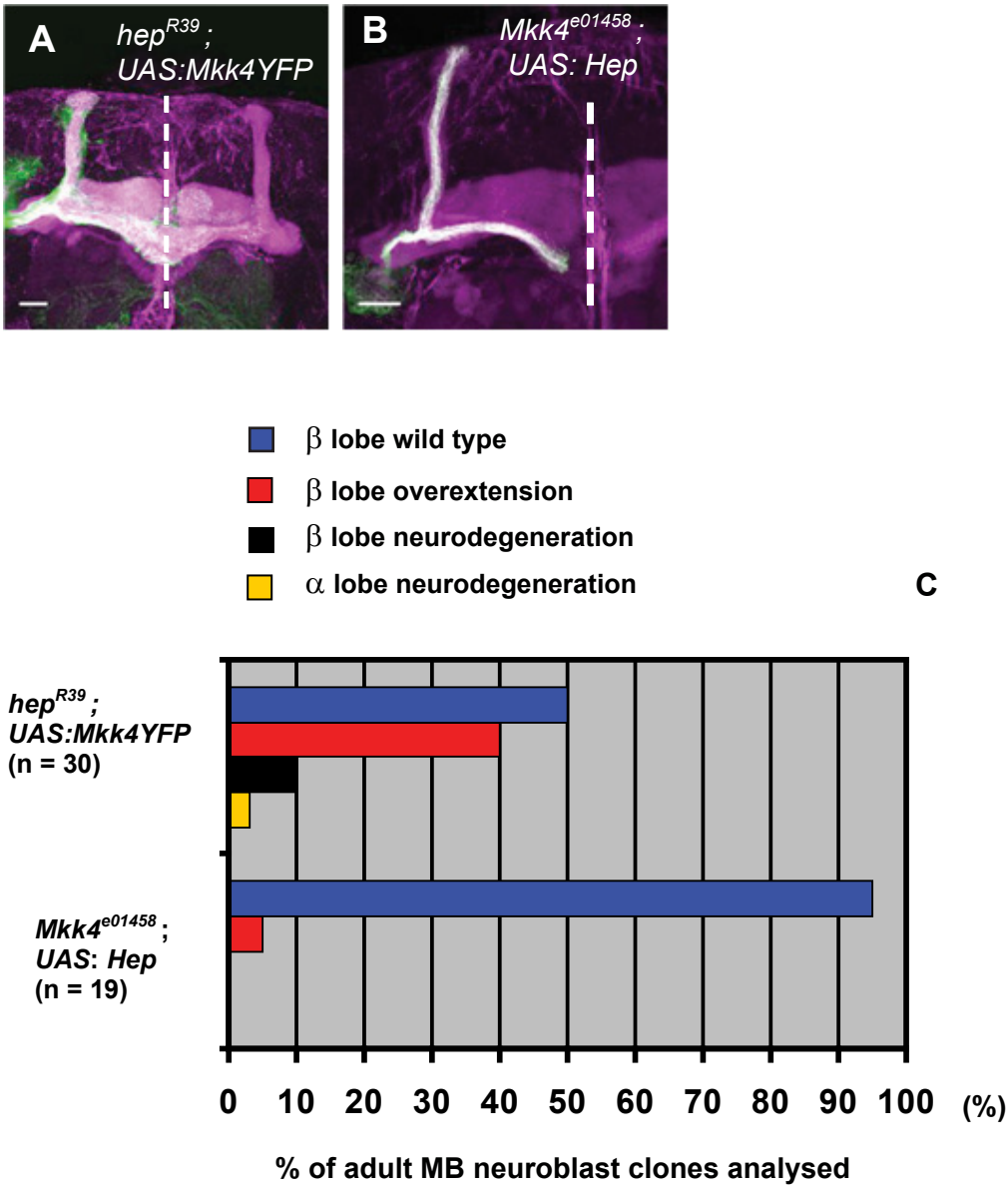

Figure 4.6.1 Ectopic *Hep* rescues *Mkk4* mutant overextension phenotypes. Representative images of *hep*^{R39} MB neuroblast clones in the presence of ectopic *MKK4* **(A)** and *Mkk4*^{e01458} in the presence of ectopic *Hep* **(B)**. Mutant phenotypes acquired with loss of Hep were not suppressed by ectopic *Mkk4*, however axon overextension phenotypes exhibited with loss of *Mkk4* can be rescued with ectopic Hep. **(C)** Quantifications illustrating the axonal phenotypes observed. Scale bars, 20μm. Genotypes are as follows (A) *hsflp122, FRT19A, GAL80/Hep* ^{R39}, *FRT19A; UAS-mCD8/ /+; UAS-Mkk4-YFP/+; GAL4 OK107/+* (B) *hsflp122/+; UAS-mCD8/UAS-Hep; FRT82B, GAL80/ FRT82B, Mkk4* ^{e01458}*; GAL4-OK107/+*

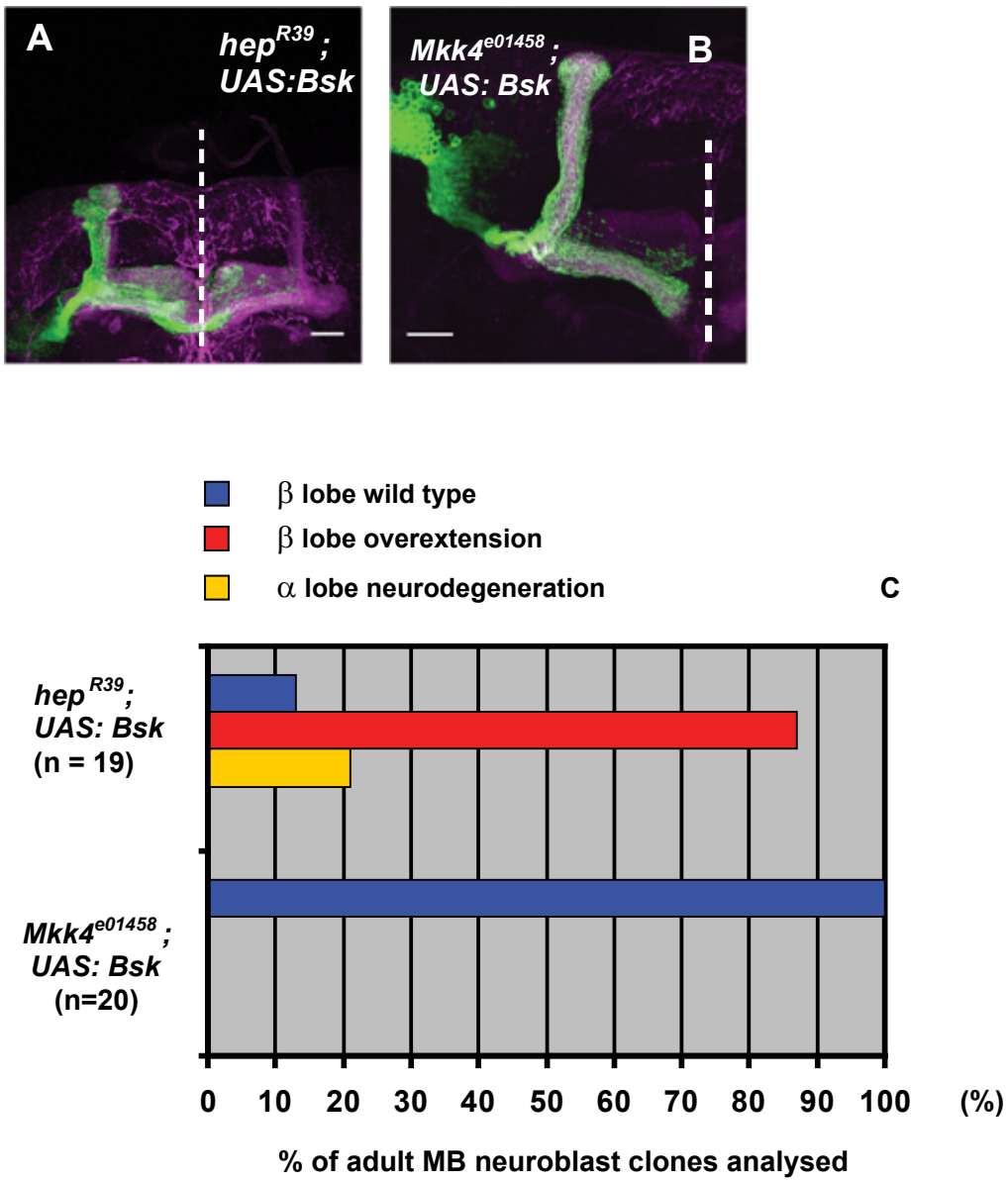

Figure 4.6.2 Ectopic expression of *Bsk* rescues the axon overextension defects observed in *Mkk4* mutant MB neuroblast clones.

Representative images of *hep*^{R39} **(A)** and *Mkk4*^{e01458} MB neuroblast clones **(B)** overexpressing *Bsk*. Ectopic *Bsk* is able to fully rescue the axon extension phenotypes exhibited with loss of *Mkk4*, however *Bsk* overexpression is unable to rescue the mutant phenotypes characteristic of loss of *Hep*. **(C)** Quantifications of these phenotypes. Scale bars, 20μm. Genotypes are as follows (A) *hsFLP122 , FRT19A, GAL80/Hep*^{R39}*, FRT19A; UAS-mCD8/UAS-Bsk; GAL4-OK107/+* (B) *hsFLP122/+; UAS-mCD8/UAS-Bsk; FRT82B, GAL80/FRT82B, Mkk4* ^{e01458} *; GAL4-OK107/+*

clones and *Mkk4* mutant MB neuroblast clones were generated with ectopic *Hep* expression. The axon overextension phenotypes observed with loss of *Mkk4* can be rescued with the introduction of *Hep* overexpression. In contrast, *Mkk4* ectopic expression in a *Hep* null background was unable to rescue the axon overextension phenotypes observed with loss of *Hep* (Figure 4.6.1 A and B; quantifications, Figure 4.6.1 C). This suggests that although both JNKKs are both able to prevent axon overextension past the correct synaptic target area, they may function differently to regulate Bsk, Hep may be the more potent activator of Bsk than Mkk4. Further evidence to reinforce this notion comes from the fact that ectopic expression of Bsk rescued the mutant phenotypes observed in Mkk4 clones but not Hep clones (Figure 4.6.2 A and B; quantifications, Figure 4.6.2 C).

4.8 Concomitant loss of *Hep* and *Mkk4* in MB neurons phenocopies the neurodegeneration observed in *Bsk* null MB neurons

If Hep and Mkk4 are the sole regulators of Bsk phosphorylation in MB neurons, concomitant loss of both Hep and Mkk4 should result in stronger Bsk inactivity, culminating in a high frequency of neurodegeneration phenotypes, similar to the phenotypes observed in a *Bsk* null scenario. I tested this by generating Hep^{R75}, $Mkk4^{e01458}$ double mutant α/β MB neuroblast clones. Both Bsk^{147e} and Hep^{R75}, $Mkk4^{e01458}$ double mutant α/β MB neuroblast clones exhibited neurodegeneration phenotypes (Figure 4.7.1 B-C), typified by loss of the entire population of β axons, however this mutant phenotype was fairly infrequent in both instances, possibly as a result of protein perdurance (Bsk^{147e}, n = 25, neurodegeneration = 8%; Hep^{R75}, $Mkk4^{e01458}$, n =10, neurodegeneration = 10%).

In order to observe the detailed morphology of these mutant neurons, I decided to generate Bsk^{147e} and Hep^{R75}, $Mkk4^{e01458}$ single-cell MB α/β clones, I found that Hep^{R75}, $Mkk4^{e01458}$ single cell MB neuroblast clones (Figure 4.7.1 D-F) exhibited a substantially higher frequency of axon breaks than Hep^{R75} or $Mkk4^{e01458}$ single mutants alone (Figure 4.7.2). The number of axon breaks in Hep^{R75}, $Mkk4^{e01458}$single cell MB α/β neuroblast clones, were comparable to *Bsk* null axons (Figure 4.7.1 G-I; quantifications, Figure 4.7.2). I also tested whether axon overextension may be linked to neurodegeneration by analysing the *babo* gene, which when inactivated results in similar axon overextensions (Ng, 2008). The *babo* overextended axons hardly has any axon breaks throughout the entire neurite (Figure 4.7.1 O; quantifications, Figure 4.7.2). This suggests that axon overextension per se does not necessarily lead to axon breaks and neurodegeneration.

Upon more thorough analysis I also observed that axon loss was more severe in aged neurons characterised by loss of the entire β axon branch. This phenotype only occurred in aged adult (15 days post-adult eclosure) Hep^{R75}, $Mkk4^{e01458}$ and Bsk^{147e} single cell MB α/β neuroblast clones (Figure 4.7.1 J-K and Figure 4.7.3), whereas this phenotype was not observed in younger adults (5 days post-eclosure; Figure 4.7.1 D-I). This large scale axon loss could be the result of dying back degeneration, which is characterised by the initial degeneration of the distal regions of axons, followed by distal-to-proximal progression (Luo and O'Leary, 2005). I also observed degeneration of the distal regions of the axons in *Bsk* null single cell clones of γ–neurons (Figure 3.3.3 M-O).

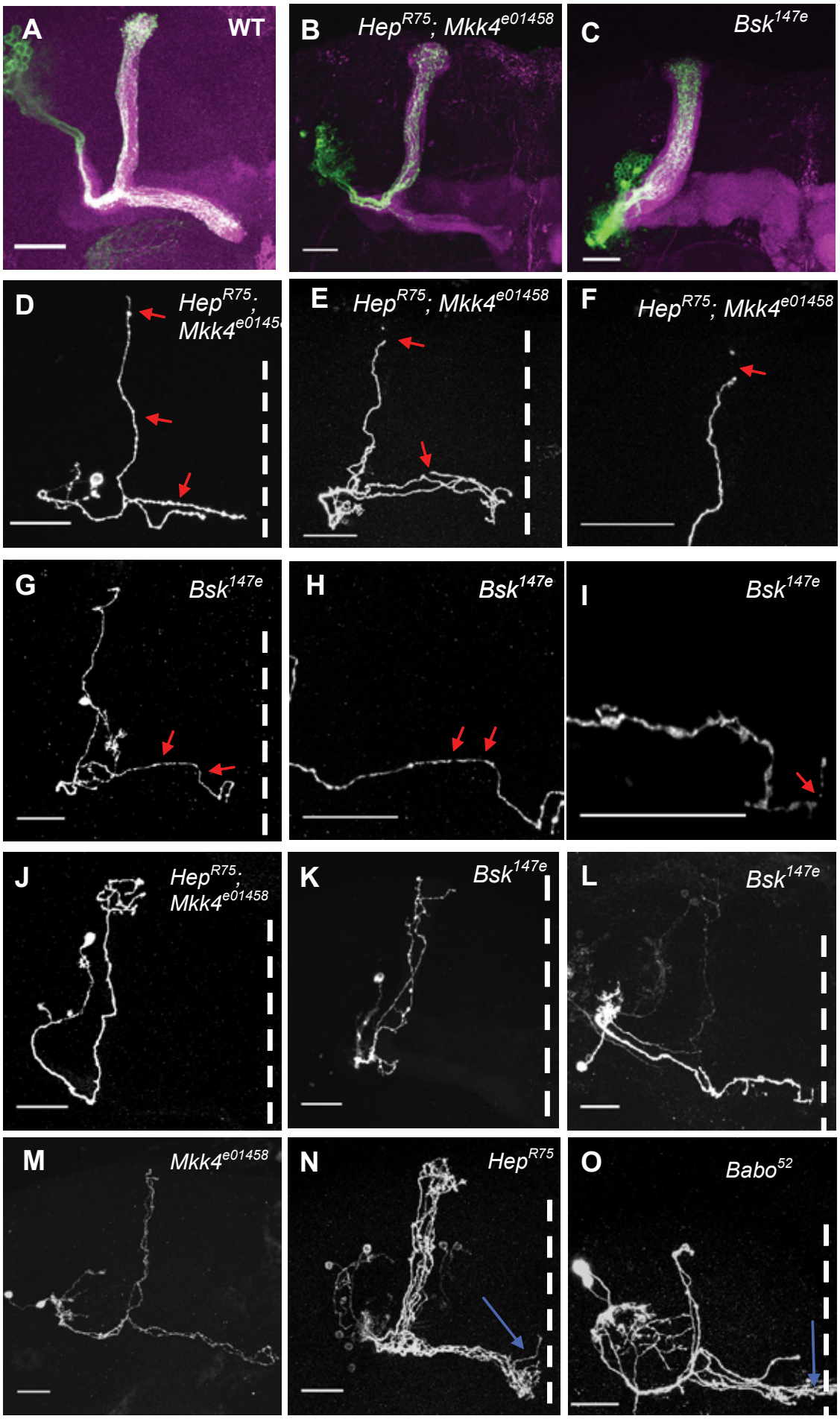
A
WT
B
Hep^R75; Mkk4^e01458
C
Bsk^147e
D
Hep^R75; Mkk4^e01458
E
Hep^R75; Mkk4^e01458
F
Hep^R75; Mkk4^e01458
G
Bsk^147e
H
Bsk^147e
I
Bsk^147e
J
Hep^R75; Mkk4^e01458
K
Bsk^147e
L
Bsk^147e
M
Mkk4^e01458
N
Hep^R75
O
Babo^52

Figure 4.7.1

Figure 4.7.1 Neurodegeneration in *Hep^{R75}, Mkk4^{e01458}* α/β single cell clones.
(A-C) Representative images of wild type **(A)**, *Hep^{R75}, Mkk4^{e01458}* **(B)** and *Bsk^{147e}* α/β neuroblast clones **(C)**. Both *Hep^{R75}, Mkk4^{e01458}* and *Bsk^{147e}* α/β mutant MB neuroblast clones exhibit loss of the entire population of β axons. **(D-E)** Overall images of entire *Hep^{R75}, Mkk4^{e01458}* α/β mutant single/two cell MB neuroblast clones exhibiting neurodegeneration (samples taken 5 days post-adult eclosure). **(F)** Magnified image of a terminal axon break, shown in the previous panel **(E)**. **(G-I)** Representative images of *Bsk^{147e}* α/β mutant MB single cell neuroblast clones displaying neurodegeneration. **(G)** Overall image of entire *Bsk^{147e}* α/β mutant single cell MB neuroblast clone. **(H)** Magnified image of mid-axon breaks, shown in the previous panel **(G)**. Terminal axon breaks were also identified in single cell *Bsk^{147e}* α/β mutant MB neuroblast clones **(I)**. **(J-K)** Loss of the entire β axon population is observed in both *Hep^{R75}, Mkk4^{e0145}* **(J)** and *Bsk^{147e}* α/β mutant single/two cell Aged (15 days post-adult eclosure) neuroblast clones. In this particular *Bsk^{147e}* α/β mutant two cell neuroblast clone, ectopic branching of the α axon projections is also observed **(K).** Loss of the α axon population was also observed in *Bsk^{147e}* α/β mutant single cell MB neuroblast clones **(L)**. Axonal loss was not exhibited in any *Mkk4^{e01458}* **(M)**, *Hep^{R75}* **(N)** or *Babo^{52}* **(O)** α/β mutant single cell neuroblast clones. Overextending axons are indicated by blue arrows, axon breaks are indicated by the red arrows. Scale bars, 20μm. Genotypes are as follows (A) *hsFLP, UAS-mCD8/+; FRT40A, GAL80/FRT40A; GAL4-OK107/+* (B, D-F, J) *hsFLP122, FRT19A/Hep^{R75} , FRT19A; UAS-mCD8/+; FRT 82B, GAL80/FRT82B, Mkk4 ^{e01458} ; GAL4-OK107/+* (C, H, I, K, L) *hsFLP, UAS-mCD8 /+; Bsk^{147e}, FRT40A/FRT40A, GAL80; GAL4-OK107/+* (M) *hsflp122/+; UAS-mCD8/+; FRT82B, GAL80/ FRT82B, Mkk4 ^{e01458}; GAL4-OK107/+* (N) *hsFLP122, FRT19A, GAL80/Hep ^{R75} , FRT19A; UAS-mCD8 (2x)/+ GAL4-OK107/+* (O) *hsFLP, UAS-mCD8/+; FRTG13, GAL80/FRTG13, Babo^{52} GAL4-OK107/+*

A

Sample no.	Location of neurodegeneration in axon														
	Cell Processes					Mid axon					Distal axon				
	No. of axon breaks					No. of axon breaks					No. of axon breaks				
1	2	2	2	1	0	6	5	2	1	1	5	13	3	1	0
2	4	5	1	0	0	9	9	1	0	1	7	4	1	1	0
3	4	5	2	0	0	4	5	0	0	0	12	7	0	0	0
4	6	3	1	0	0	8	9	2	2	0	7	8	0	1	0
5	7	2	1	0	0	4	6	2	0	2	5	4	2	0	0
6	4	6	0	0	0	5	6	0	0	0	6	11	0	1	0
7	5	3	1	0	1	7	5	1	1	0	9	4	1	2	0
8	5	3	0	0	0	7	9	0	0	0	8	8	2	0	0
9	2	2	0	1	0	5	4	2	2	0	5	4	2	0	2
10	2	2	1	0	0	6	5	2	1	1	6	5	2	1	0
Mean ($\bar{x}$)	4.1	3.3	0.9	0.2	0.1	6.1	6.3	1.2	0.7	0.5	7	6.8	1.3	0.7	0.2
Key	*Hep* ^{R75} ; *Mkk4* ^{e01458}					*Bsk* ^{147e}					*Hep*^{R75}				
											Mkk4 ^{e01458}				
													Babo^{52} (Control)		

B

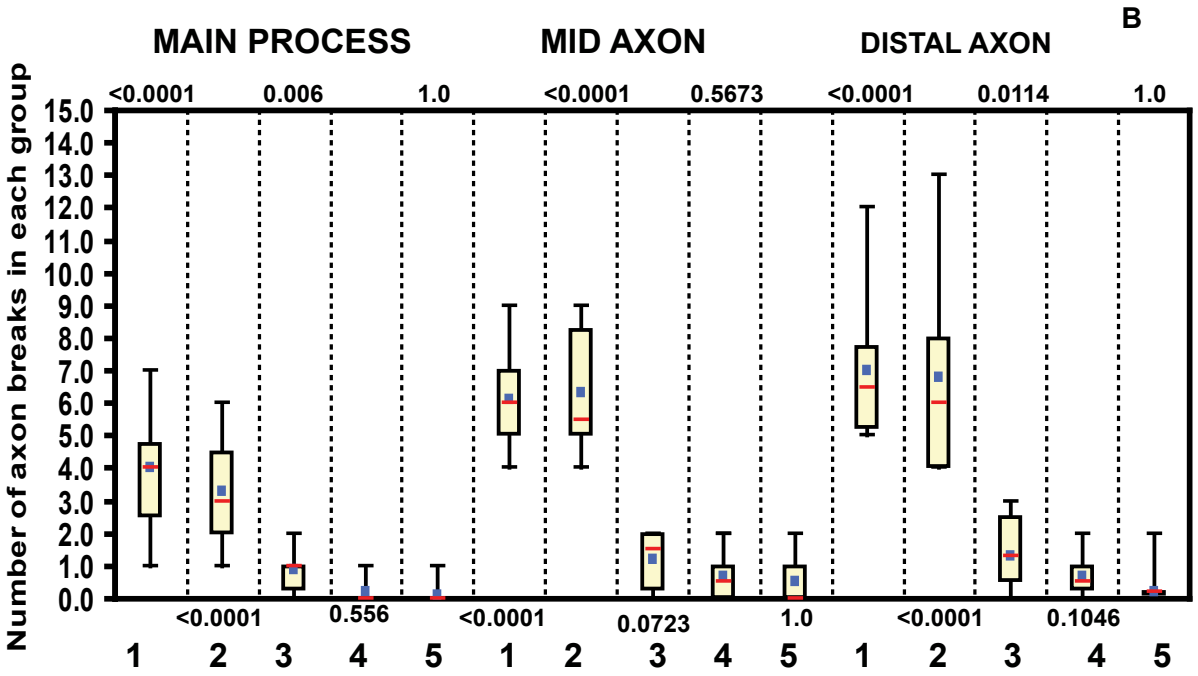

Group 1 = *Hep*^{R75}, *MKK4*^{E01458} α/β single cell clones
Group 2 = *Bsk*^{147e} α/β single cell clones
Group 3 = *Hep*^{R75} α/β single cell clones
Group 4 = *MKK4*^{E01458} α/β single cell clones
Group 5 = *Babo*^{52} α/β single cell clones

Figure 4.7.2

Figure 4.7.2 Neurodegeneration is statistically significant in double mutant *Hep^{R75}*, *Mkk4^{e01458}* and *Bsk^{147e}* MB α/β single cell clones.

(A) Table showing quantification of axon breaks in *Hep^{R75} Mkk4^{e01458}* double mutant, *Bsk^{147e}*, *Hep^{R75}*, *Mkk4^{e01458}* and *babo^{52}* MB α/β single cell clones. Ten single cell α/β clones were quantified for each genotype. **(B)** Box plot displaying quantification of axon breaks in *Hep^{R75} Mkk4^{e01458}* double mutant, *Bsk^{147e}*, *Hep^{R75}*, *Mkk4^{e01458}* and *babo^{52}* MB α/β single cell clones as indicated. Ten single cell α/β clones were analysed for each genotype. Statistical analysis shows a significant difference between *Hep^{R75}*, *Mkk4 ^{e01458}* double mutant or *bsk^{147e}* clones when compared to *Hep^{R75}* or *Mkk4^{e01458} or babo^{52}* mutants ($P<0.05$) but no significant difference between the *Hep^{R75}*, *Mkk4 ^{e01458}* double mutant compared to *bsk^{147e}* clones, or between *hep^{R75}* and *Mkk4^{e01458}* compared to *babo^{52}* mutants ($P>0.05$). The only exception is in the distal axon section of *hep^{R75}* axons, where a small proportion of degeneration was observed, as reflected in the P-value (0.014). *babo^{52}* clones were used as a control in the statistical study. **($\bar{x}$)** = mean.

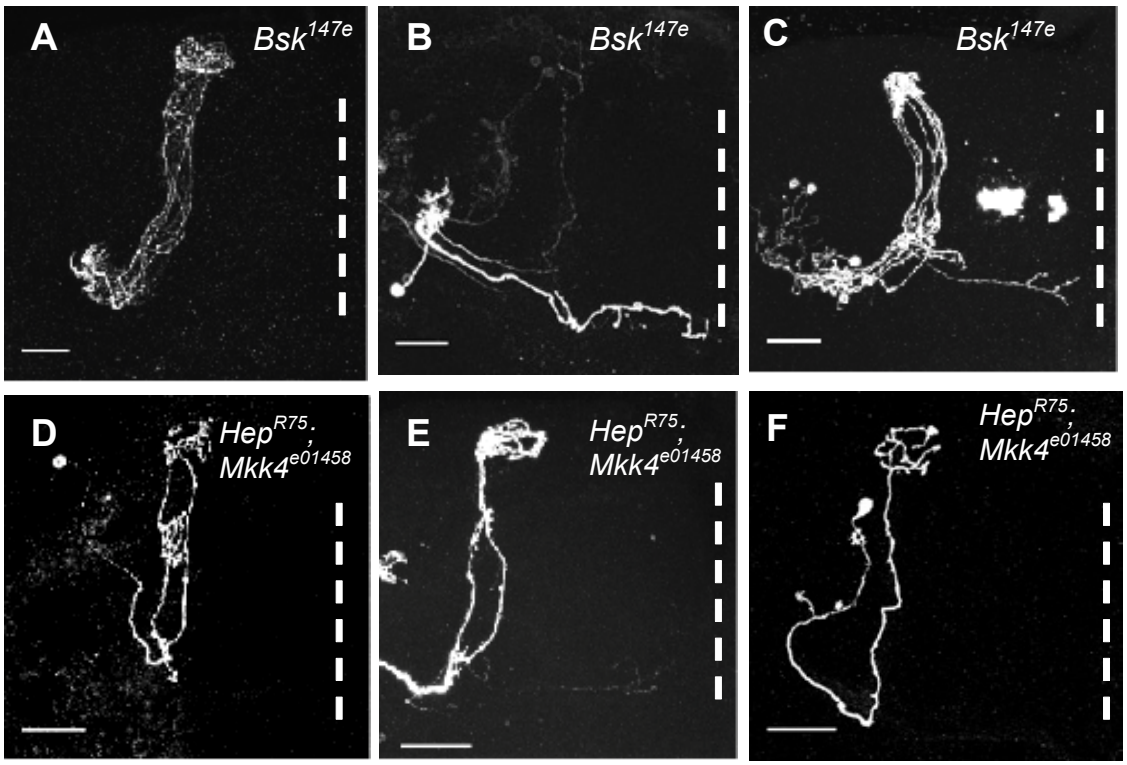

Figure 4.7.3 *Bsk*^{147e} and *Hep*^{R75}, *Mkk4*^{e01458} double mutant aged single cell α/β MB neuroblast clones both exhibit axon loss (neurodegeneration) of the β axon projections.

(A-B) Representative images of multiple single **(A)** and individual single cell **(B)** *Bsk*^{147e} α/β MB neuroblast clones, exhibiting **(A)** axon loss of the entire β axon population (n=22), and **(B)** loss of the α axon projection (n=1). **(C)** Representative image of multiple single cell *Bsk*^{147e} α'/β' MB neuroblast clones, displaying loss of the vast majority of entire β' axons (n=6, 66% of axons analysed). However remnants of the proximal part of β' axons still remain in a minority of samples (n=2, 22% of axons analysed) and one axon that terminates at the correct wild type termination point is still visible (n=1, 11% of axons analysed). **(D-F)** Representative images of single/two cell *Hep*^{R75}, *Mkk4*^{e01458} α/β MB neuroblast clones, all examples exhibited loss of the β axons (n=10). All samples displayed above were dissected at least 15 days post-eclosure. Green, CD8-GFP; FasII, Magenta. Scale bars, 20 μm. (A-C) *hsFLP, UAS-mCD8/+; Bsk*^{147e} *FRT40A/FRT40A, GAL80; GAL4-OK107/+* (D-F) *hsFLP122, FRT19A, GAL80/Hep*^{R39}*, FRT19A; UAS-mCD8/+; FRT82B, GAL80/FRT82B, Mkk4* ^{e01458} *; GAL4-OK107/+*

4.9 Constitutively active *Hep* results in MB neuron apoptosis and axon overextensions.

To determine whether there are distinct differences in the signalling mechanisms by which the JNKKs regulate Bsk I decided to take a gain of function approach by generating Hep/Mkk4-Bsk fusion transgenes. Prior to this I started by acquiring a constitutively active *Hep* transgenic line: UAS-hep^{CA} (Adachi-Yamada et al, 1999), to use as a control for comparative purposes. Expression of the constitutively active trangene Hep^{CA} at 25°C culminated in neuronal death in the majority of MB neurons. This is consistent with the cell death phenotypes observed in the adult wing (Adachi Yamada et al, 1999; Miotto et al, 2006) and wing disc (Ryoo et al, 2006) when Hep^{CA} is overexpressed (Figure 4.8.1 B; quantifications, Figure 4.8.1 C). This made it difficult to visualise axon projections as a large proportion of MB neurons are no longer present. To circumvent this I lowered the level of UAS-GAL4 expression by raising animals at 18°C (see chapter 2).

When constitutively active *Hep* was expressed at a lower level, less neuronal death was observed and the majority of β–axons exhibited overextension (Figure 4.8.2, quantifications, Figure 4.8.2 G). Surprisingly the level of phospho JNK in MB neurons expressing Hep^{CA} was significantly lower than the endogenous phospho JNK level exhibited in wild type MB neurons (Figure 4.8.2 B, E). This suggests that a negative feedback loop is in operation and a neuronally expressed phosphatase in MB neurons may be functioning to regulate phospho JNK levels. There is a precedent for this negative feedback mechanism to be operating in various developmental contexts to supress JNK activity levels. For instance Puckered, the sole *Drosophila* JNK-specific MAPK

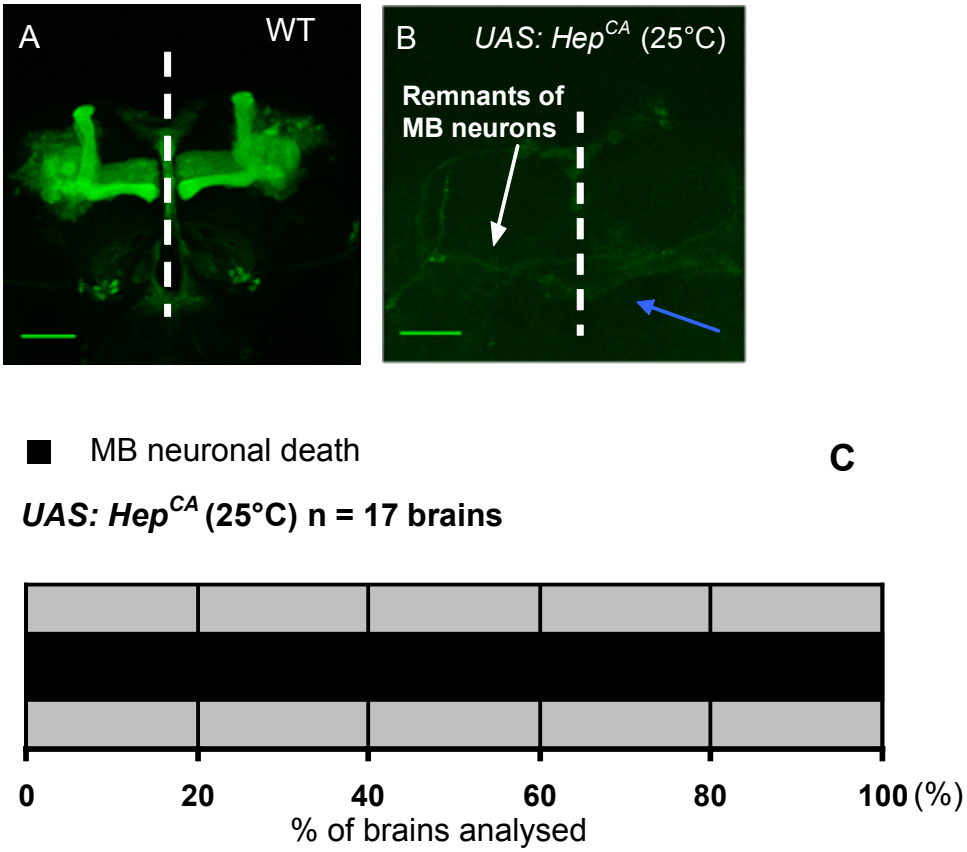

Figure 4.8.1 Overexpression of constitutively active Hep culminates in MB neuron death.

(A) Representative image of WT MB neurons and **(B)** MB neurons overexpressing a constitutively active Hep transgene (*Hep*^{CA}) at 25°C. **(C)** All samples quantified exhibited neuronal apoptosis. Scale bar, 50μm; CD8-GFP, green. The blue arrow indicates axon overextension. Genotypes are as follows (A) *UAS-mCD8-GFP/+; GAL4-OK107/+;* (B) *UAS-mCD8-GFP/+; UAS-Hep* ^{CA}*/+; GAL4-OK107/+*

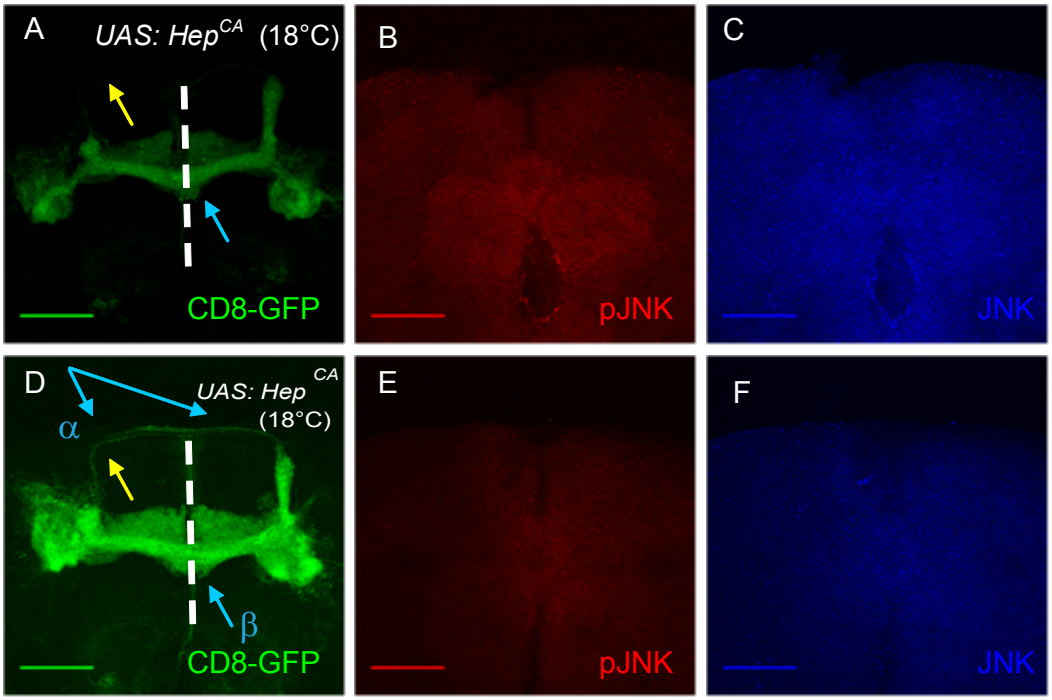

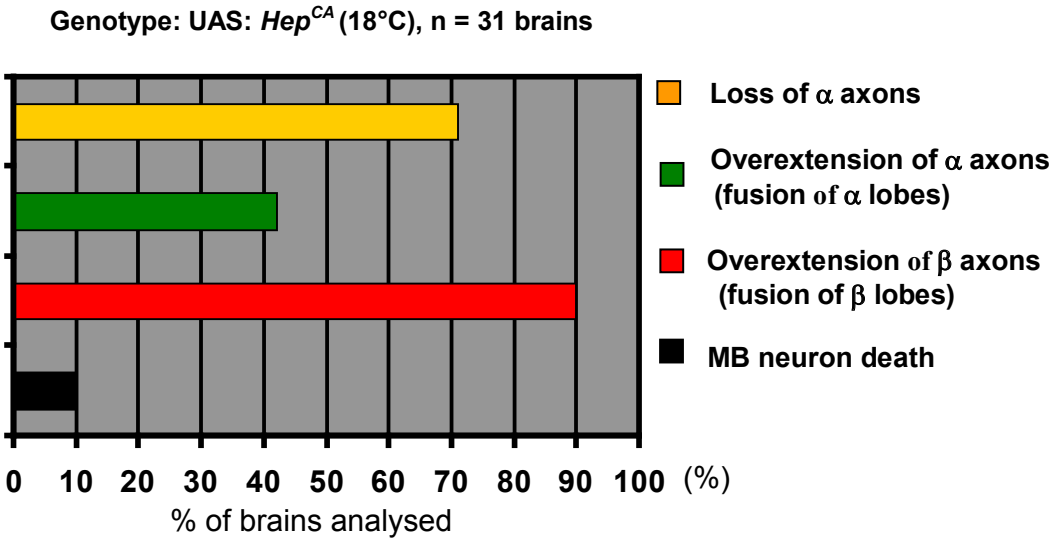

Figure 4.8.2 Overexpression of low levels of constitutively active *Hep* results in axon overextension.

Representative images of MB neurons overexpressing a constitutively active *Hep*^{CA} trangene at 18°C. The MB neuronal projections are labelled with CD8-GFP **(A)** and **(D)** and the majority of MB axons exhibit axon overextension and axon loss. Additionally the JNK and phospho JNK levels are substantially reduced; this is indicated by phospho JNK (**B** and **E**) and JNK (**C** and **F**) immunostaining. The light blue arrows indicate either α or β axon overextension, the yellow arrows indicate α axon loss. Scale bars, 50μm. **(G)** Quantifications of the above phenotypes Genotypes are as follows (A,D) *UAS-mCD8-GFP/+; UAS-Hep*^{CA}*/+; GAL4-OK107/+*

phosphatase acts a key anti-apoptotic factor that prevents apoptosis in epithelial cells by restraining JNK activity (McEwen et al, 2005).

4.10 Hep signals through Bsk to regulate neuronal death/apoptosis

I next decided to generate, Hep-Bsk and Mkk4-Bsk fusion constructs using a strategy previously described (Zheng et al, 1999). I created Hep-Bsk and Mkk4-Bsk fusion constructs by linking the respective upstream JNKK to *Bsk* via a short peptide linker (see Chapter 2). S2 cell protein homogenates from S2 cells transfected with the Hep-Bsk construct produced extremely high levels of phosphorylated JNK protein compared with S2 homogenates which had been transfected with a UASt: Bsk construct (Figure 4.9.1) confirming that the Hep-Bsk fusion protein was acting in a constitutively active manner.

I then studied the effect of overexpressing the Hep-Bsk fusion transgene *in vivo*. The majority of Hep-Bsk fusion transgenic lines when overexpressed in MB neurons exhibited large scale MB neuronal death (Figure 4.9.2; quantifications, Figure 4.9.5), reminiscent of that which occurred when the constitutively active *Hep* transgene was expressed in MB neurons. This made it difficult to visualise axon projections as a large proportion of MB neurons are no longer present. To circumvent this I analysed lower level expression lines, where a larger number of MB neurons were present. This enabled me to observe caspase activity and MB neuronal morphology in weaker expressing Hep-Bsk HA transgenic lines.

An elevated level of caspase activity was observed in MB neurons overexpressing Hep-Bsk trangenes, compared to the wild type control suggesting that any MB neuronal death occurring is caspase dependent (Figure 4.9.3). The elevated level of caspase-3

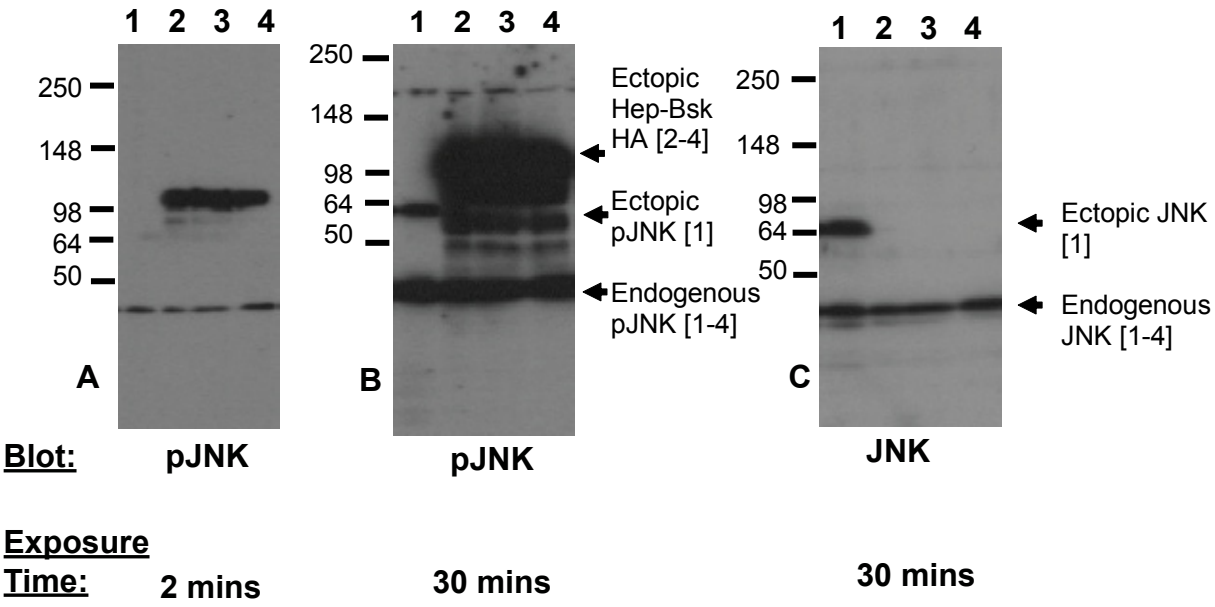

Figure 4.9.1 Elevated phospho JNK levels in S2 cells expressing Hep-Bsk fusion protein.

S2 cells were transfected with pUAST Bsk-YFP[1] and pUAST Hep-Bsk HA [2-4]. Transfected S2 cell lysates were then subjected to SDS-PAGE and immunoblot analysis using both anti-phospho JNK **(A** and **B)** and anti-JNK **(C)** antibodies. The resulting western blots detected extremely high levels of activated JNK generated from the pUAST Hep-Bsk fusion protein S2 cell homogenate, in comparison to phospho JNK levels in S2 cell homogenates transfected with JNK-YFP **(A** and **B)**. However when the same blot was stripped and stained for JNK, no visible band corresponding to JNK expression from the Hep-Bsk HA transfected S2 cell lysates (lanes 2-4) was detected **(C)**. This suggests that although the pUAST Hep-Bsk HA construct is functional, it is possible that due to high levels of toxicity or cell death it is expressed at extremely low levels in S2 cells. This would be consistent with the MB neuron data, where overexpression of a Hep-Bsk fusion transgene results in large scale MB neuron death. Three samples of transfected Hep-Bsk HA S2 cell lysates were run in each blot.

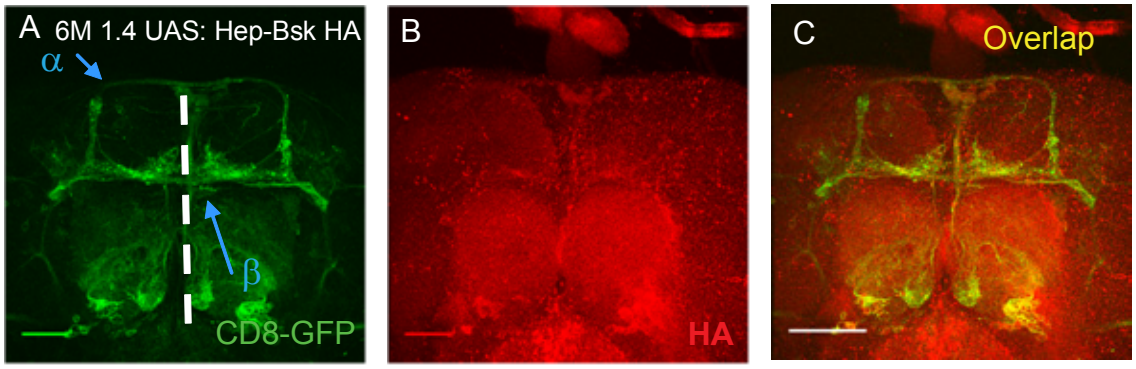

Figure 4.9.2 Overexpression of strong Hep-Bsk fusion transgenic lines results in MB neuron death.

Representative image of MB neurons overexpressing a Hep-Bsk HA fusion trangene and displaying MB neuron loss. **(A)** The MB neuron projections for this particular transgenic line also exhibit axon overextension and are labeled with CD8-GFP. **(B)** The HA tag is also detected in MB neurons ectopically expressing Hep-Bsk, however HA staining is difficult to discern due to the low numbers of MB neurons present. **(C)** The overlap between HA staining and the CD8-GFP labelled MB neurons is also shown. The light blue arrow indicates either α or β axon overextension. Scale bars, 50μm; green, CD8-GFP; red, HA staining. Genotypes are as follows (A) *UAS-mCD8-GFP/+; UAS-Hep-Bsk HA/+; GAL4-OK107/+*

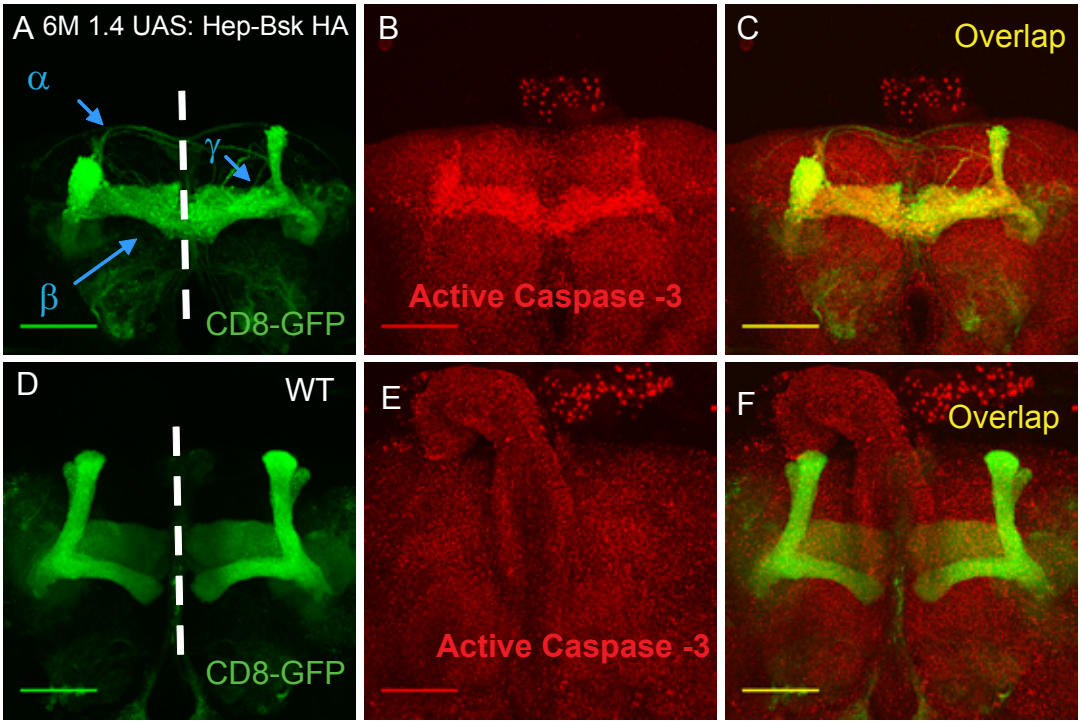

4.9.3 Overexpression of Hep-Bsk fusion transgenic lines results in an elevated level of Caspase 3 activity

(A) Representative image of MB neurons overexpressing a Hep-Bsk HA fusion transgene and displaying MB neuron loss of the α axon projections, accompanied by axon overextension of α, β and γ, neurons (indicated by the blue arrows). **(B)** Immunostaining the same brain with a caspase 3 antibody, which recognises the active (cleaved) form of caspase 3, revealed that caspase 3 activity was particularly high in MB neurons. **(C)** The overlap between the CD8-GFP labelled MB neurons and the active caspase 3 staining is also shown. **(D-F)** Wild type control stainings show caspase activity is relatively low. Scale bars, 50 μm. Green, CD8-GFP; red, active caspase 3. Genotypes are as follows (A) *UAS-mCD8-GFP/+; UAS-Hep-Bsk HA/+; GAL4-OK107/+* (B) *UAS -mCD8-GFP/+; GAL4-OK107/+*

staining in MB neurons overexpressing the Hep-Bsk fusion transgene, is not the result of cross-reactivity with CD8-GFP labelled MB axons since in the wild type control, caspase-3 staining is not visible and does not overlap with the CD8-GFP labelled MB neurons. I also noticed that in 'weaker' expressing Hep-Bsk transgenic lines, a large proportion of MB neurons exhibited β–axon overextension, which closely resembled the phenotypes observed in MB neurons expressing a lower level of constitutively active Hep (Figure 4.9.4 A; quantifications, Figure 4.9.5). However, as expected, the phospho JNK and JNK levels were elevated in the MB neurons overexpressing Hep-Bsk fusion proteins (Figure 4.9.4 B and C), compared with wild type MB neurons expressing ectopic Hep (Figure 4.9.4 D-F), confirming that the Hep-Bsk fusion transgene was acting in a constitutively active fashion in MB neurons.

I next tested whether this constitutively Hep-Bsk fusion transgene was dependent on Hep kinase activity. All the MB neurons of transgenic lines expressing Hep^{K226M}–Bsk (a kinase dead Hep-Bsk transgene) exhibited WT axonal projections (Figure 4.9.6 A; quantifications, Figure 4.9.6 D), indicating that the Hep-JNK signalling pathway that regulates neuronal death is dependent on kinase activity. It is important to note that ectopic expression of Hep or Bsk alone gives wild type axonal projections whereas overexpression of Hep^{CA} or Hep-Bsk fusion transgenes give the distinct gain-of-function MB neuronal death/axon overextension phenotype, this suggests that constitutively active Hep-Bsk signalling acts in a distinct manner.

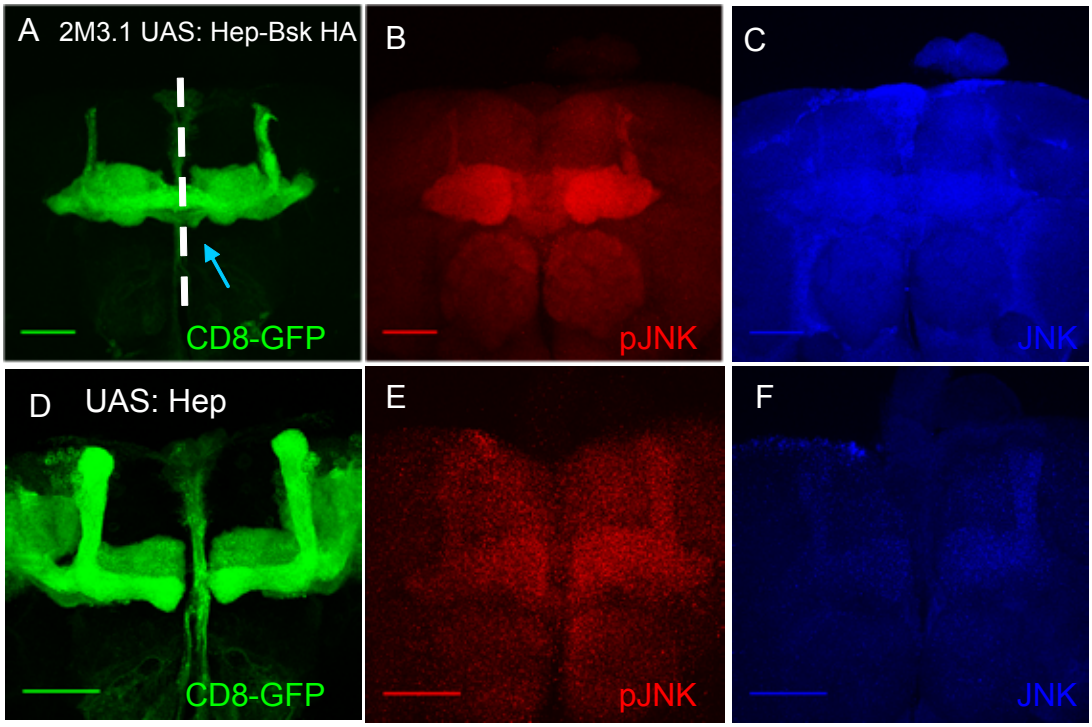

Figure 4.9.4 Overexpression of weaker expressing Hep-Bsk transgenic lines results in axon overextension

(A-C) Representative image of MB axons overexpressing the Hep-Bsk HA transgene. This particular transgenic line is characterized as weak, since when overexpressed, no large scale MB neuron loss is apparent, additionally the MB axon projections are easily discernible. **(A)** All MB axon projections analysed for this genotype exhibited axon overextension of the β neurons, (light blue arrows). Furthermore levels of activated JNK and JNK were also elevated, this was detected by staining whole mount brains with pJNK **(B)** and JNK **(C)** respectively. **(D-F)** As a control ectopic Hep was overexpressed in MB neurons, all MB axon projections analysed exhibited wild type projections **(D).** As expected there were relatively lower levels of activated JNK **(E)** and JNK **(F)**, compared with that observed in MB neurons overexpressing the Hep-Bsk fusion transgene. All Hep-Bsk HA transgenic lines used were expressed at 25°C. Scale bars, 50μm. Cell bodies have not been included in the z-projection **(A-C)**, since they were obscuring the MB neuron projections. Green, CD8-GFP; Red, pJNK staining; Blue, JNK staining. Genotypes are as follows (A) *UAS-mCD8-GFP/+; UAS-Hep-Bsk HA/+; GAL4-OK107/+* (D) *UAS-mCD8 -GFP/+; UAS-Hep/+; GAL4-OK107/+*

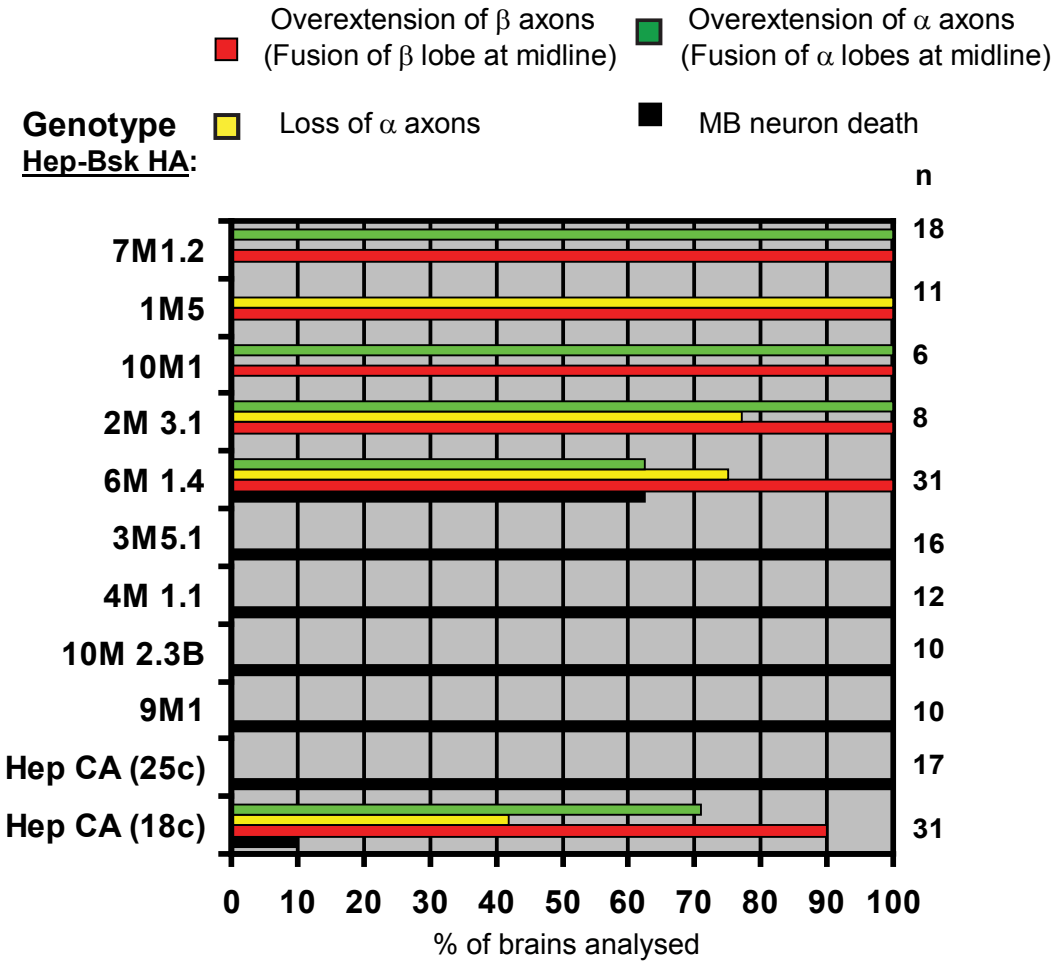

Figure 4.9.5 Quantifications of the axonal phenotypes in MB neurons acquired from overexpressing various Hep Bsk-HA transgenic lines.

Quantification of the axonal phenotypes in MB neurons overexpressing Hep-Bsk HA from 9 different transgenic lines (name of line is denoted in number form). The four trangenic lines (9M1, 10M 2.3B, 4M1.1 and 3M 5.1), where all samples exhibit large scale MB neuronal death are classified as 'strong' and the phenotypes resemble the large scale neuronal death exhibited in MB neurons overexpressing Hep^{CA} at 25°C. In the four 'weaker' expressing' lines (7M 1.2, 1M4, 10M1 and 2M 3.1) large scale MB neuronal death is not observed and the β and α axon overextension phenotypes resemble those observed when Hep^{CA} was expressed at lower levels (18°C) in MB neurons. Trangenic line 6M 1.4 may be classified as an 'intermediate' expressing line since large scale MB neuronal death is not fully penetrant and is accompanied with axon overextension. n, number of brains analysed. In some scenarios the total may not add up to 100% since some axon projections exhibit multiple phenotypes. All Bsk-HA transgenic lines were expressed at 25°C.

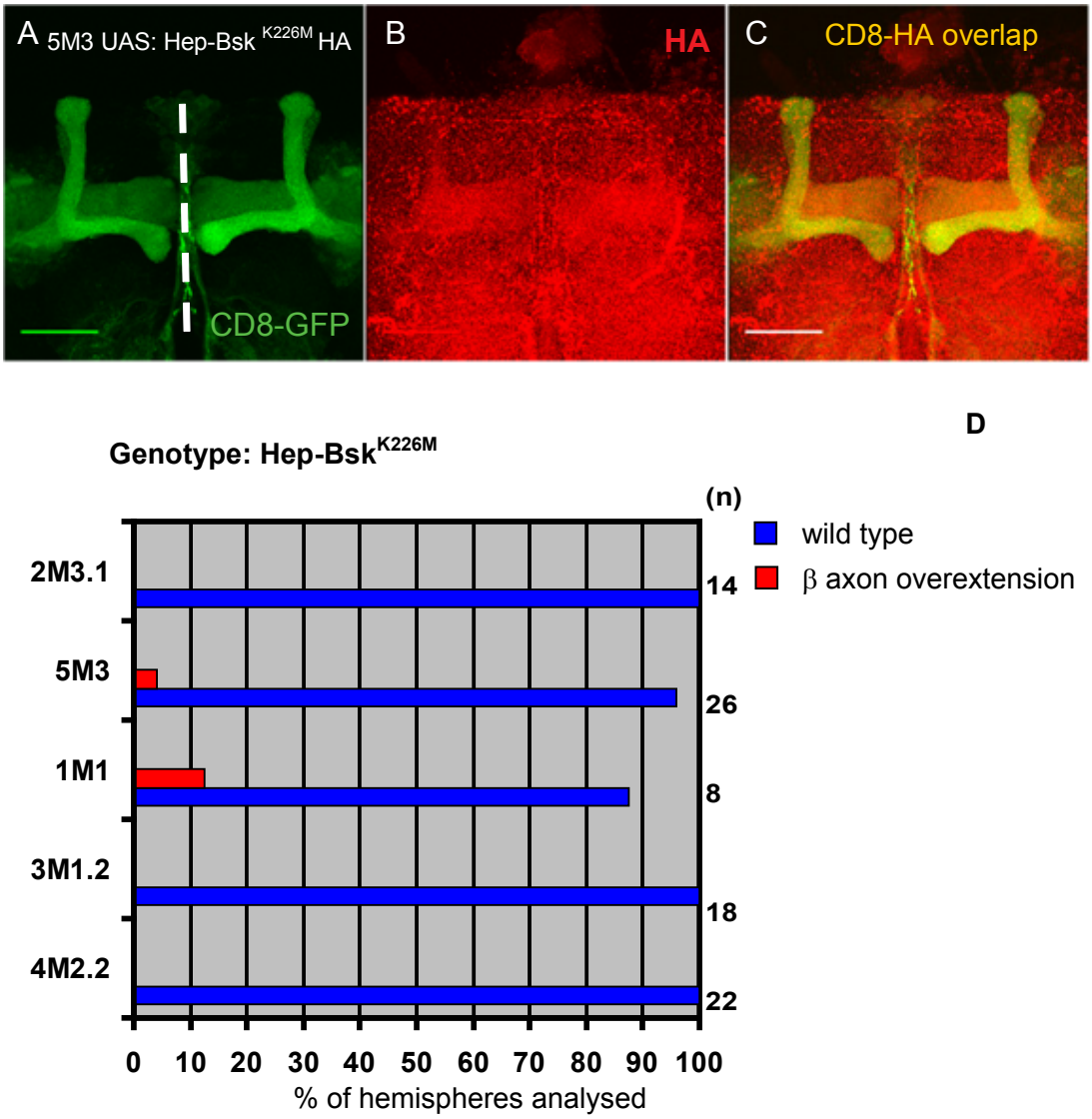

Figure 4.9.6 Hep-Bsk constitutively active signalling is kinase dependent in MB neurons.

(A) Representative image of MB neurons overexpressing the Hep-Bsk^{K226M} HA transgene. MB neurons are labelled with CD8-GFP and exhibit wild type projections in the vast majority of samples observed. **(B)** The presence of the ectopic transgene Hep-Bsk^{K226M} is confirmed by HA staining. **(C)** The overlap between CD8-GFP MB neurons and HA staining is shown in yellow. **(D).** Quantifications of the axonal phenotypes in MB neurons overexpressing Hep-Bsk HA^{K226M} from five different transgenic lines (name of line is denoted in number form). n, number of hemispheres analysed; Scale bars, 50μm. Genotypes are as follows (A) *UAS-mCD8 -GFP/+; UAS-Hep-Bsk ^{K226M} HA/+; GAL4-OK107/+*

4.11 Mkk4 is unable to constitutively activate Bsk to regulate neuronal death/apoptosis

Unlike the S2 cell protein extracts acquired from S2 cells that express Hep-Bsk , which produced extremely high levels of activated JNK, those transfected with the equivalent UASt: Mkk4-Bsk construct, exhibited no discernable phospho-JNK band on a western blot (Figure 4.10.1 A). The equivalent JNK band (Figure 4.10.1 B) was detected at a predicted size of 113.2 kDA (Mkk4 = 47.5 kDA; Bsk = 40.7 kDA + Myc 6x).

To determine whether the Mkk4-Bsk fusion transgene is able to regulate neuronal morphogenesis like the Hep-Bsk trangene it was overexpressed in MB neurons. In contrast, overexpression of the Mkk4-Bsk transgene had no significant effect on MB axon morphogenesis although subtle axon overextensions were observed infrequently (Figure 4.10.2 A; quantifications Figure 4.10.2 D). This data suggests that *Mkk4* cannot signal to Bsk in a constitutive manner to orchestrate neuronal death in MB neurons.

Overexpression of the Mkk4-Bsk fusion transgene is insufficient to generate a gain-of-function Bsk allele, as exhibited for Hep^{CA} or the Hep-Bsk fusion transgenes, possible because Mkk4 unlike Hep cannot bind to APLIP1(Horiuchi et al, 2007). This is significant since the vertebrate homologue of *APILIP1*, JIP-1, is a known scaffolding protein for JNK kinases and is able to potentiate JNK activation (Mooney and Whitmarsh, 2004).

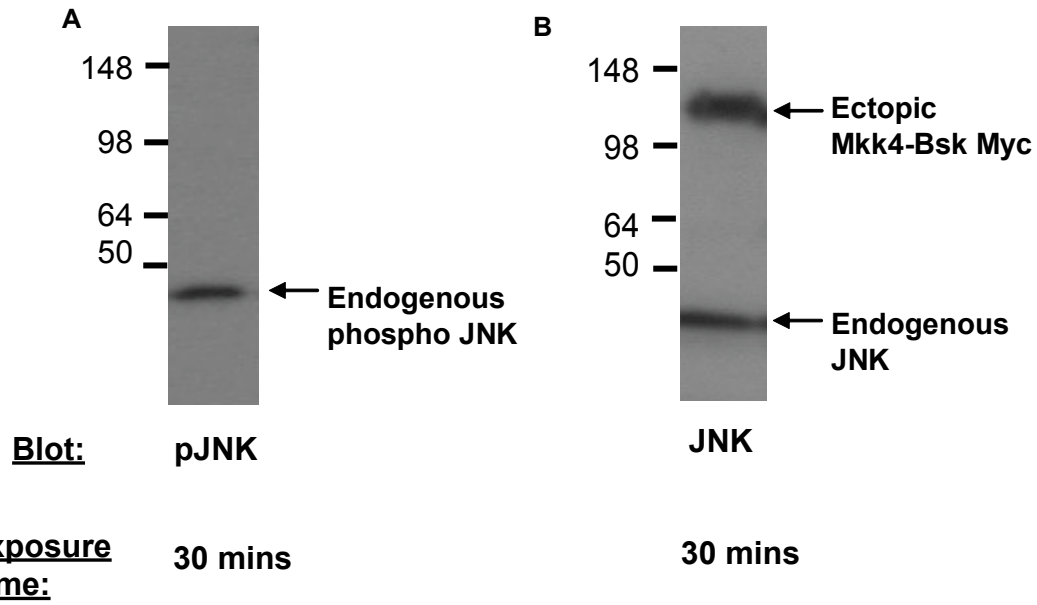

Figure 4.10.1. Phospho JNK cannot be detected in S2 cells overexpressing Mkk4-JNK fusion proteins.

S2 cells were transfected with pUAST Mkk4-Bsk Myc. Transfected S2 cell lysates were then subjected to SDS-PAGE and immunoblot analysis using both anti-phospho JNK **(A)** and anti-JNK **(B)** antibodies. The resulting western blots detected no visible phospho JNK band from the pUAST Mkk4-Bsk fusion protein S2 cell homogenate. However when the same blot was stripped and stained for JNK, a visible band corresponding to ectopic JNK expression from the Mkk4-Bsk Myc transfected S2 cell lysates was detected **(B).** This suggests that the pUAST Mkk4-Bsk Myc construct is being expressed at detectable levels, but does not have the capacity like Hep to regulate Bsk in a constitutively active manner.

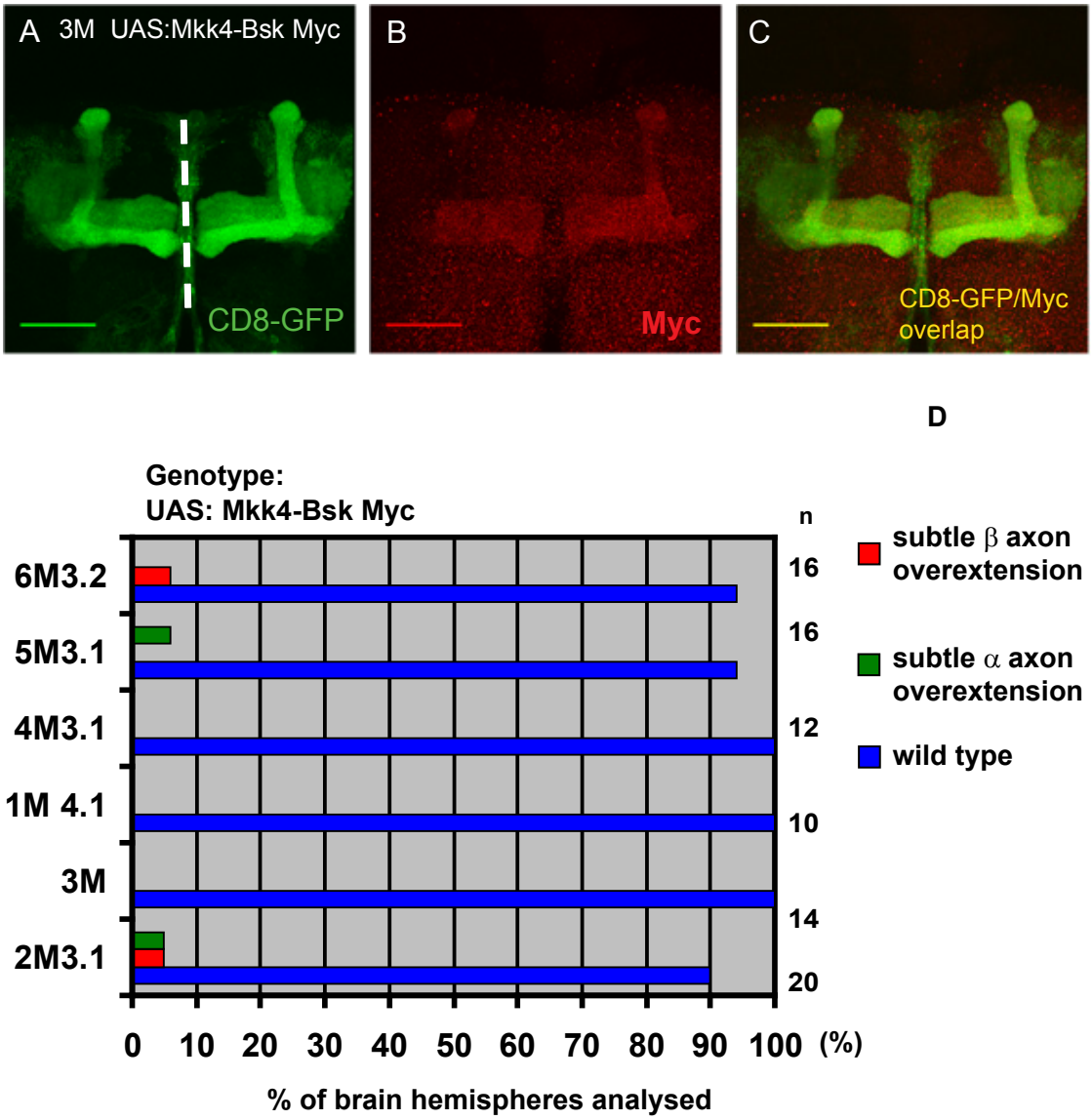

Figure 4.10.2 Overexpression of Mkk4-Bsk fusion transgenic lines has no affect on MB axon morphology

(A) Representative image of MB neurons overexpressing the Mkk4-Bsk Myc transgene. MB neurons are labelled with CD8-GFP and exhibit wild type projections in the vast majority of samples observed. **(B)** The presence of the ectopic transgene Mkk4-Bsk Myc is confirmed by Myc staining. **(C)** The overlap between CD8-GFP MB neurons and Myc staining is shown in yellow. **(D)** Quantification of the axonal phenotypes in MB neurons overexpressing Mkk4-Bsk Myc from six different transgenic lines (name of line is denoted in number form). n, number of hemispheres analysed; Scale bars, 50μm. Genotypes are as follows (A) *UAS-mCD8-GFP/+; UAS-Mkk4-Bsk Myc /+; OK107/+*

4.12 Discussion

In this chapter I presented evidence that axon stability is regulated by two distinct mechanisms, which require different threshold levels of Bsk activity. For signals that protect against neurodegeneration, the JNKKs act redundantly, as loss of either does not result in neurodegeneration, whereas loss of *Bsk* does. While relatively small levels of Bsk activity are required to prevent against axon degeneration, the mechanism that safeguards against overextension requires higher threshold levels of Bsk activity. The presence of just one JNKK activating Bsk is not sufficient to prevent axons from overshooting beyond their correct post-synaptic target. Therefore signals that regulate Bsk can potentially generate distinct axonal phenotypes depending on the signalling network, and signal intensity. The JNKK signal network is linked to signal strength since both JNKKs converge on Bsk and determine the relative activity levels. Thus the next logical questions which need addressing concerns whether Bsk acts in a graded manner to control axon morphogenesis, as suggested by the data acquired thus far and following on from this how is Bsk temporally regulated throughout development to maintain axon stability?

I initially assumed that loss of *Hep* in MB neurons would phenocopy the frequency of neurodegeneration phenotypes acquired in *Bsk* null MB neuroblast clones, based on the existing literature referring to Hep-JNK signalling as a central conduit for regulating numerous aspects of cell morphogenesis. Hep-JNK signalling has been demonstrated to regulate various morphogenetic processes (Glise et al, 1995; Risego-Escovar, 1997, Glise et al, 1995), (Agnes et al, 1999), (Bosch et al, 2005), (Sluss et al, 1996), (Weston and Davis, 2002), including axon overextension in Drosophila dorsal

cluster neurons (Srahna et al, 2006) whereas an in vivo physiological role of Mkk4 has yet to be fully determined. Recently genetic and biochemical experiments have shown a non-redundant function of Mkk4 acting as a MAPKK in parallel with Hep/Mkk7 in dTAK1 mediated JNK activation in the Eiger and Imd Pathways (Geuking et al, 2009). As of yet no phenotypic data is available on the function of Mkk4 in *Drosophila* neuron development, however mice lacking a *Mkk4* gene in the nervous system exhibit severe brain developmental defects and premature death (Wang et al, 2007).

Nonetheless my initial hypothesis proved to be incorrect as the majority of *Hep* null MB neuroblast clones exhibited axon overextension, with a minor proportion of samples displaying neurodegenerative phenotypes. Additionally loss of *Mkk4* also resulted in axon overextension. Thus both JNKKs are required to promote the extension of axons to their correct synaptic targets, as loss of either result in axon overextension. However concomitant loss of both *Hep* and *Mkk4* culminated in neurodegeneration phenotypes resembling those observed in *Bsk* null MB neuroblast clones. Additionally similar to loss of *Bsk*, loss of both JNKKs resulted in a high frequency of neurodegeneration phenotypes. The fact that loss of function of both upstream kinases phenocopies the neurodegeneration phenotypes observed in null *Bsk* MB neuroblast single cell clones shows that both *Hep* and *Mkk4* serve as upstream signalling regulators of *Bsk*.

Another salient point to make is that although both *Hep* and *Mkk4* can function to prevent the overextension of MB axons past their correct synaptic target they do not exhibit complete genetic redundancy. For instance in cross-rescue experiments only expression of *Hep* is able to rescue the axon overextension defects observed in *Mkk4*

mutant MB neuroblast clones, but Mkk4 expression was unable to rescue the *Hep* phenotype. Using a gain-of-function paradigm I also showed that a constitutively active Hep-Bsk fusion transgene is able to induce caspase activity but a similar Mkk4-Bsk fusion did not. It is important to note that the Mkk4-Bsk fusion proteins may be rendered inactive, due to possible conformational effects caused by the fusion. Furthermore loss of *Hep* results in a low frequency of neurodegeneration phenotypes, resembling those observed in Bsk null MB neurons, whereas no neurodegeneration is observed in $Mkk4^{e01458}$ MB neuroblast clones. Taken together this data suggests that Hep and Mkk4 function in a divergent manner to regulate *Bsk* activity, with Bsk being activated at higher threshold level by Hep rather than Mkk4. Therefore in their entirety the genetic results suggest that Hep is the more potent activator of *Bsk* phosphorylation.

The differential function of Mkk4 and Hep are also underlined in a recent publication, which showed that in contrast to the stronger intrinsic activity of Hep^{CA} and the weaker activity of Hep^{WT}, wild type Mkk4 is unable to activate JNK in either S2 cells or fly eyes (Geuking et al, 2009). Additionally $Mkk4^{Asp}$ a constitutively active form of Mkk4, does not act in a constitutively active manner in either flies or S2 cells (Geuking et al, 2009). A more detailed account of how and Mkk4 and Hep could potentially operate in a differential manner to regulate Bsk activation is outlined in the final discussion chapter (see chapter 7).

CHAPTER 5: Signal strength and signal duration are critical parameters in JNK-dependent axonal morphogenesis

5.1 Introduction

In the preceding chapters I established that the *in vivo* activators of Bsk, Hep and Mkk4 signal solely to Bsk to regulate MB axon stabilisation and do not utilise an independent signalling pathway. Convergent activation of both JNK kinases is required to safeguard against axon overextension beyond the correct postsynaptic target. However the presence of only one JNKK is capable of preventing MB neurodegeneration. Based on these phenotypes it can be postulated that Bsk controls axon stabilisation via two mechanisms, to prevent axons from degeneration and from overextending beyond the postsynaptic target, based on the level of signalling inputs from the JNKKs. Thus in order to examine the hypothesis that threshold activity levels of Bsk mediates two distinct aspects of JNK dependent axon stabilisation, I used genetic manipulations to induce different levels of Bsk inactivation in Drosophila MB neurons.

In this chapter I present evidence showing that inactivation of Bsk culminates in overextension and when perturbed to a greater degree neurodegeneration, confirming the hypothesis that threshold activity levels of Bsk mediates these two distinct aspects of JNK dependent axon stabilisation. I also utilise different experimental paradigms to control the timing of Bsk activity in vivo and show that sustained Bsk activity is required throughout the development of these neurons, for correct axon morphogenesis. I also demonstrate that transient Bsk activity, when confined to particular time intervals during development is not sufficient to promote optimal axon stabilisation. Finally I present

evidence suggesting a change in requirements for JNK signalling between the developing and adult brain (perhaps a switch in Bsk's role from axon stability to synaptic plasticity).

5.2 Misexpression of a Dominant negative *Bsk* transgene in MB neurons results in axon overextension

If different threshold activity levels of Bsk result in distinct axonal phenotypes, one prediction is that partial inactivation of Bsk would result in axon overextension. Given the fact that I uncovered elevated levels of Bsk activity in MB neurons, I reasoned that dominant negative (DN) *Bsk* misexpression was unlikely to result in a null, but a partial inactivation phenotype. I overexpressed a nonactivable 'kinase dead' mutant from of *Bsk* (Adachi-Yamada et al, 1999) in MB neurons and unlike in *Bsk* null neuroblast clones, axon overextension constituted the bulk of the phenotypes observed, illustrating that *Bsk* mediated axonal morphogenesis requires a functional kinase domain. (Figure 5.2.1 A, D; quantifications Figure 5.2.1 F). Interestingly overexpression of the phospho-inactive mutant $Bsk^{T181,\ Y183F}$ transgene, phenocopied the *Bsk* DN overextension phenotype acquired in MB neurons (Figure 5.2.1 E). Thus the *Bsk* phospho inactive transgene may also behave in a dominant negative manner when overexpressed in MB neurons, possibly competing with and antagonising endogenous JNK signals. The absence of phospho JNK immunoreactivity in MB neurons misexpressing DN *Bsk*, indicates that the *Bsk* dominant negative transgene has successfully perturbed the endogenous activity of Bsk (Figure 5.2 .1 C). Finally misexpression of *Bsk* DN in *Bsk* null MB neuroblast clones, does not modify the *Bsk* null phenotype, illustrating that it is specific in inactivating *Bsk* and cannot act off-target on any other signalling pathway which are needed in MB neuronal

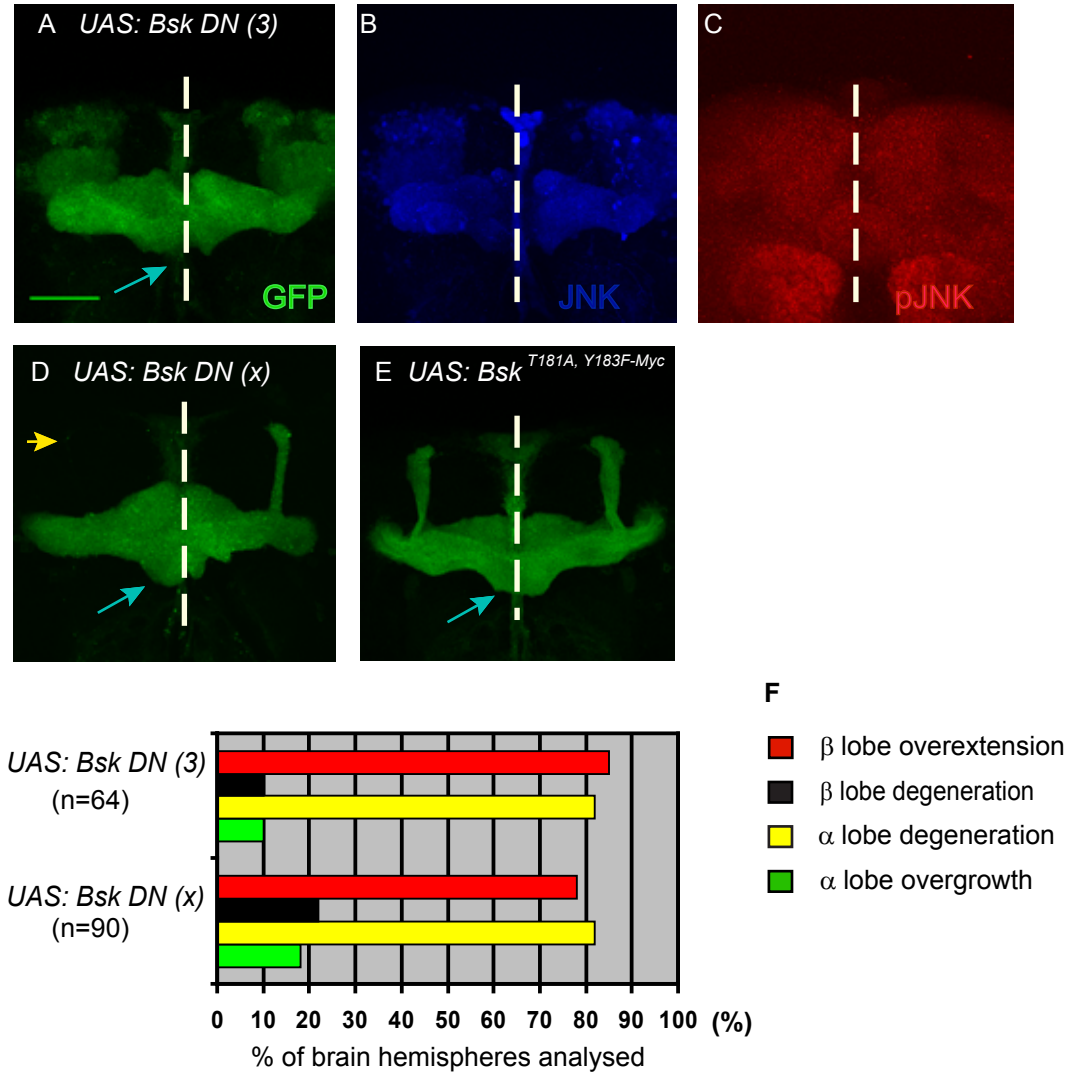

Figure 5.2.1 Partial inactivation of *Bsk* results in distinct axonal phenotypes

(A-C) Representative image of MB neurons misexpressing a dominant negative *Bsk* transgene, labeled with CD8-GFP **(A),** and immunostained with anti-JNK1 **(B)** and anti-phospho JNK **(C).** The high level of JNK staining **(B)** is reflective of the effective misexpression of DN *Bsk* in MB neurons, nonetheless misexpression of DN *Bsk* in MB neurons, **(C)** reduces the phospho JNK signal. **(D-E)** Representative images of MB neurons misexpressing one copy of dominant negative Bsk **(D)** and one copy of phospo-inactive Bsk (*Bsk* $^{T181A,\ Y183F}$) **(E).** Quantifications of the mutant phenotypes observed upon *Bsk* DN misexpression in MB neurons **(F)**. Scale Bar 50μm; n, number of hemispheres analysed. Blue arrows indicate axon overextension; yellow arrows show axon loss. Genotypes are as follows (A) *UAS-mCD8-GFP/+; UAS-Bsk DN/+; GAL4-OK107/+* (D) *UAS-Bsk DN/+; UAS-mCD8-GFP/+; GAL-OK107/+;* (E) *UAS-mCD8-GFP/+; UAS-Bsk* $^{T181A, Y183F}$ *-Myc/+; GAL4-OK107/+.*

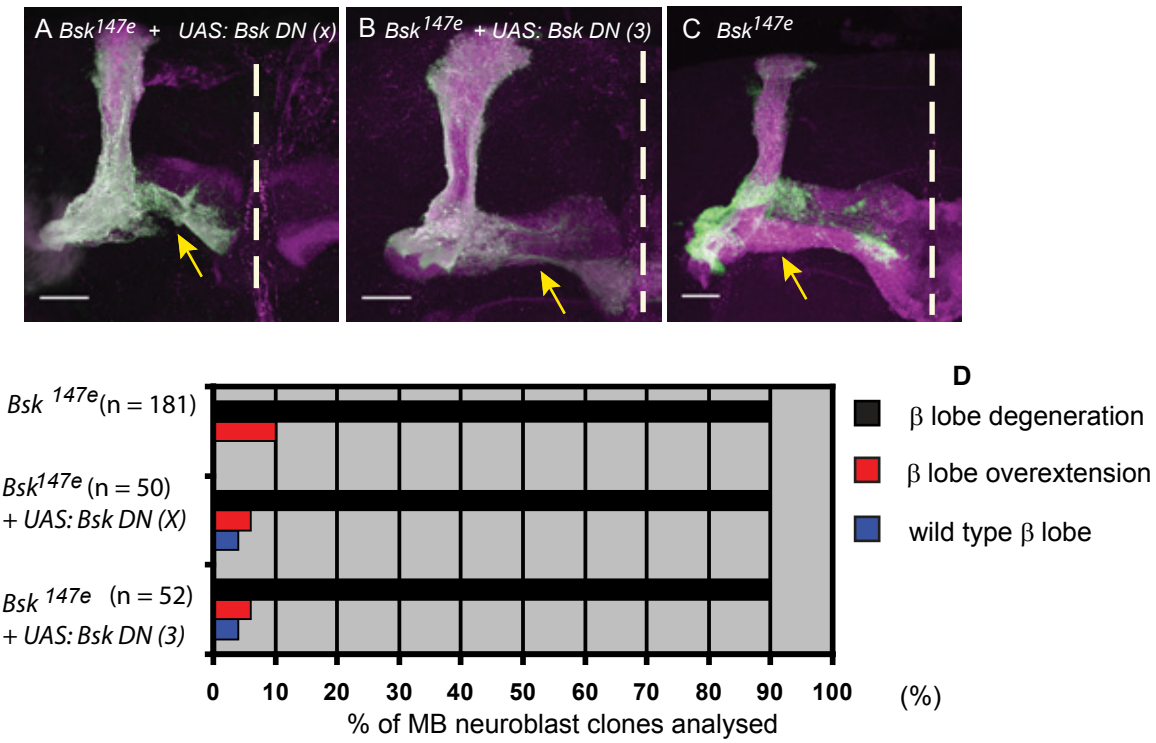

Figure 5.2.2 Misexpression of *Bsk* DN in *Bsk*^{147e} MB neuroblast clones, does not modify the *Bsk* null phenotype.

(A-B) Representative images of *Bsk*^{147e} MB neuroblast clones ectopically expressing Bsk DN transgenes on either the X **(A)** or the third chromosome **(B)**. Representative image of a *Bsk*^{147e} MB neuroblast clone is shown for comparative purposes **(C)**. All Scale bars, 20 μm. Quantification of the β projecting axon phenotypes observed for MB *Bsk*^{147e} neuroblast clones in the presence of dominant negative *Bsk* transgenes **(D).** Yellow arrows indicate regions of neurodegeneration.(A) *hsFLP, UAS-mCD8-GFP/UAS-Bsk DN; Bsk* ^{147e}*, FRT40A/FRT40, GAL80; GAL4-OK107/+;* (B) *hsFLP, UAS-mCD8-GFP/+; Bsk* ^{147e}*, FRT40A/FRT40A, GAL80;UAS-Bsk DN/+; GAL4-OK107/+* (C) *hsFLP, UAS-mCD8-GFP/+; Bsk*^{147e}*, FRT40A/ FRT40A, GAL80; GAL4-OK107/+*

morphogenesis (Figure 5.2.2; quantifications, 5.2.2 D). This experiment also shows that the DN *Bsk* phenotype is not dominant, when expressed in *Bsk* null MB neurons.

5.3 Increased levels of Bsk RNAi knockdown result in a shift of mutant phenotypes from axon overextension to neurodegeneration

I next decided to use an alternative strategy other than *Bsk* DN misexpression to induce different levels of Bsk inactivation in *Drosophila* MB neurons. I used two different Bsk RNAi lines, VDRC lines 34138 and 31439 (Dietzl et al, 2007), obtained from the same progenitor construct. They consists of a sequence of inverted repeats complementary to those located in the kinase domain of Bsk. The *Bsk* RNAi transgene was expressed in MB neurons and the level of Bsk RNAi knockdown was increased by ectopically expressing Dicer2. Dicer 2 is an endoribonuclease which cleaves dsRNA into shorter siRNAi's and subsequently promotes the activity of the RNAi induced silencing complex. Therefore by expressing ectopic Dcr together with *Bsk* RNAi, this has the effect of enhancing RNAi activity (Dietzl et al, 2007).

At 'medium' levels of *Bsk* RNAi expression (without Dcr2) I observed both axon overextension and axon degeneration in medial projecting MB β axons. Axon overextension accounted for 40% of the phenotypes observed while β lobe degeneration was observed in 26% of samples analysed. (Figure 5.3.1 D). However 'high' levels of Bsk RNAi knockdown (with Dcr2 expression) resulted in a larger proportion of mutant phenotypes exhibiting β lobe degeneration and a reduced proportion exhibiting β lobe overextension. In this scenario 38% of the phenotypes observed exhibited β lobe degeneration, while β lobe overextension was observed in 20% of the samples quantified

(Figure 5.3.1 A). A similar bias favouring axon degeneration at higher levels of Bsk RNAi knockdown was also observed in dorsal projecting MB α-axons. Under these conditions 60% of MB neurons analysed exhibited α lobe degeneration in contrast to 20% which displayed α lobe overgrowth defects (Figure 5.3.1 A; quantifications, Figure 5.3.1 G). However lower levels of Bsk RNAi knockdown resulted in the majority of mutant phenotypes displaying α lobe overgrowth defects. In this instance 25% of phenotypes observed, consisted of α lobe overgrowth defects, whereas only 12% exhibited α lobe degeneration (Figure 5.3.1 D). I found all these phenotypic differences to be statistically significant, (statistical Box plot Figure 5.3.1 F).

Further lowering the level of RNAi knockdown, by expressing the Bsk RNAi transgene at 18°C in MB neurons (the UAS-GAL4 system is temperature sensitive), resulted in subtle α overgrowth and β overextension axon defects being exhibited in a small proportion of MB neurons (Figure 5.3.1E). I found that even at low levels of RNAi knockdown (18°C), Dcr2 expression can significantly enhance Bsk RNAi phenotypes. Overall these results indicate that there is a significant shift towards degenerative phenotypes at higher levels of Bsk RNAi knockdown, whereas at lower levels of Bsk RNAi expression there is a bias towards axon overextension and overgrowth.

5.4 Sustained Bsk activity throughout development is required to maintain axon stability

I next decided to investigate how signal duration is able to regulate JNK mediated axonal stability *in vivo*. Is Bsk signaling required throughout MB development and adulthood as the phospho-JNK antibody results allude to or is the transient activity of Bsk activity at

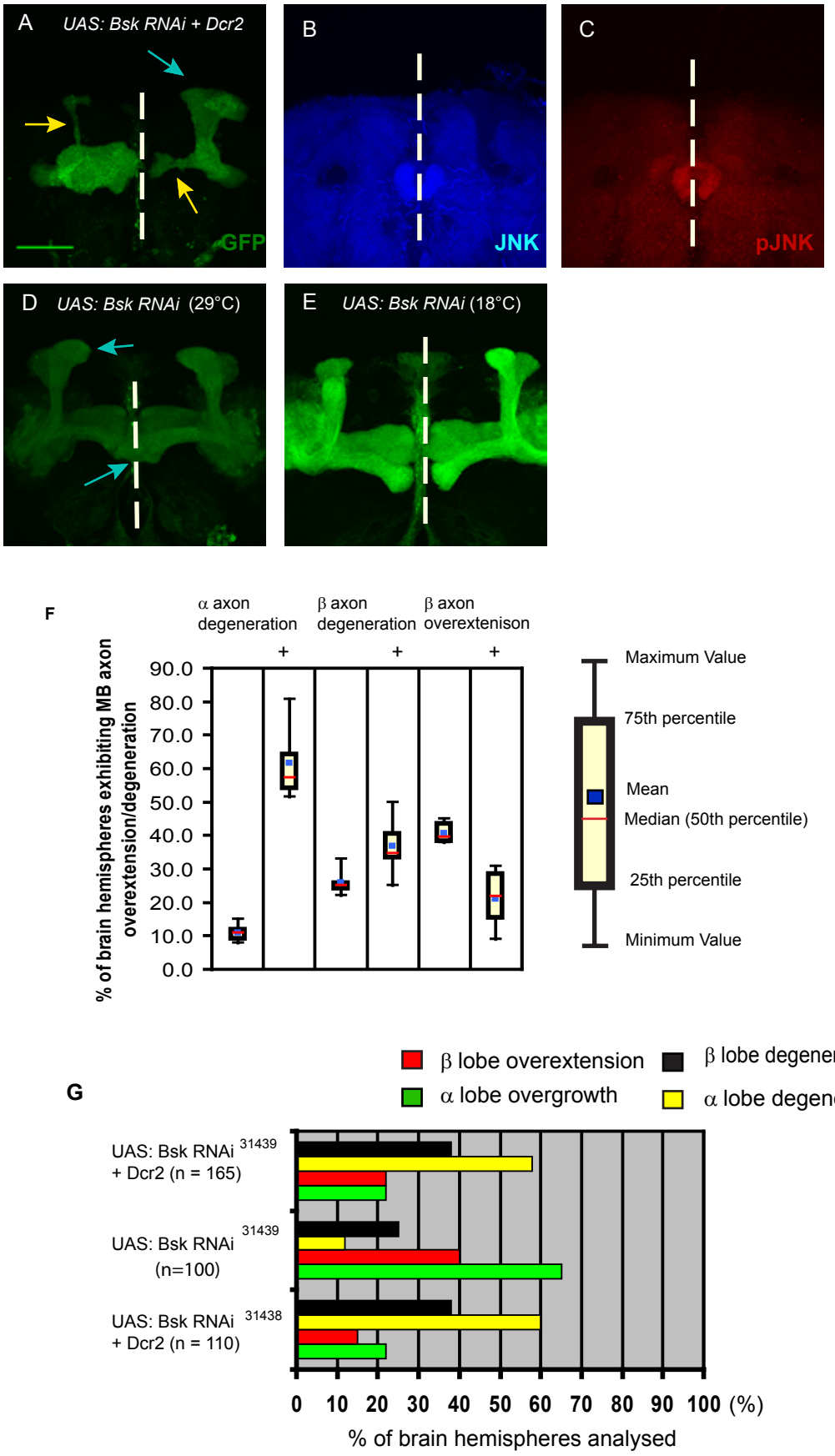
A
UAS: Bsk RNAi + Dcr2
GFP
B
JNK
C
pJNK
D
UAS: Bsk RNAi (29°C)
E
UAS: Bsk RNAi (18°C)
F
α axon degeneration
β axon degeneration
β axon overextenison
% of brain hemispheres exhibiting MB axon overextension/degeneration
90.0
80.0
70.0
60.0
50.0
40.0
30.0
20.0
10.0
0.0
Maximum Value
75th percentile
Mean
Median (50th percentile)
25th percentile
Minimum Value
G
β lobe overextension
β lobe degeneration
α lobe overgrowth
α lobe degeneration
UAS: Bsk RNAi 31439
+ Dcr2 (n = 165)
UAS: Bsk RNAi 31439
(n=100)
UAS: Bsk RNAi 31438
+ Dcr2 (n = 110)
0 10 20 30 40 50 60 70 80 90 100 (%)
% of brain hemispheres analysed

Figure 5.3.1

Figure 5.3.1 Increased levels of Bsk RNAi knockdown results in a preference towards axon degeneration, rather than axon overextension.

(A-E) Bsk RNAi expression in MB neurons. **(A-C)** Representative Images of MB neurons overexpressing Bsk RNAi along with Dcr2, labeled with CD8-GFP **(A)** and immunostained with JNK **(B)** and pJNK **(C)**. **(D)** Higher levels of Bsk RNAi knockdown leads predominantly to axon degeneration phenotypes (yellow arrows), whereas medium levels of RNAi activity leads to dorsal axon overgrowth and medial overextensions (blue arrows). **(E)** Lower levels of Bsk RNAi knockdown give a low frequency of subtle dorsal axon overgrowth and medial overextension defects. Scale bar: 50 μm. **(F)** Additional analysis on the effect of ectopic Dcr2 on the RNAi phenotype. The experiment was performed five times, and the P values are indicated for each phenotype. The presence of ectopic Dcr2 is indicated by a plus sign (+). **(G)** Quantification of the observed phenotypes. n, number of hemispheres analysed. Genotypes are as follows (A) *UAS-mCD8-GFP /+; UAS-Bsk RNAi 31439/+; UAS-Dcr2/+; GAL4-OK107/+* (D-E) *UAS-mCD8-GFP/+; UAS-Bsk RNAi 31439/+; GAL4-OK107/+*

specific periods sufficient to safeguard against defective axon morphogenesis? I used two different experimental strategies to control the timing of Bsk activity in *vivo* and both depended on the temporal and regional gene targeting (TARGET) system (McGuire et al, 2003). The TARGET system provides a method of switching UAS-GAL4 mediated transgene expression on or off by utilizing a temperature sensitive (ts) Gal80 molecule. The TsGal80 'gene switch' represses Gal4 transcriptional activity, when it is active at permissive temperatures (18°C), however in restrictive conditions (29°C) GAL80ts is suppressed and 'turned off' and so the UAS-Gal4 mediated transgene expression is active. A schematic of the TARGET system is shown in Figure 5.4.2.

In order to test the viability of the TARGET system in controlling the temporal expression of transgenes in MB neurons, I established a control experiment. I used CD8-GFP expression in MB neurons controlled under the TARGET system as a visual indicator to determine the efficiency of the TARGET system. As expected no CD8-GFP expression was detected in flies cultured at 18°C throughout (Gal4-restrictive) (Figure 5.4.1 A). Nontheless in Gal4 permissive conditions CD8-GFP expression was increasingly detected at 24hr (Figure 5.4.1 B), 48hrs (Figure 5.4.1 C) and 72hrs (Figure 5.4.1 D), confirming that the $GAL80^{ts}$ (line 7) experiment was working effectively to suppress UAS-GAL4 expression in a temperature-dependent manner.

I then performed two experiments, which enabled me to control the timing of Bsk activity *in vivo*. I initially carried out a Bsk rescue experiment, in which the timing of UAS-Bsk expression in *Bsk* null clones was under TARGET control. The results are described in Figure 5.4.3 (A-D; quantifications, E). They show that shorter periods of Bsk expression are only sufficient to partially rescue the Bsk null phenotypes and in order to

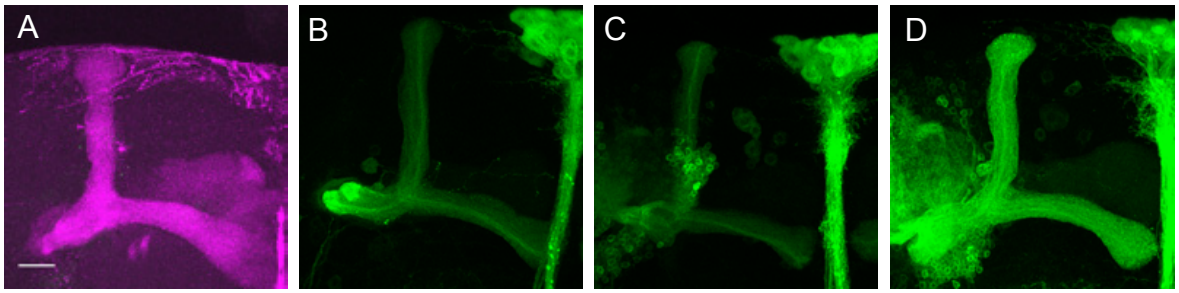

Figure 5.4.1 MB CD8-GFP expression controlled under the TARGET system. **(A)** No CD8-GFP expression was detected in flies cultured at 18°C throughout (Gal4-restrictive). **(B-D)** GAL4-permissive CD8-GFP expression is increasingly detected at 24hr **(B),** 48hrs **(C)** and 72hrs **(D)** post-induction. Scale bar: 20μm. Green, CD8-GFP. Magenta, Fas2. Genotypes are as follows (A-D) *UAS-mCD8-GFP /+; GAL80ts/+; GAL4-OK107/+*

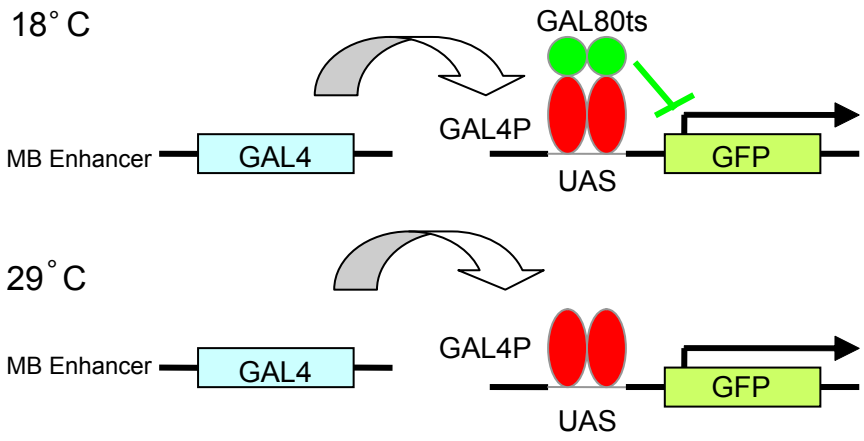

Figure 5.4.2. The TARGET system.

In the TARGET system, the conventional GAL4-UAS system is conditionally regulated by a temperature sensitive allele of gal80 (TsGal80). At 18°C the transcriptional activity of GAL4 is repressed thus preventing the expression of the desired transgene (YFP), whereas this repression is relieved by a temperature shift to 29°C, since TsGal80 becomes inactive. This allows GAL4 to drive the expression of the UAS-GFP transgene in a specific tissue or in MB neurons, if the GAL4-OK107 driver is used. Adapted from: (McGuire et al, 2003).

to fully restore the axonal projections of *Bsk* null MB neuroblast clones Bsk activity is required throughout development. In addition prolonged adult restricted expression of *Bsk* had a minimal effect in rescuing the *Bsk* null axonal phenotypes (Figure 5.4.3 D).

In a second experiment the *Bsk* RNAi transgene was also expressed under the TARGET system. This enabled me to perform tissue-specific *Bsk* inactivation in a time dependent manner. I found that perturbing endogenous JNK signals by inducing *Bsk* RNAi activity at anytime from wandering L3 through to late pupae resulted in axon overextension and to lesser degree axon degeneration phenotypes (Figure 5.4.3 F-H; quantifications, L). This suggests that no particular period during MB neuron development is dispensable for regulating Bsk mediated axon stability. Shorter or more prolonged *Bsk* RNAi activity restricted to the adult stage has very little effect on axon morphology (Figure 5.4.3 I). JNK staining confirms that Bsk RNAi knockdown is effective in these TARGET-controlled experiments (Figure 5.4.3 J-K). Taken together these experiments suggest that Bsk activity has to be sustained throughout development to ensure proper axon stability. Furthermore, Bsk RNAi knockdown over shorter latent periods during development gave a lower proportion of axonal phenotypes, compared with Bsk RNAi induction throughout development (Figure 5.4.3 L). This suggests that the 'full' Bsk inactivation phenotype reflects an accumulative period throughout development.

I also perfomed a 'reverse' protocol with an early induction of Bsk RNAi, followed by a suppression of RNAi expression from L3 or 0hr APF stages. Similar to the previous experiment, this early activation of Bsk RNAi also resulted in axonal phenotypes (Figure 5.4.4 A-B). The extent of these phenotypes was not as frequent as

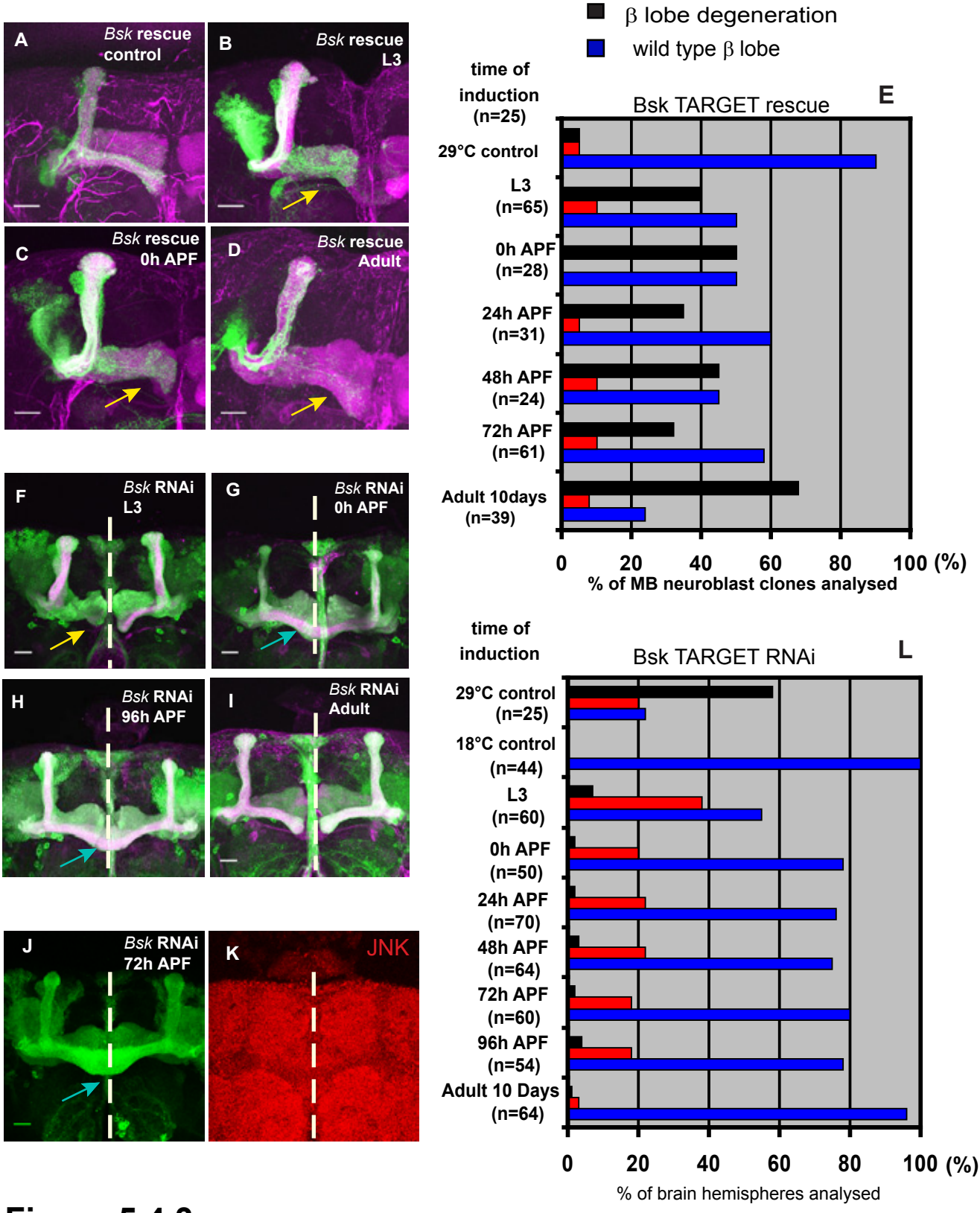
A
Bsk rescue control
B
Bsk rescue L3
C
Bsk rescue 0h APF
D
Bsk rescue Adult
F
Bsk RNAi L3
G
Bsk RNAi 0h APF
H
Bsk RNAi 96h APF
I
Bsk RNAi Adult
J
Bsk RNAi 72h APF
K
JNK
β lobe overextension
β lobe degeneration
wild type β lobe
time of induction (n=25)
Bsk TARGET rescue
E
29°C control
L3 (n=65)
0h APF (n=28)
24h APF (n=31)
48h APF (n=24)
72h APF (n=61)
Adult 10days (n=39)
0
20
40
60
80
100 (%)
% of MB neuroblast clones analysed
time of induction
Bsk TARGET RNAi
L
29°C control (n=25)
18°C control (n=44)
L3 (n=60)
0h APF (n=50)
24h APF (n=70)
48h APF (n=64)
72h APF (n=60)
96h APF (n=54)
Adult 10 Days (n=64)
0
20
40
60
80
100 (%)
% of brain hemispheres analysed

Figure 5.4.3

Figure 5.4.3 Sustained Bsk levels are essential for axon stability.

(A-D) Images of *Bsk*^{147e} neuroblast clones with the *Bsk*-myc expression under TARGET control. **(A)** As a control, Bsk TARGET flies raised at 29°C throughout (GAL4-permissive) exhibited >90% wild type projections. **(B-C)** *bsk* null clones with *Bsk*-myc expression induced at developmental stages L3 **(B)** and 0h APF **(C)**. **(D)** *bsk* null clones with *Bsk*-myc expression restricted only to the adult stage for 10 days post-eclosion. Induced at shorter periods, many flies exhibited β-axon degeneration (see E for quantifications). **(F-I)** Bsk RNAi expressed under TARGET control. Bsk RNAi expression induced at stages L3 **(F)**, 0h APF **(G)**, 96h APF **(H)** resulted in axon degeneration **(F)**, and axon overextension phenotypes **(G, H)**. **(I)** Bsk RNAi restricted to adult stages for 10 days post-eclosion show wild type projections. Bsk RNAi expression induced at 72hrs APF **(J)**, immunostained with JNK **(K)**. The low levels of JNK indicate the effectiveness of the Bsk RNAi knockdown in MB neurons. With the exception of adult-stage induced flies, all earlier induced flies were dissected as 3 day adults. Scale bars: 20 μm. Green, CD8 -GFP. Magenta, Fas2. **(E** and **L)** Quantification of these phenotypes with *bsk* rescue **(E)** and Bsk RNAi expression **(L)**. n, number of neuroblast clones **(E)** or brain hemispheres **(L)** analyzed. Note both protocols rely on the "on" kinetics of the TARGET system. In our manipulations, we detected expression from 24h and robustly at 72h post-induction (Figure 5.4.1). Therefore, a period of RNAi and Bsk-myc accumulation is required for effective downregulation of Bsk RNA transcripts and suppression of bsk-null phenotypes (respectively), and so do not reflect a strict 'on' time at the indicated developmental stages. Genotypes are as follows (A-D) *hsFLP, UAS-mCD8-GFP/ /UAS-Bsk-Myc; Bsk* ^{147e}*, FRT40A/FRT40, GAL80; GAL80ts/+; GAL4-OK107/+* (F-K) *UAS-mCD8-GFP/Bsk RNAi 31439; UAS-Dcr2/GAL80ts; GAL4-OK107/+*

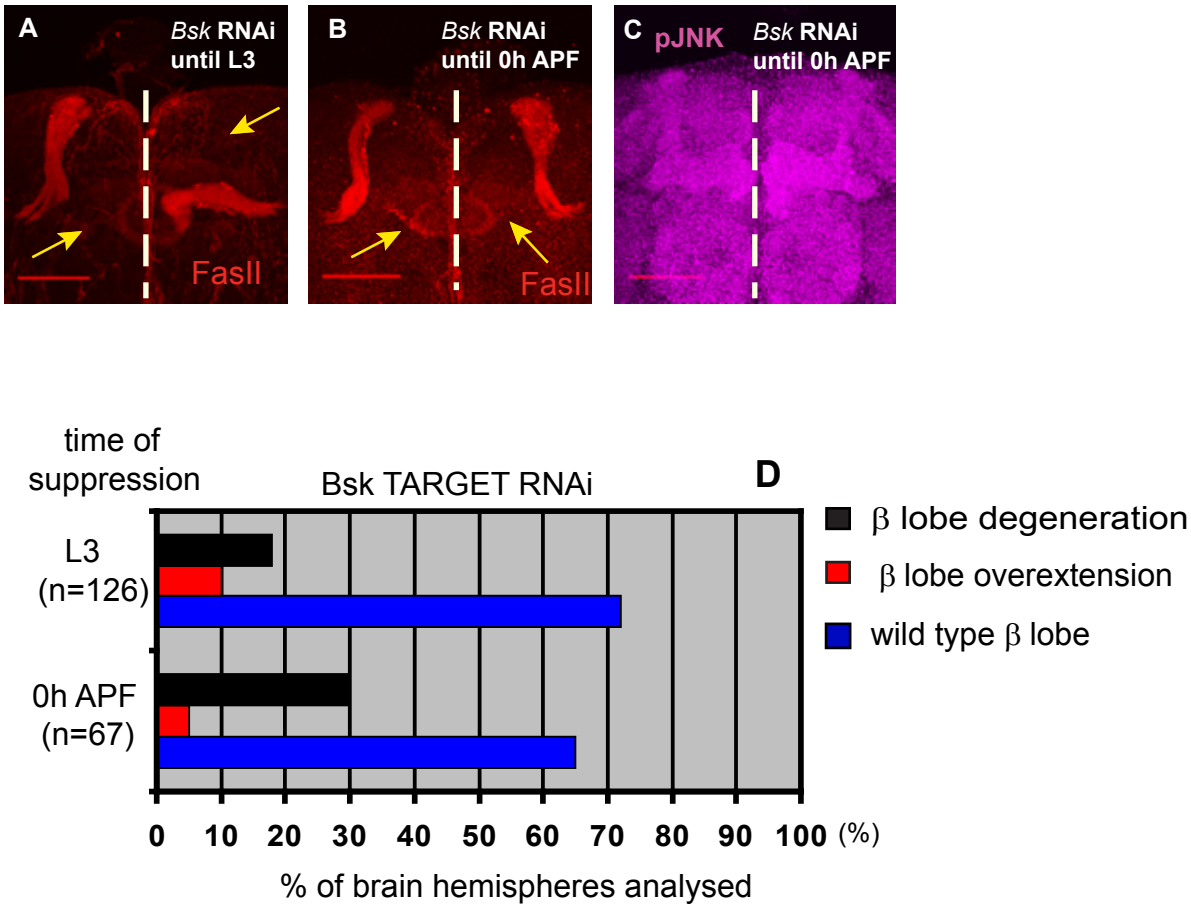

Figure 5.4.4 Early induction of Bsk RNAi followed by suppression at early developmental stages leads to an increase in neurodegeneration phenotypes. **(A-B)** Bsk RNAi expressed under TARGET control. Bsk RNAi expression was induced from the beginning of development, followed by a suppression of RNAi transgene expression at L3 **(A)** or 0h APF **(B)** as indicated. In these scenarios FasII was used to visuliase axonal projections, since CD8-GFP transgene expression was very low. **(C)** Bsk RNAi expression was suppressed at 0h APF and the resulting whole mount brains were immunostained with pJNK. As expected endogenous pJNK levels are restored, following Bsk RNAi suppression. **(D)** An increased proportion of axon degeneration over axon extension phenotypes is observed, at the early phase of Bsk inactivation. Yellow arrows indicate regions of axon loss; Red, FasII; Magenta, pJNK staining; Scale Bars, 50 μm. Genotypes are as follows: (A-C) *UAS-mCD8-GFP/ Bsk RNAi 31439; UAS-Dcr2/GAL80ts; GAL4-OK107/+*

when Bsk RNAi was induced throughout development. Interestingly, the early treatment resulted in more axon degenerations than overextensions, compared to the late induction protocol (Figure 5.4.4 D), suggesting that the degeneration phenotype is more sensitive to an early phase of Bsk inactivity. It is also important to note that the endogenous phospho JNK levels were also restored once RNAi activity had been switched off at L3 or 0hr APF (Figure 5.4.4 C). Taken together these experiments suggest Bsk activity has to be sustained throughout development to ensure proper axonal morphogenesis (see Discussion).

5.5 Discussion

Based on the JNKK data, which showed that the presence of signaling inputs from one kinase is sufficient to protect against neurodegeneration, while signaling inputs from both JNKKs are needed to prevent axon overextension, I postulated that distinct aspects of Bsk mediated axon stability are regulated by different threshold levels of Bsk activity. Indeed I found this to be the case. Misexpression of a 'kinase dead' *Bsk* dominant negative transgene resulted in an overall axon overextension phenotype in MB β neurons, typified by fusion of the medial lobe projecting neurons at the midline, additionally an overall degeneration of the dorsal projecting axons was also observed.

The RNAi knockdown approach directly reduces endogenous Bsk activity by initiating and enhancing a gene silencing mechanism which operates *in vivo* in endogenous natural physiological settings. At higher levels of Bsk RNAi knockdown, there is a greater preference for neurodegenerative mutant phenotypes in both medial and dorsal projecting axons. This shift from axon overextension/overgrowth at lower titres of

Bsk RNAi to neurodegeneration at higher levels of Bsk RNAi knockdown is not observed when reducing Bsk activity levels by increasing the dosage of Bsk DN misexpression.

Taken together these results suggest that rather than being a specific threshold level, which is able to prevent neurodegeneration or axon overextension, there is a threshold level range of signaling which meditates Bsk dependent axon stability. This dynamic range of signaling which is required to mediate Bsk dependent axon stability is reflective of the phenotypes obtained in various *in vivo* experimental paradigms. For instance under *Bsk* null conditions, the majority of MB neuroblast clones analysed exhibit degeneration, however a minority of MB neuroblast clones displayed axon overgrowth and overextension defects. Conversely at 'intermediate' Bsk activity levels (misexpression of a Bsk RNAi transgene without ectopic Dcr2) there is a bias towards axon overgrowth/overextension defects which constitute the majority of MB mutant axonal phenotypes observed, however a significant minority of MB neurons samples analysed exhibit degeneration phenotypes. Therefore it is highly probable that Bsk dependent axon stability is regulated by a graded dynamic mechanism of Bsk activity, rather than an all or none response to a precise level of active Bsk signals.

This dynamic aspect of JNK signaling then brings up the next salient question. Are active Bsk signals invoked temporarily at particular 'critical' points during development or is Bsk activity constantly required during MB neuronal development to elicit correct axonal morphogenesis? The elevated level of activated JNK throughout development, revealed by immunostaining with a phospho JNK antibody would suggest that the latter hypothesis is more probable. The data acquired from the experiments

utilizing the TARGET system to control the timing of Bsk activity *in vivo* demonstrates that sustained Bsk activity is required throughout development to maintain axonal stability. Shorter periods of Bsk inactivity and activity tend to result in a weaker effect (as opposed to no effect) compared to protocols where Bsk RNAi or rescue activity is on throughout development. Therefore based on this I propose that in order to maintain optimal axon stabilization, Bsk signals are read "additively" throughout development. Rather than as a 'temporal summation' module where signals need to reach a timed threshold level of activity to evoke an 'all-or-none' phenotype, the results suggest that shorter periods of Bsk activity can still maintain wild type axon projections, although at a lower penetrance. The fact that phospho JNK staining is noticeably higher in γ neurons rather than α/β and α'/β later born neurons suggests that active Bsk signals exert an accumulative effect during MB neuronal development.

Thus far I have shown Bsk signaling activity over different developmental phases contributes as a parameter in maintaining axon stability. However prolonged RNAi or Bsk rescue activity during adulthood does not alter the existing (pre-induced) axonal morphology of these genotypes. Therefore what accounts for the adult phospho-JNK signals observed at adulthood? It could be that there is change in the physiological requirements for JNK signaling between the developing and adult brain. The adult stage phospho JNK signals may indicate a distinct mode of MB regulation, perhaps a switch in Bsk's role from maintaining axon stability to regulating synaptic plasticity. *Bsk's* function in synaptic plasticity has already been demonstrated in Drosophila NMJ studies (Sanyal et al, 2002; Collins et al, 2006). For instance inhibiting JNK signaling by expressing *Bsk DN*, reduced the number of synaptic boutons and branches (Collins et al,

2006). Overall this data suggests that Bsk may also operate in a similar manner in adult MB neurons, although this has yet to be determined.

Another interesting inquiry which remains unanswered is what is the nature of the signaling mechanisms which prevents axon overextension and degeneration, hence maintaining axon stability? I have established that there is an activity threshold that is needed to safeguard against degeneration (relatively low) and axon overextension (relatively high). I have also demonstrated that neuroprotective signals, which safeguard against neurodegeneration, are present at earlier phases of MB neuron development; whereas signals that prevent axon overextension favor later stages of development. It is possible there are two independent JNK signals operating at different stages of development, a pro-survival (anti-neurodegeneration) signal induced in the early phases of development and a signal that ensures that axons extend to their correct synaptic target (anti-overextension) in the later phases of MB neuron development.

CHAPTER 6: A graded AP-1 response regulates axon stability

6.1 Introduction

In a wide array of diverse processes in development and physiopathology including morphogenesis, differentiation and apoptosis (Eferl and Wagner 2003; Xia and Karin 2004), the evolutionary conserved JNK pathway acts via regulation of the AP-1 transcription factor response. In response to extracellular stimulation JNK targets the phosphorylation of the Activator protein-1 (AP-1) complex, thereby reprogramming gene expression (Noselli and Agnes 1999; Kockel et al, 2001). In *Drosophila*, these transcription factors act as either heterodimers or as Fos homodimers (Perkins et al, 1990; Pearson et al, 2009), which bind DNA through conserved bZIP domains.

In this chapter I present evidence demonstrating that AP-1, operates downstream of JNK signals to regulate diverse processes in neurons such as axonal stability, axon growth and neuronal death. The AP-1 transcription factor complex operates in a graded manner to safeguard against both axon degeneration and overextension, similar to the way in which Bsk dependent axonal stability is maintained. Inactivation of Fos culminates in axon overextension, whereas inactivation of both Fos and Jun leads to a higher degree of neurodegeneration. Additionally, from co-expression assays I uncovered that Bsk activates AP-1 to promote axon growth by interacting with the actin cytoskeleton. Finally I also confirm that inactivation of Fos is able to rescue neuronal apoptosis acquired in a Hep gain of function background, implying that Fos also plays a pivotal role in inducing neuronal apoptosis.

6.2 A graded AP-1 response regulates Bsk dependent axonal stability

In order to determine whether Bsk signals are mediated through AP-1, which in *Drosophila* consists of the transcription factors Fos and Jun, I first examined the role of Jun. Through clonal analysis using strong, null alleles, or dominant-negative (JbZ) misexpression, Jun (also known as Jra) inactivation alone has no effect on gross axon morphology (*Jra* ^{1}, n=38 clones, Jra^{2}, n=30 clones, JbZ, n=36 hemispheres; all 100% wild type, Figure 6.2.1 A-C).

I next tested the role of Fos (encoded by the Kayak gene) in MB neurons by using two strong loss-of-function alleles. Using a *Kay* mutant allele (Riesgo-Escovar, et al 1997a; Zeitlinger, 1997), I generated *Kay*^{1} MB neuroblast clones. Cell proliferation defects were observed in all neuroblast clones derived from earlier born *Kay*^{1} MB neuroblast clones (Figure 6.2.2 A). In order to establish the role of *Kay* in axon morphogenesis, I then generated later born *Kay*^{1} neuroblast clones, which are comprised solely of α/β neuron subsets. These later borne *Kay*^{1} MB neuroblast clones all exhibited wild type projections (Figure 6.2.2 B), n = 21, 100% wild type. I next decided to generate *Kay*^{ED6315} MB neuroblast clones. The Kay^{ED6315} mutation (Weber et al, 2008) is caused by a chromosomal deletion, which removes a large portion of the kayak locus (approximately 58%). However the vast majority of *Kay*^{ED6315} MB neuroblast clones also exhibited wild type projections (n=30, 93.3% wild type; Figure 6.2.2 C). Given that both strong loss-of-function alleles did not give any phenotype, one possibility is that *Kay* may not be fully inactivated. It is important to note that these strong loss-of-function alleles do not remove all isoforms of Fos, therefore they may not be considered true null alleles for *Kay* (Giesen et al, 2003, Weber et al, 2008).

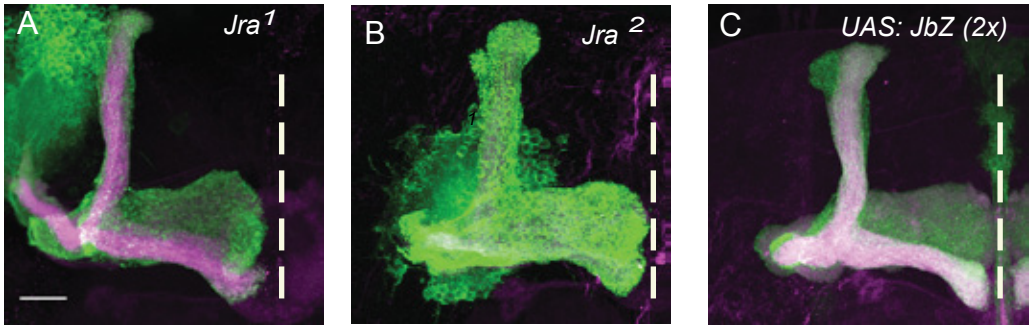

Figure 6. 2.1 Loss-of-function of *Jun* has no affect on MB axon morphology

Representative images of *Jra*[1] **(A)** and *Jra*[2] **(B)** MB neuroblast clones and MB neurons misexpressing two copies of dominant-negative *Jun* (*Jbz*) **(C)**, all exhibiting wild type axon projections. Scale bars: 20 μm. Green, CD8-GFP. Magenta, FasII. Genotypes are as follows (A) *hsFLP, UAS-mCD8-GFP/+; FRTG13, GAL80/FRTG13, Jra* [1]*, GAL4-OK107* (B) *hsFLP, UAS-mCD8-GFP/+; FRT42D, GAL80/FRT42D, Jra*[2] *; GAL4-OK107* (C) *UAS-mCD8-GFP/UAS-JbZ* [1]*; UAS-JbZ* [10]*/+; GAL4-OK107/+*

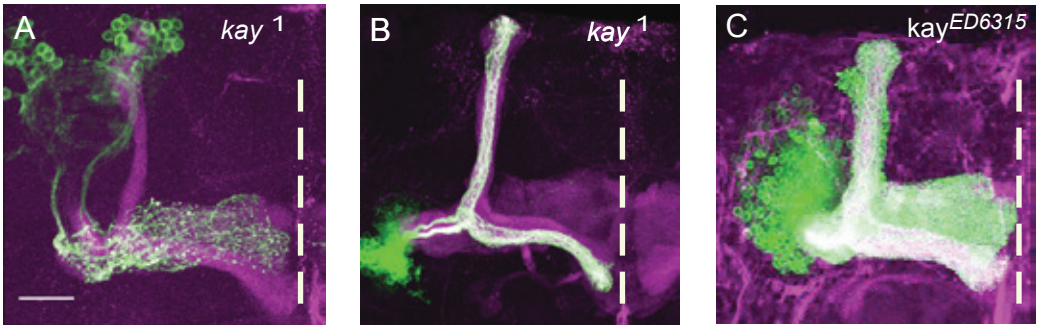

Figure 6. 2.2 Loss-of-function of *Fos* has no affect on MB axon morphology

Representative images of *kay*[1] **(A and B)** and *kay*[ED6315] **(C)** mutant MB neuroblast clones. *Kay* mutant MB neuroblast clones exhibit wild type axon projections, because these *kay* mutants are not true null alleles for kayak. Since *kay*[1] early-born neuroblast clones have cell proliferation defects **(A)**, later-born α/β neuroblast were used for the *kay* loss-of-function analysis **(B)**. Scale bars: 20 μm. Green, CD8-GFP. Magenta, FasII. Genotypes are as follows (A,B) *hsFLP122, UAS-mCD8/+; FRT82B, GAL80/FRT82B, Kay* [1]*; GAL4-OK107/+* (C) *hsFLP122, UAS-mCD8/+; FRT82B, GAL80/ FRT82B, Kay* [6315]*; GAL4-OK107/+*

I therefore decided to utilise dominant negative misexpression and RNAi approaches to inactivate *Fos*. Ectopic expression of kay RNAi (NIG fly, Mishima, Japan) predominantly resulted in axon overextension (Figure 6.2..3 A). However the RNAi phenotype was quite infrequent, which may have been the result of low transgene expression or protein perdurance. Overexpression of the same kay RNAi line along with Dcr2 resulted in a higher frequency of neurodegeneration phenotypes. (Figure 6.2.3 B and C). I next decided to utilise a dominant negative approach to interfere with Fos activity. A truncated version of Fos (Fbz) has previously been described (Eresh et al, 1997), which consists of the basic region leucine zipper (bZIP) domain only. Fbz is thought to act in a dominant negative fashion, since it consists only of the domain which confers DNA binding and dimerisation. Misexpression of two copies of dominant negative kayak (FbZ) in MB neurons resulted in predominantly axon overextension (Figure 6.2.3 D) and to a lesser degree axon degeneration. However a higher frequency of axon degeneration phenotypes was observed when two copies of FbZ were misexpressed in MB neurons with two copies of JbZ, (Figure 6.2.3 E; quantifications, Figure 6.2.3 F).

In a similar manner to Bsk-dependent axon stability, in which weak Bsk signals safeguard against neurodegeneration and stronger Bsk activity prevents axon overextension, weak AP-1 signals are able to protect against neurodegeneration and stronger AP-1 signals prevent axon overextension, with Kay playing the major role in these neurons.

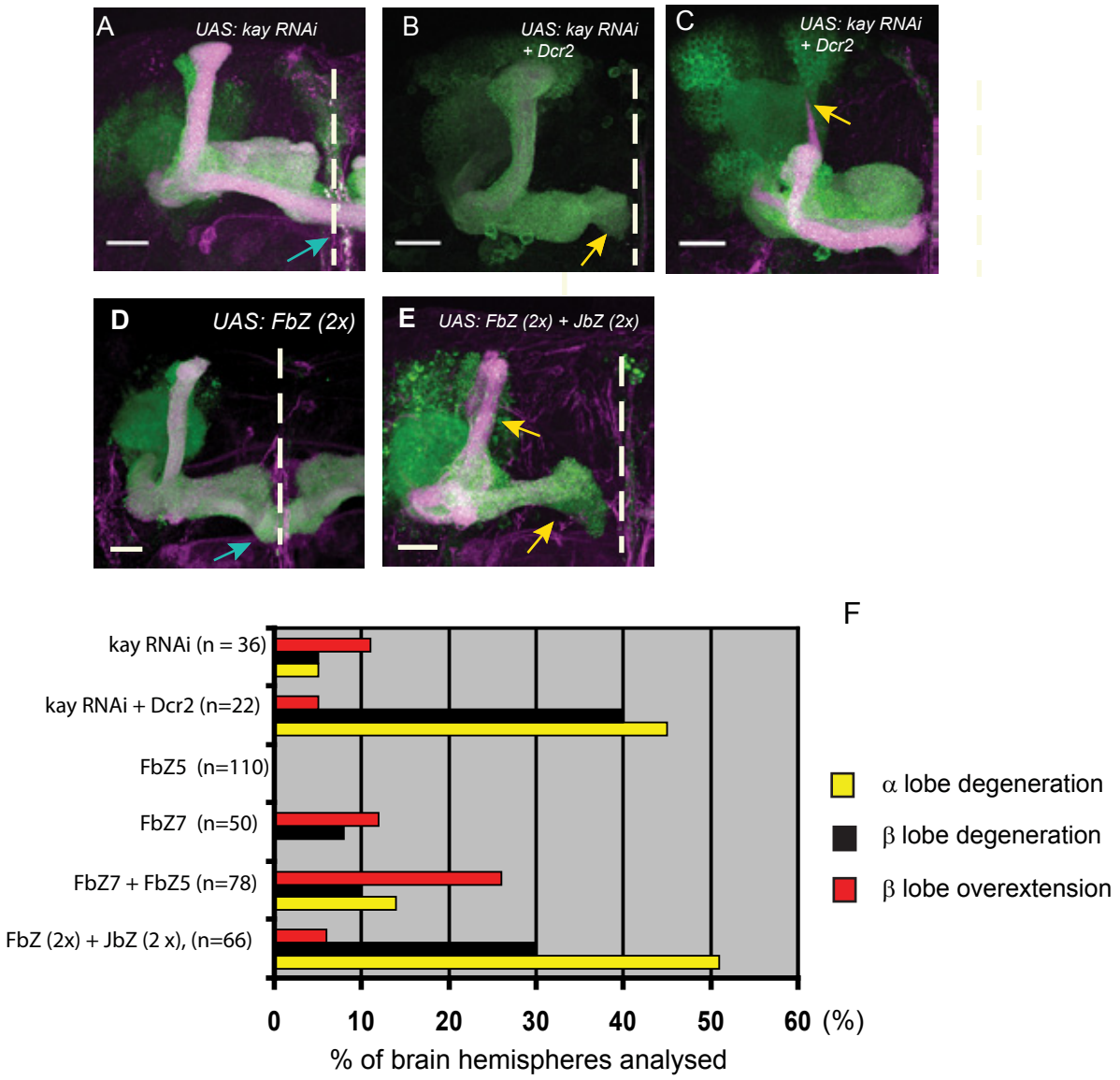

Figure 6.2.3 A graded AP-1 signal mediates Bsk responses

Representative images of MB neurons expressing **(A)** *kay RNAi* (without Dcr2) and the same *kay RNAi* line with Dcr2 **(B-C)**, exhibiting axon overextension **(A)** and degeneration phenotypes respectively **(B-C)**. MB neurons misexpressing two copies of Fbz **(D)** or two copies of Fbz along with two copies of JbZ **(E)** displayed axon overextension **(D)** and degeneration **(E)** phenotypes. Copy numbers of expressed transgenes are indicated in parenthesis. Progeny derived from Fbz and Jbz crosses were raised at 29°C to increase the possibility of detecting any axonal phenotypes due to misexpression. Scale bars: 20 µm. Green, CD8-GFP. Magenta, FasII. **(F)** Quantification of these phenotypes. Genotypes are as follows (A) *UAS-mCD8-GFP/+; UAS-kay RNAi/+; GAL4-OK107/+;* (B-C) *UAS-mCD8-GFP /+; UAS-kay RNAi/UAS-Dcr2; GAL4-OK107/+* (D) *UAS-mCD8-GFP/UAS-FbZ; UAS-FbZ/+*; *GAL4-OK107/+*; (E) *UAS-mCD8-GFP/UAS-FbZ, UAS-JbZ; UAS-FbZ, UAS-JbZ/+; GAL4-OK107/+*

6.3 Bsk genetically interacts with the transcription factors Fos and Jun.

I examined whether there was a genetic interaction between Bsk and AP-1 components Fos and Jun. I achieved this by establishing a sensitised co-expression assay. In the control scenario an intermediate expressing Bsk RNAi line [31438] was ectopically expressed along with Dcr2. I then used this senstised background to examine whether overexpression of FbZ or JbZ along with Bsk RNAi could enhance the axon degeneration phenotypes acquired in Bsk RNAi overexpressing MB neurons. I overexpressed either one copy of Fbz or Jbz along with Bsk RNAi. This was done to avoid additive effects, since misexpression of one copy of FbZ or JbZ alone gives wild type axon projections. Misexpression of either FbZ or JbZ transgenic lines in a Bsk RNAi knockdown background did in fact enhance the Bsk RNAi knockdown phenotypes and a higher frequency of degeneration phenotypes were observed (quantifications, Figure 6.3.1).

6.4 Bsk activation of the AP-1 transcription factor complex regulates axon growth

Another initial objective outlined at the beginning of my PhD was to identify whether Bsk could signal via AP-1 transcription regulation to interact with the cytoskeleton and promote axon growth. I therefore used a gain-of-function co-expression assay and identified that Bsk acts via the activation of the AP-1 transcription factor response, (in a pak independent signalling pathway) to promote axon growth.

Firstly a sensitized genetic background was established, in which LIMK was overexpressed. In this control scenario, ectopic expression of LIMK, gave an axon stalled phenotype, characterized by dorsal lobe axon growth defects (Figure 6.4.1 A). I then used

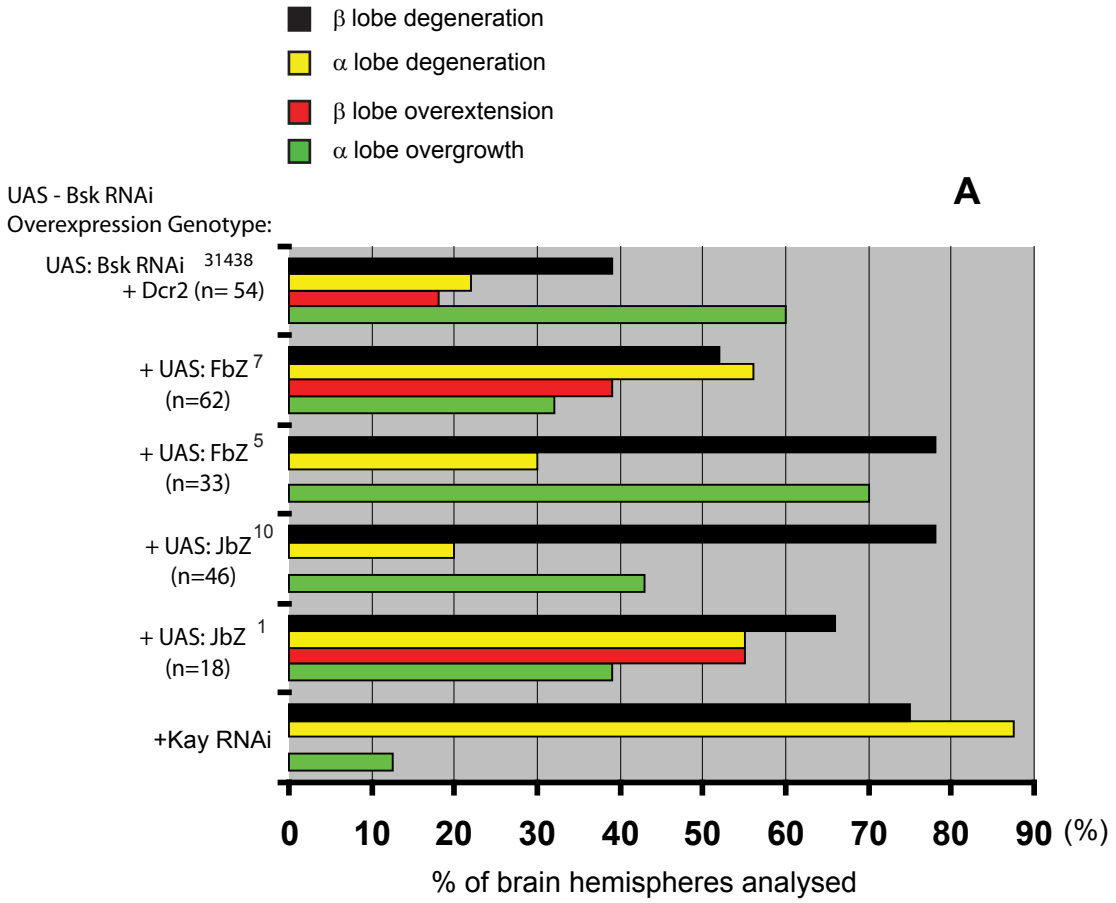

Figure 6.3.1 Bsk genetically interacts with Fos and Jun

(A) Quantification of axon overextension/overgrowth and degeneration defects in Bsk RNAi overexpressing neurons in the presence of Fbz or Jbz expression transgenes (UAS-FbZ or JbZ) or Kay RNAi. Inactivation of Fos or Jun in Bsk RNAi MB expressing neurons enhances the neurodegeneration phenotypes observed. The different transgenic lines are expressed after the genotype, i.e. FbZ 7. n, number of brain hemispheres examined. The following genotype was used: *UAS-mCD8-GFP/UAS-Bsk RNAi 31438; UAS-Dcr2/(X); OK107/+ Where (X) is either UAS-FbZ, UAS-JbZ or UAS-Kay RNAi.*

this sensitized background to examine whether overexpression of AP-1, Fos or Jun alone could suppress the axon stalled phenotype induced by LIMK gain of function. I found that AP-1 overexpression was able to rescue the gain-of-function LIMK phenotype and restore wild type MB axon projections (Figure 6.4.1 B). Additionally overexpression of Fos alone and not Jun is sufficient to suppress the LIMK gain-of-function phenotype and restore wild type MB axon projections (Figure 6.4.1C-D; quantifications 6.4.1 E). Overall these results suggest that Fos operates in a signalling pathway antagonistic to LIMK, promoting axon growth. Additionally Fos as oppose to Jun seems to play the major role indicating that Fos signals independently of Jun to promote axon growth in MB neurons.

In order to determine whether Fos phosphorylation is required to regulate axon growth, I examined whether ectopic expression of D-Fos$^{N\text{-}ALA}$, (a mutated form of Fos lacking all phosphorylation sites at the N-terminus), D-Fos$^{C\text{-}ALA}$ (a mutated form of Fos lacking all phosphorylation sites at the C-terminus) or D-Fos$^{PAN\text{-}ALA}$ (a mutated form of Fos lacking all phosphorylation sites), was able to modify the LIMK gain-of-function phenotype. I found that only D-Fos$^{PAN\text{-}ALA}$ overexpression was able to enhance the LIMK gain-of-function phenotype. In this case the majority of axons displayed severe axon growth defects (Figure 6.4.2 D). However ectopic expression of either D-Fos$^{N\text{-}ALA}$ (Figure 6.4.2 B) or D-Fos$^{C\text{-}ALA}$ (Figure 6.4.2 C) was not sufficient to modify the LIMK gain-of-function phenotype (Figure 6.4.2 A; quantifications 6.4.2 E). This suggests that Fos requires phosphorylation sites on both the N and the C-termini to regulate axon growth. These residues serve as phosphorylation sites for both MAP kinases Bsk (JNK) and Rolled (ERK).

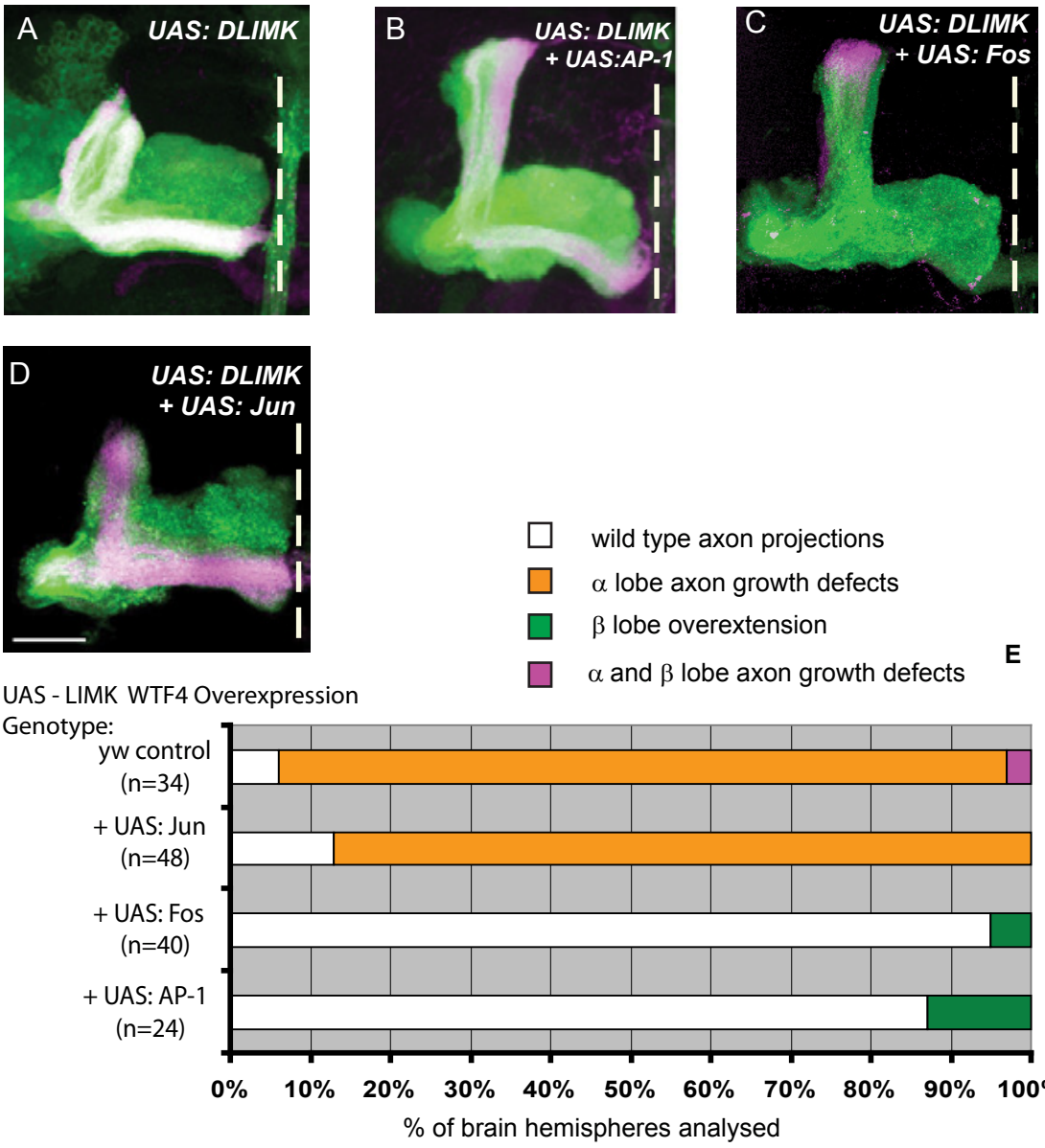

Figure 6.4.1 Overexpression of Fos suppresses the gain-of-function LIMK axon stalled phenotype

(A-D) Representative Images of LIMK overexpressing MB neurons **(A)** in the presence of wild type AP-1 (Fos and Jun) **(B)**, Fos **(C)** and Jun **(D)** expression transgenes. Overexpression of both AP-1 and Fos is able to suppress the gain-of-function LIMK axon stalled phenotype **(A)** and restore wild type axon projections (**B** and **C**, respectively). Quantification of these phenotypes **(D)**. Scale bars: 20 μm. Green, CD8-GFP. Magenta, FasII. n, number of brain hemispheres examined. Genotypes are as follows (A) *UAS-mCD8 -GFP/+; UAS: DLIMK/+; OK107/+;* (B) *UAS-mCD8-GFP/UAS-Fos; UAS-Jun/UAS: DLIMK; GAL4-OK107/+;* (C) *UAS-mCD8-GFP/UAS-Fos; UAS: DLIMK/+; GAL4-OK107/+* (D) *UAS-mCD8-GFP/+; UAS: DLIMK/UAS-Jun; GAL4-OK107/+*

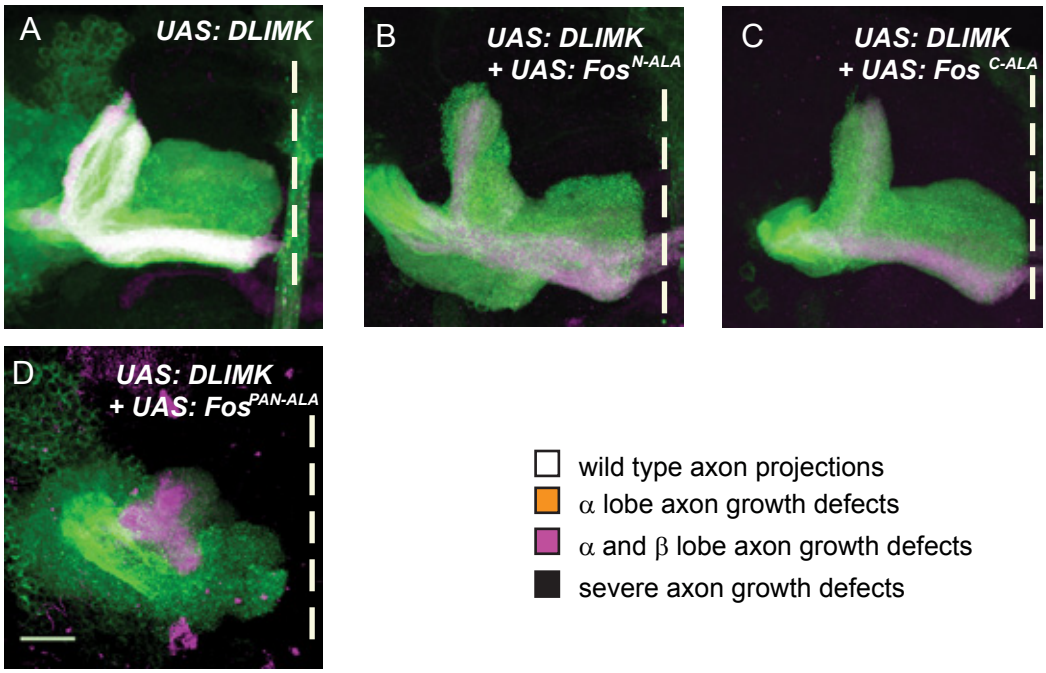

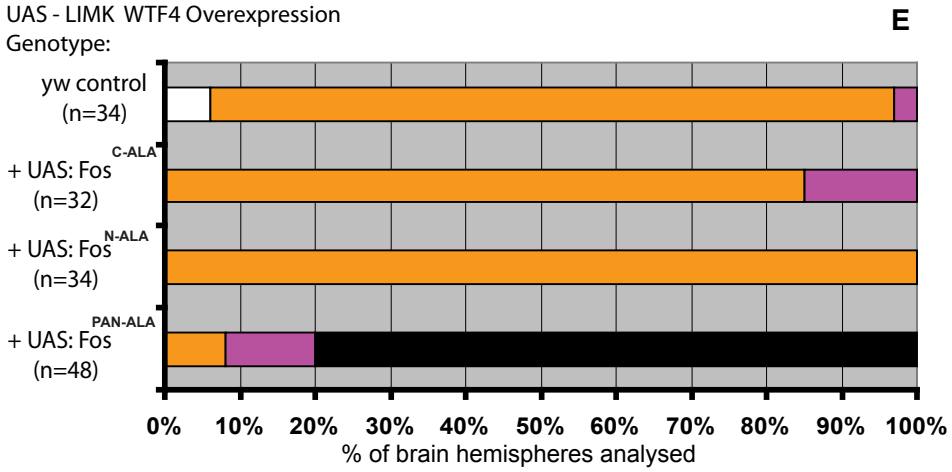

Figure 6.4.2 Overexpression of a Fos mutant phospho inactive transgene enhances the gain-of-function LIMK axon stalled phenotype

(A-D) Representative Images of LIMK overexpressing MB neurons **(A)** in the presence of Fos mutant expression trangenes D-Fos^{N-ALA} **(B)** , D-Fos^{C-ALA} **(C)** and D-Fos$^{PAN-ALA}$ **(D)**. Overexpression of only D-Fos$^{PAN-ALA}$ is able to enhance the gain-of-function LIMK axon stalled phenotype and give severe axon projections **(D)**. Quantification of these phenotypes **(E)**. Scale bars: 20 μm. Green, CD8-GFP. Magenta, FasII. n, number of brain hemispheres examined. Genotypes are as follows (A) *UAS-mCD8-GFP/+; UAS-DLIMK/+; GAL4-OK107/+* (B) *UAS-mCD8-GFP/+; UAS-DLIMK/UAS-Fos^{N-ALA}; GAL4-OK107/+* (C) *UAS-mCD8-GFP/+; UAS-DLIMK/UAS-Fos^{C-ALA}; GAL4-OK107/+* (D) *UAS-mCD8-GFP/+; UAS-DLIMK/UAS-Fos$^{PAN-ALA}$; GAL4-OK107/+*

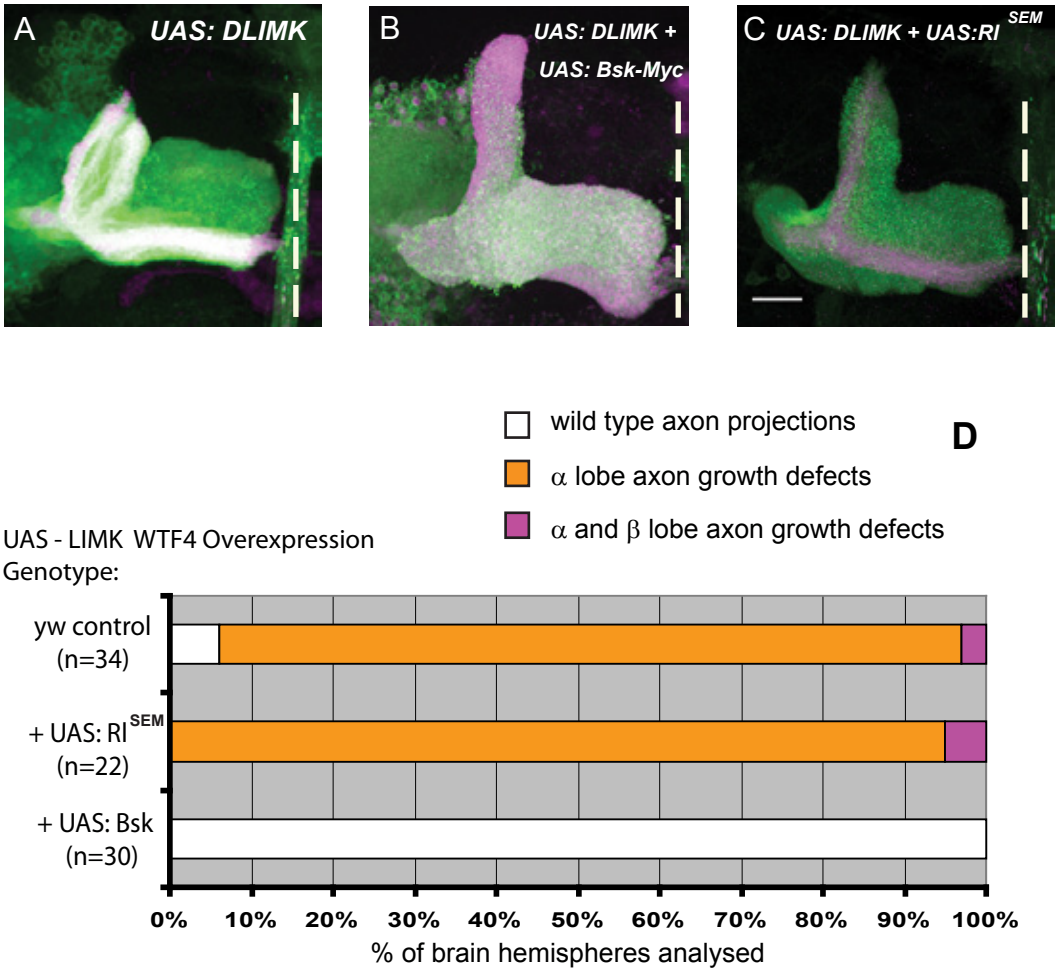

Figure 6.4.3 Overexpression of a wild type Bsk transgene rescues the gain-of-function LIMK axon stalled phenotype

(A-C) Representative Images of LIMK overexpressing MB neurons **(A)** in the presence of Bsk-Myc WT and **(B)** constitutively active Rolled (RI^{SEM}) expression trangenes **(C).** Overexpression of only Bsk-Myc is able to rescue the gain-of-function LIMK axon stalled phenotype and restore wild type axon projections **(B).** Quantification of these phenotypes **(D).** Scale bars: 20 μm. Green, CD8-GFP. Magenta, FasII for **A** and **C**; Myc for **B**. n, number of brain hemispheres examined. Genotypes are as follows (A) *UAS-mCD8-GFP/+; UAS-DLIMK/+; GAL4-OK107/+;* (B) *UAS-Bsk-Myc/+; UAS-mCD8-GFP/+; UAS-DLIMK/+; GAL4-OK107/+* (C) *UAS-mCD8 -GFP/UAS-RI ^{SEM}, UAS-DLIMK/+; GAL4-OK107/+*

In vitro kinase assays have confirmed that Bsk is able to phosphorylate sites in both the N and C-terminus of Fos, whereas Rolled phosphorylation of Fos is confined to the N-terminal sites (Ciapponi et al, 2001). The fact that Fos requires phosphorylation sites on both the N and the C-termini to regulate axon growth suggests that Fos responds to JNK rather than ERK signalling inputs to regulate axon growth. I also tested whether overexpression of Bsk or a constitutively activated form of Rolled could suppress the LIMK gain-of-function phenotype. I found that only Bsk was able to fully rescue the LIMK gain-of-function phenotype and restore wild type projections whereas Rolled did not modify the LIMK gain-of-function phenotype (Figure 6.4.3 B-C; quantifications, 6.4.3 D). Taken together these results indicate that Bsk phosphorylation of Fos is critical in promoting axon growth in MB neurons.

6.5 How does AP-1 act to regulate constitutively active Bsk signalling which is required for neuronal apoptosis?

I have already established that overexpression of a constitutively active Hep (Hep^{CA}) transgene or a Hep-Bsk fusion transgene induces large scale neuronal death in MB neurons. However when one copy of dominant negative Fos (FbZ) is misexpressed in a Hep^{CA} gain-of-function background, it is able to fully rescue the neuronal death phenotype and restore wild type projections (Figure 6.5.1 A). Furthermore both phospho JNK and JNK levels are significantly higher in a Hep^{CA} gain-of-function background, misexpressing one copy of FbZ than with overexpression of Hep^{CA} alone (compare Figure 6.5.1 B and C, with 6.5.1 H and I). I then decided to misexpress one copy of JbZ in a Hep^{CA} gain-of-function background to determine whether JbZ could also rescue the

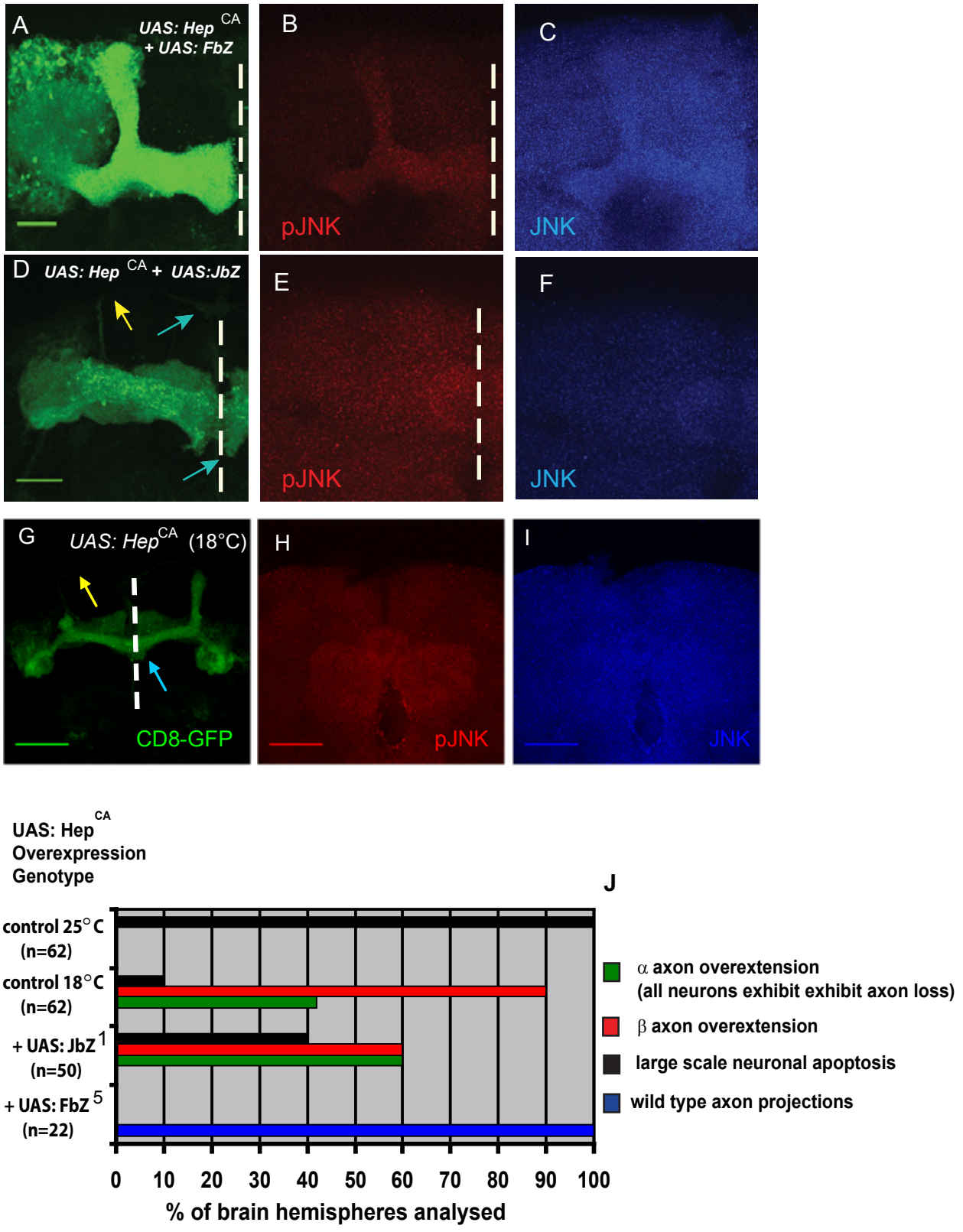
A
UAS: Hep CA
+ UAS: FbZ
B
pJNK
C
JNK
D
UAS: Hep CA + UAS:JbZ
E
pJNK
F
JNK
G
UAS: HepCA (18°C)
CD8-GFP
H
pJNK
I
JNK
J
UAS: Hep CA
Overexpression
Genotype
control 25°C
(n=62)
control 18°C
(n=62)
+ UAS: JbZ 1
(n=50)
+ UAS: FbZ 5
(n=22)
0
10
20
30
40
50
60
70
80
90
100
% of brain hemispheres analysed
α axon overextension
(all neurons exhibit exhibit axon loss)
β axon overextension
large scale neuronal apoptosis
wild type axon projections

Figure 6.5.1

Figure 6.5.1 Neuronal death of MB neurons induced by ectopic expression of Hep^{CA} can be rescued by inactivating Fos.

Representative Images of Hep^{CA} gain-of-function MB neurons overexpressing FbZ or JbZ **(A or D)**, immunostained with pJNK **(B,E)** and JNK antibodies **(C,F).** Inhibiting Fos signaling is able to fully rescue large scale neuronal death observed in MB neurons induced by constitutively active Hep overexpression and restore wild type axon projections **(A).** Whereas perturbing Jun activity fails to rescue MB neuronal death, however a high frequency of mutant phenotypes exhibit axon overextension **(D).** Furthermore endogenous phospho JNK/JNK levels are restored when FbZ is overexpressed in a Hep^{CA} gain-of-function background **(B,C)**; this is not the case when JbZ is overexpressed in the same genetic paradigm **(E,F)**. As a control overexpression of Hep^{CA} alone **(G)** gives relatively low phospho JNK/JNK levels **(H-I)**. **(J)** Quantification of the above phenotypes. Green, CD8-GFP; Red, pJNK Ab staining; Blue, JNK Ab staining. Scale Bar, 20μm, pale blue arrows indicate axon overextensions, yellow arrows show axon loss. Genotypes are as folllows (A) *UAS-mCD8-GFP/UAS-FbZ; UAS-Hep^{CA} /+; GAL4-OK107/+* (B) *UAS-mCD8-GFP/UAS-JbZ; UAS-Hep^{CA}/+; GAL4-OK107/+* (C) *UAS-mCD8 -GFP/+; UAS-Hep^{CA} ; GAL4-OK107/+*

neuronal death phenotype induced by Hep^{CA} overexpression. Unlike FbZ, dominant negative Jun misexpression only partially rescued the Hep^{CA} gain-of-function neuronal death phenotype. Approximately 60% of mutant phenotypes exhibited axon overextensions (Figure 6.5.1 D; quantifications, Figure 6.5.1 J) the remaining 40% displayed large scale neuronal death. Additionally in this scenario both phospho JNK and JNK levels were reduced compared to the higher levels of pJNK/JNK staining observed in a Hep CA gain-of-function background, misexpressing FbZ (compare Figure 6.5.2 B-C with E-F). Overall these results suggest that constitutively active JNK signals operate through Fos to induce neuronal death. Furthermore it is likely that Fos is the principle AP-1 component with Jun playing an ancillary role, since inactivation of Fos and not Jun is able to fully rescue the Bsk gain-of-function MB neuronal death phenotype.

6.6 Constitutively active Jun induces axon overextension in MB neurons

A potential method to establish an ancillary role for Jun in neuronal morphogenesis would be to overexpress a constitutively active form of Jun in MB neurons. The Jun^{Asp} transgene consists of mutated serine/threonine phosphorylation sites, which have been substituted to Aspartic Acid (Treier et al, 1995) rendering it constitutively active. Overexpression of Jun^{Asp} resulted in overextension of both medial and dorsal projecting axons, with fusion of both sets of axons at the midline. All phenotypes also exhibited axon loss of the dorsal axons (n=36) (Figure 6.6.1 A). These phenotypes closely resembled those observed in MB neurons overexpressing Hep-Bsk fusion transgenes (weaker expressing lines) and low levels of constitutively active Hep (Figure 6.6.1 B and C). What could account for this similarity? A possible explanation could be that Jun

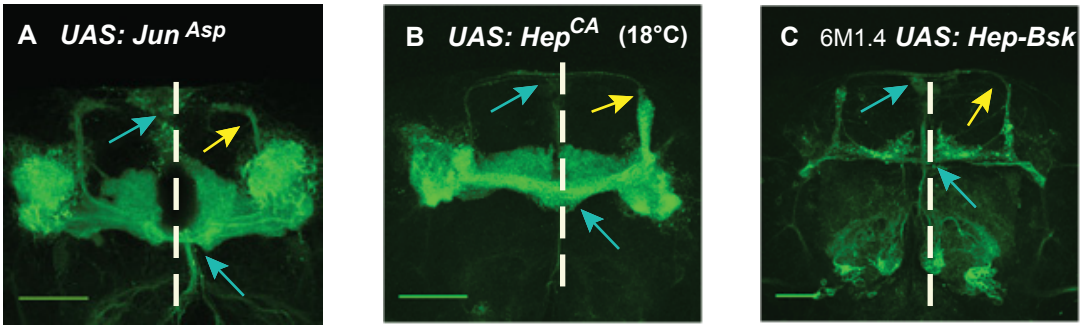

Figure 6.6.1. Overexpressing constitutively active Jun MB neurons resemble mutant phenotypes acquired for Hep ^{CA} gain-of-function MB neurons.

(A-C) Representative images of MB neurons overexpressing constitutively active forms of Jun **(A)**, Hep **(B)** and a Hep-Bsk fusion transgene **(C)**. Overexpressing Jun^{Asp} MB neurons exhibit overextending dorsal and medial axon projections, characterized by partial loss of the medial axon **(A)**, this is the case for all samples observed (n=40). MB neurons overexpressing low levels of constitutively active Hep **(B)** and weak Hep-Bsk transgenic lines **(C)**, also exhibit mutant phenotypes with similar morphological features. Hence they are shown for comparative purposes. Green, CD8-GFP; Scale Bar, 50μm, pale blue arrows indicate axon overextensions, yellow arrows show axon loss. Genotypes are as follows (A) *UAS-mCD8-GFP/UAS-Jun* ^{Asp} *; GAL4-OK107/+* (B) *UAS-mCD8-GFP/UAS -Hep* ^{CA} *; GAL4-OK107/+* (C) *UAS-mCD8-GFP/UAS-Hep Bsk HA; GAL4-OK107/+*

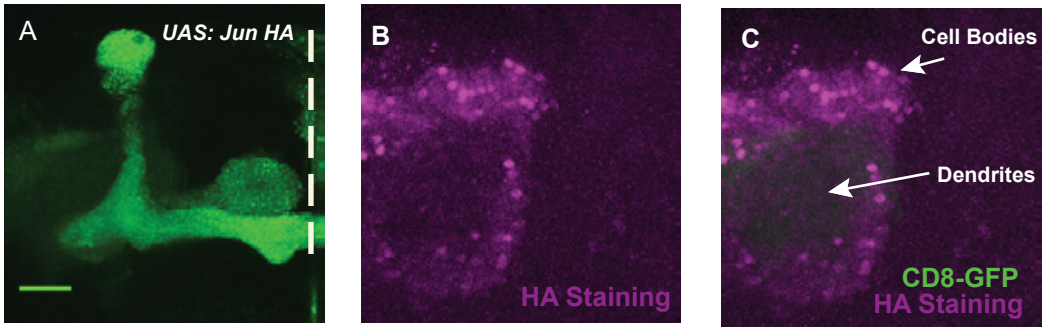

Figure 6.7.1. Jun is exclusively localized to cell bodies of MB neurons

(A-C) Representative Images of MB neurons overexpressing a tagged Jun-HA trangene. MB neuron projections are labelled by overexpressing CD8-GFP in these neurons **(A)**. Immunostaining with an HA antibody reveals that tagged Jun HA protein is solely localized to the cell bodies and cannot be detected in either the dendrites or axons **(B)**. Overlap between Mushroom Body neurons labelled with CD8-GFP (Green) and HA staining (Magenta). For clarity only a z projection of the Cell Body/dendritic region is shown **(C)**. Scale bar: 20 μm. Genotypes are as follows (A) *UAS-mCD8-GFP/UAS-Jun HA; GAL4-OK107/+*

responds to lower intensity of constitutively active JNK signals, whereas Fos comprises the major component of the AP-1 transcription factor complex receiving the vast majority of constitutively active JNK signalling inputs.

6.7 Jun localisation is confined to the cell bodies in MB neurons.

The AP-1 complex is an immediate early transcription factor, which operates in the cell nucleus to regulate the transcription of downstream targets. What evidence is there in MB neurons that the AP-1 complex is localised exclusively to the cell bodies? In order to ascertain whether the AP-1 transcription factor complex is localised solely to the MB neuronal cell bodies, I ectopically expressed a Jun-HA tagged transgene. As expected, I found that Jun was solely confined to the MB cell bodies (Figure 6.7.1 C) and was not localised to either the dendrites or the axons (Figure 6.7.1 A and B).

6.8 Discussion

The results thus far suggest that axon based Bsk signals are translated into a graded nuclear based AP-1 readout, to maintain axon stability and prevent axon overextension and neurodegeneration, however how predominantly this occurs awaits further investigation. One common theme, which did emerge from this study nonetheless, is that Fos rather than Jun forms the major component of the AP-1 response, which regulates various aspects of neuronal morphogenesis. For instance loss of function or inactivation of Jun has no effect on axon stability, additionally it is overexpression of Fos rather than Jun than it able to rescue the gain-of-function LIMK axon stalled phenotype. Furthermore only misexpression of dominant negative Fos is able to fully restore wild type axon

projections in a Hep^{CA} gain-of-function background and rescue the neuronal death phenotype. So what accounts for the fact that predominantly Fos, rather than Jun is able to regulate diverse processes in MB neurodevelopment and physiopathology such as axon growth and neuronal death?

Previous studies show that Jun and Fos do not always play equal roles in mediating AP-1 responses. There is a precedent for Fos rather than Jun being the principle AP-1 component, mediating varied morphological events in diverse cell types. For instance during Drosophila endoderm induction it is Fos and not Jun, which is responsible for activating labial, a selector gene with a role in cellular differentiation in the larval midgut. Furthermore Fbz interferes with cell differentiation in the larval midgut whereas as JbZ does not (Riese et al, 2003). Additionally in imaginal discs *Jun* mutant clones display only mild mutant phenotypes and do not affect proliferation/survival, whereas as strong loss of function *Kayak*/*Fos* alleles exhibit severe defects (Ciapponi et al, 2001). Consistent with this, recent studies on the role of Fos, show it is required for cell cycle regulation and proliferation in wing and eye discs. In fact cyclin B was identified as a direct downstream transcriptional target of Fos *in vivo* (Hyun et al, 2006). Fos also controls the expression of ecdysone inducible genes to regulate glial cell number and differentiation in the developing ventral nerve cord of Drosphila (Giesen et al, 2003). Reinforcing the notion that Fos is required for cell proliferation, loss-of-function of Fos in MB neurons using Kay^{1} mutant MB neuroblast clones, resulted in neuroblast proliferation defects, in which the later born neurons failed to form (Figure 6.2.2 A). However why is it that the kay^{1} mutation had no effect on the axonal architecture of later-born MB neuroblast clones?

It has been well documented that multiple Fos isoforms exist in Drosophila, whereas this is not the case for Jun. The structure of the Fos gene has been demonstrated to be complex and the gene is spread over 28kb of genomic DNA harbouring the expression of five different promoters directing the expression of six different isoforms. In fact the *Kay*^{1} mutation is not likely to be a true 'null' mutation since it is known to affect only two Fos isoforms (Giesen et al, 2003). Consequently in order to perturb Fos function many studies have opted for a dominant negative approach, which offers a method to inhibit the activity of multiple Fos proteins. This strategy has been used to investigate the role of AP-1 in various developmental processes such as dendrite growth, endoderm induction, wing vein formation, photoreceptor differentiation and neuronal development and plasticity (Hartwig et al, 2008; Riese et al, 1997; Ciapponi et al, 2001; Franciscovich et al, 2008; Collins et al, 2006).

In my study misexpression of dominant negative Fos also proved informative. I demonstrated that overexpressing two copies of FbZ, culminated in MB axon overextension, this process also seems to be dose dependent, since misexpression of one copy of FbZ resulted in a very lower penetrance of MB axon overextension. Increasing the level of Fos inactivation resulted in predominantly neurodegeneration as oppose to axon overextensions. Overexpressing Kay RNAi also resulted in MB axon overextension; however when the Kay RNAi knockdown was increased by ectopically expressing Dcr2, an increased proportion of MB neurons exhibited neurodegeneration (Figure 6.2.3). Additionally overexpression of FbZ in conjunction with JbZ, culminated in predominantly neurodegeneration and a lower frequency of axon overextension, this suggests that the two AP-1 components are able to cooperate with each other as

heterodimers, to induce transcription of downstream targets which probably confer neuroprotective effects on MB neurons. However the results also suggest that Fos plays the major role in safeguarding against neurodegeneration in the AP-1 response.

I also uncovered that misexpression of dominant negative Fos could fully rescue the neuronal death phenotype acquired in a Hep gain of function background, whereas dominant negative Jun was unable to restore wild type projections in this paradigm. This experiment establishes that constitutively active JNK signals can operate solely through Fos to induce neuronal apoptosis and Jun is surplus to requirements. Additionally caspase-3 activity is elevated in Bsk gain-of function MB neurons, underlining the pro-apoptotic function of Bsk. In fact it has been widely reported that JNK signalling is implicated in apoptosis and activation of JNK signalling induces cell death via the transcriptional activation of the pro-apoptotic genes *reaper*, *grim* and *hid*. (Griswold et al, 2008; Hong et al, 2009). It has also has been found that Fos is required to activate the pro-apoptotic gene hid downstream of JNK signalling in response to UV induced DNA damage in the developing Drosphila retina (Luo et al, 2006).

Interestingly overexpression of constitutively activated Hep resulted in a reduced level of JNK/pJNK (Figure 4.7.1), whereas inactivation of Fos in a constitutively active Hep background, restored endogenous JNK/pJNK levels. I previously speculated that this could be a result of an unknown JNK specific phosphatase, which has responded to the artificially high level of JNK activity and restrained it below a certain threshold. There is a precedent for this, for instance in one study it has been found that loss of puckered (a JNK specific phosphatase) triggers apoptosis in epithelia. It was demonstrated that in puckered's absence intrinsic JNK activity exceeds a certain threshold and culminates in

epithelial cell death (McEwen et al, 2005). It could be that a similar situation is occurring in MB neurons, although further investigation would be needed to confirm the relevance of a phosphatase in regulating JNK signalling in MB neurons. One could potentially envisage a scenario in which Fos is upregulating this unknown phosphatase. In fact it has been demonstrated that AP-1 activity levels mediate puckered activity during follicle cell morphogenesis (Dobens et al, 2001) and dorsal closure (Martin Blanco, 1998).

Finally I have also revealed that JNK signals operate through Fos to promote axon growth in a pathway antagonistic to LIMK. It is known that the Rho GTPases via their downstream effector proteins Pak and Rho kinase are able to activate LIMK, which in turn is able to phosphorylate and deactive cofilin. It is slingshot phosphatase which is able to dephosphorylate cofilin, facilitating actin turnover and thereby promoting axon growth (Ng and Luo, 2004). However both ectopic expression of Bsk and Fos suppress the LIMK axon stalled gain-of-function phenotype, restoring wild type projections and overexpression of a phospho inactive form of Fos enhances the LIMK gain-of-function phenotype. This strong genetic interaction between LIMK and the JNK signalling pathway components Bsk and Fos, suggest that they constitute part of an alternative pathway which promotes axon growth via transcriptional regulation of target genes. Thus far, these AP-1 target genes which promote axon elongation in MB neurons have yet to be elucidated, although there is a large array of candidates which could potentially regulate the cytoskeleton and axon growth (see chapter 7).

In conclusion, I have identified that Fos responds to instructive JNK signals independently of Jun to regulate both neuronal apoptosis and axon growth. I have also demonstrated that axon stability could at least in part be regulated by a graded AP-1

transcriptional output, which responds to graded levels of JNK signalling inputs. Distinct Fos isoforms could potentially form heterodimers between themselves or Jun, which could in theory induce the transcription of a number of different downstream target genes. Therefore future research should focus on which isoforms of Fos are required in which biological context and how they interact with Jun.

CHAPTER 7: Discussion

7.1 The significance of the JNK signalling pathway in neuronal morphogenesis

I initially set out to understand how the JNK signalling pathway is able to regulate distinct aspects of neuronal morphogenesis. A lot of research has gone into axon guidance, morphogenesis and signalling, however key issues have not yet been addressed. For instance how is it that the sole *Drosophila* JNK homologue Bsk is able to regulate diverse processes in neurodevelopment and physiopathology, which in mammals are mediated by three JNK genes and multiple spliced isoforms and more generally how can the same signalling molecules regulate different aspects of neuronal morphogenesis?

In my study I have established that the level of JNK activity is crucial in mediating axon stability, growth and neuronal apoptosis. The JNK pathway regulates axon stability by preventing axon overextension, (which requires a higher threshold of Bsk activity) and axonal degeneration, (which needs a relatively lower level of Bsk activity). To understand how defective neuronal morphogenesis is prevented during development, I have demonstrated that the level of JNK activity, its duration and the developmental phase of the organism are crucial in determining how developing axons respond to JNK signalling inputs.

I have also demonstrated that Bsk activates the AP-1 transcription factor complex and like Bsk, AP-1 signals are similarly graded to maintain axon stability. Furthermore I have shown that Bsk signals through AP-1 to induce MB neuronal apoptosis. However MB neuronal apoptosis only occurs in a Bsk gain-of-function paradigm, further highlighting the importance of JNK activity levels in eliciting different processes in

cellular morphogenesis. I have provided evidence that Bsk and AP-1 are able to interact with the cytoskeleton, since overexpression of Bsk or AP-1 is able to rescue the axon growth inhibited phenotypes induced in a LIMK gain-of-function background.

Finally I have established that the two *Drosophila* JNKKs Hep and Mkk4 are needed to maintain JNK-dependent axon stability. Furthermore Hep and Mkk4 differentially regulate Bsk activity. Biochemical and genetic data confirm that Hep is a more potent activator of Bsk activity. For instance overexpression of only Hep-Bsk fusion transgenes can invoke MB neuronal death, whereas overexpression of Mkk4-Bsk fusion trangenes cannot. The divergent functions of Hep and Mkk4 are confirmed by antibody studies, which show they are differentially localised in MB neurons

7.2 The importance of the relative activity level of Bsk in regulating axon stability *in vivo*

Signalling parameters such as signal strength and duration governs how cells respond to multiple stimuli to elicit the relevant biological response and previous studies have shown that signal strength and signal duration can bias MAPK responses. For instance several studies demonstrate that activation of sustained ERK signalling is responsible for initiating the differentiation of rat PC12 pheochromocytoma cells into sympathetic like neurons (Yaka et al, 1998; Qui & Green, 1992; Marshall 1998; Sun et al, 2006). However this has been studied mainly in the context of Erk responses towards cell proliferation and differentiation in cultured neuronal and non-neuronal cells (Marshall et al, 1995; Murphy and Blenis, 2006). How these parameters regulate ERK signals have been investigated

2006). However it is yet to be determined how signal strength and duration are able to modulate JNK-dependent axonal stability in vivo.

This study shows how JNK signalling can potentially regulate multiple aspects of neuronal morphogenesis in *Drosophila*, with the protein kinase *Bsk* (*Drosophila JNK*) acting as the central signalling conduit. Contrastingly in vertebrates, multiple JNK isoforms have been demonstrated to exhibit isoform specific functions and regulate various aspects of neurodevelopment (Coffey et al, 2002; Chang et al, 2003; Brecht et al, 2005, Zhao and Herdegen, 2009; Yang et al, 1997; Kuan et al, 1999). Signals that regulate Bsk activity can generate distinct axonal phenotypes depending on the signalling network, strength and duration. Both JNKKs, Mkk4 and Hep converge on Bsk and determine its relative activity level, hence the JNKK signal network is related to signal strength (Figure 7.1 A). In order to prevent axons from overextending past their post-synaptic target region, the signals require the activity of both Hep and Mkk4, since loss of either will result in axon overextension. This phenotype is phenocopied by either a *Bsk* hypomorph mutation or *Bsk* RNAi knockdown, where Bsk activity is partially inactivated. However for signals that protect against neurodegeneration and axonal loss, the JNKKs seem to act redundantly, as loss of either kinase does not result in a significant proportion of neurodegenerative phenotypes being observed, whereas *Bsk* null conditions or loss of both Mkk4 and Hep concomitantly, result in a large proportion of neurodegenerative phenotypes being observed. This bias in responses suggests while lower levels of *Bsk* activity are sufficient to protect against neurodegeneration, the mechanism that safeguards against axon overextension requires higher levels of *Bsk* activity. In order to prevent defective axonal morphogenesis and maintain axonal

stability, JNKK inputs are critical as loss of their phosphorylation sites on *Bsk* renders *Bsk* fully inactive.

What is currently unknown is the nature of the signals upstream of the JNKKs that regulate Bsk mediated axon stability in MB neurons. These unidentified upstream signals are likely to be active throughout development to maintain Bsk mediated axon stability by preventing axon degeneration and axon overextension. Furthermore it is unclear whether there are distinct divergent upstream signals which converge on the JNK signalling pathway to protect against axon degeneration and axon overextension respectively. In one scenario there could be different growth factors or signalling molecules, which could differentially regulate JNK signalling via distinct modi operandi. One signal could act to prevent degeneration, while another stabilises axons at the correct termini by preventing overextension. In a separate scenario, this may be one and the same factor, which acts to promote axon stability by preventing defective axon extension beyond the synaptic target region and neurodegeneration. Nonetheless, the results suggest that these two distinct aspects of JNK-dependent axon stabilisation require different threshold levels of Bsk activity.

7.3 The importance of the signal duration of Bsk activity in regulating neuronal morphogenesis *in vivo*

The phospho-JNK staining results show that Bsk is active throughout MB development and adulthood (Figure 7.1B). Interestingly in adult MB neurons the level of activated JNK is substantially higher in the earlier born γ-neurons, than in the later borne α'/β' and α/β neurons. This could be due to the fact that phosphorylated JNK has accumulated in

these neurons over a greater time period during development. Unlike the phospho-JNK immunostaining results, the genetic results show that *Bsk* activity is only required throughout development to regulate MB neuronal morphogenesis. Prolonged Bsk RNAi knockdown during adulthood does not modify the existing pre-induced wild type axonal phenotype. In concurrence, with this finding, introduction of *Bsk* rescue activity at adulthood, in *Bsk* null MB neurons, does not modify the existing pre-induced neurodegenerative phenotype. These results suggest that JNK-dependent physiology changes occur between development and adulthood, and the adult-stage phospho-JNK signals most likely reflect a distinct mode of MB neuron regulation. The switch from JNK signalling being required during development for correct axonal morphogenesis and an unknown function in adulthood may reflect a cell-context requirement of JNK signalling. Although yet to be defined, it is possible that JNK signalling is needed during adulthood for synaptic plasticity and growth, as shown in *Drosophila* NMJ studies (Collins et al, 2006; Sanyal et al, 2002). For instance one could potentially envisage that JNK signals to AP-1 in a differential manner in the adult neuron, facilitating the transcription of genes needed for synaptic plasticity and higher order processes such as memory and learning. Conversely JNK may be surplus to requirements at adulthood as axons become stabilised and another signalling molecule may perform adult specific functions in the MB neuron.

Using different experimental paradigms to control the timing of Bsk activity in vivo, I found that Bsk activity is required throughout development to maintain optimal axon stabilisation. The shorter duration of Bsk inactivity and activity results in a weaker effect, or a lower penetrance of mutant phenotypes compared with protocols where Bsk

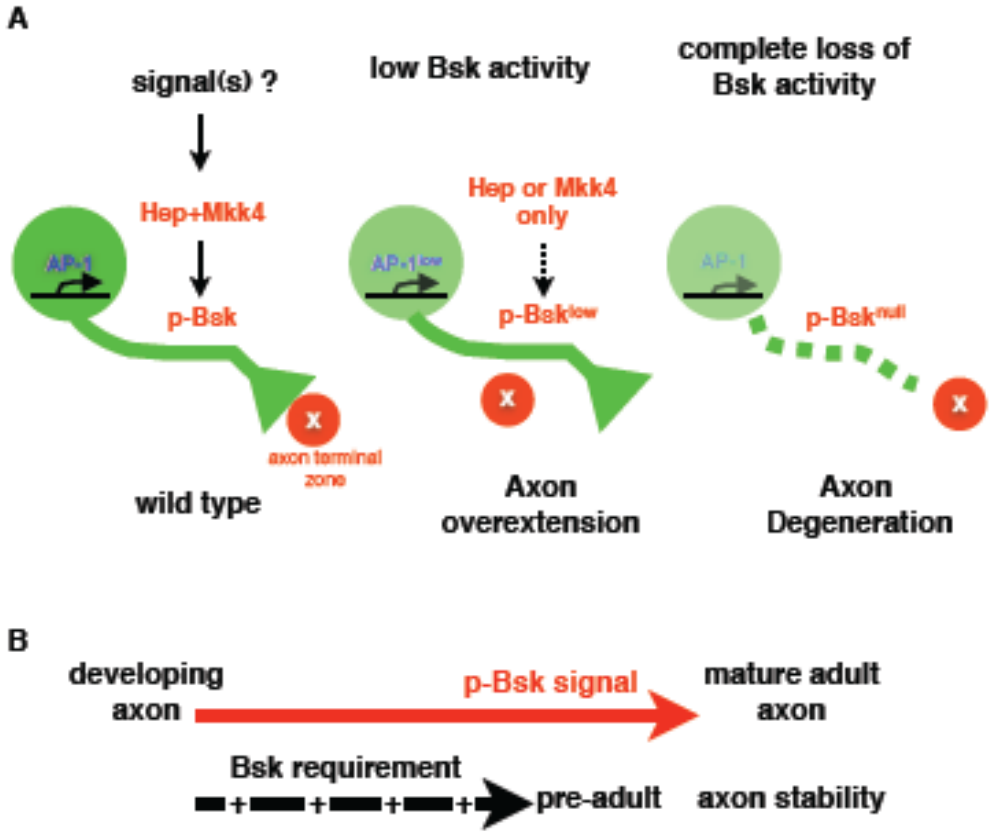

Figure 7.1. Working model of the role activity level and temporal duration plays in Bsk signaling in neurons

A working model of Bsk-dependent axon stability derived from this study. **(A)** The levels of Hep and Mkk4 determine the level of Bsk/AP-1 activity in MB neurons resulting in wild-type (normal activity), axon overextension (partial activity), or degenerating (completely loss of Bsk/AP-1) axons. **(B)** A temporal model of Bsk-dependent axonal morphogenesis. Bsk activity (measured by the P-Bsk signal) is detected throughout development and adulthood (observed in 14 day old adults). The genetic results show, to maintain axonal stability, Bsk is required mainly during the developmental phase (pre-adult). Furthermore, the Bsk TARGET RNAi and rescue studies show these signals act additively. In the *bsk*-null analysis, axon phenotypes were not detected until mid-pupal stages (from 30h APF onwards) and resulted in accumulative incidence of axon degeneration. Together with the TARGET results, this suggests the *bsk* axon degeneration phenotype reflects a late-onset event due to loss of earlier Bsk signals.

RNAi or rescue activity is 'on' throughout development'. Based on these results, I propose that for maintaining optimal axon stabilisation, Bsk signals are read "additively" throughout development (Figure 7.1B). Rather than as a 'temporal summation' module, where signals are required to reach a timed threshold level of activity to evoke an 'all-or-none' response, I find that shorter periods of Bsk activity, are still able to generate the correct wild type morphogenetic response (albeit sub-optimal). Nonetheless there is still a threshold level of JNK activity, needed to protect against neurodegeneration (relatively low) and axon overextension (relatively high). Interestingly the signals that prevent neurodegeneration, seems to be more sensitive to an early inactivation of Bsk whereas those that safeguard against axon overextension, seem to be more sensitive to JNK inactivation at later stages of development. This suggests that JNK signalling predominantly mediates pro-survival (anti-neurodegenerative) effects early in development and regulates axon extension in the later stages of development.

7.4 Differential regulation of Bsk activity by the JNKKs: Hep and Mkk4

Another salient point to make is that although both *Hep* and *Mkk4* can function to prevent the overextension of MB axons past their correct synaptic target they do not exhibit complete genetic redundancy. For instance only expression of *Hep* is able to rescue the axon overextension defects observed in *Mkk4* mutant MB neuroblast clones, not vice-versa. Additionally in a different gain of function genetic paradigm, where Hep-Bsk fusion transgene are overexpressed in MB neurons *Hep* is able to constitutively activate *Bsk* to induce large scale neuronal death whereas equivalent overexpression of Mkk-Bsk

fusion transgenes in MB neurons has no effect on MB axon projections. Furthermore loss of *Hep* results in a low frequency of neurodegeneration phenotypes, resembling those observed in *Bsk* null MB neurons, whereas no neurodegeneration is observed in *Mkk4* MB neuroblast clones. Taken together this data suggests that Hep and Mkk4 function in a divergent manner to regulate Bsk activity, with Bsk being activated at higher threshold level by Hep rather than Mkk4. Therefore the genetic results suggest that Hep is the more potent activator of *Bsk* phosphorylation.

What could account for the differential manner in which Hep and Mkk4 operate to activate *Bsk*? First of all Hep and Mkk4 are strongly expressed in different axon subsets of MB neurons. Mkk4 is localised in the later born α/β and α'/β' axons whereas Hep is localised in all three MB neuron subsets: γ, α/β and α'/β' axons. This is consistent with the loss of function data which shows that *Mkk4* is required for the formation of the later born α/β and α'/β' MB neuron subsets. Additionally unlike ectopic Hep, which exhibited preferential localisation to the MB axons, ectopic Mkk4-YFP when expressed in MB neurons was strongly localised in the cell bodies and the axons.

Based on the differential localisation of the JNKKs it is possible that discrete signals from different locations in the brain can activate JNKKs, which in turn would leads to a local activation of Bsk at the relevant subcellular location. This distinct localisation of the JNKKs is likely to be achieved by the presence of particular JNK scaffolding proteins (Figure 1.12 and Figure 1.13). For instance it is thought that both JNKKs Mkk4 and Hep may bind to Syd (Ito et al, 1999; Kelkar et al, 2000). In sciatic nerves of mice Sunday driver (Syd) has been found on vesicular structures in axons that are transported in both anterograde and retrograde axonal transport pathways, and interact

with kinesin-1 and the dynactin complex. Furthermore it has been found that activated JNK and Syd co-localise with $p150^{Glued}$, a subunit of the dynactin complex and with dynein (Cavalli et al, 2005). This suggests that Syd may have the potential to bind to Mkk4 and transport into the neuronal cell body via a retrograde axonal transport mechanism. The appropriate downstream effectors can then presumably elicit the required morphogenetic change. Additionally it is known that *Hep* unlike *Mkk4* is able to bind directly to *APLIP1* (Horiuchi et al, 2007). This is significant since the vertebrate homologue of *APILIP1*, JIP-1, is a known scaffolding protein for JNK kinases and is able to potentiate JNK activation (Mooney and Whitmarsh, 2004), this could account for that fact that Hep rather than Mkk4 is the more potent activator of Bsk.

7.5 The role of JNK signalling in neurodegeneration

The neurodegenerative phenotypes described in a *Bsk* null situation in adult MB neurons, are the result of a progressive late onset neurodegeneration, which is initiated during the mid-pupal stage of development. Analysis of *Bsk* null MB single cell and neuroblast clones confirms that they are morphologically altered compared to their wild type counterparts, with multiple axon breaks being exhibited in the cell processes, mid-axon and especially the axon termini. These findings are consistent with a previous study in mice, which showed that JNK1 loss resulted in degeneration of the anterior commissure during embryonic development (Chang et al, 2003). Interestingly ectopic expression of p35 (a pan-caspase anti apoptotic baculovirus gene), rescues the neurodegeneration observed in *Bsk* null MB neuroblast clone; this suggests that neurodegeneration is accompanied by caspase-dependent apoptosis.

The neurodegenerative phenotype is exacerbated in aged adult *Bsk* null MB neurons and specific axon projections are completely absent. For instance in aged single cell and neuroblast α/β clones, the entire medial projecting β axon population is absent. This could be the result of dying back degeneration, which is characterised by the initial degeneration of the distal regions of axons, followed by distal to proximal progression. Dying back degeneration is observed in a number of disorders including amyotrophic lateral sclerosis (ALS), spinal muscular atrophy, spinocerebellar disorders, peripheral neuropathies and nutritional neurological disorders (Cavanagh 1964, Berger and Schaumburg 1995, Raff et al, 2002, Luo and O'Leary, 2005).

A possible cause for the neurodegenration observed in *Bsk* null MB neurons could be a failure of axonal transport. For instance late pupal and young adult (5 days post-eclosure) *Bsk* null single cell MB neuroblast clones possess abnormal axon morphology, characterised by the presence of 'spheroid' like structures throughout the axonal shaft (Chapter 3). Upon further genetic analysis it has been found that these 'spheroid' like protrusions, consisted of accumulations of both synaptobrevin and mitochondria (preliminary data). One possibility is that the disruption of JNK signalling results in defective APLIP-1/JIP-1 linked kinesin-cargo transport, as has been described previously in *Drosophila* motor neurons (Horiuchi et al, 2005, Horiuchi et al, 2007; Verhey, 2007).

New morphological methods have found that spheroids arise prior to neurodegeneration in a wide range of disorders. Longitudinal axon imaging using transgenic mice has revealed that in models of Alzheimer's disease (Tsai et al, 2004), ALS (Coleman et al, 2005) gracile axonal dystrophy (Mi et al, 2005) and in a wide variety of other CNS disorders (Coleman, 2005) spheroids and protrusions begin on

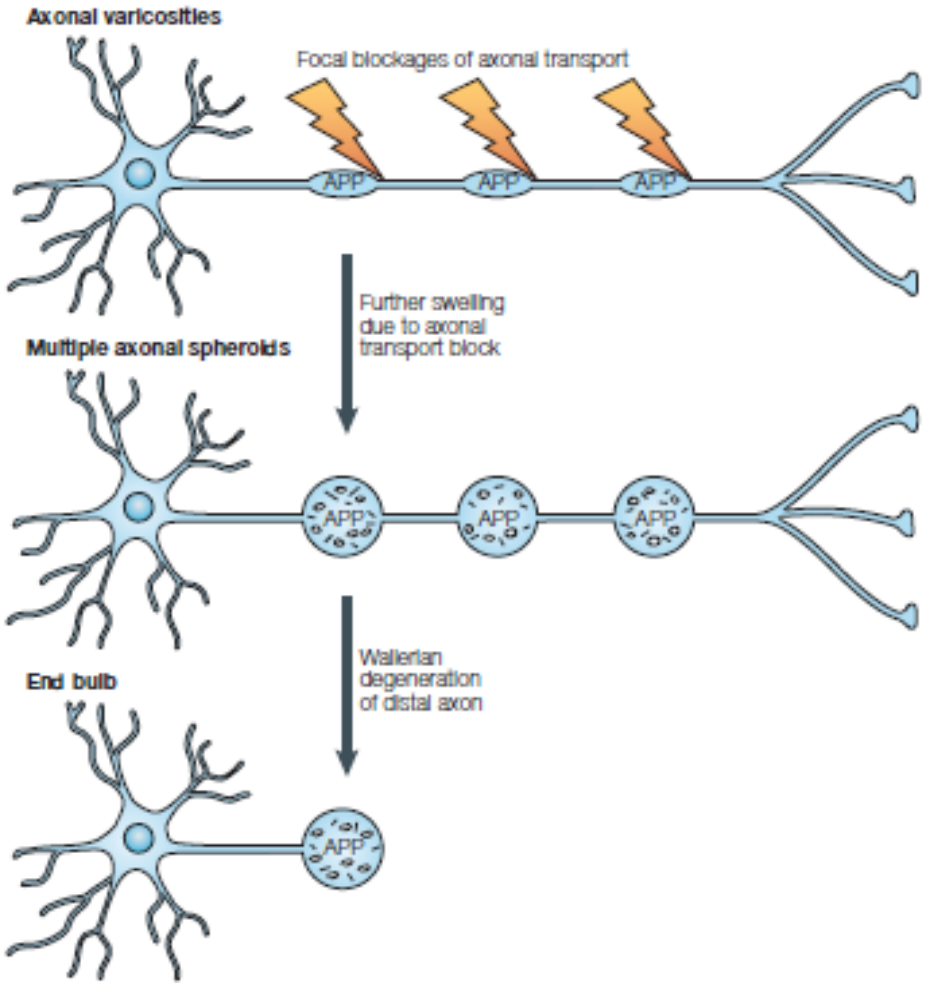

Figure 7.2 Potential mechanism of dying back degeneration in *Bsk* null MB neurons

The disruption of JNK signalling may result in defective APLIP-1/JIP-1 linked kinesin-cargo transport; this could lead to multiple blockages of axonal transport, which would cause the accumulation of organelles and vesicles such as mitochondria and synaptobrevin. It is likely that APP would also accumulate in these swellings (top). These axonal swellings would subsequently increase in size to form axonal spheroids (middle). As these spheroids expand, axonal transport becomes increasing impaired, to such a point that block of axonal transport is so severly disrupted to induce Wallerian degeneration of the distal axon (bottom). Adapted from: (Coleman, 2005).

many unbroken axons. Indicative of this axonal transport impairment is the accumulation of APP in axonal spheroids and varicosities in a multitude of neurodegenerative disorders, including Alzheimer's disease (Stokin et al, 2005), Creutzfeldt-Jakob disease (Liberski and Budka, 1999) and Parkinson's disease (Schwab et al, 1997). It would be interesting to determine whether the protrusions observed in *Bsk* null MB single cell neurons, contained accumulations of APP, this may be probable since it is well documented that APP binds directly to APLIP-1, the *Drosophila* orthologue of JIP-1 (Taru et al, 2002; Horiuchi et al, 2007). A potential mechanism by which defective axonal transport culminates in dying back degeneration is shown in Figure 7.2.

7.6 Gain of function of Bsk induces neuronal apoptosis

Constitutively active JNK signalling in MB neurons results in large scale neuronal death of the vast majority of all MB neuron subtypes; to such an extent that only relatively few MB neurons are present in a total population of approximately 2,500 (Ito et al, 1997). This finding is consistent with many other studies that show that large scale neuronal death takes place upon the induction of constitutively active JNK signalling in response to a wide range of genetic, environmental and stress stimuli, including ischemia and trophic factor deprivation (Miller et al, 2009; Morfini et al, 2006; Waetzig et al, 2006; Putcha et al, 2003). Interestingly inactivation of Fos, is able to fully rescue the neuronal apoptotic phenotype observed in a constitutively active JNK background and restore wild type MB neuron projections. Furthermore there is an elevated level of cleaved caspase-3 in MB neurons where constitutively active JNK is expressed compared with wild type MB neurons. Overall these results suggest that the transcription factor Fos (in response to

constitutively active JNK signals), could potentially promote the upregulation of pro-apoptotic genes, which in turn could facilitate the activation of the caspase-dependent apoptotic signalling cascade, ultimately resulting in neuronal death. For instance it has been documented that Fos is required to activate the pro-apoptotic gene hid downstream of JNK signalling in response to UV induced DNA damage in the developing Drosophila retina (Luo et al, 2006).

Additionally JNK and AP-1 activity is often upregulated in response to nerve injury and thought to be essential for axonal repair post-injury (Herdegen et al, 1998, Raivich et al, 2004). How my study relates to these different models of disease, development, injury and repair remains speculative, however my findings do propose that parameters such as activity levels, timing and developmental stages, may be crucial in understanding JNK-dependent dysfunction in the nervous system.

7.7 Bsk maintains axon stability through AP-1 transcriptional regulation

In a similar respect to *Bsk*, stronger inactivation of AP-1 signals results in neurodegeneration and axon loss, whereas partial inactivation of AP-1 activity culminates in axon overextension. Therefore like *Bsk*, AP-1 signals are similarly graded to maintain axon stability, with a high level of AP-1 activity needed to prevent axon overextension beyond the correct post-synaptic target and a lower threshold activity level of AP-1 required to safeguard against neurodegeneration. It is possible that the pro-survival signals, which confer neuroprotective (anti-degenerative) effects during MB neuron development and adulthood, could be the result of AP-1 transcriptional regulation of a

Nerve Growth Factor (NGF)-like homologue in *Drosophila*. In mammals it has been found that the NGF promoter contains an AP-1 consensus sequence, furthermore a correlation has been found between increased AP-1-NGF binding activity and the induction of NGF mediated transcription in rat glioma cells (Colangelo et al, 1996). Trophic factors and contact dependent processes are essential in maintaining a growing and healthy cell; however whether JNK signalling is implicated in regulating these factors remains speculative.

7.8 The JNK signalling pathway interacts with the cytoskeleton via AP-1 transcriptional regulation.

Previous studies show Bsk signals result in distinct transcriptional responses, involving gene targets linked to the actin cytoskeleton, cell adhesion, oxidative stress, extracellular matrix, autophagy, cell cycle and apoptotic control (Homsy et al., 2006; Hyun et al., 2006; Jasper et al., 2001; Moreno et al., 2002; Uhlirova and Bohmann, 2006; Wang et al., 2003; Wu et al., 2009). Many of these are important for the Bsk-regulated morphogenetic changes and cytoskeletal regulation. In our preliminary analysis, we found Bsk/AP-1 signals do lead to changes in the actin and microtubule cytoskeleton, axonal transport and caspase-related activities (preliminary observations). Therefore, in our paradigm, Bsk/AP-1 signals most likely lead to multiple transcriptional targets, leading to different cellular responses during axonal morphogenesis.

In order to ascertain whether Bsk-AP-1 signalling is able to interact genetically with the cytoskeleton, I established co-expression assays using a LIMK gain-of-function background. LIMK inhibits axon growth through phosphorylating and inactivating cofilin

(Ng and Luo, 2004). As mentioned previously cofilin is required to promote the rapid turnover of actin filaments and depolymerise actin filaments from their pointed ends (Bamburg, 1999) Ectopic expression of either Bsk or AP-1 was able to fully rescue the axon stalled phenotype induced in a LIMK gain-of-function background and restore wild type projections. Furthermore overexpression of a mutant phospho-inactive form of Fos (which lacked all Bsk phosphoacceptor sites) enhanced the LIMK gain-of-function axon stalled phenotype. This suggests that Bsk-AP-1 signals upregulate downstream transcriptional targets, which are required in regulating cytoskeletal dynamics.

It is highly probable that AP-1 transcription could upregulate genes which are required in axonal outgrowth and cytoskeleton regulation. For instance during Drosophila embryogenesis Bsk/AP-1 signalling upregulates chickadee (chic), this encodes Drosophila profilin. Additionally Chic-deficient embryos fail to execute JNK mediated cytoskeletal reorganisation during dorsal closure (Jasper et al, 2001). However Chic alone is unlikely to be the sole downstream target of Bsk/AP-1, required in promoting axon growth, since overexpression of Chic fails to suppress the gain-of-function LIMK axon stalled phenotype (Ng and Luo, 2004). Additionally Fos controls Decapentaplegic (Dpp) expression in Drosophila dorsal closure (Riesgo-Escovar and Hafen, 1997b); Zeitlinger et al, 1997). Dpp co-ordinates cell shape changes and cytoskeletal dynamics by binding to the TGF-β like receptors Thickveins (Tkv) and Punt (Put), which activates a TGF-β like pathway (Ricos et al, 1999). It has also been found that Fos activation can stimulate matrix metalloproteinase (MMP) production, which probably functions via the reorganisation of the actin cytoskeleton (Zeigler et al, 1999; Ispanovic and Haas, 2006). MMPs play a crucial role in cell motility and extracellular matrix induced cell migration.

In *C-elegans* an MMP has been identified as a transcriptional target of Fos (Sherwood et al, 2005).

In mammals it is known promoters of the genes galanin, α7β1–integrin and CD44 all contain identified AP-1 sites (Anouar et al, 1999; Lee et al, 1993; Raivich et al, 2004). The AP-1 transcription target genes galanin, α7β1–integrin and CD44 all play prominent roles in promoting axonal outgrowth. Galanin is neuropeptide which exerts trophic actions on neurite outgrowth, including in DRG neurons (Mahoney et al, 2003; Hobson et al, 2006; Sanford et al, 2008). Activation of the receptor α7β1–integrin promotes the axonal outgrowth of retinal axons (Siddiqui et al, 2009) and stimulates neurite extension in cerebellar granule cells (Mercado et al, 2004). Finally reduction in the activity of CD44 a cell surface glycoprotein expressed in the neurons and glia of the CNS and PNS culminated in a failure in axon growth of retinal ganglion cells (Ries et al, 2007).

A central role for AP-1, has also been demonstrated in the regulation of cell morphology and motility. It is well documented that AP-1 can regulate the expression of target genes such as Mts-1, stromelysin 1, ezrin, and urokinase-type plasminogen activator (Hennigan et al, 1994; Miao and Curran; 1994, Jooss and Müller, 1995; Lamb et al, 1997). All these gene have been clearly implicated in cytoskeletal organisation, cell motility or remodelling of the extracellular Matrix (ECM) in *fos*-transformed fibroblasts (Lamb et al, 1997; Malliri et al, 1998). Furthermore expression of a c-jun deletion mutant in a human derived squamous cell carcinoma (SCC) line inhibits epidermal growth factor (EGF) activation of the Rho GTPases. (Malliri et al, 1998) The Rho GTPases are critical in regulating remodelling of the cytoskeleton, which in turn is required for processes such as membrane ruffling, lamellipodia formation, cell rounding and motility. Nonetheless

further investigation is needed to identify which target genes are upregulated by AP-1 transcriptional regulation in order to promote axon growth in MB neurons, this could be carried out using DNA microarray analysis.

7.9 The molecular interpretation of JNK signal duration and signal strength by AP-1.

The MAPK family of proteins have been implicated in numerous and diverse aspects of cellular behaviour and several hypotheses have been proposed, to account for their pleiotrophic behaviour. Previous in vitro studies have confirmed that signal strength and signal duration is able to bias MAPK responses. These parameters have been studied, primarily in the context of Erk responses towards cell proliferation and differentiation in cultured cells (Marshall, 1995; Murphy and Blenis, 2006). It has been found that the immediate early gene product c-Fos functions as a sensor for ERK signal duration and accumulative signal strength. Newly synthesised c-fos has a relatively short half life of about 30-45 minutes, but when it is phosphorylated by ERK the half life is extended to two hours (Okazaki and Sagata, 1995; Chen et al, 1996). Therefore when ERK activation is transient, c-Fos is present in the nucleus, but it is not phosphorylated and is therefore unstable and degraded. Conversely when ERK activation is sustained, c-Fos is phosphorylated, this stabilises c-Fos and primes additional phosphorylation, by exposing a docking site for ERK termed the DEF domain (signal sensor). Putative DEF domains have been found in four additional AP-1 proteins such as Fra-1, Fra-2, JunB and JunD (Murphy et al, 2002) as well as *Drosophila* Jun (Vinciguerra et al, 2004) and *Drosophila*

Fos. Since c-Fos is an integral component of the dimeric AP-1 transcription factor, an increase in its stability results in greater promoter occupancy and expression of target genes (Murphy et al, 2002). ERK docking to the DEF domain of the immediate early gene c-Fos, results in sensor phosphorylation. Docking and phosphorylation alters the biological activity and this directs the biological outcome.

Thus far, the mechanisms by which signal strength and signal duration regulate MAPK signals have been explored using only *in vitro* experimental and theoretical approaches (Kholodenko, 2006; Murphy and Blenis, 2006). In my project I focused on how timing and the activity level of JNK signalling regulate JNK-dependent axonal stability *in vivo*. Sustained JNK signalling is essential in regulating axon stability, this is probably due to the fact that JNK signal transduction is crucial throughout neurodevelopment and is needed to elicit the appropriate morphogenetic response via AP-1 transcriptional regulation at any given time. As demonstrated transient JNK signalling results in defective axonal morphogenesis, since the transcription of all the necessary downstream targets of the AP-1 immediate early gene products cannot occur. Additionally partial loss of JNK activity also results in defective axonal morphogenesis. This suggests that the JNK signal is not sufficient to adequately phosphorylate AP-1 and evoke the required morphogenetic response. Like Bsk, AP-1 signals are similarly graded, this suggests that AP-1 possibly contains DEF domains that sense the phosphorylation state of the AP-1 immediate early gene products and evokes the appropriate biological response (Figure 7.3). Further research would need to be carried out to test the relevance of the DEF domain in *Drosophila* Fos and Jun. This could be achieved be generating Fos and Jun DEF mutant *Drosophila* strains or non-nuclear/nuclear inhibited forms of JNK.

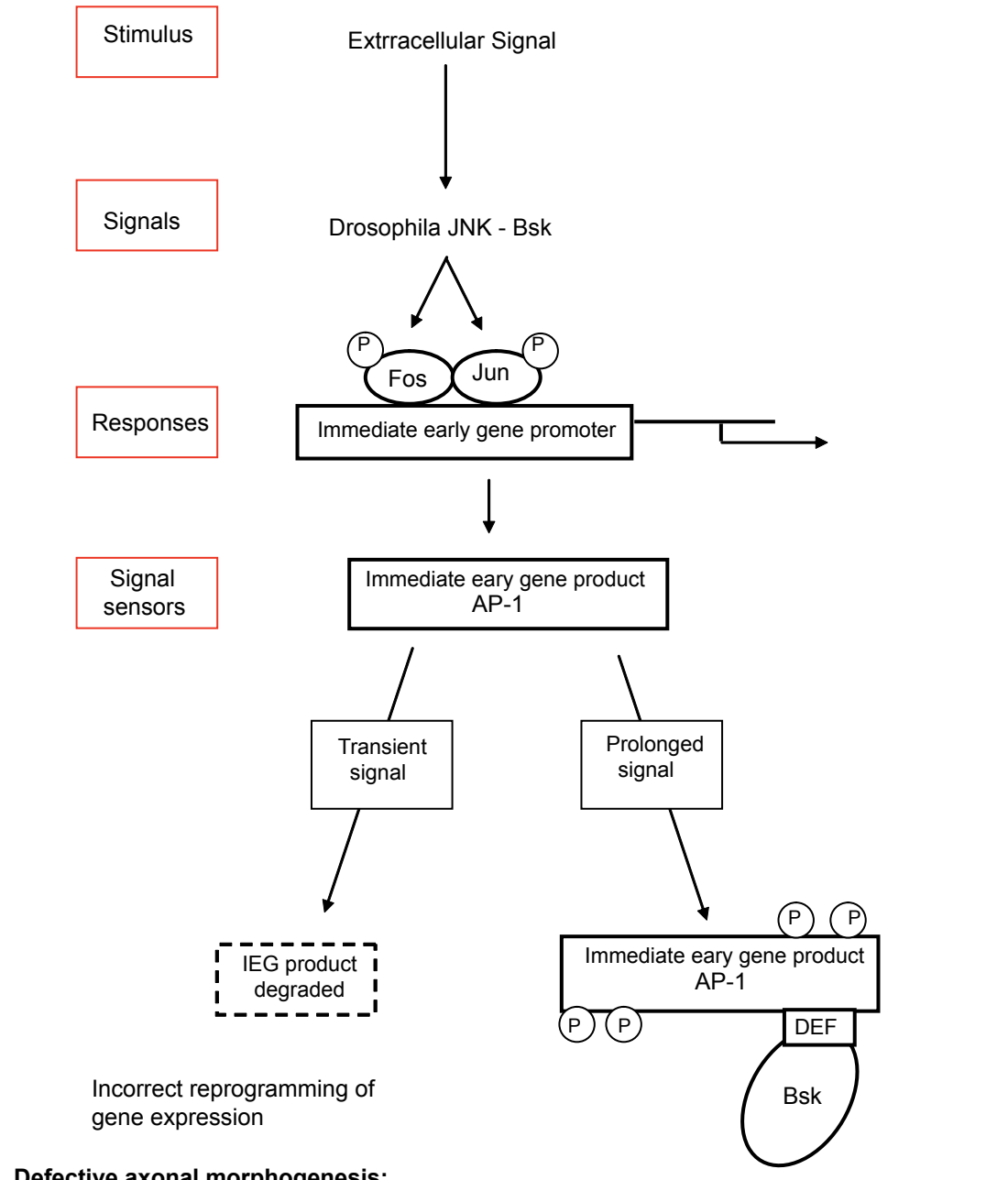
Stimulus
Extrracellular Signal
Signals
Drosophila JNK - Bsk
P
P
Fos
Jun
Responses
Immediate early gene promoter
Signal sensors
Immediate eary gene product AP-1
Transient signal
Prolonged signal
IEG product degraded
P
P
Immediate eary gene product AP-1
P
P
DEF
Bsk
Incorrect reprogramming of gene expression
Defective axonal morphogenesis:
- Neurodegeneration
- Axon overextension
Increase in stabilty of AP-1 results in greater promoter occupancy and expression of the relevant target genes
Non-defective neurodevelopmet:
-Protection against Neurodegeneration
-Prevention of axon overextensiuon

Figure 7.3

Figure 7.3. Molecular Interpretation of JNK signal duration.

An instructive extracellular signal (stimulus) induces activation of JNK signaling (signals) that results in rapid transcriptional induction of AP-1, consisting of the canonical immediate early genes Fos and Jun (response). The duration and strength of JNK signaling is then interpreted by the AP-1 immediate early gene products that are composed of DEF domains (signal sensors). Docking of nuclear residing JNK to the DEF domain results in sensor phosphorylation. Docking and phosphorylation alters the biological activity of AP-1, and this dictates how AP-1 regulates the transcription of a number of downstream targets in the cell, to elicit the appropriate morphogenetic response. Adapted from: (Murphy et al, 2002).

However the question remains as to how graded levels of AP-1 transcriptional activity are able to activate the relevant downstream target genes to induce the necessary cellular response during development. It is possible that similar to the Dorsal gradient networks in the Drosophila embryo which specify different thresholds of gene activity and tissue differentiation (Stathopoulos and Levine, 2002), graded AP-1 activity may control different events in neuronal morphogenesis during MB neuron development. Our data suggests that a low level of basal activity of pJNK/AP-1 is sufficient to protect against neurodegeneration and promote neuronal survival. It is probable that the pro-survival genes (which consist of AP-1 DNA recognition elements) have a high binding affinity to AP-1, and can therefore be induced at relatively low titres of AP-1 activity. It then follows that genes able to regulate axon overextension are activated at higher titres of pJNK/AP-1 activity, since they have a relatively lower binding affinity to AP-1.

Nevertheless this simplified mechanistic explanation, based on marginally different binding affinities of AP-1 for specific response element sequences, may only hold true in an *in vitro* scenario. In reality however drastic changes in the cellular environment during MB neuron development, could cause fluctuations in JNK signalling, this could potentially lead to an AP-1 graded signalling readout, which consists of various ensembles of transcription factors, with different DNA binding properties. Furthermore different combinations of Fos/Jun heterodimers and Fos homodimers in the appropriate conformational states may recognise different sequence elements in the promoters and enhancers of target genes, facilitating the desired biological outcome. One could potentially envisage a scenario where varying phospho-JNK levels are mirrored in the phosphorylation state of AP-1. Thus allosterically altering the AP-1 transcription factor

ensemble, would have a crucial role in determining the selectivity of AP-1 towards a particular DNA AP-1 binding site. A phosophomimetic approach could be taken to determine which AP-1 phosphorylation sites are needed to protect against neurodegeneration and prevent axon overextension. It must also be noted that DFos phosphorylation, also has the ability to co-ordinate chromatin dynamics. In fact it has been found that DFos phosphorylation, downstream of JNK signalling plays a key role in regulating the dynamics of the histone acetyltransferase (HAT) Chameau and recruiting the histone deactylase DRpd3 (Miotto et al, 2006). Therefore in MB neurons dynamic changes in AP-1 mediated gene transcription, necessary for proper MB neuronal morphogenesis most likely involve chromatin modifications.

7.10 Future experiments

In order to further investigate how the relative level of JNK/AP-1 signalling, affects MB neuronal morphology, I am currently utilising Electron Microscopy. This will enable me to observe how the neuronal ultrastructure is altered in various genetic paradigms. In fact immunogold labelling has been used to visualise fine structures such as synaptic vesicles, the endoplasmic reticulum, mitochondria and the plasma membrane in the ventral nerve cords of *C. elegans*. (Rostaing et al, 2004) and *Drosophila* (Pan et al, 2008). At present it is unclear as to how the MB neuronal cytoskeleton is modified in Bsk null and hypomorphic MB Neuroblast clones. I have already attempted to use acetylated and detyrosinated microtubule antibodies to determine if the stability of microtubules is affected in MB neurons expressing various transgenes, such as Bsk RNAi and Bsk DN. However the method of using antibody staining to examine the microtubule stability of

MB neurons for the whole mount Drosophila brain proved to be ineffective, since microtubules are ubiquitously present in the Drosophila brain and as a consequence of this, I was unable to differentiate the tubulin staining of the MB neurons from the surrounding brain tissue.

At present I have not yet identified the genes downstream of AP-1 responsible for maintaining JNK mediated axon stability in MB neurons. DNA microarray analysis could be used to determine changes in gene expression levels in various transgenic scenarios and at different developmental phases of MB neuron development. This could potentially inform me which genes are responsible for preventing axon overextension and protecting against neurodegeneration. Chromatin immunoprecipitation could also be utilised to determine the location of the DNA binding sites for AP-1 in the Drosophila genome. This technique could give us an insight into the protein-DNA interactions that occur in MB neurons in different genetic, temporal and developmental paradigms.

Finally the late onset degeneration phenotype I observe in *Bsk* null MB Neuroblast and single cell clones, may be due to the accumulation of aberrant protein aggregates. The preliminary data suggests that proteinaceous deposits, such as mitochondria, and membrane trafficking proteins such as synaptotagmin and synaptobrevin, accumulate in *Bsk* null single cell clones, giving a 'bead on a string' phenotype. The bead being the spheroid-like aggregate and the string, the smooth axonal shaft (see Figure 3.3.3). In many instances these abnormal axonal deposits may be composed of ubiquitin conjugates, which overwhelm and impair the ubiqutin/proteosome system as is this case in polyglutamine disorders such as Huntington's disease (Maynard et al, 2009). Interestingly overexpression of UBP-2, (a ubiquitin-specific protease that

removes ubiquitin from ubiquitinated proteins) enhances the neurodegenerative phenotype acquired with *Bsk* null MB Neuroblast clones. Therefore a method, in which the level of ubiquitination, could be deciphered in a wild type or *Bsk* null scenario, could potentially be useful in understanding whether the neurodegeneration, I observe can be attributed to defective ubiquitination. One way to detect varying ubiquitination levels could be to overexpress tagged ubiquitin molecules in *Bsk* null and wild type clones.

Furthermore overexpression of the slow Wallerian degeneration (Wlds) gene rescues the *Bsk* null neurodegeneration phenotype observed in *Bsk* Neuroblast clones. This is consistent with the neuroprotective effects of *Wlds* observed in transgenic mice (Mack et al, 2001), rats and *Drosophila melanogaster* (Adalbert et al, 2005, Hoopfer et al, 2006, MacDonald et al, 2008). I also proposed that Wallerian degeneration could potentially be occurring in *Bsk* null clones based on the neurodegeneration phenotype observed in aged *Bsk* null MB neurons (see Section 7.5, Page 202). As a result of this preliminary data, I am currently carrying out detailed analysis of *Bsk* null single cell clones, which express the Wlds-Myc tagged transgene, to gain a better understanding of the protective effects that Wlds is exerting in this neurodegenerative paradigm.

7.10 Conclusions

In conclusion, the overall results underline the signalling mechanisms that can regulate the JNK pathway during neuronal morphogenesis. The maintenance of axon stability *in vivo* can be accounted for by the graded signals by which JNK input signals are mediated and the means by which AP-1 transcriptional output signals are generated as well as the duration of JNK signal propagation within neurons. These findings potentially explain

how the ‘pleiotrophic’ JNK signaling cascade, which has been implicated in diverse processes in neurodevelopment, is able to regulate axon stability through the differential activation of the Drosophila JNK *Bsk*. Therefore understanding how the JNK signaling pathway is able to impart signaling specificity and effect particular changes in axon morphology, will inevitably assist in developing therapeutic strategies to combat neurodegenerative disorders and advance our current knowledge on neuroregeneration.

References

Adachi-Yamada T, Fujimura-Kamada K, Nishida Y, Matsumoto K. (1999). Distortion of proximodistal information causes JNK-dependent apoptosis in Drosophila wing. *Nature.* 400, 166-9.

Adachi-Yamada T, Nakamura M, Irie K, Tomoyasu Y, Sano Y, Mori E, Goto S, Ueno N, Nishida Y, Matsumoto K. (1999b). p38 mitogen-activated protein kinase can be involved in transforming growth factor beta superfamily signal transduction in Drosophila wing morphogenesis. *Mol Cell Biol* 19, 2322-9.

Adalbert R, Gillingwater TH, Haley JE, Bridge K, Beirowski B, Berek L, Wagner D, Grumme D, Thomson D, Celik A, Addicks K, Ribchester RR, Coleman MP. (2005). A rat model of slow Wallerian degeneration (WldS) with improved preservation of neuromuscular synapses. *Eur. J. Neurosci.* 21, 271–277

Agnes, F., Suzanne, M. and Noselli, S. (1999). The Drosophila JNK pathway controls the morphogenesis of imaginal discs during metamorphosis. *Development* 126, 5453-62.

Akechi M, Ito M, Uemura K, Takamatsu N, Yamashita S, Uchiyama K, Yoshioka K, Shiba T. (2001). Expression of JNK cascade scaffold protein JSAP1 in the mouse nervous system. *Neurosci Res* 39, 391-400.

Akhmanova A, Hoogenraad CC. (2005). Microtubule plus-end-tracking proteins: mechanisms and functions. *Curr Opin Cell Biol* 17, 47-54. Review

Amagasaki K, Kaneto H, Heldin CH, Lennartsson J. (2006). c-Jun N-terminal kinase is necessary for platelet-derived growth factor-mediated chemotaxis in primary fibroblasts. *J Biol Chem* 281, 22173-9.

Anouar Y, Lee HW, Eiden LE. (1999). Both inducible and constitutive activator protein-1-like transcription factors are used for transcriptional activation of the galanin gene by different first and second messenger pathways. *Mol Pharmacol* 56, 162-9.

Arber S, Barbayannis FA, Hanser H, Schneider C, Stanyon CA, Bernard O, Caroni P. (1998). Regulation of actin dynamics through phosphorylation of cofilin by LIM-kinase. *Nature* 393, 805-9.

Arévalo JC, Chao MV. (2005). Axonal growth: where neurotrophins meet Wnts. *Curr Opin Cell Biol.* 17, 112-5. Review.

Bagowski CP, Ferrell JE Jr. (2001). Bistability in the JNK cascade. *Curr Biol* 11, 1176-82.

Bamburg JR. (1999). Proteins of the ADF/cofilin family: essential regulators of actin dynamics. *Annu Rev Cell Dev Biol*, 15, 185-230. Review.

Barr RK, Bogoyevitch MA. (2001). The c-Jun N-terminal protein kinase family of mitogen-activated protein kinases (JNK MAPKs). *Int J Biochem Cell Biol* 33, 1047-63. Review.

Berger AR, Schaumberg HH. (1995). Human peripheral nerve disease (peripheral neuropathies). In The Axon: Structure, Function and Pathophysiology, ed. SG Waxman, JD Kocsis, PK Sytys, 648-60. New York: Oxford Univ. Press.

Berger, J., Senti, K. A., Senti, G., Newsome, T. P., Asling, B., Dickson, B. J. and Suzuki, T. (2008). Systematic identification of genes that regulate neuronal wiring in the Drosophila visual system. *PLoS Genet* 4, e1000085.

Bettencourt-Dias, M., Giet, R., Sinka, R., Mazumdar, A., Lock, W. G., Balloux, F., Zafiropoulos, P. J., Yamaguchi, S., Winter, S., Carthew, R. W. et al. (2004). Genome-wide survey of protein kinases required for cell cycle progression. *Nature* 432, 980-7.

Billuart P, Winter CG, Maresh A, Zhao X, Luo L. (2001). Regulating axon branch stability: the role of p190 RhoGAP in repressing a retraction signaling pathway. *Cell* 107, 195-207.

Björkblom B, Ostman N, Hongisto V, Komarovski V, Filén JJ, Nyman TA, Kallunki T, Courtney MJ, Coffey ET. (2005). *J Neurosci* 25, 6350-61.

Bjorklund, M., Taipale, M., Varjosalo, M., Saharinen, J., Lahdenpera, J. and Taipale, J. (2006). Identification of pathways regulating cell size and cell-cycle progression by RNAi. *Nature* 439, 1009-13.

Blasius TL, Cai D, Jih GT, Toret CP, Verhey KJ. (2007). Two binding partners cooperate to activate the molecular motor Kinesin-1. *J Cell Biol* 176, 11-7.

Bogoyevitch MA, Kobe B. (2006). Uses for JNK: the many and varied substrates of the c-Jun N-terminal kinases. *Microbiol Mol Biol Rev*. 70, 1061-95. Review.

Bohmann D, Ellis MC, Staszewski LM, Mlodzik M. (1994). Drosophila Jun mediates Ras-dependent photoreceptor determination. *Cell.* 78, 973-86.

Bosch, M., Serras, F., Martin-Blanco, E. and Baguna, J. (2005). JNK signaling pathway required for wound healing in regenerating Drosophila wing imaginal discs. *Dev Biol* 280, 73-86.

Brachmann CB, Jassim OW, Wachsmuth BD, Cagan RL. (2000). The Drosophila bcl-2 family member dBorg-1 functions in the apoptotic response to UV-irradiation. *Curr Biol*. 10, 547-50.

Brand AH, Perrimon N. (1993). Targeted gene expression as a means of altering cell fates and generating dominant phenotypes. *Development* 118, 401-15.

Bray D, Chapman K. (1985). Analysis of microspike movements on the neuronal growth cone. *J Neurosci* 5, 3204-13

Brecht, S., Kirchhof, R., Chromik, A., Willesen, M., Nicolaus, T., Raivich, G., Wessig, J., Waetzig, V., Goetz, M., Claussen, M., Pearse, D., Kuan, C. Y., Vaudano, E., Behrens, A., Wagner, E., Flavell, R. A., Davis, R. J. & Herdegen, T. (2005) Specific patho-physiological functions of JNK isoforms in the brain. *Eur J Neurosci,* 21**,** 363-77.

Bridgman PC, Dailey ME. (1989). The organization of myosin and actin in rapid frozen nerve growth cones. *J Cell Biol* 108, 95-109.

Brown MD, Cornejo BJ, Kuhn TB, Bamburg JR. (2000). Cdc42 stimulates neurite outgrowth and formation of growth cone filopodia and lamellipodia. *J Neurobiol* 43, 352-64.

Brown MC, Turner CE. (2004). Paxillin: adapting to change. *Physiol Rev* 84, 1315-39. Review.

Buchsbaum RJ, Connolly BA, Feig LA. (2002). Interaction of Rac exchange factors Tiam1 and Ras-GRF1 with a scaffold for the p38 mitogen-activated protein kinase cascade. *Mol Cell Biol* 22, 4073-85.

Burbelo PD, Drechsel D, Hall A. (1995). A conserved binding motif defines numerous candidate target proteins for both Cdc42 and Rac GTPases. *J Biol Chem* 270, 29071-4.

Cavalli V, Kujala P, Klumperman J, Goldstein LS. (2005). Sunday Driver links axonal transport to damage signaling. *J Cell Biol* 168, 775-87.

Cavanagh JB. (1964). The significance of the "dying back" process in experimental and human neurological disease. *Int Rev Exp Pathol* 3, 219-67.

Chang, L., Jones, Y., Ellisman, M. H., Goldstein, L. S. and Karin, M. (2003). JNK1 is required for maintenance of neuronal microtubules and controls phosphorylation of microtubule-associated proteins. *Dev Cell* 4, 521-33.

Chang, L. & Karin, M. (2001) Mammalian MAP kinase signalling cascades. *Nature,* 410**,** 37-40.

Charbaut E, Curmi PA, Ozon S, Lachkar S, Redeker V, Sobel A. (2001). Stathmin family proteins display specific molecular and tubulin binding properties. *J Biol Chem*. 276, 16146-54

Chen GC, Turano B, Ruest PJ, Hagel M, Settleman J, Thomas SM. (2005). Regulation of Rho and Rac signaling to the actin cytoskeleton by paxillin during Drosophila development. *Mol Cell Biol* 25, 979-87.

Chen HW, Marinissen MJ, Oh SW, Chen X, Melnick M, Perrimon N, Gutkind JS, Hou SX. (2002). CKA, a novel multidomain protein, regulates the JUN N-terminal kinase signal transduction pathway in Drosophila. *Mol Cell Biol* 22, 1792-803.

Chen RH, Juo PC, Curran T, Blenis J. (1996). Phosphorylation of c-Fos at the C-terminus enhances its transforming activity. *Oncogene* 12, 1493-502.

Chilton JK. (2006). Molecular mechanisms of axon guidance. *Dev Biol* 292, 13-24. Review

Chipuk JE, Fisher JC, Dillon CP, Kriwacki RW, Kuwana T, Green DR. (2008). Mechanism of apoptosis induction by inhibition of the anti-apoptotic BCL-2 proteins. *Proc Natl Acad Sci U S A*. 105, 20327-32.

Ciani L, Salinas PC. (2007). c-Jun N-terminal kinase (JNK) cooperates with Gsk3beta to regulate Dishevelled-mediated microtubule stability. *BMC Cell Biol* 8, 27.

Ciapponi, L., Jackson, D. B., Mlodzik, M. and Bohmann, D. (2001). Drosophila Fos mediates ERK and JNK signals via distinct phosphorylation sites. *Genes Dev* 15, 1540-53.

Coffey ET, Hongisto V, Dickens M, Davis RJ, Courtney MJ. (2000). Dual roles for c-Jun N-terminal kinase in developmental and stress responses in cerebellar granule neurons. *J Neurosci* 20, 7602-13.

Coffey ET, Smiciene G, Hongisto V, Cao J, Brecht S, Herdegen T, Courtney MJ. c-Jun N-terminal protein kinase (JNK) 2/3 is specifically activated by stress, mediating c-Jun activation, in the presence of constitutive JNK1 activity in cerebellar neurons. *J Neurosci*. 22, 4335-45.

Colamarino SA, Tessier-Lavigne M. (1995). The axonal chemoattractant netrin-1 is also a chemorepellent for trochlear motor axons. *Cell* 81, 621-9.

Colangelo AM, Pani L, Mocchetti I. (1996). Correlation between increased AP-1NGF binding activity and induction of nerve growth factor transcription by multiple signal transduction pathways in C6-2B glioma cells. *Brain Res Mol Brain Res* 35, 1-10

Coleman M. (2005). Axon degeneration mechanisms: commonality amid diversity. *Nat Rev* 6, 889-98. Review

Coleman MP, Adalbert R, Beirowski B. (2005). Neuroprotective strategies in MS: lessons from C57BL/Wld(S) mice. *J Neurol Sc*i 233, 133-8. Review.

Collins, C. A., Wairkar, Y. P., Johnson, S. L. and DiAntonio, A. (2006). Highwire restrains synaptic growth by attenuating a MAP kinase signal. *Neuron* 51, 57-69.

Colussi PA, Quinn LM, Huang DC, Coombe M, Read SH, Richardson H, Kumar S. (2000). Debcl, a proapoptotic Bcl-2 homologue, is a component of the Drosophila melanogaster cell death machinery. *J Cell Biol* 148, 703-14.

Coso OA, Chiariello M, Yu JC, Teramoto H, Crespo P, Xu N, Miki T, Gutkind JS. (1995). The small GTP-binding proteins Rac1 and Cdc42 regulate the activity of the JNK/SAPK signaling pathway. *Cell* 81, 1137-46

Craig CR, Fink JL, Yagi Y, Ip YT, Cagan RL. (2004). A Drosophila p38 orthologue is required for environmental stress responses. *EMBO Rep* 5, 1058-63.

Crittenden JR, Skoulakis EM, Han KA, Kalderon D, Davis RL. (1998). Tripartite mushroom body architecture revealed by antigenic markers. *Learn Mem* 5, 38-51.

Davidson FF, Steller H. (1998). Blocking apoptosis prevents blindness in Drosophila retinal degeneration mutants. *Nature* 391, 587-91.

Davis MM, Primrose DA, Hodgetts RB. (2008). A member of the p38 mitogen-activated protein kinase family is responsible for transcriptional induction of Dopa decarboxylase in the epidermis of Drosophila melanogaster during the innate immune response. *Mol Cell Biol*. 28, 4883-95.

Davis, R. J. (1999) Signal transduction by the c-Jun N-terminal kinase. *Biochem Soc Symp,* 64**,** 1-12.

Davis RJ. (2000). Signal transduction by the JNK group of MAP kinases. *Cell* 103, 239-52

Delaney, J. R., Stoven, S., Uvell, H., Anderson, K. V., Engstrom, Y. and Mlodzik, M. (2006). Cooperative control of Drosophila immune responses by the JNK and NF-kappaB signaling pathways. *EMBO J* 25, 3068-77.

Dent EW, Gertler FB. (2003) Cytoskeletal dynamics and transport in growth cone motility and axon guidance. *Neuron* 40, 209-27.

Dent EW, Kalil K. (2001). Axon branching requires interactions between dynamic microtubules and actin filaments. *J Neurosci* 21, 9757-69.

Deveraux QL, Reed JC. (1999). IAP family proteins--suppressors of apoptosis. *Genes Dev*. 13, 239-52. Review.

Dickson BJ. (2001). Rho GTPases in growth cone guidance. *Curr Opin Neurobiol* 11, 103-10. Review.

Dietzl, G., Chen, D., Schnorrer, F., Su, K. C., Barinova, Y., Fellner, M., Gasser, B., Kinsey, K., Oppel, S., Scheiblauer, S. et al. (2007). A genome-wide transgenic RNAi library for conditional gene inactivation in Drosophila. *Nature* 448, 151-6.

Dingwell KS, Holt CE, Harris WA. (2000). The multiple decisions made by growth cones of RGCs as they navigate from the retina to the tectum in Xenopus embryos. *J Neurobiol* 44, 246-59. Review.

Dobens LL, Martín-Blanco E, Martínez-Arias A, Kafatos FC, Raftery LA. (2001). Drosophila puckered regulates Fos/Jun levels during follicle cell morphogenesis. *Development* 128, 1845-56.

Dotti CG, Sullivan CA, Banker GA. (1988). The establishment of polarity by hippocampal neurons in culture. *J Neurosci* 8, 1454-68.

Dragunow M, Xu R, Walton M, Woodgate A, Lawlor P, MacGibbon GA, Young D, Gibbons H, Lipski J, Muravlev A, Pearson A, During M. (2000). c-Jun promotes neurite outgrowth and survival in PC12 cells. *Mol Brain Res* 83, 20-33.

Du C, Fang M, Li Y, Li L, Wang X. (2000). Smac, a mitochondrial protein that promotes cytochrome c-dependent caspase activation by eliminating IAP inhibition. *Cell* 102, 33-42.

Eden S, Rohatgi R, Podtelejnikov AV, Mann M, Kirschner MW. (2002). Mechanism of regulation of WAVE1-induced actin nucleation by Rac1 and Nck. *Nature* 418, 790-3.

Eferl R, Wagner EF. (2003). AP-1: a double-edged sword in tumorigenesis. *Nat Rev Cancer* 3, 859-68. Review.

Eickholt BJ, Walsh FS, Doherty P. (2002). An inactive pool of GSK-3 at the leading edge of growth cones is implicated in Semaphorin 3A signaling. *J Cell Biol*. 157, 211-7.

Enslen H, Davis RJ. (2001). Regulation of MAP kinases by docking domains. *Biol Cell* 93, 5-14. Review.

Eresh, S., Riese, J., Jackson, D. B., Bohmann, D. and Bienz, M. (1997). A CREB-binding site as a target for decapentaplegic signalling during Drosophila endoderm induction. *EMBO J* 16, 2014-22.

Etienne-Manneville S, Hall A. (2002). Rho GTPases in cell biology. *Nature* 420, 629-35. Review.

Evangelista M, Blundell K, Longtine MS, Chow CJ, Adames N, Pringle JR, Peter M, Boone C. (1997). Bni1p, a yeast formin linking cdc42p and the actin cytoskeleton during polarized morphogenesis. *Science*. 276, 118-22.

Ferrell JE Jr. (2002). Self-perpetuating states in signal transduction: positive feedback, double-negative feedback and bistability. *Curr Opin Cell Biol* 14, 140-8. Review.

Forscher P, Smith SJ. (1988). Actions of cytochalasins on the organization of actin filaments and microtubules in a neuronal growth cone. *J Cell Biol* 107, 1505-16.

Franciscovich AL, Mortimer AD, Freeman AA, Gu J, Sanyal S. (2008). Overexpression screen in Drosophila identifies neuronal roles of GSK-3 beta/shaggy as a regulator of AP-1-dependent developmental plasticity. *Genetics* 180, 2057-71.

Galko, M. J. and Krasnow, M. A. (2004). Cellular and genetic analysis of wound healing in Drosophila larvae. *PLoS Biol* 2, E239.

Gallo G. (2004). Myosin II activity is required for severing-induced axon retraction in vitro. *Exp Neurol* 189, 112-21.

Gallo G. (2006). RhoA-kinase coordinates F-actin organization and myosin II activity during semaphorin-3A-induced axon retraction. *J Cell Sci* 119, 3413-23.

Gallo G, Letourneau PC. (1998). Axon guidance: GTPases help axons reach their targets. *Curr Biol* 8, 80-2.

Gallo KA, Johnson GL. (2002). Mixed-lineage kinase control of JNK and p38 MAPK pathways. *Nat Rev Mol Cell Biol* 3, 663-72. Review.

Garel S, Rubenstein JL. (2004). Intermediate targets in formation of topographic projections: inputs from the thalamocortical system. *Trends Neurosci* 27, 533-9. Review

Gdalyahu A, Ghosh I, Levy T, Sapir T, Sapoznik S, Fishler Y, Azoulai D, Reiner O. (2004). DCX, a new mediator of the JNK pathway. *EMBO J* 23, 823-32.

Geuking P, Narasimamurthy R, Lemaitre B, Basler K, Leulier F (2009). A non-redundant role for Drosophila Mkk4 and hemipterous/Mkk7 in TAK1-mediated activation of JNK. *PLoS One* 4(11):e7709

Ghosh A, Antonini A, McConnell SK, Shatz CJ. (1990). Requirement for subplate neurons in the formation of thalamocortical connections. *Nature* 347, 179-81.

Giesen, K., Lammel, U., Langehans, D., Krukkert, K., Bunse, I. and Klambt, C. (2003). Regulation of glial cell number and differentiation by ecdysone and Fos signaling. *Mech Dev* 120, 401-13.

Gitai Z, Yu TW, Lundquist EA, Tessier-Lavigne M, Bargmann CI. (2003). The netrin receptor UNC-40/DCC stimulates axon attraction and outgrowth through enabled and, in parallel, Rac and UNC-115/AbLIM. *Neuron* 37, 53-65.

Glise, B., Bourbon, H. and Noselli, S. (1995). hemipterous encodes a novel Drosophila MAP kinase kinase, required for epithelial cell sheet movement. *Cell* 83, 451-61.

Goedert M, Hasegawa M, Jakes R, Lawler S, Cuenda A, Cohen P. (1997). Phosphorylation of microtubule-associated protein tau by stress-activated protein kinases. *FEBS Lett*. 409, 57-62.

Goldberg DJ, Burmeister DW. (1986). Stages in axon formation: observations of growth of Aplysia axons in culture using video-enhanced contrast-differential interference contrast microscopy. *J Cell Biol* 103, 1921-31.

Gomez TM, Zheng JQ. (2006). The molecular basis for calcium-dependent axon pathfinding. *Nat Rev Neurosci* 7, 115-25. Review.

Gong Q, Shipley MT. (1995). Evidence that pioneer olfactory axons regulate telencephalon cell cycle kinetics to induce the formation of the olfactory bulb. *Neuron* 14, 91-101.

Gordon-Weeks PR. (2004). Microtubules and growth cone function. *J Neurobiol* 58, 70-83. Review.

Govek EE, Newey SE, Van Aelst L. (2005). The role of the Rho GTPases in neuronal development. *Genes Dev* 19, 1-49. Review.

Griswold AJ, Chang KT, Runko AP, Knight MA, Min KT. (2008). Sir2 mediates apoptosis through JNK-dependent pathways in Drosophila. *Proc Natl Acad Sci U S A*. 105, 8673-8.

Guirland C, Buck KB, Gibney JA, DiCicco-Bloom E, Zheng JQ. (2003). Direct cAMP signaling through G-protein-coupled receptors mediates growth cone attraction induced by pituitary adenylate cyclase-activating polypeptide. *J Neurosci* 23, 2274-83.

Gundersen GG, Gomes ER, Wen Y. (2004). Cortical control of microtubule stability and polarization. *Curr Opin Cell Biol* 16, 106-12. Review.

Gupta, S., Barrett, T., Whitmarsh, A. J., Cavanagh, J., Sluss, H. K., Derijard, B. & Davis, R. J. (1996) Selective interaction of JNK protein kinase isoforms with transcription factors. *EMBO J,* 15**,** 2760-70.

Gupta S, Campbell D, Dérijard B, Davis RJ. (1995). Transcription factor ATF2 regulation by the JNK signal transduction pathway. *Science* 267, 389-93.

Hai T, Wolfgang CD, Marsee DK, Allen AE, Sivaprasad U. (1999). ATF3 and stress responses. *Gene Expr* 7, 321-35. Review.

Hakeda-Suzuki S, Ng J, Tzu J, Dietzl G, Sun Y, Harms M, Nardine T, Luo L, Dickson BJ. (2002). Rac function and regulation during Drosophila development. *Nature* 416, 438-42.

Hall A. (1998). Rho GTPases and the actin cytoskeleton. *Science* 279, 509-14. Review.

Hall AC, Lucas FR, Salinas PC. (2000). Axonal remodeling and synaptic differentiation in the cerebellum is regulated by WNT-7a signaling. *Cell* 100, 525-35.

Hanks SK, Quinn AM, Hunter T. (1988). The protein kinase family: conserved features and deduced phylogeny of the catalytic domains. *Science* 241, 42-52. Review.

Han, Z. S., Enslen, H., Hu, X., Meng, X., Wu, I. H., Barrett, T., Davis, R. J. and Ip, Y. T. (1998). A conserved p38 mitogen-activated protein kinase pathway regulates Drosophila immunity gene expression. *Mol Cell Biol* 18, 3527-39.

Harris CA, Johnson EM Jr. (2001). BH3-only Bcl-2 family members are coordinately regulated by the JNK pathway and require Bax to induce apoptosis in neurons. *J Biol Chem* 276, 37754-60.

Hartwig CL, Worrell J, Levine RB, Ramaswami M, Sanyal S. (2008). Normal dendrite growth in Drosophila motor neurons requires the AP-1 transcription factor. Dev Neurobiol. 68, 1225-42

Hay BA. (2000). Understanding IAP function and regulation: a view from Drosophila. *Cell Death Differ* 7, 1045-56. Review.

Hay BA, Wolff T, Rubin GM. (1994). Expression of baculovirus P35 prevents cell death in Drosophila. *Development* 120, 2121-9.

He JC, Neves SR, Jordan JD, Iyengar R. (2006). Role of the Go/i signaling network in the regulation of neurite outgrowth. *Can J Physiol Pharmacol* 84, 687-94. Review.

Henley JR, Huang KH, Wang D, Poo MM. (2004). Calcium mediates bidirectional growth cone turning induced by myelin-associated glycoprotein. *Neuron* 44, 909-16.

Hennigan RF, Hawker KL, Ozanne BW. (1994). Fos-transformation activates genes associated with invasion. *Oncogene* 9, 3591-600.

Herdegen, T., Claret, F. X., Kallunki, T., Martin-Villalba, A., Winter, C., Hunter, T. and Karin, M. (1998). Lasting N-terminal phosphorylation of c-Jun and activation of c-Jun N-terminal kinases after neuronal injury. *J Neurosci* 18, 5124-35.

Herdegen T, Leah JD. (1998). Inducible and constitutive transcription factors in the mammalian nervous system: control of gene expression by Jun, Fos and Krox, and CREB/ATF proteins. *Brain Res Rev* 28, 370-490. Review.

Herdegen T, Skene P, Bähr M. (1997). The c-Jun transcription factor--bipotential mediator of neuronal death, survival and regeneration. *Trends Neurosci* 20, 227-31. Review

Hirokawa N, Takemura R. (2004). Kinesin superfamily proteins and their various functions and dynamics. *Exp Cell Res* 301, 50-9. Review.

Ho DT, Bardwell AJ, Grewal S, Iverson C, Bardwell L. (2006). Interacting JNK-docking sites in MKK7 promote binding and activation of JNK mitogen-activated protein kinases. *J Biol Chem* 281, 13169-79.

Hobson SA, Holmes FE, Kerr NC, Pope RJ, Wynick D. (2006). Mice deficient for galanin receptor 2 have decreased neurite outgrowth from adult sensory neurons and impaired pain-like behaviour. *J Neurochem* 99, 1000-10.

Homsy JG, Jasper H, Peralta XG, Wu H, Kiehart DP, Bohmann D. (2006). JNK signaling coordinates integrin and actin functions during Drosophila embryogenesis. *Dev Dyn*. 235, 427-34.

Hong K, Nishiyama M, Henley J, Tessier-Lavigne M, Poo M. (2000). Calcium signalling in the guidance of nerve growth by netrin-1. *Nature* 403, 93-8.

Hong YK, Lee NG, Lee MJ, Park MS, Choi G, Suh YS, Han SY, Hwang S, Jeong G, Cho KS. (2009). dXNP/DATRX increases apoptosis via the JNK and dFOXO pathway in Drosophila neurons. *Biochem Biophys Res Commun* 384, 160-6.

Hoopfer ED, McLaughlin T, Watts RJ, Schuldiner O, O'Leary DD, Luo L. (2006). Wlds protection distinguishes axon degeneration following injury from naturally occurring developmental pruning. *Neuron 50, 883-95.*

Horiuchi D, Barkus RV, Pilling AD, Gassman A, Saxton WM. (2005). APLIP1, a kinesin binding JIP-1/JNK scaffold protein, influences the axonal transport of both vesicles and mitochondria in Drosophila. *Curr Biol* 15, 2137-41.

Horiuchi D, Collins CA, Bhat P, Barkus RV, Diantonio A, Saxton WM. (2007). Control of a kinesin-cargo linkage mechanism by JNK pathway kinases. *Curr Biol* 17, 1313-7.

Horwitz SB, Shen HJ, He L, Dittmar P, Neef R, Chen J, Schubart UK. (1997). The microtubule-destabilizing activity of metablastin (p19) is controlled by phosphorylation. *J Biol Chem* 272, 8129-32.

Hou XS, Goldstein ES, Perrimon N. (1997). Drosophila Jun relays the Jun amino-terminal kinase signal transduction pathway to the Decapentaplegic signal transduction pathway in regulating epithelial cell sheet movement. *Genes Dev* 11, 1728-37.

Howard J, Hyman AA. (2003). Dynamics and mechanics of the microtubule plus end. *Nature* 422, 753-8. Review.

Huang C, Rajfur Z, Borchers C, Schaller MD, Jacobson K. (2003). JNK phosphorylates paxillin and regulates cell migration. *Nature* 424, 219-23.

Huber AB, Kolodkin AL, Ginty DD, Cloutier JF. (2003). Signaling at the growth cone: ligand-receptor complexes and the control of axon growth and guidance. *Annu Rev Neurosci*. 26, 509-63.

Hyun, J., Becam, I., Yanicostas, C. and Bohmann, D. (2006). Control of G2/M transition by Drosophila Fos. *Mol Cell Biol* 26, 8293-302.

Igaki T, Kanuka H, Inohara N, Sawamoto K, Núñez G, Okano H, Miura M. (2000). Drob-1, a Drosophila member of the Bcl-2/CED-9 family that promotes cell death. *Proc Natl Acad Sci U S A* 97, 662-7.

Ispanovic E, Haas TL. (2006). JNK and PI3K differentially regulate MMP-2 and MT1-MMP mRNA and protein in response to actin cytoskeleton reorganization in endothelial cells. *Am J Physiol Cell Physiol*, 291, 579-88.

Ito K, Hotta Y (1992) Proliferation pattern of postembryonic neuroblasts in the brain of Drosophila melanogaster. *Dev Biol*. 149(1):134-48.

Ito, K., Awano, W., Suzuki, K., Hiromi, Y. and Yamamoto, D. (1997). The Drosophila mushroom body is a quadruple structure of clonal units each of which contains a virtually identical set of neurones and glial cells. *Development* 124, 761-71.

Ito M, Yoshioka K, Akechi M, Yamashita S, Takamatsu N, Sugiyama K, Hibi M, Nakabeppu Y, Shiba T, Yamamoto KI. (1999). JSAP1, a novel jun N-terminal protein kinase (JNK)-binding protein that functions as a Scaffold factor in the JNK signaling pathway. *Mol Cell Biol* 19, 7539-48.

Jareb M, Banker G. (1997). Inhibition of axonal growth by brefeldin A in hippocampal neurons in culture. *J Neurosci* 17, 8955-63.

Jasper H, Benes V, Schwager C, Sauer S, Clauder-Münster S, Ansorge W, Bohmann D. (2001). The genomic response of the Drosophila embryo to JNK signaling. *Dev Cell*. 1, 579-86.

Jooss KU, Müller R. (1995). Deregulation of genes encoding microfilament-associated proteins during Fos-induced morphological transformation. *Oncogene* 10, 603-8

Jurney WM, Gallo G, Letourneau PC, McLoon SC. (2002). Rac1-mediated endocytosis during ephrin-A2- and semaphorin 3A-induced growth cone collapse. *J Neurosci* 22, 6019-28.

Kalil K, Dent EW. (2005) Touch and go: guidance cues signal to the growth cone cytoskeleton. *Curr Opin Neurobio*l 15 521-6. Review.

Kallunki, T., Deng, T., Hibi, M. & Karin, M. (1996) c-Jun can recruit JNK to phosphorylate dimerization partners via specific docking interactions. *Cell,* 87**,** 929-39.

Katoh H, Aoki J, Ichikawa A, Negishi M. (1998). p160 RhoA-binding kinase ROKalpha induces neurite retraction. *J Biol Chem* 273, 2489-92.

Keino-Masu K, Masu M, Hinck L, Leonardo ED, Chan SS, Culotti JG, Tessier-Lavigne M. (1996). Deleted in Colorectal Cancer (DCC) encodes a netrin receptor. *Cell*. 87, 175-85.

Kelkar N, Gupta S, Dickens M, Davis RJ. (2000). Interaction of a mitogen-activated protein kinase signaling module with the neuronal protein JIP3. *Mol Cell Biol*. 20, 1030-43.

Kenney AM, Kocsis JD. (1998). Peripheral axotomy induces long-term c-Jun amino-terminal kinase-1 activation and activator protein-1 binding activity by c-Jun and junD in adult rat dorsal root ganglia in vivo. *J Neurosci* 18, 1318-28.

Kholodenko, B. N. (2006). Cell-signalling dynamics in time and space. *Nat Rev Mol Cell Biol* 7, 165-76.

Kita Y, Kimura KD, Kobayashi M, Ihara S, Kaibuchi K, Kuroda S, Ui M, Iba H, Konishi H, Kikkawa U, Nagata S, Fukui Y. (1998). Microinjection of activated phosphatidylinositol-3 kinase induces process outgrowth in rat PC12 cells through the Rac-JNK signal transduction pathway. *J Cell Sci*. 111, 907-15.

Klose M, Bentley D. (1989). Transient pioneer neurons are essential for formation of an embryonic peripheral nerve. *Science* 245, 982-4

Klueg, K. M., Alvarado, D., Muskavitch, M. A. and Duffy, J. B. (2002). Creation of a GAL4/UAS-coupled inducible gene expression system for use in Drosophila cultured cell lines. *Genesis* 34, 119-22.

Kockel, L., Zeitlinger, J., Staszewski, L. M., Mlodzik, M. and Bohmann, D. (1997). Jun in Drosophila development: redundant and nonredundant functions and regulation by two MAPK signal transduction pathways. *Genes Dev* 11, 1748-58.

Kockel L, Homsy JG, Bohmann D. (2001). Drosophila AP-1: lessons from an invertebrate. *Oncogene* 20, 2347-64. Review.

Kolodziej PA, Timpe LC, Mitchell KJ, Fried SR, Goodman CS, Jan LY, Jan YN. (1996). frazzled encodes a Drosophila member of the DCC immunoglobulin subfamily and is required for CNS and motor axon guidance. *Cell* 87,197-204.

Koushika SP. (2008). "JIP"ing along the axon: the complex roles of JIPs in axonal transport. *Bioessays* 30, 10-4. Review.

Kreutz MR, Bien A, Vorwerk CK, Böckers TM, Seidenbecher CI, Tischmeyer W, Sabel BA. (1999). Co-expression of c-Jun and ATF-2 characterizes the surviving retinal ganglion cells which maintain axonal connections after partial optic nerve injury. *Brain Res Mol Brain Res* 69, 232-41.

Krylova O, Messenger MJ, Salinas PC. (2000). Dishevelled-1 regulates microtubule stability: a new function mediated by glycogen synthase kinase-3beta. *J Cell Biol* 151, 83-94.

Kuan CY, Yang DD, Samanta Roy DR, Davis RJ, Rakic P, Flavell RA. (1999). The Jnk1 and Jnk2 protein kinases are required for regional specific apoptosis during early brain development. *Neuron* 22, 667-76.

Kuhn TB, Brown MD, Bamburg JR (1998). Rac1-dependent actin filament organization in growth cones is necessary for beta1-integrin-mediated advance but not for growth on poly-D-lysine. *J Neurobiol* 37, 524-40

Kuhn TB, Meberg PJ, Brown MD, Bernstein BW, Minamide LS, Jensen JR, Okada K, Soda EA, Bamburg JR. (2000). Regulating actin dynamics in neuronal growth cones by ADF/cofilin and rho family GTPases. *J Neurobiol* 44, 126-44. Review.

Kurusu, M., Awasaki, T., Masuda-Nakagawa, L. M., Kawauchi, H., Ito, K. and Furukubo-Tokunaga, K. (2002). Embryonic and larval development of the Drosophila mushroom bodies: concentric layer subdivisions and the role of fasciclin II. *Development* 129, 409-19.

Lagalwar S, Guillozet-Bongaarts AL, Berry RW, Binder LI. (2006). Formation of phospho-SAPK/JNK granules in the hippocampus is an early event in Alzheimer disease *Acta Neuropath* 113(1):63-73

Lamb RF, Ozanne BW, Roy C, McGarry L, Stipp C, Mangeat P, Jay DG. (1997). Essential functions of ezrin in maintenance of cell shape and lamellipodial extension in normal and transformed fibroblasts. *Curr Biol* 7, 682-8.

Lawler S, Fleming Y, Goedert M, Cohen P. (1998). Synergistic activation of SAPK1/JNK1 by two MAP kinase kinases in vitro. *Curr Biol*, 8, 1387-90.

Lebrand C, Dent EW, Strasser GA, Lanier LM, Krause M, Svitkina TM, Borisy GG, Gertler FB. (2004). Critical role of Ena/VASP proteins for filopodia formation in neurons and in function downstream of netrin-1. *Neuron* 42, 37-49.

Lee H, Engel U, Rusch J, Scherrer S, Sheard K, Van Vactor D. (2004). The microtubule plus end tracking protein Orbit/MAST/CLASP acts downstream of the tyrosine kinase Abl in mediating axon guidance. *Neuron* 42, 913-26.

Lee, T., Lee, A. and Luo, L. (1999). Development of the Drosophila mushroom bodies: sequential generation of three distinct types of neurons from a neuroblast. *Development* 126, 4065-76.

Lee, T. and Luo, L. (1999). Mosaic analysis with a repressible cell marker for studies of gene function in neuronal morphogenesis. *Neuron* 22, 451-61.

Lee TH, Klampfer L, Shows TB, Vilcek J. (1993). Transcriptional regulation of TSG6, a tumor necrosis factor- and interleukin-1-inducible primary response gene coding for a secreted hyaluronan-binding protein. *J. Biol. Chem* 268 6154–6160.

Letourneau PC. (1996). The cytoskeleton in nerve growth cone motility and axonal pathfinding. *Perspect Dev Neurobiol* 4, 111-23. Review.

Letourneau PC, Shattuck TA, Ressler AH. (1987). "Pull" and "push" in neurite elongation: observations on the effects of different concentrations of cytochalasin B and taxol. *Cell Motil Cytoskeleton* 8, 193-209.

Li X, Saint-Cyr-Proulx E, Aktories K, Lamarche-Vane N. (2002). Rac1 and Cdc42 but not RhoA or Rho kinase activities are required for neurite outgrowth induced by the Netrin-1 receptor DCC (deleted in colorectal cancer) in N1E-115 neuroblastoma cells. *J Biol Chem* 277, 15207-14.

Liberski PP, Budka H. (1999). Neuroaxonal pathology in Creutzfeldt-Jakob disease. *Acta Neuropathol* 97, 329-34.

Lin CH, Forscher P. (1995). Growth cone advance is inversely proportional to retrograde F-actin flow. *Neuron* 14, 763-71.

Lindwall C, Kanje M. (2005). Retrograde axonal transport of JNK signaling molecules influence injury induced nuclear changes in p-c-Jun and ATF3 in adult rat sensory neurons. *Mol Cell Neurosci* 29, 269-82

Liu X, Rubin JS, Kimmel AR. (2005). Rapid, Wnt-induced changes in GSK3beta associations that regulate beta-catenin stabilization are mediated by Galpha proteins. *Curr Biol* 15, 1989-97.

Llense F, Martín-Blanco E (2008). JNK signaling controls border cell cluster integrity and collective cell migration. *Curr Biol* 18, 538-44.

Lucas FR, Goold RG, Gordon-Weeks PR, Salinas PC. (1998). Inhibition of GSK-3beta leading to the loss of phosphorylated MAP-1B is an early event in axonal remodelling induced by WNT-7a or lithium. *J Cell Sci* 111, 1351-61.

Lundquist EA, Reddien PW, Hartwieg E, Horvitz HR, Bargmann CI. (2001). Three C. elegans Rac proteins and several alternative Rac regulators control axon guidance, cell migration and apoptotic cell phagocytosis. *Development* 128, 4475-88.

Luo L. (2000). Rho GTPases in neuronal morphogenesis. *Nat Rev Neurosci.* 1, 173-80. Review.

Luo L, Liao YJ, Jan LY, Jan YN. (1994). Distinct morphogenetic functions of similar small GTPases: Drosophila Drac1 is involved in axonal outgrowth and myoblast fusion. *Genes Dev* 8, 1787-802.

Luo L, O'Leary DD. (2005). Axon retraction and degeneration in development and disease. *Annu Rev Neurosci* 28, 127-56. Review.

Luo X, Puig O, Hyun J, Bohmann D, Jasper H. (2007). Foxo and Fos regulate the decision between cell death and survival in response to UV irradiation. *EMBO J.* 26, 380-90.

Lyuksyutova AI, Lu CC, Milanesio N, King LA, Guo N, Wang Y, Nathans J, Tessier-Lavigne M, Zou Y. (2003). Anterior-posterior guidance of commissural axons by Wnt-frizzled signaling. *Science* 302, 1984-8.

MacDonald JM, Beach MG, Porpiglia E, Sheehan AE, Watts RJ, Freeman MR. (2006). The Drosophila cell corpse engulfment receptor Draper mediates glial clearance of severed axons. *Neuron 50, 869-81.*

Mack TG, Reiner M, Beirowski B, Mi W, Emanuelli M, Wagner D, Thomson D, Gillingwater T, Court F, Conforti L, Fernando FS, Tarlton A, Andressen C, Addicks K, Magni G, Ribchester RR, Perry VH, Coleman MP. (2001). Wallerian degeneration of injured axons and synapses is delayed by a Ube4b/Nmnat chimeric gene. *Nat Neurosci. 4, 1199-206.*

Maekawa M, Ishizaki T, Boku S, Watanabe N, Fujita A, Iwamatsu A, Obinata T, Ohashi K, Mizuno K, Narumiya S. (1999). Signaling from Rho to the actin cytoskeleton through protein kinases ROCK and LIM-kinase. *Science* 285, 895-8.

Mahoney SA, Hosking R, Farrant S, Holmes FE, Jacoby AS, Shine J, Iismaa TP, Scott MK, Schmidt R, Wynick D. (2003). The second galanin receptor GalR2 plays a key role in neurite outgrowth from adult sensory neurons. *J Neurosci* 23, 416-21.

Malliri A, Symons M, Hennigan RF, Hurlstone AF, Lamb RF, Wheeler T, Ozanne BW. (1998). The transcription factor AP-1 is required for EGF-induced activation of rho-like GTPases, cytoskeletal rearrangements, motility, and in vitro invasion of A431 cells. *J Cell Biol* 143, 1087-99.

Marinissen MJ, Gutkind JS. (2005). Scaffold proteins dictate Rho GTPase-signaling specificity. *Trends Biochem Sci* 30, 423-6.

Markus A, Patel TD, Snider WD. (2002). Neurotrophic factors and axonal growth. *Curr Opin Neurobiol* 12, 523-31. Review.

Marsh L, Letourneau PC. (1984). Growth of neurites without filopodial or lamellipodial activity in the presence of cytochalasin. *B. J Cell Biol* 99, 2041-7.

Marshall, C. J. (1995). Specificity of receptor tyrosine kinase signaling: transient versus sustained extracellular signal-regulated kinase activation. *Cell* 80, 179-85.

Marshall CJ. (1998). Signal transduction. Taking the Rap. *Nature* 392, 553-4.

Martin JH, Mohit AA, Miller CA. (1996). Developmental expression in the mouse nervous system of the p493F12 SAP kinase. *Brain Res Mol Brain Res*. 35, 47-57.

Martín-Blanco E. (1998) Regulatory control of signal transduction during morphogenesis in Drosophila. *Int J Dev Biol* 42, 363-8

Matsuda S, Yasukawa T, Homma Y, Ito Y, Niikura T, Hiraki T, Hirai S, Ohno S, Kita Y, Kawasumi M, Kouyama K, Yamamoto T, Kyriakis JM, Nishimoto I. (2001). c-Jun N-terminal kinase (JNK)-interacting protein-1b/islet-brain-1 scaffolds Alzheimer's amyloid precursor protein with JNK. *J Neurosci* 21, 6597-607.

Matsuura R, Tanaka H, Go MJ. (2004). Distinct functions of Rac1 and Cdc42 during axon guidance and growth cone morphogenesis in Drosophila. *Eur J Neurosci* 19, 21-31.

Mattila, J., Omelyanchuk, L., Kyttala, S., Turunen, H. and Nokkala, S. (2005). Role of Jun N-terminal Kinase (JNK) signaling in the wound healing and regeneration of a Drosophila melanogaster wing imaginal disc. *Int J Dev Biol* 49, 391-9.

Maynard CJ, Böttcher C, Ortega Z, Smith R, Florea BI, Díaz-Hernández M, Brundin P, Overkleeft HS, Li JY, Lucas JJ, Dantuma NP. (2009). Accumulation of ubiquitin conjugates in a polyglutamine disease model occurs without global ubiquitin/proteasome system impairment. *Proc Natl Acad Sci U S A*. 106, 13986-91

McCall K, Steller H. (1997). Facing death in the fly: genetic analysis of apoptosis in Drosophila. *Trends Genet* 13, 222-6. Review.

McEwen DG, Peifer M. (2005). Puckered, a Drosophila MAPK phosphatase, ensures cell viability by antagonizing JNK-induced apoptosis. *Development* 132, 3935-46.

McGuire, S. E., Le, P. T., Osborn, A. J., Matsumoto, K. and Davis, R. L. (2003). Spatiotemporal rescue of memory dysfunction in Drosophila. *Science* 302, 1765-8.

Mercado ML, Nur-e-Kamal A, Liu HY, Gross SR, Movahed R, Meiners S. (2004). Neurite outgrowth by the alternatively spliced region of human tenascin-C is mediated by neuronal alpha7beta1 integrin. *J Neurosci* 24, 238-47.

Meyer D, Liu A, Margolis B. (1999). Interaction of c-Jun amino-terminal kinase interacting protein-1 with p190 rhoGEF and its localization in differentiated neurons. *J Biol Chem*. 274, 35113-8.

Mi W, Beirowski B, Gillingwater TH, Adalbert R, Wagner D, Grumme D, Osaka H, Conforti L, Arnhold S, Addicks K, Wada K, Ribchester RR, Coleman MP. (2005). The slow Wallerian degeneration gene, WldS, inhibits axonal spheroid pathology in gracile axonal dystrophy mice. *Brain* 128, 405-16.

Miao GG, Curran T. (1994). Cell transformation by c-fos requires an extended period of expression and is independent of the cell cycle. *Mol Cell Biol* 14, 4295-310.

Miller, B. R., Press, C., Daniels, R. W., Sasaki, Y., Milbrandt, J. and DiAntonio, A. (2009). A dual leucine kinase-dependent axon self-destruction program promotes Wallerian degeneration. *Nat Neurosci* 12, 387-9.

Minden A, Lin A, Claret FX, Abo A, Karin M. (1995). Selective activation of the JNK signaling cascade and c-Jun transcriptional activity by the small GTPases Rac and Cdc42Hs. *Cell* 81, 1147-57.

Miotto B, Sagnier T, Berenger H, Bohmann D, Pradel J, Graba Y. (2006). Chameau HAT and DRpd3 HDAC function as antagonistic cofactors of JNK/AP-1-dependent transcription during Drosophila metamorphosis. *Genes Dev* 20, 101-12.

Mohit AA, Martin JH, Miller CA. (1995). p493F12 kinase: a novel MAP kinase expressed in a subset of neurons in the human nervous system. *Neuron* 14, 67-78

Mooney LM, Whitmarsh AJ. (2004). Docking interactions in the c-Jun N-terminal kinase pathway. *J Biol Chem* 279, 11843-52.

Moreno E, Yan M, Basler K (2002). Evolution of TNF signaling mechanisms: JNK-dependent apoptosis triggered by Eiger, the Drosophila homolog of the TNF superfamily. *Curr Biol*. 12, 1263-8.

Morfini, G., Pigino, G., Szebenyi, G., You, Y., Pollema, S. and Brady, S. T. (2006). JNK mediates pathogenic effects of polyglutamine-expanded androgen receptor on fast axonal transport. *Nat Neurosci* 9, 907-16.

Morrison DK, Davis RJ. (2003). Regulation of MAP kinase signaling modules by scaffold proteins in mammals. *Annu Rev Cell Dev Biol* 19, 91-118. Review.

Murphy, L. O. and Blenis, J. (2006). MAPK signal specificity: the right place at the right time. *Trends Biochem Sci* 31, 268-75.

Murphy LO, Smith S, Chen RH, Fingar DC, Blenis J. (2002). Molecular interpretation of ERK signal duration by immediate early gene products. *Nat Cell Biol*. 2002 4(8):556-64.

Ng, J. (2008). TGF-beta signals regulate axonal development through distinct Smad-independent mechanisms. *Development* 135, 4025-35.

Ng J, Luo L. (2004). Rho GTPases regulate axon growth through convergent and divergent signaling pathways. *Neuron* 44, 779-93.

Ng J, Nardine T, Harms M, Tzu J, Goldstein A, Sun Y, Dietzl G, Dickson BJ, Luo L. (2002). Rac GTPases control axon growth, guidance and branching. *Nature* 2002 416, 442-7.

Nihalani D, Meyer D, Pajni S, Holzman LB. (2001). Mixed lineage kinase-dependent JNK activation is governed by interactions of scaffold protein JIP with MAPK module components. *EMBO J* 20, 3447-58.

Nishiyama M, Hoshino A, Tsai L, Henley JR, Goshima Y, Tessier-Lavigne M, Poo MM, Hong K. Cyclic AMP/GMP-dependent modulation of Ca2+ channels sets the polarity of nerve growth-cone turning. *Nature* 423, 990-5.

Niwa R, Nagata-Ohashi K, Takeichi M, Mizuno K, Uemura T (2002). Control of actin reorganization by Slingshot, a family of phosphatases that dephosphorylate ADF/cofilin. *Cell* 108, 233-46.

Noselli, S. (1998). JNK signaling and morphogenesis in Drosophila. *Trends Genet* 14, 33-8.

Noselli S, Agnès F. (1999). Roles of the JNK signaling pathway in Drosophila morphogenesis. *Curr Opin Genet Dev* 9, 466-72. Review.

Oliva, A. A., Jr., Atkins, C. M., Copenagle, L. and Banker, G. A. (2006). Activated c-Jun N-terminal kinase is required for axon formation. *J Neurosci* 26, 9462-70.

Okazaki K, Sagata N. (1995). The Mos/MAP kinase pathway stabilizes c-Fos by phosphorylation and augments its transforming activity in NIH 3T3 cells. *EMBO J* 14, 5048-59.

Okazawa H, Estus S. (2002) The JNK/c-Jun cascade and Alzheimer's disease. *Am J Alzheimers Dis Other Demen* 17(2):79-88

Ozon S, Guichet A, Gavet O, Roth S, Sobel A. (2002). Drosophila stathmin: a microtubule-destabilizing factor involved in nervous system formation. *Mol Biol Cell* 13, 698-710.

Palazzo AF, Cook TA, Alberts AS, Gundersen GG. (2001). mDia mediates Rho-regulated formation and orientation of stable microtubules. *Nat Cell Biol* 3, 723-9.

Pan L, Broadie KS. (2007). Drosophila fragile X mental retardation protein and metabotropic glutamate receptor A convergently regulate the synaptic ratio of ionotropic glutamate receptor subclasses. *J Neurosci* 27, 12378-89.

Pastor-Pareja, J. C., Grawe, F., Martin-Blanco, E. and Garcia-Bellido, A. (2004). Invasive cell behavior during Drosophila imaginal disc eversion is mediated by the JNK signaling cascade. *Dev Cell* 7, 387-99.

Pearson AG, Gray CW, Pearson JF, Greenwood JM, During MJ, Dragunow M. ATF3 enhances c-Jun-mediated neurite sprouting. (2003). *Mol Brain Res* 120, 38-45.

Pearson, J. C., Juarez, M. T., Kim, M. and McGinnis, W. (2009). Multiple transcription factor codes activate epidermal wound-response genes in Drosophila. *Proc Natl Acad Sci U S A* 106, 2224-9.

Peng J, Andersen JK. (2003). The role of c-Jun N-terminal kinase (JNK) in Parkinson's disease. *IUBMB Life*. 55(4-5):267-71

Perkins, K. K., Admon, A., Patel, N. and Tjian, R. (1990). The Drosophila Fos-related AP-1 protein is a developmentally regulated transcription factor. *Genes Dev* 4, 822-34.

Perrin V, Dufour N, Raoul C, Hassig R, Brouillet E, Aebischer P, Luthi-Carter R, Déglon N. Perrin V, Dufour N, Raoul C, Hassig R, Brouillet E, Aebischer P, Luthi-Carter R, Déglon N. (2009) Implication of the JNK pathway in a rat model of Huntington's disease. *Exp Neurol*. 215(1):191-200

Pollard TD, Blanchoin L, Mullins RD. (2000). Molecular mechanisms controlling actin filament dynamics in nonmuscle cells. *Annu Rev Biophys Biomol Struct* 29, 545-76. Review

Putcha GV, Le S, Frank S, Besirli CG, Clark K, Chu B, Alix S, Youle RJ, LaMarche A, Maroney AC, Johnson EM Jr. (2003). JNK-mediated BIM phosphorylation potentiates BAX-dependent apoptosis. *Neuron* 38, 899-914.

Putcha GV, Moulder KL, Golden JP, Bouillet P, Adams JA, Strasser A, Johnson EM. (2001). Induction of BIM, a proapoptotic BH3-only BCL-2 family member, is critical for neuronal apoptosis. *Neuron* 29, 615-28.

Qui MS, Green SH. (1992). PC12 cell neuronal differentiation is associated with prolonged p21ras activity and consequent prolonged ERK activity. *Neuron* 9, 705-17.

Quinn L, Coombe M, Mills K, Daish T, Colussi P, Kumar S, Richardson H. (2003). Buffy, a Drosophila Bcl-2 protein, has anti-apoptotic and cell cycle inhibitory functions. *EMBO J* 22, 3568-79.

Raff MC, Whitmore AV, Finn JT (2002). Axonal self-destruction and neurodegeneration. *Science* 296, 868-71. Review.

Raivich G, Behrens A. (2006). Role of the AP-1 transcription factor c-Jun in developing, adult and injured brain. *Prog Neurobiol* 78, 347-63. Review.

Raivich, G., Bohatschek, M., Da Costa, C., Iwata, O., Galiano, M., Hristova, M., Nateri, A. S., Makwana, M., Riera-Sans, L., Wolfer, D. P. et al. (2004). The AP-1 transcription factor c-Jun is required for efficient axonal regeneration. *Neuron* 43, 57-67.

Ramet, M., Lanot, R., Zachary, D. and Manfruelli, P. (2002). JNK signaling pathway is required for efficient wound healing in Drosophila. *Dev Biol* 241, 145-56.

Ravelli RB, Gigant B, Curmi PA, Jourdain I, Lachkar S, Sobel A, Knossow M. (2004). Insight into tubulin regulation from a complex with colchicine and a stathmin-like domain. *Nature* 428, 198-202.

Reiner O, Gdalyahu A, Ghosh I, Levy T, Sapoznik S, Nir R, Sapir T. (2004). DCX's phosphorylation by not just another kinase (JNK). *Cell Cycle* 3, 747-51. Review

Reynolds AJ, Bartlett SE, Hendry IA. (2000). Molecular mechanisms regulating the retrograde axonal transport of neurotrophins. *Brain Res Rev* 33, 169-78. Review

Reynolds CH, Utton MA, Gibb GM, Yates A, Anderton BH. (1997). Stress-activated protein kinase/c-jun N-terminal kinase phosphorylates tau protein. *J Neurochem*. 68, 1736-44.

Richardson H, Kumar S. (2002). Death to flies: Drosophila as a model system to study programmed cell death. *J Immunol Methods* 265, 21-38. Review.

Ridley AJ, Hall A. (1992). Distinct patterns of actin organization regulated by the small GTP-binding proteins Rac and Rho. *Cold Spring Harb Symp Quant Biol* 57, 661-71.

Ries A, Goldberg JL, Grimpe B. (2007). A novel biological function for CD44 in axon growth of retinal ganglion cells identified by a bioinformatics approach. *J Neurochem* 103, 1491-505.

Riese J, Tremml G, Bienz M. (1997). D-Fos, a target gene of Decapentaplegic signalling with a critical role during Drosophila endoderm induction. *Development* 124, 3353-61.

Riesgo-Escovar, J. R., Jenni, M., Fritz, A. & Hafen, E. (1996) The Drosophila Jun-N-terminal kinase is required for cell morphogenesis but not for DJun-dependent cell fate specification in the eye. *Genes Dev,* 10**,** 2759-68.

Riesgo-Escovar, J. R. and Hafen, E. (1997a). Common and distinct roles of DFos and DJun during Drosophila development. *Science* 278, 669-72.

Riesgo-Escovar, J. R. and Hafen, E. (1997b). Drosophila Jun kinase regulates expression of decapentaplegic via the ETS-domain protein Aop and the AP-1 transcription factor DJun during dorsal closure. *Genes Dev* 11, 1717-27.

Rincon, M., Flavell, R. A. & Davis, R. J. (2001) Signal transduction by MAP kinases in T lymphocytes. *Oncogene,* 20**,** 2490-7.

Robinson GA. (1996). Changes in the expression of transcription factors ATF-2 and Fra-2 after axotomy and during regeneration in rat retinal ganglion cells. *Brain Res Mol Brain Res* 41, 57-64.

Robles E, Woo S, Gomez TM. (2005). Src-dependent tyrosine phosphorylation at the tips of growth cone filopodia promotes extension. *J Neurosci* 25, 7669-81.

Rosso, S. B., Sussman, D., Wynshaw-Boris, A. and Salinas, P. C. (2005). Wnt signaling through Dishevelled, Rac and JNK regulates dendritic development. *Nat Neurosci* 8, 34-42.

Rostaing P, Weimer RM, Jorgensen EM, Triller A, Bessereau JL. (2004). Preservation of immunoreactivity and fine structure of adult C. elegans tissues using high-pressure freezing. *J Histochem Cytochem*. 52, 1-12

Rothenberg ME, Rogers SL, Vale RD, Jan LY, Jan YN. (2003). Drosophila pod-1 crosslinks both actin and microtubules and controls the targeting of axons. *Neuron* 39, 779-91.

Ryoo, H. D., Gorenc, T. and Steller, H. (2004). Apoptotic cells can induce compensatory cell proliferation through the JNK and the Wingless signaling pathways. *Dev Cell* 7, 491-501.

Sabapathy K, Jochum W, Hochedlinger K, Chang L, Karin M, Wagner EF. (1999). Defective neural tube morphogenesis and altered apoptosis in the absence of both JNK1 and JNK2. *Mech Dev* 89, 115-24.

Sambrook, J., Fritsch, E.F., and Maniatis, T. (1989). Molecular Cloning: A Laboratory Manual, Second Edition (Cold Spring Harbor, New York: Cold Spring Harbor Laboratory).

Sanford SD, Gatlin JC, Hökfelt T, Pfenninger KH. (2008). Growth cone responses to growth and chemotropic factors. *Eur J Neurosci* 28, 268-78.

Sanyal S, Narayanan R, Consoulas C, Ramaswami M. (2003). Evidence for cell autonomous AP1 function in regulation of Drosophila motor-neuron plasticity. *BMC Neurosci* 4, 20.

Sanyal, S., Sandstrom, D. J., Hoeffer, C. A. and Ramaswami, M. (2002). AP-1 functions upstream of CREB to control synaptic plasticity in Drosophila. *Nature* 416, 870-4.

Sato S, Sanjo H, Takeda K, Ninomiya-Tsuji J, Yamamoto M, Kawai T, Matsumoto K, Takeuchi O, Akira S. (2005). Essential function for the kinase TAK1 in innate and adaptive immune responses. *Nat Immunol* 6, 1087-95.

Schaefer AW, Kabir N, Forscher P. (2002). Filopodia and actin arcs guide the assembly and transport of two populations of microtubules with unique dynamic parameters in neuronal growth cones. *J Cell Biol* 158, 139-52.

Schmitt AM, Shi J, Wolf AM, Lu CC, King LA, Zou Y. (2006). Wnt-Ryk signalling mediates medial-lateral retinotectal topographic mapping. *Nature* 439, 31-7.

Schwab C, Steele JC, McGeer PL. (1997). Dystrophic neurites are associated with early stage extracellular neurofibrillary tangles in the parkinsonism-dementia complex of Guam. *Acta Neuropathol* 94, 486-92.

Segal RA. (2003). Selectivity in neurotrophin signaling: theme and variations. *Annu Rev Neurosci* 26, 299-330. Review.

Sharrocks AD, Yang SH, Galanis A. (2000). Docking domains and substrate-specificity determination for MAP kinases. *Trends Biochem Sci* 25, 448-53. Review.

Shekarabi M, Kennedy TE. (2002). The netrin-1 receptor DCC promotes filopodia formation and cell spreading by activating Cdc42 and Rac1. *Mol Cell Neurosci* 19, 1-17.

Sherwood DR, Butler JA, Kramer JM, Sternberg PW (2005). FOS-1 promotes basement-membrane removal during anchor-cell invasion in C. elegans. *Cell* 121, 151-62.

Siddiqui S, Horvat-Bröcker A, Faissner A. (2009). The glia-derived extracellular matrix glycoprotein tenascin-C promotes embryonic and postnatal retina axon outgrowth via the alternatively spliced fibronectin type III domain TNfnD. *Neuron Glia Biol* 10, 1-13.

Sluss, H. K., Han, Z., Barrett, T., Goberdhan, D. C., Wilson, C., Davis, R. J. and Ip, Y. T. (1996). A JNK signal transduction pathway that mediates morphogenesis and an immune response in Drosophila. *Genes Dev* 10, 2745-58.

Song HJ, Ming GL, Poo MM. (1997). cAMP-induced switching in turning direction of nerve growth cones. *Nature* 388, 275-9.

Smith SJ. (1988). Neuronal cytomechanics: the actin-based motility of growth cones. *Science.* 242, 708-15. Review.

Srahna, M., Leyssen, M., Choi, C. M., Fradkin, L. G., Noordermeer, J. N. and Hassan, B. A. (2006). A signaling network for patterning of neuronal connectivity in the Drosophila brain. *PLoS Biol* 4, 348.

Stathopoulos A, Levine M (2002). Dorsal gradient networks in the Drosophila embryo. *Dev Biol* 246, 57-67. Review.

Stockinger W, Brandes C, Fasching D, Hermann M, Gotthardt M, Herz J, Schneider WJ, Nimpf J. (2000). The reelin receptor ApoER2 recruits JNK-interacting proteins-1 and -2. *J Biol Chem* 275, 25625-32.

Stokin GB, Lillo C, Falzone TL, Brusch RG, Rockenstein E, Mount SL, Raman R, Davies P, Masliah E, Williams DS, Goldstein LS (2005). Axonopathy and transport deficits early in the pathogenesis of Alzheimer's disease. *Science* 307, 1282-8.

Stronach, B. (2005). Dissecting JNK signaling, one KKKinase at a time. *Dev Dyn* 232, 575-84.

Stronach B, Perrimon N. (2002). Activation of the JNK pathway during dorsal closure in Drosophila requires the mixed lineage kinase, slipper. *Genes Dev* 16, 377-87.

Su YC, Maurel-Zaffran C, Treisman JE, Skolnik EY. (2000). The Ste20 kinase misshapen regulates both photoreceptor axon targeting and dorsal closure, acting downstream of distinct signals. *Mol Cell Biol* 20, 4736-44.

Su, Y. C., Treisman, J. E. and Skolnik, E. Y. (1998). The Drosophila Ste20-related kinase misshapen is required for embryonic dorsal closure and acts through a JNK MAPK module on an evolutionarily conserved signaling pathway. *Genes Dev* 12, 2371-80.

Sun P, Watanabe H, Takano K, Yokoyama T, Fujisawa J, Endo T. (2006). Sustained activation of M-Ras induced by nerve growth factor is essential for neuronal differentiation of PC12 cells. *Genes Cells* 11, 1097-113.

Tanaka E, Sabry J. (1995). Making the connection: cytoskeletal rearrangements during growth cone guidance. *Cell* 83, 171-6. Review

Tanoue T, Nishida E. (2003). Molecular recognitions in the MAP kinase cascades. *Cell Signal* 15, 455-62. Review.

Tapon N, Hall A. (1997). Rho, Rac and Cdc42 GTPases regulate the organization of the actin cytoskeleton. *Curr Opin Cell Biol* 9, 86-92.

Tararuk T, Ostman N, Li W, Björkblom B, Padzik A, Zdrojewska J, Hongisto V, Herdegen T, Konopka W, Courtney MJ, Coffey ET. (2006). JNK1 phosphorylation of SCG10 determines microtubule dynamics and axodendritic length. *J Cell Biol*. 173, 265-77.

Van Dam H, Wilhelm D, Herr I, Steffen A, Herrlich P, Angel P. (1995). ATF-2 is preferentially activated by stress-activated protein kinases to mediate c-jun induction in response to genotoxic agents. *EMBO J* 14, 1798-811.

Varela-Echavarría A, Tucker A, Püschel AW, Guthrie S. (1997) Motor axon subpopulations respond differentially to the chemorepellents netrin-1 and semaphorin D. *Neuron*. 18, 193-207.

Ventura, J. J., Hubner, A., Zhang, C., Flavell, R. A., Shokat, K. M. and Davis, R. J. (2006). Chemical genetic analysis of the time course of signal transduction by JNK. *Mol Cell* 21, 701-10.

Verhagen AM, Ekert PG, Pakusch M, Silke J, Connolly LM, Reid GE, Moritz RL, Simpson RJ, Vaux DL. (2000). Identification of DIABLO, a mammalian protein that promotes apoptosis by binding to and antagonizing IAP proteins. *Cell* 102, 43-53.

Verhey KJ. (2007). Motor proteins: trafficking and signaling collide. *Curr Biol*. 17, 804-6

Verhey KJ, Meyer D, Deehan R, Blenis J, Schnapp BJ, Rapoport TA, Margolis B. (2001). Cargo of kinesin identified as JIP scaffolding proteins and associated signaling molecules. *J Cell Biol* 152, 959-70.

Vidal, S., Khush, R. S., Leulier, F., Tzou, P., Nakamura, M. and Lemaitre, B. (2001). Mutations in the Drosophila dTAK1 gene reveal a conserved function for MAPKKKs in the control of rel/NF-kappaB-dependent innate immune responses. *Genes Dev* 15, 1900-12.

Vinciguerra M, Vivacqua A, Fasanella G, Gallo A, Cuozzo C, Morano A, Maggiolini M, Musti AM. Differential phosphorylation of c-Jun and JunD in response to the epidermal growth factor is determined by the structure of MAPK targeting sequences. *J Biol Chem*. 279, 9634-41.

Viswanath V, Wu Z, Fonck C, Wei Q, Boonplueang R, Andersen JK. (2000). Transgenic mice neuronally expressing baculoviral p35 are resistant to diverse types of induced apoptosis, including seizure-associated neurodegeneration. *Proc Natl Acad Sci U S A* 97, 2270-5.

Waetzig, V., Zhao, Y. and Herdegen, T. (2006). The bright side of JNKs-Multitalented mediators in neuronal sprouting, brain development and nerve fiber regeneration. *Prog Neurobiol* 80, 84-97.

Wahl S, Barth H, Ciossek T, Aktories K, Mueller BK. (2000). Ephrin-A5 induces collapse of growth cones by activating Rho and Rho kinase. *J Cell Biol* 149, 263-70.

Wang J, Zugates CT, Liang IH, Lee CH, Lee T. (2002). Drosophila Dscam is required for divergent segregation of sister branches and suppresses ectopic bifurcation of axons. *Neuron* 33, 559-71.

Wang, M. C., Bohmann, D. and Jasper, H. (2003). JNK signaling confers tolerance to oxidative stress and extends lifespan in Drosophila. *Dev Cell* 5, 811-6.

Wang X, Nadarajah B, Robinson AC, McColl BW, Jin JW, Dajas-Bailador F, Boot-Handford RP, Tournier C. (2007). Targeted deletion of the mitogen-activated protein kinase kinase 4 gene in the nervous system causes severe brain developmental defects and premature death. *Mol Cell Biol* 27, 7935-46.

Weber, U., Pataki, C., Mihaly, J. and Mlodzik, M. (2008). Combinatorial signaling by the Frizzled/PCP and Egfr pathways during planar cell polarity establishment in the Drosophila eye. *Dev Biol* 316, 110-23.

Wen Z, Guirland C, Ming GL, Zheng JQ. (2004). A CaMKII/calcineurin switch controls the direction of Ca(2+)-dependent growth cone guidance. *Neuron* 43, 835-46.

Weston, C. R. and Davis, R. J. (2002). The JNK signal transduction pathway. *Curr Opin Genet Dev* 12, 14-21.

Whitfield J, Neame SJ, Paquet L, Bernard O, Ham J. (2001). Dominant-negative c-Jun promotes neuronal survival by reducing BIM expression and inhibiting mitochondrial cytochrome c release. *Neuron* 29, 629-43

Whitmarsh AJ. (2006). The JIP family of MAPK scaffold proteins. *Biochem Soc Trans*. 34, 828-32

Whitmarsh AJ, Cavanagh J, Tournier C, Yasuda J, Davis RJ. (2002). A mammalian scaffold complex that selectively mediates MAP kinase activation. *Science*. 281, 1671-4.

Wills Z, Marr L, Zinn K, Goodman CS, Van Vactor D. (1999). Profilin and the Abl tyrosine kinase are required for motor axon outgrowth in the Drosophila embryo. *Neuron* 22, 291-9.

Wong K, Ren XR, Huang YZ, Xie Y, Liu G, Saito H, Tang H, Wen L, Brady-Kalnay SM, Mei L, Wu JY, Xiong WC, Rao Y. (2001). Signal transduction in neuronal migration: roles of GTPase activating proteins and the small GTPase Cdc42 in the Slit-Robo pathway. *Cell* 107, 209-21.

Wu H, Wang MC, Bohmann. (2009). JNK protects Drosophila from oxidative stress by trancriptionally activating autophagy. *Mech Dev*. 126, 624-37.

Wu, J. S. and Luo, L. (2006a). A protocol for dissecting Drosophila melanogaster brains for live imaging or immunostaining. *Nat Protoc* 1, 2110-5.

Wu, J. S. and Luo, L. (2006b). A protocol for mosaic analysis with a repressible cell marker (MARCM) in Drosophila. *Nat Protoc* 1, 2583-9.

Wylie SR, Chantler PD. (2003). Myosin IIA drives neurite retraction. *Mol Biol Cell*. 14, 4654-66.

Yaka R, Gamliel A, Gurwitz D, Stein R. (1998). NGF induces transient but not sustained activation of ERK in PC12 mutant cells incapable of differentiating. *J Cell Biochem* 70, 425-32.

Yamauchi J, Miyamoto Y, Sanbe A, Tanoue A. (2006). JNK phosphorylation of paxillin, acting through the Rac1 and Cdc42 signaling cascade, mediates neurite extension in N1E-115 cells. *Exp Cell Res* 312, 2954-61

Yang DD, Kuan CY, Whitmarsh AJ, Rincón M, Zheng TS, Davis RJ, Rakic P, Flavell RA. (1997). Absence of excitotoxicity-induced apoptosis in the hippocampus of mice lacking the Jnk3 gene. *Nature* 389, 865-70.

Yang N, Higuchi O, Ohashi K, Nagata K, Wada A, Kangawa K, Nishida E, Mizuno K. (1998). Cofilin phosphorylation by LIM-kinase 1 and its role in Rac-mediated actin reorganization. *Nature* 393, 809-12.

Yao R, Osada H. (1997). Induction of neurite outgrowth in PC12 cells by gamma-lactam-related compounds via Ras-MAP kinase signaling pathway independent mechanism. *Exp Cell Res* 234, 233-9.

Yasuda J, Whitmarsh AJ, Cavanagh J, Sharma M, Davis RJ. (1999). The JIP group of mitogen-activated protein kinase scaffold proteins. *Mol Cell Biol* 19, 7245-54.

Yoshida H, Hastie CJ, McLauchlan H, Cohen P, Goedert M. (2004). Phosphorylation of microtubule-associated protein tau by isoforms of c-Jun N-terminal kinase (JNK). *J Neurochem* 90, 352-8.

Yu TW, Hao JC, Lim W, Tessier-Lavigne M, Bargmann CI. (2002). Shared receptors in axon guidance: SAX-3/Robo signals via UNC-34/Enabled and a Netrin-independent UNC-40/DCC function. *Nat Neurosci* 5, 1147-54.

Zeitlinger, J., Kockel, L., Peverali, F. A., Jackson, D. B., Mlodzik, M. and Bohmann, D. (1997). Defective dorsal closure and loss of epidermal decapentaplegic expression in Drosophila fos mutants. *EMBO J* 16, 7393-401.

Zhao Y, Herdegen T. (2009). Cerebral ischemia provokes a profound exchange of activated JNK isoforms in brain mitochondria. *Mol Cell Neurosci*. 2009 41, 186-95.

Zheng C, Xiang J, Hunter T, Lin A. (1999). The JNKK2-JNK1 fusion protein acts as a constitutively active c-Jun kinase that stimulates c-Jun transcription activity. *J Biol Chem* 274, 28966-71.

Zhou FQ, Cohan CS. (2004). How actin filaments and microtubules steer growth cones to their targets. *J Neurobiol* 58, 84-91. Review.

Zhou FQ, Waterman-Storer CM, Cohan CS. (2002). Focal loss of actin bundles causes microtubule redistribution and growth cone turning. *J Cell Biol* 157, 839-49.

Zhou FQ, Zhou J, Dedhar S, Wu YH, Snider WD. (2004). NGF-induced axon growth is mediated by localized inactivation of GSK-3beta and functions of the microtubule plus end binding protein APC. *Neuron 42, 897-912.*

Zhou Q, Krebs JF, Snipas SJ, Price A, Alnemri ES, Tomaselli KJ, Salvesen GS. (1998). Interaction of the baculovirus anti-apoptotic protein p35 with caspases. Specificity, kinetics, and characterization of the caspase/p35 complex. *Biochemistry* 37, 10757-65.

Zou H, Henzel WJ, Liu X, Lutschg A, Wang X. (1997). Apaf-1, a human protein homologous to C. elegans CED-4, participates in cytochrome c-dependent activation of caspase-3. *Cell* 90, 405-13.

Zumbrunn J, Kinoshita K, Hyman AA, Näthke IS. (2001). Binding of the adenomatous polyposis coli protein to microtubules increases microtubule stability and is regulated by GSK3 beta phosphorylation. *Curr Biol* 11, 44-9.

Developmental Biology 339 (2010) 65–77

Contents lists available at ScienceDirect

Developmental Biology

journal homepage: www.elsevier.com/developmentalbiology

Signal strength and signal duration define two distinct aspects of JNK-regulated axon stability

Andrew Rallis, Coralie Moore, Julian Ng *

MRC Centre for Developmental Neurobiology, New Hunt's House, Guy's Campus, King's College, London SE1 1UL, UK

ARTICLE INFO

Article history:
Received for publication 16 September 2009
Revised 10 December 2009
Accepted 11 December 2009
Available online 24 December 2009

Keywords:
Jun N-terminal kinase
Fos
Jun
AP-1
Axonal morphogenesis
Neurodegeneration
Neural development
Drosophila

ABSTRACT

Signaling proteins often control multiple aspects of cell morphogenesis. Yet the mechanisms that govern their pleiotropic behavior are often unclear. Here we show activity levels and timing mechanisms determine distinct aspects of Jun N-terminal kinase (JNK) pathway dependent axonal morphogenesis in *Drosophila* mushroom body (MB) neurons. In the complete absence of *Drosophila* JNK (Basket), MB axons fail to stabilize, leading to their subsequent degeneration. However, with a partial loss of Basket (Bsk), or of one of the upstream JNK kinases, Hemipterous or Mkk4, these axons overextend. This suggests that Bsk activity prevents axons from destabilizing, resulting in degeneration and overextension beyond their terminal targets. These distinct phenotypes require different threshold activities involving the convergent action of two distinct JNK kinases. We show that sustained Bsk signals are essential throughout development and act additively but are dispensable at adulthood. We also suggest that graded Bsk inputs are translated into AP-1 transcriptional outputs consisting of Fos and Jun proteins.

Introduction

To reach maturity, developing neurons undergo many morphogenetic changes including axon and dendrite formation/polarity, neurite extension, guidance, branching and synaptogenesis. The mechanisms that underlie these distinct steps are not well understood. This results partly from the observation that, although many molecules are involved, they exhibit pleiotropy, controlling several aspects of neuronal morphogenesis. The MAPK family of signaling proteins epitomizes such pleiotropic factors. They are present throughout eukaryotes and control many cellular responses, such as proliferation, differentiation, stress and apoptotic control (Weston and Davis, 2002). MAPKs (Erk, JNK or p38 members) are activated through phosphorylation by upstream kinases, which are themselves regulated by other protein kinases. Several studies show the Jun N-terminal kinase (JNK) pathway is involved in axon formation/polarization, extension, synaptic plasticity and dendrite development (Oliva et al., 2006; Rosso et al., 2005; Sanyal et al., 2002; Srahna et al., 2006). Many non-neuronal models have been used to explain how JNKs regulate multiple aspects of cell regulation. For example, one proposal is that the core-signaling component is linked to distinct specialized complexes. JNKs are regulated by distinct upstream kinases through interactions with scaffold proteins (Weston and Davis, 2002). These link JNK responses to particular stimuli, such as morphogenetic, stress or apoptotic regulation. However, timing mechanisms can also play a role. From chemical genetic paradigms using JNK mutant mice, transient or prolonged JNK inactivation can affect distinct JNK-dependent immune responses (Ventura et al., 2006). Another possibility is that signaling molecules have context-dependent roles in different cell types. Thus, while in mammalian hippocampal cells, JNKs are involved in dendritogenesis (Rosso et al., 2005) and axonal polarity/formation (Oliva et al., 2006), in *Drosophila* dorsal cluster (DC) neurons, JNK is involved in axon extension (Srahna et al., 2006), and at the *Drosophila* neuromuscular junction (NMJ), JNK regulates synaptic plasticity and growth (Collins et al., 2006; Sanyal et al., 2002).

In *Drosophila*, the JNK signaling network consists of one JNK, Basket (Bsk), which is regulated by two JNK kinases (JNKKs), Hemipterous (Hep) and MAP kinase kinase 4 (MKK4) (Glise et al., 1995; Han et al., 1998; Riesgo-Escovar and Hafen, 1997b). Six JNKK kinases (JNKKKs) exist, which control the JNKKs (Stronach, 2005). Further upstream, a single JNKKKK, Misshapen (Msn), regulates the JNKKKs (Su et al., 1998). Like in many other model systems studied, Bsk responses in *Drosophila* are varied. While first shown to control epithelial morphogenesis during embryonic dorsal closure, Bsk also contributes to imaginal disk development, apoptotic regulation, wound healing, tissue regeneration, tissue homeostasis and innate immunity (Agnes et al., 1999; Bosch et al., 2005; Delaney et al., 2006; Galko and Krasnow, 2004; Mattila et al., 2005; Noselli, 1998; Pastor-Pareja et al., 2004; Ramet et al., 2002; Ryoo et al., 2004; Sluss et al., 1996; Vidal et al., 2001; Zeitlinger et al., 1997). Additionally, Bsk

* Corresponding author.
E-mail address: julian.ng@kcl.ac.uk (J. Ng).

0012-1606/$ – see front matter © 2009 Elsevier Inc. All rights reserved.
doi:10.1016/j.ydbio.2009.12.016

signals can prolong lifespan and protect against oxidative stress in flies (Wang et al., 2003).

In many of these responses, Bsk targets the phosphorylation of the Activator protein-1 (AP-1) complex, composed of the transcription factors Fos and Jun (Ciapponi et al., 2001; Kockel et al., 1997). In *Drosophila*, these act either as heterodimers or as Fos homodimers (Pearson et al., 2009; Perkins et al., 1990). In many studies, distinct JNKKKs are thought to represent stimulus-specific regulators and the

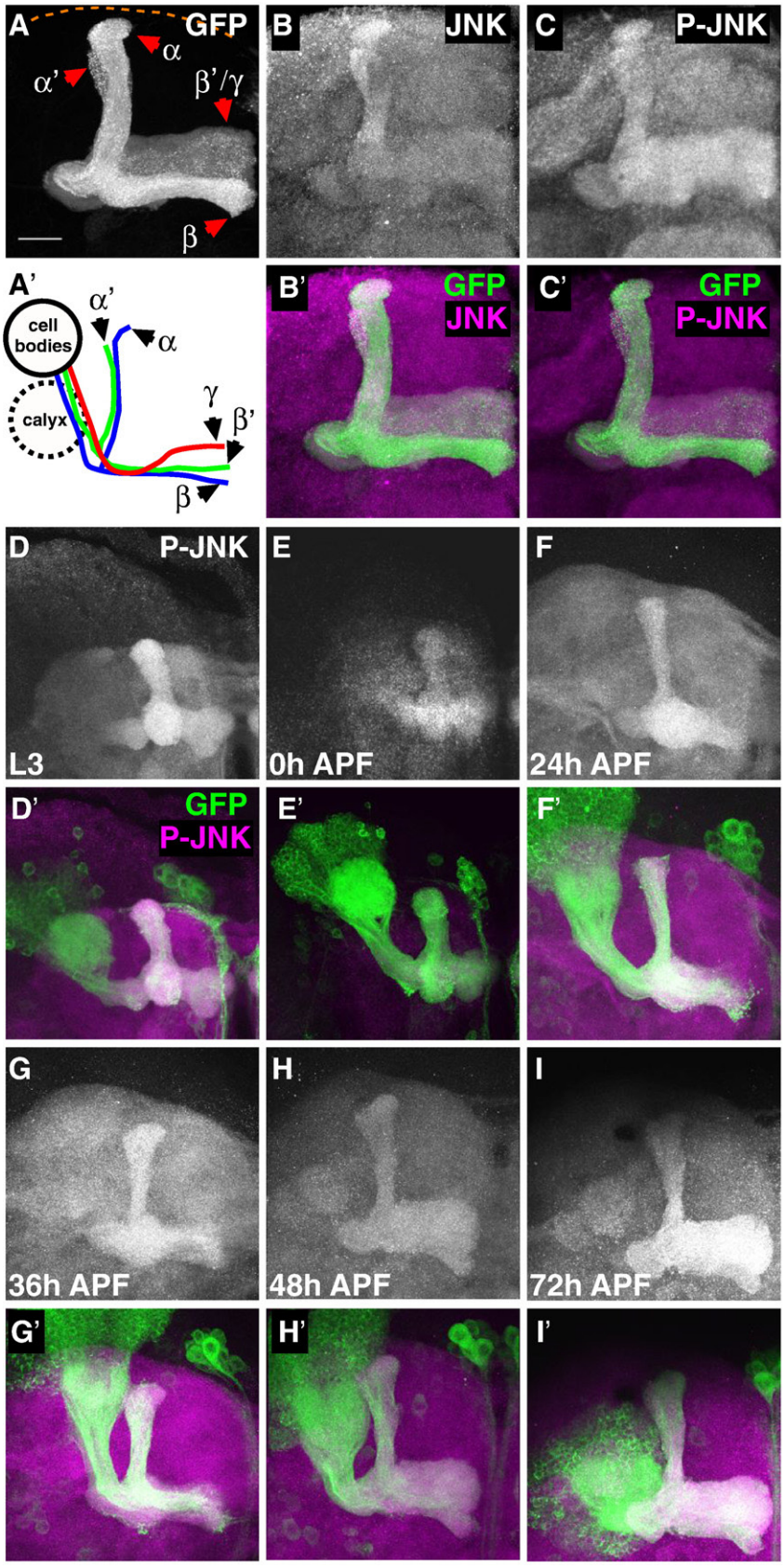

core components are represented by the Hep→Bsk→AP-1 response (Stronach, 2005). The in vivo role of MKK4 has not been previously described.

Here we show that *Drosophila* JNK controls two distinct axonal phenotypes in mushroom body (MB) neurons. Depending on the level of Bsk inactivation, this results in a bias towards axon degeneration or overextension. Based on these phenotypes, we propose that Bsk controls axon stabilization via two mechanisms, to prevent axons from degenerating and from overextending beyond the postsynaptic target. These mechanisms require different threshold activity levels, involving the upstream JNKKs, Hep and Mkk4. We show that sustained Bsk activity is required throughout development to maintain axonal stability. These phenotypes are mediated through AP-1, which shows a similar graded response to these axonal phenotypes.

Materials and methods

Drosophila strains

bsk^{147e}and *hep* mutant strains (*hep*^{R39}and *hep*^{75}) are null mutations, as previously described (Glise et al., 1995; Sluss et al., 1996). The *bsk*^{H15} allele (Berger et al., 2008) encodes a missense mutation (I212F-PB isoform) within the kinase domain, which is likely to result in a hypomorphic allele (see quantifications in Fig. 6I) The *Mkk4*^{e01458} allele is derived from a *PiggyBac* insertion (Thibault et al., 2004). *Mkk4*^{e01458}complemented the lethality associated with chromosomal deficiencies *Df(3R)Dhod15*, *Df(3R)BSC195* and *Df(3R)BSC197* but failed to complement *Df(3R)p13* and *Df(3R)Exel6149* (Flybase). Ubiquitous expression of Mkk4 (*tub-GAL4>MKK4YFP*) fully rescued the lethality associated with *Mkk4*^{e01458}/*Df(3R)p13* transheterozygotes, confirming that the insertion disrupts the *Mkk4* locus.

The following additional strains were also used in our study; *UAS-Bskmyc, UAS-Mkk4Venus* (this study); *UAS-Bsk RNAi, UAS-Mkk4 RNAi* (VDRC lines 34138, 34139 and 26928), *UAS-Dcr2* (Dietzl et al., 2007); *UAS-Bsk DN*, *UAS-Hep.B*^{2}, *UAS-Hep.CA*^{4} and *GAL80*^{ts7} (Bloomington Drosophila Stock Center); *Jun*^{2}, *Jun*^{1} (Kockel et al., 1997); *UAS-Jbz, UAS-Fbz,* (Eresh et al., 1997); *UAS-kay RNAi, UAS-hep RNAi* (NIG-Fly, Mishima; lines 15507R-4 and 2190R-1); *kay*^{1}(Riesgo-Escovar and Hafen, 1997a; Zeitlinger et al., 1997); *kay*^{ED6315} (Weber et al., 2008). These *kay* alleles are not true nulls, as they do not disrupt all Kay isoforms (Giesen et al., 2003; Weber et al., 2008). *Drosophila* strains for MARCM analysis have previously been described (Lee and Luo, 1999) and mutant strains were generated by standard recombination techniques.

Molecular biology

To generate expression vectors *pUAST-Bskmyc* and *pUAST-Mkk4YFP*, Bsk and Mkk4 cDNAs (a gift from D. Bohmann and BDGP clone RE70055, respectively) were cloned into a pENTR vector (Invitrogen) by PCR and TOPO® cloning. The resulting pENTR-*Bsk* and pENTR-*Mkk4* clones were ligated to the destination vectors (pTWM or pTWV, respectively; T. Murphy, Carnegie *Drosophila* Gateway® vectors) using the Gateway® system (Invitrogen). *pUAST-BskMyc*$^{T181A,\ Y183F}$ was constructed by site directed mutagenesis (Quikchange®, Stratagene) and cloning into the pTWM vector, as above. Germline transformations were performed commercially (Aktogen, Cambridge, UK).

Generation of MARCM clones, UAS-Gal4, RNAi and TARGET expression analysis

Homozygous mutant clones that are positively labeled were generated using the MARCM method. MB neuroblast and single-cell clones were generated as previously described (Wu and Luo, 2006b). A single neuroblast clone can give rise to ~600 Kenyon cells (Ito et al., 1997). Neurons were visualized using the OK107-Gal4 driver expressing mCD8GFP. The Gal4-OK107 driver was also used in misexpression studies, along with one copy of UAS-CD8GFP. Flies were reared at 25 °C, unless otherwise stated such as in RNAi and TARGET experiments. For 'high' level of RNAi knockdown, flies were cultured at 29 °C in the presence of ectopic Dicer (Dcr2), to increase the level of UAS expression and RNAi efficiency (Dietzl et al., 2007). For 'medium' RNAi activity, flies were raised at 29 °C without ectopic Dcr2. We found that even at low levels of RNAi expression (18 °C), Dcr2 expression can significantly enhance RNAi phenotypes. Ectopic expression of Dcr2 alone does not disrupt MB axon projections (data not shown). Flies were dissected within 3–7 days post-eclosion. For the TARGET protocol, flies were grown at 18 °C and UAS-GAL4 expression was induced by transferring to 29 °C at the indicated stages. In the 'reverse' protocol, flies were grown at 29 °C and shifted to 18 °C. These flies were maintained in the shifted temperatures and analyzed at 3 days post-eclosion, unless indicated otherwise.

Immunohistochemistry

Fly brains were dissected at various stages and stained as previously described (Wu and Luo, 2006a). For MARCM neuroblast and single-cell clones, axon projections were visualized using anti-FasII (1:5) and anti-mCD8, 1:200. The following additional antibodies were used: anti-JNK1 (Santa Cruz Biotechnology, sc-571, 1:250), anti-phospho JNK (Cell Signalling, no. 9255, 1:250), anti-Myc (Santa Cruz Biotechnology, clone 9E10; 1:100 or Cell Signalling, no. 2272; 1:200), anti-GFP (Molecular Probes, A11122, 1:100 or Roche, 11814460001, 1:200), anti-MKK4 (1:50) and anti-Hep (1:100). Anti-Hep and anti-Mkk4 antibodies were generated commercially using rabbit and guinea pig hosts, respectively, using a DXP protocol (Eurogentec, Seraing, Belgium). The following peptide sequences were used as immunogens (QSLEAKLQAQNESHDC and CLRANGDPTLQRLPNS for Hep; MAERPKNLFATGSSRC and CKDGITQFTANQQAES for Mkk4). Stained brains were imaged by confocal microscopy (using Zeiss 510 and processed using Zeiss LSM and Adobe photoshop software).

S2 cell culture, expression and Western blotting analysis

Drosophila S2 cells were maintained at 25 °C in Schneider's media, supplemented with 10% fetal bovine serum. S2 transfections were performed using the pMT-GAL4 binary system (Klueg et al., 2002). Briefly, 2×10^{6} cells (50% confluent) were plated in 2 ml of medium 24 h prior to the transfection. 2 μg of pUAST and 2 μg of pMT-GAL4 plasmids were then added per well (90% cell confluent stage), along with 30 μl of Cellfectin (Invitrogen) in 2 ml of antibiotic-free, Schneider's Media. The media were removed 3 h post-transfection and replaced with media supplemented with 10% fetal bovine serum, 1% streptomycin (Gibco BRL). Twelve hours later, the media were replaced with media containing 1% $CuSO_4$ to induce protein expression. S2 cells were subsequently harvested 24 h later. Cells

Fig. 1. JNK is highly expressed in MB axons and dendrites. (A) MB axons labeled by CD8-GFP expression, using the OK107-Gal4 driver. These adult MB axonal projections are wild type. Axons terminate close to the midline (to the right of all images, unless indicated with a dashed white line), or close to the anterior dorsal cortex (dashed orange line). The different axon lobes (γ, α'β', αβ) are indicated, as previously (Lee et al., 1999). (A') A schematic of these MB neuron subtypes (γ, α'β', αβ) and the relative location of cell bodies, dendrite ('calyx') and axon projections. (B) The same brain immunostained with anti-JNK1, the overlap with the GFP marker (magenta in B') shows axonal localization. (C) The same brain also immunostained with anti-phospho JNK (P-JNK). (C') The overlap shows high JNK activity in MB axons. (D–I) P-JNK brain staining at various developmental stages, from wandering larvae L3 and pupae at different time-points after puparium formation (APF), indicated in hours (h). The additional panels (D'–I') show the corresponding overlap between P-JNK and the GFP labeled MB axons at these stages. Unless indicated otherwise, these and subsequent images are *z*-stack of serial confocal images taken at 1-μm thickness. In some images (such as in A), cell body sections have been omitted to clearly reveal axonal projections. Scale bar: 20 μm.

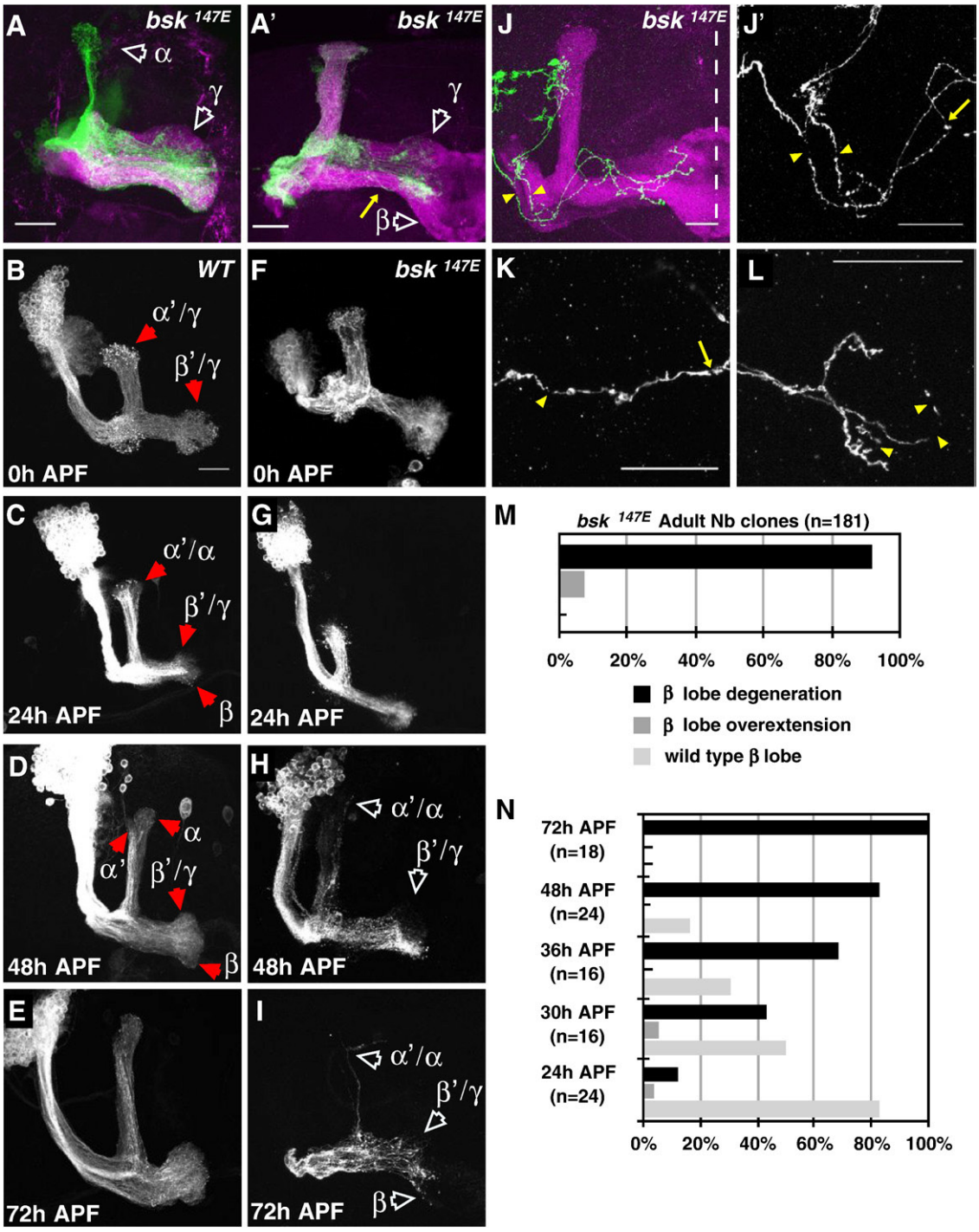

Fig. 2. JNK loss results in axon destabilization. (A, A') Adult MB *bsk*^{147e}neuroblast clones show axon thinning (yellow arrow) and termination defects (open white arrowheads). (B–I) Images of CD8-GFP labeled wild-type (B–E) and *bsk*^{147e} (F–I) neuroblast clones analyzed at developmental stages: 0 h (B, F), 24 h (C, G), 48 h (D, H) and 72 h APF (E, I). At the onset of puparium formation (0 h APF), the majority of wild-type MB neurons consist of γ and α'β' neurons (B). A phase of neurogenesis occurs at this period and MB neuroblasts give rise to αβ neurons, which are visible at 24 h APF (C). As axon continue to grow, dorsal α and medial β lobes become more prominent. At 48 h APF, these lobes are similar to adult MB projections (D compare with Fig. 1A, respectively). Note *bsk* axonal defects at later stages of development (quantified in N). Axon defects were also more pronounced at later stages (compare H to I). The cell body section has been omitted from I. (J–L) Images of *bsk*^{147e} single cell clones (γ-neurons) showing breaks (yellow arrowheads) along different regions of the axon. (J', K and L) Higher magnification of MB axons shows breaks and axon thinning in the proximal and mid-axonal shaft (J',K, respectively) and in the distal section (L). Scale bars: 20 μm. Unless indicated otherwise, CD8-GFP labeled neurons are shown in green or grayscale and Fas2 immunostaining (magenta) labels a subset (γ weakly and αβ strongly) of all MB axons. (M–N) Quantification of β-axon termination defects in adult MB *bsk*^{147e} neuroblast clones (M), and at specific time points in development (N). *n*, number of neuroblast clones analyzed. While all MB axons displayed degeneration phenotypes to some extent, to simplify this study, we decided to focus on the medially projecting β-lobe. For *bsk* additional images and quantifications of other MB projections, see Supplementary Fig. 2.

were harvested by centrifugation at 1000 *g* for 5 min and lysed on ice for 30 min in RIPA buffer [10 mM Tris (pH 7.4), 10 mM NaH_2PO_4, 150 mM NaCl, 1% Triton X-100], supplemented with protease and phosphatase inhibitors (Halt® protease inhibitor from Pierce, 10 mM NaF and 1 mM Na_3VO_4). Lysates were spun for 10 min at 21,000 *g*. The supernatant was added to reducing sample loading buffer (2) in equal quantity. Reduced protein samples were run on 10% polyacrylamide Tris–HCl gels and transferred to Invitrolon® membranes (Invitrogen),

using standard methods (Bio-Rad). Immunoblots were probed with phospho-JNK (Cell Signalling, no. 9255, 1:1000) and JNK1 (Santa Cruz Biotechnology, sc-571, 1:4000), Hep (ab1956; 1:2000 and ab1957; 1:250) and Mkk4 antibodies (ab1954 and 1955; both at 1:5000). Additional antibodies used were GFP (Molecular Probes, A11122, 1:4000) and myc (Santa Cruz Biotechnology, clone 9E10, 1:4000) using standard protocols. Blots were developed with Pico-ECL chemiluminescence reagents (Pierce) and exposed to ECL hyperfilm (Amersham Biosciences).

Results

Drosophila JNK activity is detected in MB axons

MB neurons (Kenyon cells) in the *Drosophila* brain were used as a model to analyze Bsk signaling in vivo (Ito et al., 1997; Kurusu et al., 2002; Lee et al., 1999). Adult MB neurons are composed of three distinct sets (γ, α'β' and αβ) with each set having distinct axonal projections (Lee et al., 1999)(Figs. 1A and A'). MB axons extend from posterior located cell bodies and lead to dorsal and medial projections in the anterior part of the brain. These projections terminate in the anterior dorsal cortex (α' and α), or close to the midline (γ, β' and β). Antibodies were used in whole-mount immunohistochemistry to determine Bsk activity in these neurons. Using a human JNK1 antibody that cross-reacts with the *Drosophila* protein, Bsk was detected in MB axons (Fig. 1B). Using a phosphorylation-specific antibody that detects active forms of JNK, we found that Bsk was highly phosphorylated in adult MB axons (Fig. 1C). Low Bsk and p-Bsk signals were also present throughout the brain. Other notable structures that showed high Bsk/p-Bsk signals included the antennal lobe (AL) and ellipsoid body (eb) regions (Supplementary Fig. 1). As antibody controls, JNK and phospho-JNK immunoreactivity were not present when Bsk was lost or when its activity was inhibited in MB neurons (Supplementary Fig. 1). Analysis at different developmental stages showed that Bsk is active in axons throughout development, from wandering L3 larvae to adulthood (Fig. 1).

Bsk loss results in axon degeneration

The effect of Bsk inactivation was determined by generating MARCM neuroblast clones in MB neurons (see Methods). Analyzed at the adult stage, most *bsk*-null axons failed to reach the wild-type termination point (Figs. 2A, A', arrows). Many *bsk* clones also showed discontinuous thinning along the axon tracts, suggesting a possible axon loss (yellow arrow in Fig. 2A'). Interestingly, a minority of *bsk* axons displayed the converse phenotype with axon overextensions beyond their normal termination points (Supplementary Fig. 2A, B, open white arrows; quantifications in Fig. 2M and Supplementary Fig. 2I).

To determine whether this phenotype resulted from a failure in axon extension or stabilization, leading to subsequent degeneration, we analyzed *bsk* clones at different stages of development. The results showed the majority of *bsk* axons had normal, wild-type projections at early stages, but axonal defects characteristic of the adult stage were observed from 30 h after puparium formation (APF) onwards (Figs. 2F–I compared to wild type, Figs. 2B–E; quantified in Fig. 2N). These axon defects were often subtle at early to mid-pupal stages (data not shown; Fig. 2H) but becomes more acute in late pupae (Fig. 2I). At the adult stages, the entire axon lobe is often missing (Fig. 2A').

We analyzed this further by generating *bsk* single-cell clones. We found many fully extended axons showed thinning and breaks (Figs. 2J–L; compared to wild-type images in Supplementary Fig. 2C–E). This was not confined to axons, but also found in the main process close to the cell body, indicating an overall degeneration was taking place (Supplementary Fig. 2F, G compared to wild type, Fig. 2H). This was statistically significant when compared to wild-type clones for all axon regions analyzed (Supplementary Fig. 2J). We found that Bsk inactivation also resulted in many changes in the axonal architecture, with the increased presence of large protrusions and swellings (Supplementary Fig. 2B compared to wild type, Fig. 2C–E). Together these results strongly suggest that Bsk loss does not result in an initial defect of axon extension but in the subsequent failure in axon stabilization, leading to neurodegeneration and axon loss.

Bsk phosphorylation is essential for axonal morphogenesis

Bsk is activated by phosphorylation by the JNKKs, Hep and MKK4, on two predicted residues on threonine 181 and tyrosine 183 (Glise et al., 1995; Han et al., 1998). We first determined the relevance of these sites by generating a Bsk mutant that removes the phospho-acceptor sites (Bsk T181A, Y183F, or Bsk mTPY). By Western blotting, the phospho-JNK antibody does not detect Bsk mTPY (Supplementary Fig. 3A). Interestingly, overexpression of Bsk mTPY partially mimics the dominant negative (DN) Bsk misexpression phenotype when expressed in wild-type MB neurons (Supplementary Fig. 3B; see below). We determined whether Bsk mTPY expression would rescue the *bsk* phenotype. The results show, in contrast to the wild-type Bsk, Bsk mTPY expression failed to rescue the *bsk* axonal phenotypes, not only in MB neurons but also in optic lobe contralateral projecting (OL) neurons where *bsk* axon extension phenotypes were also observed (Fig. 3 and Supplementary Fig. 3, respectively; quantified in Supplementary Fig. 3G). These results show phosphorylation of these residues are critical for axonal morphogenesis and that the phospho-JNK antibody serves as a valid marker of Bsk activity in these neurons.

Role of the Drosophila JNKK Hep in axonal morphogenesis

Given the importance of JNK phosphorylation, we next determined the expression pattern of the JNKK, Hep. Hep antibodies were generated and used in western blotting (Supplementary Fig. 4A) and immunohistochemistry (Figs. 4A–C, G). Hep was detected in all MB axons but was less prominent in the cell bodies (Figs. 4A–C). Additional Hep signals were also observed throughout the brain, including the AL. By *UAS-Hep* expression, ectopic Hep staining also showed preferential localization to MB axons (Fig. 4G).

The role of Hep was determined by loss-of-function analysis. In *hep*-null clones, while axon degeneration was detected, it was not the major phenotype (Figs. 5A, I). Instead, axon overextensions were mainly observed (Figs. 5B, I). This is surprising, given that Hep is consistently described as a central regulator of Bsk (Stronach, 2005), *hep*-null clones might be expected to phenocopy *bsk* phenotypes to the same extent (Fig. 2M).

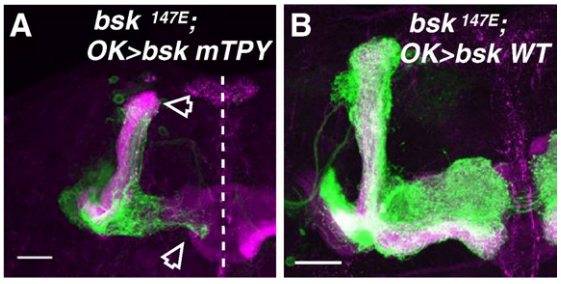

Fig. 3. JNK phosphorylation is essential for axonal morphogenesis. (A, B) *bsk*^{147e} neuroblast clones in the presence of Bsk mTPY (A), or wild-type Bsk (B). Wild-type Bsk, but not Bsk mTPY, expression rescues the axon phenotype. Cell body sections have been omitted in both panels. Scale bars: 20 μm. Green, CD8-GFP. Magenta, Fas2.

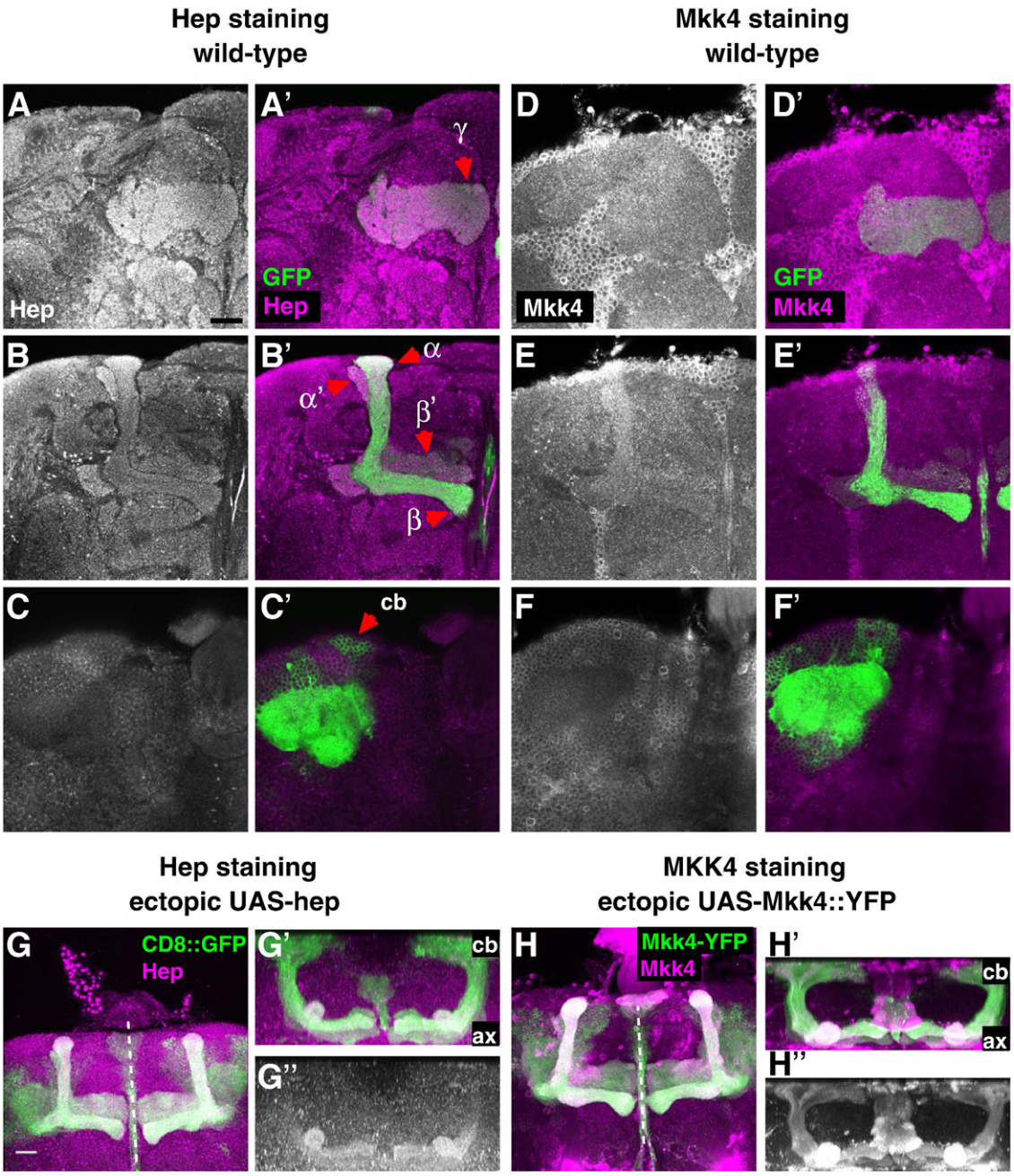

Fig. 4. Expression study of JNK kinases Hep and MKK4. (A–F ') Single confocal sections of MB neurons labeled with CD8-GFP and immunostained with Hep (A–C') or Mkk4 (D–F') antibodies. The corresponding panels (A'–F') show overlap between Hep and Mkk4 signals and CD8-GFP labeling. Single sections show γ (A, D), α/β and α'/β' axons (B, E) and MB cell bodies (cb) (C, F), as indicated in A'–C'. (G–G) CD8-GFP labeled MB neurons (green) expressing ectopic Hep (shown in magenta in G and G' and grayscale in G). Dorsal (*y*) projection views (G' and G) show Hep is mainly localized to axons (ax). (H–H) Representative image of MB neurons expressing MKK4YFP (green) and stained with anti-MKK4 (magenta in H and H' and white in H). Dorsal views (H' and H) show MKK4 is localized to axons and cell bodies (cb). Scale bar: 20 μm (*x*-only).

Role of Drosophila MKK4 in MB neurons

Another JNKK regulator of Bsk is MKK4 (Han et al., 1998). Antibodies to Mkk4 were generated and used in Western blotting and immunohistochemistry (Supplementary Fig. 4B; Figs. 4D–F). Mkk4 was detected in MB axons (particularly in α'β' and αβ axons) and cell bodies (Figs. 4D, E and F, respectively). This was confirmed by the expression of Mkk4-YFP fusion protein in these neurons (Fig. 4H). Using a recently described *MKK4* mutant allele (Thibault et al., 2004) (see Methods), we generated $MKK4^{e01485}$ MB clones. This also resulted in axon overextension (Fig. 5C), although this phenotype was less frequently observed than in *hep* clones (Fig. 5I). Cell proliferation defects were also observed in neuroblasts derived from earlier-born $MKK4^{e01485}$clones (Fig. 5D). This is consistent with recent reports, which show MKK4 loss results in cytokinetic defects in cultured *Drosophila* S2 cells (Bettencourt-Dias et al., 2004; Bjorklund et al., 2006).

Given the similar axon overextension phenotypes, we tested whether Hep and MKK4 are interchangeable. Ectopic Mkk4 was expressed in *hep* clones and *Mkk4* clones were generated with ectopic Hep. *hep* phenotypes were not suppressed by ectopic Mkk4, but the loss of Mkk4 can be rescued by increased Hep (Figs. 5E and G, respectively). In control experiments, these same UAS lines could rescue the corresponding *hep* or *Mkk4* phenotypes (Figs. 5F and H,

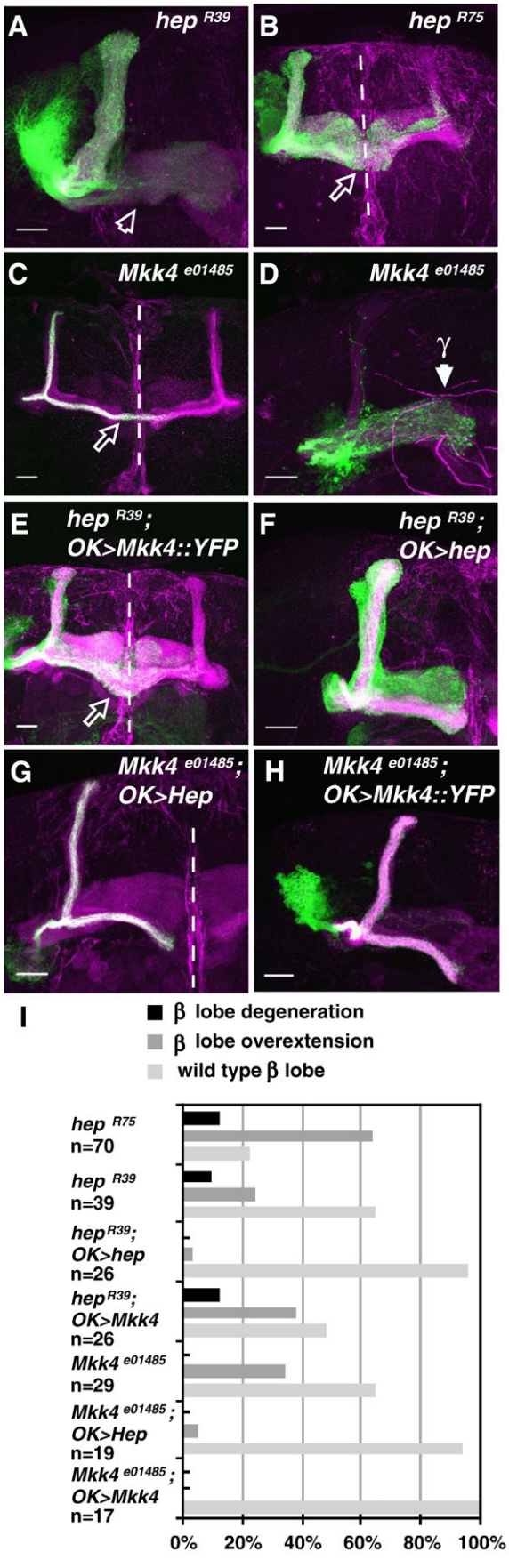

respectively; quantified in Fig. 5I). These results suggest that while both JNKKs regulate axon growth, Hep plays a more prominent role in these axons (see also Supplementary Fig. 5).

Partial inactivation of Bsk results in axon overextension

As loss of either JNKK results in the same phenotype, one explanation is that partial Bsk inactivity leads to a bias towards axon overextension. To test this, two strategies were used to partially reduce Bsk signals in MB neurons. Given the high level of Bsk in these neurons, we reasoned that either RNAi or DN Bsk misexpression are unlikely to result in a null, but a partial inactivation phenotype. *Bsk* RNAi or DN Bsk expression in all MB neurons resulted in a number of axon defects, with defasciculation, degeneration and overextension phenotypes (Figs. 6A–C). Notably, while *Bsk* RNAi expression resulted in many degenerating axons, axon overextension was also observed, particularly at lower titres of RNAi activity (Figs. 6A, B, respectively; quantified in Fig. 6D and Supplementary Fig. 6A; see Methods). Axon overextensions were also observed by DN Bsk misexpression, and this constituted the major phenotype observed (Figs. 6C, D). Therefore, distinct from the *bsk-null* phenotype where axon degeneration predominates, these results suggest that a partial loss of Bsk leads to axon overextension.

These results, together with the JNKK study, make two further predictions: that concomitant loss of Hep and Mkk4 would result in stronger Bsk inactivity, resulting in degeneration phenotypes, and that hypomorphic *bsk* alleles would lead to less axon degeneration and a higher proportion of axon overextension phenotypes. Indeed, we found that *hep, Mkk* double mutant clones showed a higher frequency of axon breaks than *hep* or *Mkk4* single mutants (Figs. 6E, H). The number of axon breaks in *hep, Mkk* double mutants were comparable to *bsk*-null axons (Fig. 6H; data not shown). We also analyzed the *babo* gene, which when inactivated results in similar axon overextensions (Ng, 2008). We found that *babo* overextended axons had hardly any axon breaks throughout the entire neurite (data not shown; Fig. 6H). This suggests that axon overextension does not necessarily lead to axon breaks and neurodegeneration.

A number of *bsk* hypomorphic alleles were analyzed. bsk^{1} and bsk^{2} clones gave wild-type projections (data not shown). bsk^{H15}, which carries a missense mutation in the kinase domain (Berger et al., 2008) resulted in axon degeneration and overextension (Figs. 6F, G, respectively). Our analysis showed while a large fraction of axons were wild type (46.4%), 32.1% gave degeneration phenotypes, while 21.4% exhibited axon overextensions (Fig. 6I). This result shows while the *bsk*-null allele results in predominantly axon degeneration, weaker alleles do result in axon overextension, consistent with the JNKK results.

Sustained Bsk activity is essential for axon stabilization

Is Bsk activity required throughout MB development and adulthood, as the phospho-JNK antibody results would suggest, or at specific periods? This was investigated by temporally controlling Bsk expression in two ways (Fig. 7A). First, a Bsk rescue experiment was performed. By placing *UAS-Bsk* under the control of the TARGET system (McGuire et al., 2003), raising animals at GAL4-restrictive

Fig. 5. Loss of function of Hep and MKK4 in MB neurons. Representative images of hep^{R39} (A), hep^{R75} (B) and $MKK4^{e01458}$ (C, D) neuroblast clones exhibiting β lobe axon degeneration (A), axon overextension (B, C) and cell proliferation (D) phenotypes. Neuroblast proliferation phenotypes are characterized by the presence of early-born γ neurons and absent later-born α'β' and αβ neurons. (E–H) hep^{R39} (E, F) and $MKK4^{e01458}$(G, H) clones in the presence of ectopic MKK4YFP (E, H) or Hep (F, G). Scale bars: 20 μm. Green, CD8-GFP. Magenta, Fas2. (I) Quantification of the β axon phenotypes. As *Mkk4* leads to proliferation defects in early-born neuroblast clones, later-born αβ neuroblast clones were generated for axon studies. *n*, number of neuroblast clones analyzed.

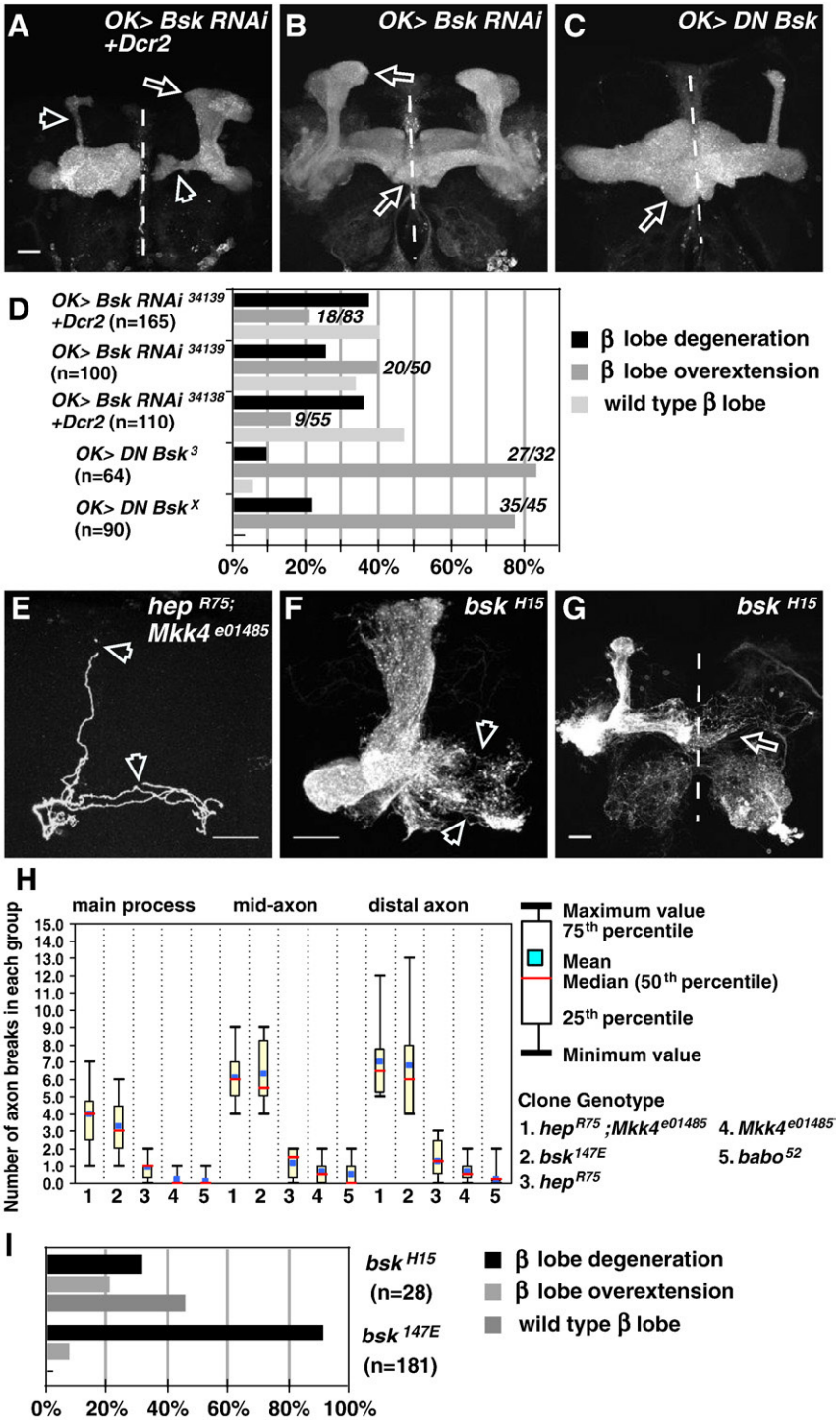

Fig. 6. Partial inactivation of Bsk leads to axon overextension. (A, B) MB neurons expressing *Bsk* RNAi. High level of *Bsk* RNAi knockdown leads to a bias in axon degeneration phenotypes (open arrowheads in A), whereas medium RNAi activity levels lead to dorsal axon overgrowth and medial overextensions (open arrows in B). (C) Dominant-negative Bsk (DN Bsk) misexpression resulted in similar phenotypes. We found that pan-MB inactivation of Bsk also resulted in defasciculation defects, characterized by wider, splayed-out axon lobes (for example, the dorsal projection in A, indicated by the open arrow). (D) Quantification of these phenotypes. n, number of hemispheres analyzed. Given that, in many instances, the β-lobe overextension from one hemisphere overlaps against either a similarly overextending, or otherwise wild-type, axon from the contralateral side, we also present a different analysis of the medial projections for all (pan-MB) overexpression genotypes as the number of brains that have β-lobe overextensions over the total number of brains analyzed (in italics next to the relevant bar). Additional analysis and quantifications for dorsal projections are in Supplementary Fig. 6. (E) Representative image of a hep^{R75}, $MKK4^{e01458}$ mutant single-cell αβ clone. Note axon breaks in the dorsal and medial branch (open arrowheads). Similar breaks were also observed in bsk^{147E} single-cell αβ clones (data not shown; quantified in H). (F, G) Representative image of bsk^{H15} neuroblast clones showing axon degeneration (F) and overextension (G) phenotypes. Cell body sections were removed from A, C and F to clearly reveal axon projections. Scale bars: 20 μm. (H) Quantification of axon breaks in hep^{R75}, $MKK4^{e01458}$ double, bsk^{147E}, hep^{R75} or $MKK4^{e01458}$ or $babo^{52}$ mutants, as indicated. Ten single-cell αβ clones were analyzed for each genotype. Statistical analysis show a significant difference between hep^{R75}, $MKK4^{e01458}$ double or bsk^{147E} clones when compared to hep^{R75} or $MKK4^{e01458}$ or $babo^{52}$ mutants ($P<0.05$) but no significant difference between hep^{R75}, $MKK4^{e01458}$ double compared to bsk^{147E} clones, or between hep^{R75} and $MKK4^{e01458}$ or $babo^{52}$ mutants ($P>0.05$). The only exception is in the distal axon section of hep^{R75} axons, where a small proportion of degeneration was observed, as reflected in the *P*-value (0.014). $babo^{52}$ clones were used as the control in the statistical study. (I) Quantification of the bsk^{H15} axon phenotypes in neuroblast clones, with a comparison to the null (147E) clones.

(18 °C) or GAL4-permissive (29 °C) conditions enabled us to control the timing of Bsk rescue transgene expression in *bsk*-null clones (Fig. 7A and Supplementary Fig. 7; see Methods). The results are summarized in Figs. 7B–E (quantified in F). They show that Bsk activity is required throughout development to completely rescue the axonal phenotypes. Shorter, latent periods of Bsk expression only partially rescued the *bsk*-null phenotypes. In addition, prolonged adult-restricted expression had very little effect.

In a second experiment, a *Bsk RNAi* trangene was expressed also under TARGET control. This enabled us to perform tissue-specific inactivation in a stage-dependent manner. We found that inducing *Bsk* RNAi expression from larval (wandering L3) to late pupal (48–96 h APF) stages resulted in axon overextension and, to a smaller extent, axon degeneration phenotypes (Figs. 7G–J, quantified in K). Prolonged *Bsk* RNAi activity restricted to the adult stage had very little effect, suggesting that Bsk activity is dispensable in adults (Figs. 7J, K). When expressed at shorter, later periods, these axonal phenotypes were also not as frequent as when the *Bsk* RNAi was induced throughout development. This suggests that the 'full' Bsk inactivation phenotype reflects an accumulative period of Bsk signaling throughout development (see Discussion).

We also performed a 'reverse' protocol with an early induction of *Bsk* RNAi, followed by a suppression of RNAi expression from L3 or 0h APF stages. Similar to the above treatment, this also resulted in axonal phenotypes (Fig. 7L; data not shown). Again, the extent of these phenotypes was not as frequent as when *Bsk* RNAi was induced throughout development. Interestingly, the early treatment resulted in more axon degenerations than overextensions, when compared to the late induction protocol (Fig. 7J), suggesting that the degeneration phenotype is more sensitive to an early phase of Bsk inactivity, while the overextension phenotype is prevented more by a later phase of Bsk.

Together these experiments suggest Bsk activity has to be sustained throughout development to ensure proper axonal morphogenesis.

A graded AP-1 response regulates Bsk-dependent axon stability

We determined whether Bsk signals are mediated through AP-1, which in *Drosophila* consists of the transcription factors Fos and Jun. Through clonal analysis using strong, null alleles or dominant-negative (Jbz) misexpression, Jun (also known as Jra) inactivation alone had no effect on gross axon morphology (Jra^1, $n=38$ clones, Jra^2, $n=30$ clones, *Jbz*, $n=36$ hemispheres; both 100% wild type; Supplementary Fig. 8A,B and E, respectively). Loss-of-function analysis on *Fos* (also know as *kayak*, or *kay*) was performed. These axons appeared wild type (kay^1, $n=21$, 100% wild type; kay^{ED6315}, $n=30$, 93.3% wild type; Supplementary Fig. 7C, D), most likely because true null alleles for *kay* do not exist (Giesen et al., 2003; Weber et al., 2008). Therefore, RNAi and dominant-negative misexpression approaches were used. *Kay* RNAi expression resulted in axon overextension (Fig. 8A). In the presence of Dcr2, stronger *Kay* RNAi resulted in axon degeneration phenotypes (Fig. 8B), and this was the dominant phenotype observed (Fig. 8E). Axon overextensions were also observed when Fbz was misexpressed (Fig. 8C). However, axon degeneration phenotypes were observed when Fbz was co-expressed with Jbz (Fig. 8D; quantified in E). To test whether these AP-1 phenotypes are linked to Bsk, we performed genetic interaction assays by expressing *Bsk* RNAi together with Jbz or Fbz (data not shown; Fig. 8F). We found that the *Bsk* RNAi effect was strongly enhanced by single copy expression of Fbz, and by two copies of Jbz.

These results suggest the AP-1 complex mediates the Bsk response in MB neurons. These signals were similarly graded, whereby weak AP-1 inactivation leads to axon overextension but stronger loss results in a bias towards axon degeneration, with Kay playing the major role in these neurons.

Discussion

This study shows that the JNK pathway regulates distinct aspects of axonal morphogenesis, namely to prevent axon overextension and axonal degeneration. To understand the underlying differences, we showed that the level of Bsk activity, its duration and the developmental phase of an organism determine how developing axons respond to these signals. The JNK signals are converted into a transcriptional response through AP-1 and that these signals are similarly graded in axonal morphogenesis.

The MAPK family of proteins are involved in many aspects of cellular behavior and several hypotheses have been put forward to account for their diverse action. Previous in vitro studies show signal duration and signal strength can bias MAPK responses. This has been studied mainly in the context of Erk responses towards cell proliferation and differentiation in cultured cells (Marshall, 1995; Murphy and Blenis, 2006). How these parameters regulate Erk signals have been explored using experimental and theoretical approaches (Kholodenko, 2006; Murphy and Blenis, 2006). Below we discuss the results of this study and focus on the parameters that regulate JNK-dependent axonal stability in vivo.

Our study explains how a single protein kinase can potentially regulate multiple aspects of neuronal morphogenesis. Signals that regulate Bsk activity can generate distinct axonal phenotypes depending on the signaling network, strength and duration. The JNKK signal network is linked to signal strength, since both JNKKs converge on Bsk and determine its relative activity levels (Supplementary Fig. 9A). In the case where the signal ensures axons do not overextend, both Hep and Mkk4 are essential as the loss of either input leads to axon overextension. This is phenocopied by hypomorphic conditions of Bsk. However, for signals that protect against neurodegeneration and axonal loss, the JNKKs seem to act redundantly, as loss of either JNKK does not result in axon degeneration, whereas loss of Bsk, or Hep together with Mkk4 does. The bias in responses suggest while lower levels of Bsk activity are sufficient to protect against axon degeneration, the mechanism that protects against axon overextension requires higher threshold levels of Bsk activity. In both cases, Bsk phosphorylation is critical for as loss of their sites renders Bsk fully inactive.

What is currently unknown is the nature of the signal(s) that regulate the JNK responses in these neurons, although it is likely to be active throughout development. Also unclear is whether the signal that protects against neurodegeneration is linked to axon overextension, although we show overextended axons *per se* do not necessarily lead to axon breaks. In one scenario, these could be represented by distinct molecules and signaling mechanisms: one signal acts to prevent degeneration, while another stabilizes axons at the correct termini by preventing overextension. In a distinct scenario, this may be one and the same factor, which acts to promote both axon stability and termination at the correct target site. Nonetheless, our results suggest these responses require different Bsk threshold activities.

The phospho-JNK staining results show Bsk is active throughout MB development and adulthood (Supplementary Fig. 9B). The genetic results show, for axonal morphogenesis, sustained Bsk activity is essential only throughout development, but it is not restricted to a narrow, critical period within development. As Bsk activity (or inactivity) during adulthood does not change the pre-existing axonal morphology of these genotypes, this suggests JNK-dependent physiology changes between development and adulthood, and the adult-stage phospho-JNK signals most likely reflect a distinct mode of MB regulation. This switch may be an example of a cell-context requirement of JNK signaling at different developmental stages. Although yet to be defined, one possibility is an adult role in synaptic plasticity and growth, as shown in *Drosophila* NMJ studies (Collins et al., 2006; Sanyal et al., 2002).

We found that shorter periods of Bsk inactivity and activity tend to result in a weaker effect (as opposed to no effect at all) compared to protocols where *Bsk* RNAi or rescue activity is 'on' throughout development. Based on these results, we propose, for maintaining optimal axon stability, Bsk signals are read 'additively' throughout development (Supplementary Fig. 9B). Rather than as a 'temporal

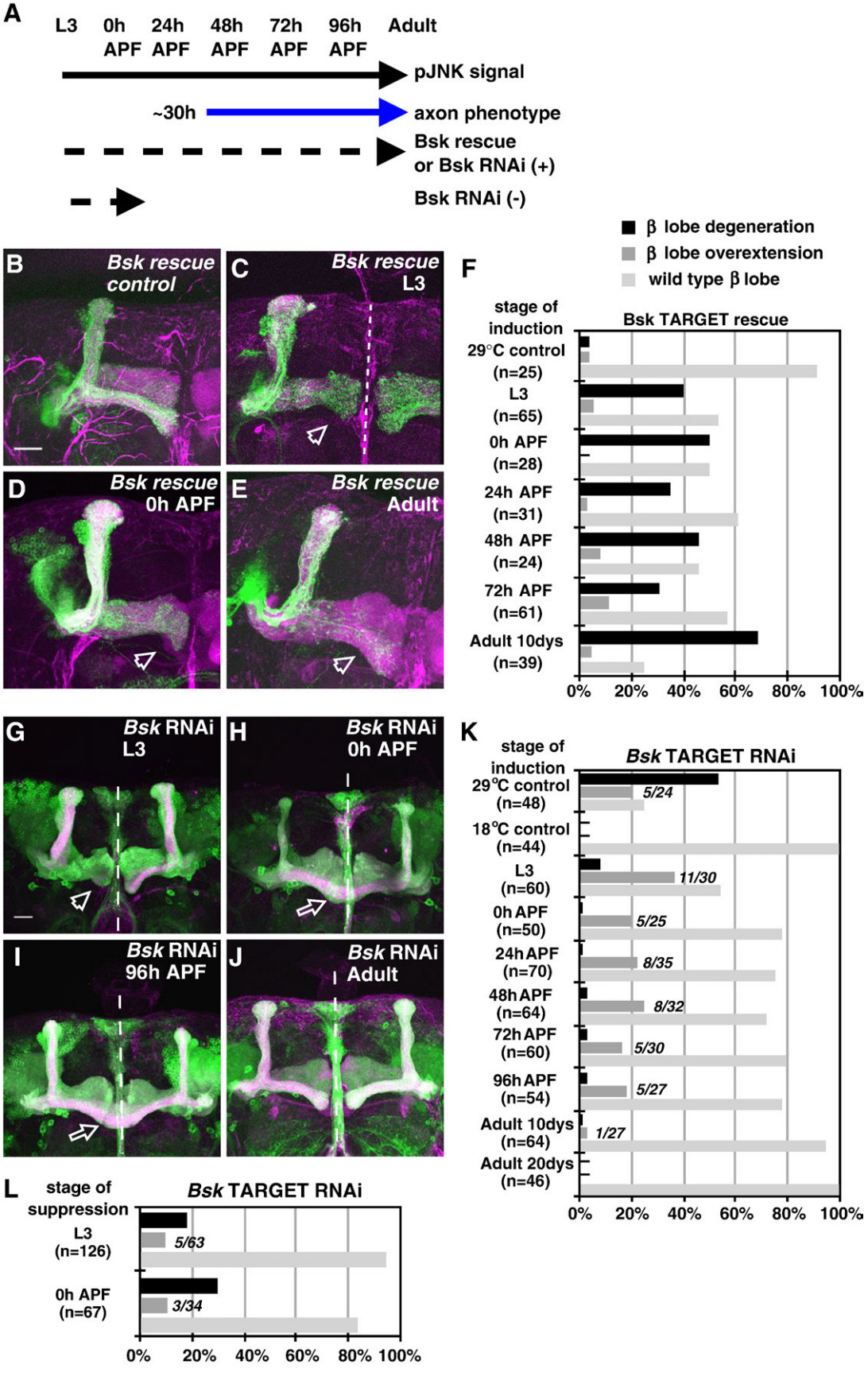

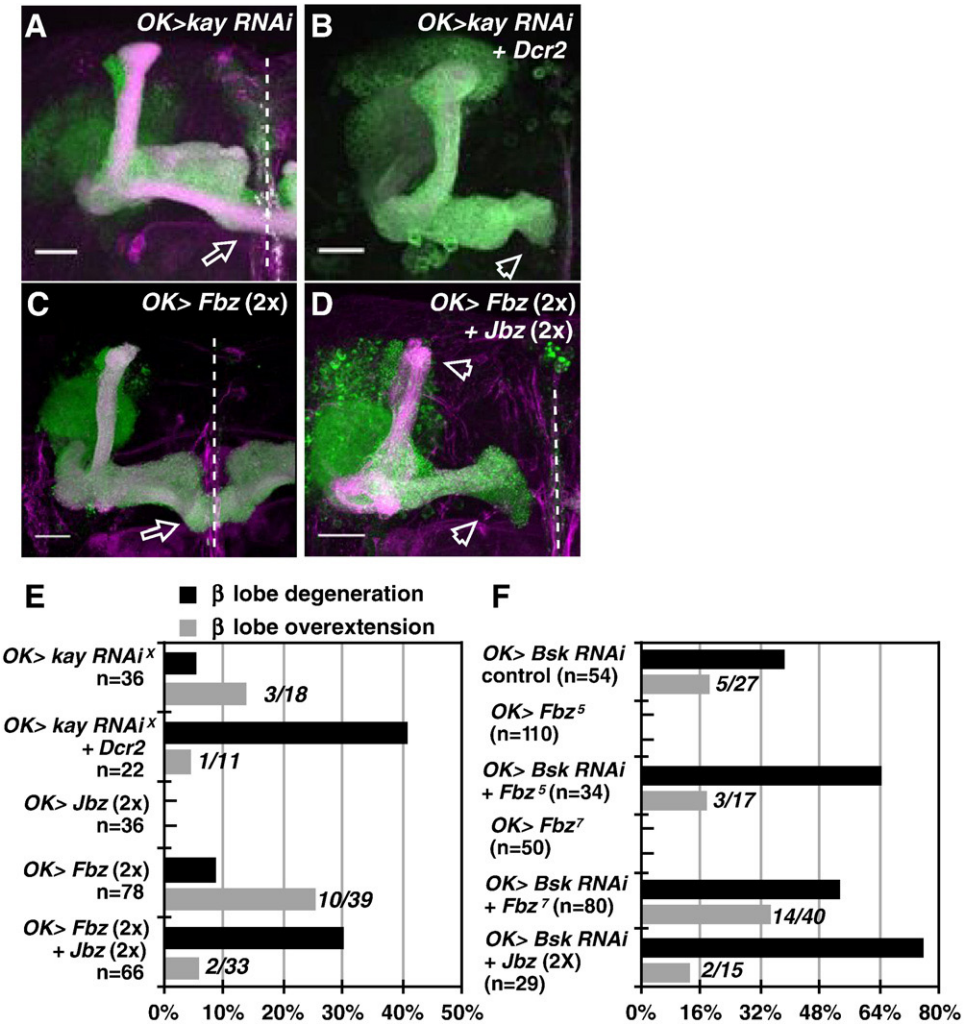

Fig. 8. A graded AP-1 signal mediates Bsk responses. (A–D) MB neurons expressing *kay* RNAi (A), *kay* RNAi plus *Dcr2* (B), Fbz (C), or Fbz plus Jbz (D) showed axon overextension (A, C) and degeneration (B, D) phenotypes. Copy numbers of expressed transgenes are indicated in parenthesis. Progeny derived from Fbz and Jbz crosses were raised at 29 °C to increase the possibility of detecting any axonal phenotypes due to misexpression. Scale bars: 20 μm. Green, CD8-GFP. Magenta, Fas2. (E) Quantification of these phenotypes. In E and F, also shown is the β-lobe overextension analysis expressed as the number of overextended brains over the total number of brains analyzed (italics). (F) Genetic interaction assay using *Bsk* RNAi (line 34138) with dominant-negative AP-1. *Bsk* RNAi expressing flies were grown at 29 °C, in presence of one copy of Fbz or two copies of Jbz, showed an enhancement in axonal defects. As controls, *Bsk* RNAi flies were expressed with CD8GFP alone. Single copy expression of Fbz (line 5 or 7) or two copies of Jbz (lines 1 and 10) (E) did not result in gross axon defects. n, number of hemispheres analyzed.

summation' module, where signals need to reach a timed threshold level of activity to evoke 'all-or-none' response, we find the shorter periods of Bsk activity can still derive a (albeit sub-optimal) morphogenetic response. Nonetheless, there is still an activity threshold required to protect against degeneration (relatively low) and axon overextension (relatively high).

Note that in our genetic paradigm JNK activity protects against neurodegeneration and axonal loss. In many studies, JNK activity provokes these effects, in response to physical injury, genetic, environmental and stress stimuli (Miller et al., 2009; Morfini et al., 2006; Waetzig et al., 2006). One previous study in mutant mice showed that JNK inactivation also leads to axonal loss. These studies

Fig. 7. Sustained Bsk levels are essential for axon stability. (A) Bsk activity (as measured by the P-Bsk signal) is detected throughout development and adulthood (black arrow). Yet the axonal phenotypes are observed only at later stages (~30 h after puparium formation, APF) (blue arrow). To determine the temporal requirements of Bsk-dependent phenotypes, we used the TARGET system to determine whether the induction (+) or suppression (−) of TARGET expression (see schematic in Supplementary Fig. 7A), by transgenic rescue analysis or RNAi at specific stages (larval, pupal or adult) alters the extent of the observed phenotypes. The dashed arrows indicate the extent of the TARGET expression under different temporal and developmental settings. (B–E) Images of bsk^{147e}neuroblast clones with the Bsk-myc expression under TARGET control. As a control, Bsk TARGET flies raised at 29 °C (GAL4-permissive) throughout exhibited >90% wild type projections (B). bsk^{147e}clones with Bsk-myc expression induced at developmental stages L3 (C), and 0h APF (D). (E) bsk^{147e}clones with Bsk-myc expression restricted only to the adult stage for 10 days post-eclosion. (F) Quantification of these *bsk* rescue phenotypes. Induced at shorter periods, many flies exhibited β-axon degeneration. *n*, number of neuroblast clones analyzed. (G–J) *Bsk* RNAi expressed under TARGET control. *Bsk* RNAi expression induced at stages L3 (G), 0 h (H), or 96 h APF (I) resulted in axon degeneration (G), and axon overextension phenotypes (H, I). (J) *Bsk* RNAi restricted to adult stages for 10–20 days post-eclosion showed wild-type projections. With the exception of adult-stage induced flies, all earlier induced flies were dissected as 3-day adults. Scale bars: 20 μm. Green, CD8-GFP. Magenta, Fas2. (K) Quantification of the *Bsk* TARGET RNAi phenotypes. *n*, number of brain hemispheres analyzed. In K and L, the β-lobe overextension analysis is also presented as the number of overextended brains over the total number of brains analyzed (italics). Note both protocols do not reflect a strict 'on' time at the indicated developmental stages but rely on the 'on' kinetics of the TARGET system. In our manipulations, we detected expression from 24 h and robustly at 72 h post-induction (Supplementary Fig. 7B–E; data not shown). Therefore, a period of RNAi and Bsk-myc accumulation is required for effective downregulation of *Bsk* mRNA transcripts and suppression of *bsk*-null phenotypes (respectively). (L) Quantification of the *Bsk* RNAi phenotype using a reverse TARGET protocol, with an early induction followed by a suppression of RNAi transgene expression at L3 or 0 h APF, as indicated. Note the increased representation of axon degeneration over overextension phenotypes at the early phase of Bsk inactivity.

also showed JNK loss does not affect initial axon commissure formation (Chang et al., 2003). Interestingly, JNK and AP-1 activity is often upregulated in response to nerve injury and thought to be essential for axonal repair post-injury (Herdegen et al., 1998; Raivich et al., 2004). How our study relates to these models of disease, injury and repair remains speculative, however, it shows parameters such as activity levels, timing and developmental stages may be key to understanding JNK-dependent dysfunctions in the nervous system.

Our study also raises the possibility that JNK signals are related to developmentally regulated degenerative events such as axonal pruning (Lee et al., 1999). However, this is unlikely, as our results show (1) all adult *bsk* γ-axons exhibit only a single, medial projection (Fig. 2J), showing that mutant axons prune properly, (2) neither is there a delay in pruning (Figs. 2G–I), as aberrant, non-pruned, dorsal projections are not visible at mid-pupal stages, when pruning (followed by re-extension) has completed (Lee et al., 1999), and (3) forced ectopic activation of the JNK pathway also does not block axon pruning (Supplementary Fig. 10). Together these results suggest Bsk signals (its loss or gain) does not affect developmental pruning in MB neurons.

Our results show AP-1 signals are similarly graded to these distinct phenotypes (Supplementary Fig. 9A). How predominantly axon-based Bsk signals are translated into a graded, nuclear-based AP-1 transcriptional readout awaits further investigation. One can potentially envisage that the different axonal behaviors derived from graded AP-1 responses result from gene expression programs involving separate pools of immediate early gene products, or the same set of transcriptional targets expressed in different quantities, and/or perhaps even under different temporal settings.

Currently, it is unclear how the Bsk/AP-1 signaling program regulates these changes in axonal behaviors. Previous studies show Bsk signals result in transcriptional responses involving distinct gene targets linked to the actin cytoskeleton, cell adhesion, oxidative stress, extracellular matrix, autophagy, cell cycle and apoptotic control (Homsy et al., 2006; Hyun et al., 2006; Jasper et al., 2001; Moreno et al., 2002; Uhlirova and Bohmann, 2006; Wang et al., 2003; Wu et al., 2009). Many of these processes control Bsk-regulated morphogenesis. In our preliminary analysis, we found Bsk/AP-1 signals do lead to changes in the actin and microtubule cytoskeleton, axonal transport and caspase-related activities (unpublished observations). These preliminary results may be related to the axonal breaks and to changes in the axonal architecture (such as swellings, filopodia and lamellipodia protrusions) that were observed in *bsk* single-cell clones.

While we show AP-1 mechanisms are involved, it is likely that not all of these cellular changes are AP-1 related. For example, the axonal swellings observed in *bsk* clones may arise from defects in axonal transport, which was recently reported to be perturbed in different JNK settings (Horiuchi et al., 2007), and our preliminary results show many of these swellings do contain an accumulation of axonal transport cargo, such as organelles and vesicles, as measured using mitochondrial and synaptic markers. Many AP-1-independent targets have been reported in mammalian JNK studies and direct JNK regulation of the actin and microtubule cytoskeleton has been proposed (Bjorkblom et al., 2005; Chang et al., 2003; Gdalyahu et al., 2004; Huang et al., 2003; Tararuk et al., 2006; Yoshida et al., 2004). Currently, it is unclear how relevant these targets are in Bsk responses in vivo. In some instances, these targets are not relevant as either there are no obvious homologs in Drosophila (such as DCX), or the fly proteins do not have the equivalent JNK phospho-regulatory sites (such as paxillin).

In summary, our results highlight the signaling mechanisms that control the JNK pathway during neuronal morphogenesis. The basis of distinct morphogenetic functions can be accounted by the graded levels by which JNK input signals are mediated and the way AP-1 transcriptional output signals are generated, as well as the duration of the signal propagation within developing neurons.

Acknowledgments

This work was supported by the Wellcome Trust (078045). A. Rallis was supported by a studentship from the Medical Research Council (MRC). We thank M. Fanto, S. Guthrie, A. Ridley and O. Schuldiner and members of the Ng lab for comments on the manuscript. M. Bienz, D. Bohmann, M. Mlodzik, M. Ramaswami, T. Suzuki, D. Strutt, together with the Bloomington Drosophila Stock Center, NIG-FLY Stock Center, Vienna Drosophila RNAi Center and DGRC, Bloomington provided critical reagents used in this study.

Appendix A. Supplementary data

Supplementary data associated with this article can be found, in the online version, at doi:10.1016/j.ydbio.2009.12.016.

References

Agnes, F., Suzanne, M., Noselli, S., 1999. The Drosophila JNK pathway controls the morphogenesis of imaginal discs during metamorphosis. Development 126, 5453–5462.
Berger, J., Senti, K.A., Senti, G., Newsome, T.P., Asling, B., Dickson, B.J., Suzuki, T., 2008. Systematic identification of genes that regulate neuronal wiring in the Drosophila visual system. PLoS Genet. 4, e1000085.
Bettencourt-Dias, M., Giet, R., Sinka, R., Mazumdar, A., Lock, W.G., Balloux, F., Zafiropoulos, P.J., Yamaguchi, S., Winter, S., Carthew, R.W., Cooper, M., Jones, D., Frenz, L., Glover, D.M., 2004. Genome-wide survey of protein kinases required for cell cycle progression. Nature 432, 980–987.
Bjorkblom, B., Ostman, N., Hongisto, V., Komarovski, V., Filen, J.J., Nyman, T.A., Kallunki, T., Courtney, M.J., Coffey, E.T., 2005. Constitutively active cytoplasmic c-Jun N-terminal kinase 1 is a dominant regulator of dendritic architecture: role of microtubule-associated protein 2 as an effector. J. Neurosci. 25, 6350–6361.
Bjorklund, M., Taipale, M., Varjosalo, M., Saharinen, J., Lahdenpera, J., Taipale, J., 2006. Identification of pathways regulating cell size and cell-cycle progression by RNAi. Nature 439, 1009–1013.
Bosch, M., Serras, F., Martin-Blanco, E., Baguna, J., 2005. JNK signaling pathway required for wound healing in regenerating Drosophila wing imaginal discs. Dev. Biol. 280, 73–86.
Chang, L., Jones, Y., Ellisman, M.H., Goldstein, L.S., Karin, M., 2003. JNK1 is required for maintenance of neuronal microtubules and controls phosphorylation of microtubule-associated proteins. Dev. Cell 4, 521–533.
Ciapponi, L., Jackson, D.B., Mlodzik, M., Bohmann, D., 2001. Drosophila Fos mediates ERK and JNK signals via distinct phosphorylation sites. Genes Dev. 15, 1540–1553.
Collins, C.A., Wairkar, Y.P., Johnson, S.L., DiAntonio, A., 2006. Highwire restrains synaptic growth by attenuating a MAP kinase signal. Neuron 51, 57–69.
Delaney, J.R., Stoven, S., Uvell, H., Anderson, K.V., Engstrom, Y., Mlodzik, M., 2006. Cooperative control of Drosophila immune responses by the JNK and NF-kappaB signaling pathways. EMBO J. 25, 3068–3077.
Dietzl, G., Chen, D., Schnorrer, F., Su, K.C., Barinova, Y., Fellner, M., Gasser, B., Kinsey, K., Oppel, S., Scheiblauer, S., Couto, A., Marra, V., Keleman, K., Dickson, B.J., 2007. A genome-wide transgenic RNAi library for conditional gene inactivation in Drosophila. Nature 448, 151–156.
Eresh, S., Riese, J., Jackson, D.B., Bohmann, D., Bienz, M., 1997. A CREB-binding site as a target for decapentaplegic signalling during Drosophila endoderm induction. EMBO J. 16, 2014–2022.
Galko, M.J., Krasnow, M.A., 2004. Cellular and genetic analysis of wound healing in Drosophila larvae. PLoS Biol. 2, E239.
Gdalyahu, A., Ghosh, I., Levy, T., Sapir, T., Sapoznik, S., Fishler, Y., Azoulai, D., Reiner, O., 2004. DCX, a new mediator of the JNK pathway. EMBO J. 23, 823–832.
Giesen, K., Lammel, U., Langehans, D., Krukkert, K., Bunse, I., Klambt, C., 2003. Regulation of glial cell number and differentiation by ecdysone and Fos signaling. Mech. Dev. 120, 401–413.
Glise, B., Bourbon, H., Noselli, S., 1995. Hemipterous encodes a novel Drosophila MAP kinase kinase, required for epithelial cell sheet movement. Cell 83, 451–461.
Han, Z.S., Enslen, H., Hu, X., Meng, X., Wu, I.H., Barrett, T., Davis, R.J., Ip, Y.T., 1998. A conserved p38 mitogen-activated protein kinase pathway regulates Drosophila immunity gene expression. Mol. Cell. Biol. 18, 3527–3539.
Herdegen, T., Claret, F.X., Kallunki, T., Martin-Villalba, A., Winter, C., Hunter, T., Karin, M., 1998. Lasting N-terminal phosphorylation of c-Jun and activation of c-Jun N-terminal kinases after neuronal injury. J. Neurosci. 18, 5124–5135.
Homsy, J.G., Jasper, H., Peralta, X.G., Wu, H., Kiehart, D.P., Bohmann, D., 2006. JNK signaling coordinates integrin and actin functions during Drosophila embryogenesis. Dev. Dyn. 235, 427–434.
Horiuchi, D., Collins, C.A., Bhat, P., Barkus, R.V., Diantonio, A., Saxton, W.M., 2007. Control of a kinesin-cargo linkage mechanism by JNK pathway kinases. Curr. Biol. 17, 1313–1317.
Huang, C., Rajfur, Z., Borchers, C., Schaller, M.D., Jacobson, K., 2003. JNK phosphorylates paxillin and regulates cell migration. Nature 424, 219–223.
Hyun, J., Becam, I., Yanicostas, C., Bohmann, D., 2006. Control of G2/M transition by Drosophila Fos. Mol. Cell. Biol. 26, 8293–8302.

Ito, K., Awano, W., Suzuki, K., Hiromi, Y., Yamamoto, D., 1997. The Drosophila mushroom body is a quadruple structure of clonal units each of which contains a virtually identical set of neurones and glial cells. Development 124, 761–771.
Jasper, H., Benes, V., Schwager, C., Sauer, S., Clauder-Munster, S., Ansorge, W., Bohmann, D., 2001. The genomic response of the Drosophila embryo to JNK signaling. Dev. Cell 1, 579–586.
Kholodenko, B.N., 2006. Cell-signalling dynamics in time and space. Nat. Rev. Mol. Cell Biol. 7, 165–176.
Klueg, K.M., Alvarado, D., Muskavitch, M.A., Duffy, J.B., 2002. Creation of a GAL4/UAS-coupled inducible gene expression system for use in Drosophila cultured cell lines. Genesis 34, 119–122.
Kockel, L., Zeitlinger, J., Staszewski, L.M., Mlodzik, M., Bohmann, D., 1997. Jun in Drosophila development: redundant and nonredundant functions and regulation by two MAPK signal transduction pathways. Genes Dev. 11, 1748–1758.
Kurusu, M., Awasaki, T., Masuda-Nakagawa, L.M., Kawauchi, H., Ito, K., Furukubo-Tokunaga, K., 2002. Embryonic and larval development of the Drosophila mushroom bodies: concentric layer subdivisions and the role of fasciclin II. Development 129, 409–419.
Lee, T., Luo, L., 1999. Mosaic analysis with a repressible cell marker for studies of gene function in neuronal morphogenesis. Neuron 22, 451–461.
Lee, T., Lee, A., Luo, L., 1999. Development of the Drosophila mushroom bodies: sequential generation of three distinct types of neurons from a neuroblast. Development 126, 4065–4076.
Marshall, C.J., 1995. Specificity of receptor tyrosine kinase signaling: transient versus sustained extracellular signal-regulated kinase activation. Cell 80, 179–185.
Mattila, J., Omelyanchuk, L., Kyttala, S., Turunen, H., Nokkala, S., 2005. Role of Jun N-terminal Kinase (JNK) signaling in the wound healing and regeneration of a Drosophila melanogaster wing imaginal disc. Int. J. Dev. Biol. 49, 391–399.
McGuire, S.E., Le, P.T., Osborn, A.J., Matsumoto, K., Davis, R.L., 2003. Spatiotemporal rescue of memory dysfunction in Drosophila. Science 302, 1765–1768.
Miller, B.R., Press, C., Daniels, R.W., Sasaki, Y., Milbrandt, J., DiAntonio, A., 2009. A dual leucine kinase-dependent axon self-destruction program promotes Wallerian degeneration. Nat. Neurosci. 12, 387–389.
Moreno, E., Yan, M., Basler, K., 2002. Evolution of TNF signaling mechanisms: JNK-dependent apoptosis triggered by Eiger, the Drosophila homolog of the TNF superfamily. Curr. Biol. 12, 1263–1268.
Morfini, G., Pigino, G., Szebenyi, G., You, Y., Pollema, S., Brady, S.T., 2006. JNK mediates pathogenic effects of polyglutamine-expanded androgen receptor on fast axonal transport. Nat. Neurosci. 9, 907–916.
Murphy, L.O., Blenis, J., 2006. MAPK signal specificity: the right place at the right time. Trends Biochem. Sci. 31, 268–275.
Ng, J., 2008. TGF-beta signals regulate axonal development through distinct Smad-independent mechanisms. Development 135, 4025–4035.
Noselli, S., 1998. JNK signaling and morphogenesis in Drosophila. Trends Genet. 14, 33–38.
Oliva Jr., A.A., Atkins, C.M., Copenagle, L., Banker, G.A., 2006. Activated c-Jun N-terminal kinase is required for axon formation. J. Neurosci. 26, 9462–9470.
Pastor-Pareja, J.C., Grawe, F., Martin-Blanco, E., Garcia-Bellido, A., 2004. Invasive cell behavior during Drosophila imaginal disc eversion is mediated by the JNK signaling cascade. Dev. Cell 7, 387–399.
Pearson, J.C., Juarez, M.T., Kim, M., McGinnis, W., 2009. Multiple transcription factor codes activate epidermal wound-response genes in Drosophila. Proc. Natl. Acad. Sci. U. S. A. 106, 2224–2229.
Perkins, K.K., Admon, A., Patel, N., Tjian, R., 1990. The Drosophila Fos-related AP-1 protein is a developmentally regulated transcription factor. Genes Dev. 4, 822–834.
Raivich, G., Bohatschek, M., Da Costa, C., Iwata, O., Galiano, M., Hristova, M., Nateri, A.S., Makwana, M., Riera-Sans, L., Wolfer, D.P., Lipp, H.P., Aguzzi, A., Wagner, E.F., Behrens, A., 2004. The AP-1 transcription factor c-Jun is required for efficient axonal regeneration. Neuron 43, 57–67.
Ramet, M., Lanot, R., Zachary, D., Manfruelli, P., 2002. JNK signaling pathway is required for efficient wound healing in Drosophila. Dev. Biol. 241, 145–156.
Riesgo-Escovar, J.R., Hafen, E., 1997a. Common and distinct roles of DFos and DJun during Drosophila development. Science 278, 669–672.
Riesgo-Escovar, J.R., Hafen, E., 1997b. Drosophila Jun kinase regulates expression of decapentaplegic via the ETS-domain protein Aop and the AP-1 transcription factor DJun during dorsal closure. Genes Dev. 11, 1717–1727.
Rosso, S.B., Sussman, D., Wynshaw-Boris, A., Salinas, P.C., 2005. Wnt signaling through Dishevelled, Rac and JNK regulates dendritic development. Nat. Neurosci. 8, 34–42.
Ryoo, H.D., Gorenc, T., Steller, H., 2004. Apoptotic cells can induce compensatory cell proliferation through the JNK and the Wingless signaling pathways. Dev. Cell 7, 491–501.
Sanyal, S., Sandstrom, D.J., Hoeffer, C.A., Ramaswami, M., 2002. AP-1 functions upstream of CREB to control synaptic plasticity in Drosophila. Nature 416, 870–874.
Sluss, H.K., Han, Z., Barrett, T., Goberdhan, D.C., Wilson, C., Davis, R.J., Ip, Y.T., 1996. A JNK signal transduction pathway that mediates morphogenesis and an immune response in Drosophila. Genes Dev. 10, 2745–2758.
Srahna, M., Leyssen, M., Choi, C.M., Fradkin, L.G., Noordermeer, J.N., Hassan, B.A., 2006. A signaling network for patterning of neuronal connectivity in the Drosophila brain. PLoS Biol. 4, e348.
Stronach, B., 2005. Dissecting JNK signaling, one KKKinase at a time. Dev. Dyn. 232, 575–584.
Su, Y.C., Treisman, J.E., Skolnik, E.Y., 1998. The Drosophila Ste20-related kinase misshapen is required for embryonic dorsal closure and acts through a JNK MAPK module on an evolutionarily conserved signaling pathway. Genes Dev. 12, 2371–2380.
Tararuk, T., Ostman, N., Li, W., Bjorkblom, B., Padzik, A., Zdrojewska, J., Hongisto, V., Herdegen, T., Konopka, W., Courtney, M.J., Coffey, E.T., 2006. JNK1 phosphorylation of SCG10 determines microtubule dynamics and axodendritic length. J. Cell Biol. 173, 265–277.
Thibault, S.T., Singer, M.A., Miyazaki, W.Y., Milash, B., Dompe, N.A., Singh, C.M., Buchholz, R., Demsky, M., Fawcett, R., Francis-Lang, H.L., Ryner, L., Cheung, L.M., Chong, A., Erickson, C., Fisher, W.W., Greer, K., Hartouni, S.R., Howie, E., Jakkula, L., Joo, D., Killpack, K., Laufer, A., Mazzotta, J., Smith, R.D., Stevens, L.M., Stuber, C., Tan, L.R., Ventura, R., Woo, A., Zakrajsek, I., Zhao, L., Chen, F., Swimmer, C., Kopczynski, C., Duyk, G., Winberg, M.L., Margolis, J., 2004. A complementary transposon tool kit for Drosophila melanogaster using P and piggyBac. Nat. Genet. 36, 283–287.
Uhlirova, M., Bohmann, D., 2006. JNK- and Fos-regulated Mmp1 expression cooperates with Ras to induce invasive tumors in Drosophila. EMBO J. 25, 5294–5304.
Ventura, J.J., Hubner, A., Zhang, C., Flavell, R.A., Shokat, K.M., Davis, R.J., 2006. Chemical genetic analysis of the time course of signal transduction by JNK. Mol. Cell 21, 701–710.
Vidal, S., Khush, R.S., Leulier, F., Tzou, P., Nakamura, M., Lemaitre, B., 2001. Mutations in the Drosophila dTAK1 gene reveal a conserved function for MAPKKKs in the control of rel/NF-kappaB-dependent innate immune responses. Genes Dev. 15, 1900–1912.
Waetzig, V., Zhao, Y., Herdegen, T., 2006. The bright side of JNKs-multitalented mediators in neuronal sprouting, brain development and nerve fiber regeneration. Prog. Neurobiol. 80, 84–97.
Wang, M.C., Bohmann, D., Jasper, H., 2003. JNK signaling confers tolerance to oxidative stress and extends lifespan in Drosophila. Dev. Cell 5, 811–816.
Weber, U., Pataki, C., Mihaly, J., Mlodzik, M., 2008. Combinatorial signaling by the Frizzled/PCP and Egfr pathways during planar cell polarity establishment in the Drosophila eye. Dev. Biol. 316, 110–123.
Weston, C.R., Davis, R.J., 2002. The JNK signal transduction pathway. Curr. Opin. Genet. Dev. 12, 14–21.
Wu, J.S., Luo, L., 2006a. A protocol for dissecting Drosophila melanogaster brains for live imaging or immunostaining. Nat. Protoc. 1, 2110–2115.
Wu, J.S., Luo, L., 2006b. A protocol for mosaic analysis with a repressible cell marker (MARCM) in Drosophila. Nat. Protoc. 1, 2583–2589.
Wu, H., Wang, M.C., Bohmann, D., 2009. JNK protects Drosophila from oxidative stress by trancriptionally activating autophagy. Mech. Dev. 126, 624–637.
Yoshida, H., Hastie, C.J., McLauchlan, H., Cohen, P., Goedert, M., 2004. Phosphorylation of microtubule-associated protein tau by isoforms of c-Jun N-terminal kinase (JNK). J. Neurochem. 90, 352–358.
Zeitlinger, J., Kockel, L., Peverali, F.A., Jackson, D.B., Mlodzik, M., Bohmann, D., 1997. Defective dorsal closure and loss of epidermal decapentaplegic expression in Drosophila fos mutants. EMBO J. 16, 7393–7401.
Zheng, X., Wang, J., Haerry, T.E., Wu, A.Y., Martin, J., O'Connor, M.B., Lee, C.H., Lee, T., 2003. TGF-beta signaling activates steroid hormone receptor expression during neuronal remodeling in the Drosophila brain. Cell 112, 303–315.